

This file is part of the following work:

**Kuddus, Md Abdul (2021) *Using mathematical models to develop tuberculosis control strategies in Bangladesh*. PhD Thesis, James Cook University.**

Access to this file is available from:

<https://doi.org/10.25903/8erm%2D4476>

Copyright © 2020 Md Abdul Kuddus.

The author has certified to JCU that they have made a reasonable effort to gain permission and acknowledge the owners of any third party copyright material included in this document. If you believe that this is not the case, please email

[researchonline@jcu.edu.au](mailto:researchonline@jcu.edu.au)

# Using mathematical models to develop tuberculosis control strategies in Bangladesh

Thesis submitted by

Md Abdul Kuddus, BSc, MSc, MPH

Assistant Professor

University of Rajshahi, Bangladesh

in February 2021



for the Degree of Doctor of Philosophy (Health)

in the College of Medicine and Dentistry

James Cook University, Australia

# **SUPERVISOR**

## **PRINCIPAL SUPERVISOR**

Professor Emma McBryde, MBBS, MBios, FRACP, PhD  
James Cook University

## **CO-SUPERVISOR**

Dr Michael Meehan, BSc, PhD  
James Cook University

## **ASSOCIATE SUPERVISOR**

Professor Lisa White (University of Oxford)  
A/Prof. James Trauer (Monash University)  
Dr Tan Doan (University of Melbourne)

# DECLARATION

I, the undersigned declare that the work presented in this thesis is carried out on my research during the academic program towards the degree of Doctor of Philosophy (Health) of James Cook University. The work has not been previously submitted anywhere for another degree or diploma at any university of the institution of tertiary education in or out of Australia. Information derived from the published or unpublished works of others has been acknowledged in the text and a list of references is given.

February 2021

Date \_\_\_\_\_

Content has been removed  
for privacy reasons

Signature

Md Abdul Kuddus

\_\_\_\_\_  
Name

## STATEMENT OF ACCESS

I, the undersigned, the author of this research work, understand that James Cook University will make this thesis accessible for wider use within the University library and via the Australian Digital Theses Network, for use elsewhere.

I understand that, as an unpublished work, a thesis has significant defense under the Copyright Act. All users referring this thesis will have to sign the following statement.

“In referring this thesis I approve not to copy or closely paraphrase it in entire or in partial without the written agreement of the author; and to make appropriate written acknowledgement for any support which I have achieved from it”

Beyond this, I do not wish to place any additional constraint on access to this research work.

February 2021

Date \_\_\_\_\_

Content has been removed  
for privacy reasons

Signature

Md Abdul Kuddus

\_\_\_\_\_  
Name

## DECLARATION ON ETHICS

This research presented and reported in this thesis was conducted within the guidelines for human research ethics outlined in the James Cook University Human Ethics Policy. Human studies were approved by the Human Ethics Committee in accordance with the institutional ethical guidelines of James Cook University. All of the protocols were approved by the Human Ethics Committee of James Cook University (Approval number: H7300)

February 2021

Date \_\_\_\_\_

Content has been removed  
for privacy reasons

Signature

Md Abdul Kuddus

\_\_\_\_\_  
Name

## ACKNOWLEDGEMENTS

My enormous gratitude goes to my supervisory panel – Emma McBryde, Michael Meehan, Lisa White, James Trauer, and Tan Doan for their patience, direction, and inspiration. Each of them contributed to my understanding of the topic in diverse and extremely significant ways.

I thank Dr Rouseli Haque, Dr Ahmadul Hasan Khan (Sumon) and Dr Md. Abu Sayem from the National TB Control Program (NTP), Directorate General of Health Services in Bangladesh, for kindly providing TB surveillance data. I also thank the climate division in Bangladesh for providing weather data. I am also thankful to Dr Jahirul Karim who helped to source the TB surveillance data. A special thanks to Dr Oyelola Adegboye and Dr Adeshina Adekunle for their kind help on statistical and mathematical analyses. Besides, I would like to thank, Narayan, Samson, and Eike for giving me the warmth of family and making my life abroad full of fun and color.

In undertaking this research, I was supported financially by the James Cook University Postgraduate Research Scholarship (International), a Top-up and a Thesis Write-up Scholarship from College of Medicine and Dentistry at James Cook University. The Policy relevant infectious disease simulation and mathematical modelling (PRISM<sup>2</sup>) Centre of Research Excellence provided financial support to attend infectious diseases modelling conferences in Thailand and Australia. The College of Medicine and Dentistry also provided financial support to publish papers in open access journals.

I am eternally grateful to my parents, sisters, and brothers for their infinite support, and for always encouraging me to follow my dreams, no matter how far they take me. My gratitude goes out to my wife, Farha, and my son, Arav for their loving support and endless encouragement that kept me alive on the rocky road of the PhD journey.

Lastly, I am sincerely grateful to my M.Sc. thesis supervisor Professor Ashabul Hoque, MPH thesis supervisor Professor Nuntavarn Vichit-Vadakan, and Professor Marc Van der Putten. I am also grateful to Professor Mamunur Rashid Talukder who made me realise my capability of becoming a researcher.

## STATEMENT ON THE CONTRIBUTION OF OTHERS

<b>Nature of Assistant</b>	<b>Contribution</b>	<b>Names, Titles and Affiliations of Co-Contributors</b>
Thesis presentation	Thesis formatting ESL editing	Prof. Emma McBryde, JCU Dr Michael Meehan, JCU Dr Tan Doan, University of Melbourne
Chapter 1: Intellectual support	Editorial assistance	Prof. Emma McBryde, JCU Dr Michael Meehan, JCU Prof. Lisa White, University of Oxford A/Prof. James Trauer, Monash University Dr Tan Doan, University of Melbourne A/Prof. Elizabeth Tynan, JCU
Chapter 2: Intellectual support  Financial support	Editorial assistance	Prof. Emma McBryde, JCU Dr Michael Meehan, JCU Prof. Lisa White, University of Oxford A/Prof. James Trauer, Monash University Dr Tan Doan, University of Melbourne A/Prof. Elizabeth Tynan, JCU  College of Medicine and Dentistry, JCU
Chapter 3: Intellectual support  Financial support	Editorial assistance	Prof. Emma McBryde, JCU Dr Oyelola Adegboye, JCU Dr Michael Meehan, JCU  College of Medicine and Dentistry, JCU
Chapter 4: Intellectual support	Editorial assistance	Prof. Emma McBryde, JCU Dr Michael Meehan, JCU Prof. Lisa White, University of Oxford Dr Adeshina Adekunle, JCU

Financial support		College of Medicine and Dentistry, JCU
Chapter 5: Intellectual support	Editorial assistance	Prof. Emma McBryde, JCU Dr Michael Meehan, JCU Prof. Lisa White, University of Oxford Dr Adeshina Adekunle, JCU
Chapter 6: Intellectual support	Editorial assistance	Prof. Emma McBryde, JCU Dr Michael Meehan, JCU Prof. Lisa White, University of Oxford Dr Adeshina Adekunle, JCU
Financial support		College of Medicine and Dentistry, JCU
Chapter 7: Intellectual support	Editorial assistance	Prof. Emma McBryde, JCU Dr Michael Meehan, JCU Dr Md. Abu Sayem, NTP
Financial support		College of Medicine and Dentistry, JCU
Chapter 8: Intellectual support	Editorial assistance	Prof. Emma McBryde, JCU Dr Michael Meehan, JCU Dr Tan Doan, University of Melbourne

## ABSTRACT

*Mycobacterium tuberculosis* (*Mtb*) kills more people each year than any other infectious disease, including HIV and malaria, despite substantial efforts to control it. Currently, multidrug-resistant (MDR) TB is emerging as the greatest threat to TB control globally. The world's highest TB burden occurs in the World Health Organization's (WHO) South-East Asian Region. Bangladesh is a lower-middle income country located in South Asia, with strong seasonal weather variation and ranks sixth among 22 high TB burden countries. The transmission dynamics and epidemiology of TB in the country are poorly understood. The aim of my research was to investigate the influence of weather variables and the transmission dynamics of drug-susceptible (DS) TB and multidrug-resistant (MDR) TB in Bangladesh. To achieve this aim, I conducted a time series analysis to explore the association between weather variables and TB epidemic. I also developed a mathematical model of the transmission dynamics of DS-TB and MDR-TB in Bangladesh and performed extensive formal analysis of the system properties and solutions. I also assessed specific intervention strategies to identify the most effective programs for achieving TB control in Bangladesh – an area of study that remains relatively neglected in the literature.

In a narrative literature review (Chapter 2), I discussed the emergence and establishment of DS-TB and MDR-TB along with the possibility of future epidemics of severe TB. Numerous structural risk factors can lead to an outbreak of TB disease. These risk factors include, but are not limited to, health system factors, environmental factors, host related factors and sociological factors. These factors are culturally sensitive, contributing to a worrisome problem in developing countries such as Bangladesh. TB impacts poor populations more because of a lack of health facilities and services, poor nutrition, and crowded housing, facilitating the spread of TB disease and worsening outcomes. As a consequence, TB continues to be the world's biggest infectious disease killer and disproportionately impacts developing countries such as Bangladesh.

From a generalized linear Poisson regression model (Chapter 3), developed using quarterly TB cases in three known endemic districts of North-East Bangladesh from 2007 to 2012, I found that TB risk increased with prolonged exposure to temperature and rainfall, and persisted at lag periods beyond 6 quarters. The association between humidity and TB is strong and immediate at low humidity, but the risk decreases with increasing lag. Using the optimum weather values corresponding to the lowest risk of infection, the risk of TB is highest at low temperature, low humidity and low rainfall. Measures of the risk attributable to weather variables revealed that TB cases attributed to humidity are higher than that of temperature and rainfall in each of the three districts. The results have relevance for the

Bangladesh National TB Control Program (NTP) and act as a practical reference for the early warning of TB cases.

In Chapter 4, I developed a two-strain Susceptible-Infected-Recovered (SIR) disease model. The first strain represents drug-susceptible (DS) and the other is drug-resistant (DR). In this analysis, I also modeled the emergence of drug resistance as a consequence of inadequate treatment, i.e. amplification. I performed a dynamical analysis of the resulting system and found that the model contains three equilibrium points: a disease-free equilibrium, a mono-existent disease-endemic equilibrium with respect to the DR strain and a co-existent disease-endemic equilibrium where both the DS and DR strains persist. I conducted a local stability analysis of the system equilibrium points using the Routh-Hurwitz conditions and a global stability analysis using appropriate Lyapunov functions. I also investigated the impact of amplification and treatment/recovery rates of both strains on the equilibrium prevalence of infection and found that if amplification and DS treatment/recovery rates increase then DR prevalence increases but DS prevalence declines. Further, if amplification and DR treatment/recovery rates increase then DR prevalence declines but DS prevalence increases. Following this, I performed a sensitivity analysis to investigate the model parameters that have the greatest influence on the prevalence.

In Chapter 5, I developed a parsimonious model structure capable of accurately reproducing observed TB epidemiology dynamics, particularly the prolonged latency period and the possibility of fast and slow progression to active TB. Similar to the model investigated in Chapter 4, I included an amplification pathway for individuals that acquire drug resistance during treatment. I performed a rigorous analytical analysis of the system properties and solutions to predict both the early- and late-time behaviour of the model. I again found resistance to drugs increases with increasing drug use, that is, active TB treatment results in a reduction of drug sensitive cases and an increase in DR-TB cases because of amplification. I also fitted the model to TB prevalence and notification data and performed a sensitivity analysis, finding that the contact rate of both strains had the largest influence on DS and DR-TB prevalence.

In Chapter 6, an extended version of mathematical two-strain TB model fitted to Bangladesh TB data to understand the transmission dynamics of DS-TB and MDR-TB. I performed a sensitivity analysis to identify the parameters with the greatest influence on the overall epidemic. I found that the transmission rate for DS and MDR-TB is the most important parameter. Different control strategies, including distancing, latent case finding, case holding, active case finding, and their combinations are investigated within the optimal control framework. Optimal control strategies are used for reducing the number of DS and MDR-TB patients with minimum intervention implementation costs. Results recommend that

the distancing control strategy is the most cost-effective single intervention that can be applied. My findings also recommended that enhancing active case finding instead of case holding together with distancing and latent case finding can significantly reduce the rate of spread of DS and MDR-TB in Bangladesh.

In Chapter 7, I developed four potential specific intervention scenarios in consultation with the local staff of the NTP in Bangladesh during the period from 2020 to 2035. These include increasing the detection proportion, DS and MDR-TB treatment rates and drug-susceptibility testing rate from baseline to explore the impact of each intervention on TB incidence and mortality. My findings suggest that the detection proportion is the most important intervention for decreasing DS and MDR-TB incidence and mortality in Bangladesh. However, focusing on the DS and MDR-TB treatment rate alone will not dramatically affect the decline in DS and MDR-TB incidence and mortality in the country. Varying more key interventions simultaneously is the most effective way to reduce the burden of DS and MDR-TB incidence and mortality in Bangladesh.

In summary, this thesis provides a better understanding of the changing epidemiology of DS-TB and emerging MDR-TB epidemics and will support future policy and planning of TB control efforts in Bangladesh. Finally, this flexible modelling (both transmission and economic) framework will be adaptable to other settings that are experiencing high burden of DS and MDR-TB.

## **KEYWORDS**

Mathematical modelling

Epidemic modelling

Infectious diseases

Epidemiology

Public Health

Tuberculosis

Stability analysis

Sensitivity analysis

Optimal control strategy

Economical modelling

Distributed lag models

Scenario analysis

# LIST OF PUBLICATIONS

## PUBLISHED

**Kuddus, M. A.,** Meehan, T. M., Sayem, A., McBryde, E. S. (2021). Scenario analysis for programmatic tuberculosis control in Bangladesh: A mathematical modelling study. *Scientific Reports*, 11(1), 4354.

**Kuddus, M. A.,** McBryde, E. S., Adekunle, I. A., White, J. L., Meehan, T. M. (2021). Mathematical analysis of a two-strain disease model with amplification. *Journal of Chaos, Soliton's & Fractals*, 143 (2021), 110594.

**Kuddus, M. A.,** Meehan, M. T., White, L. J., McBryde, E. S., & Adekunle, A. I. (2020). Modelling drug-resistant tuberculosis amplification rates and intervention strategies in Bangladesh. *PLOS ONE*, 15(7), e0236112.

**Kuddus, M. A.,** Tynan, E., McBryde, E. (2020). Urbanization: a problem for the rich and the poor? *Public Health Reviews*, 41(1), 1.

**Kuddus, M. A.,** McBryde, E. S., Adegboye, O. A. (2019). Delay effect and burden of weather-related tuberculosis cases in Rajshahi province, Bangladesh, 2007–2012. *Scientific Reports*, 9(1), 1-13.

## UNDER REVIEW

**Kuddus, M. A.,** McBryde, E. S., Adekunle, I. A., White, J. L., Meehan, T. M. (2021). Mathematical analysis of a two-strain tuberculosis model in Bangladesh. *Journal of Applied Mathematics and Computation*.

**Kuddus, M. A.,** Meehan, T. M., Doan, T., McBryde, E. S. (2021). The epidemiological presentation and management of tuberculosis: A literature review. *Antimicrobial Resistance & Infection Control*.

**Kuddus, M. A.,** Meehan, T. M., Doan, T., McBryde, E. S. (2021). Tuberculosis in different setting and opportunity for modelling: A review. *Current Infectious Diseases Reports*.

## OTHER PUBLICATIONS

### PUBLISHED

Corwin, A., Plipat, T., Phetsouvanh, R., Mayxay, M., Sangxayalath, P., Mai, L., Oum, S., **Kuddus, M. A.** (2021). The impact of preparedness in defying COVID-19 pandemic expectations in the lower mekong region: a case study. *American Journal of Tropical Medicine and Hygiene*, tpmd201499.

Rahman, A., **Kuddus, M. A.** (2021). Modelling the transmission dynamics of COVID-19 in six high burden countries. *Biomed Research International*. Accepted for publication.

Rahman, A., **Kuddus, M. A.** (2020). Cost-effective modelling of the transmission dynamics of malaria: A case study in Bangladesh. *Communications in Statistics: Case Studies, Data Analysis and Applications*, 1-17.

Saffary, T., Adegboye, O. A., Gayawan, E., Elfaki, F., **Kuddus, M. A.**, & Saffary, R. (2020). Analysis of COVID 19 cases' spatial dependence in US counties reveals health inequalities. *Frontiers in Public Health*, 8, 728.

### UNDER REVIEW

**Kuddus, M. A.**, Rahman A. (2021). Analysis of COVID-19 using a modified SLIR model with nonlinear incidence. *Results in Physics*.

**Kuddus, M. A.**, Rahman, A., (2021). Climate change and its impact on different types of transitions: A review. *Current Environmental Health Reports*.

**Kuddus, M. A.**, Rahman A. (2021). Modelling and analysis of human-mosquito malaria transmission dynamics in Bangladesh. *Mathematics and Computer in Simulation*.

**Kuddus, M. A.**, Mohiuddin, M., Rahman A. (2021). Mathematical analysis of a measles transmission dynamics model in Bangladesh with double dose vaccination. *Scientific Reports*.

Rahman, A., **Kuddus, M. A.**, Ryan, H., Demskoy, D., Bewong, M. (2021). A review of COVID-19 modelling strategies in three countries to develop a research framework for New South Wales, Australia. *Public Health Reviews*.

Rahman, A., **Kuddus, M. A.**, Ryan, H., Demskoy, D., Bewong, M. (2021). Modelling COVID-19 control strategies between metropolitan and rural health districts in New South Wales, Australia. *American Journal of Tropical Medicine and Hygiene*.

### IN PROGRESS

**Kuddus, M. A.**, McBryde, E. S., Adekunle, I. A., Meehan, T. M. (2021). Analysis and simulation of a two-strain disease model with nonlinear incidence.

**Kuddus, M. A.**, Mohiuddin, M., Alam, F., Rahman A. (2021). Scenario analysis for programmatic measles control in Bangladesh: a modelling study.

Mohiuddin, M., Alam, F., Rahman A., **Kuddus, M. A.** (2021). Mathematical analysis of COVID-19 transmission dynamics model in Bangladesh.

Hussain, M., Shimul, S., Faisal A. J., Hamid, S.A., Jabin, N., Sultana, N., **Kuddus, M. A.** (2021). Impact of alternative non-pharmaceutical interventions strategies for controlling COVID-19 outbreak in Bangladesh: a modelling study.

# COMMUNICATIONS

## ORAL COMMUNICATIONS

**Kuddus, M. A.,** Meehan, T. M., McBryde, E. S. (2019). Mathematical model and intervention strategies for controlling tuberculosis in Bangladesh, Policy relevant infectious disease simulation and mathematical modelling (PRISM) annual conference, November 2019.

**Kuddus, M. A.,** Meehan, T. M., McBryde, E. S. (2019). Mathematical analysis of a two-strain tuberculosis model in Bangladesh, My research rules, James Cook University, October 2019.

**Kuddus, M. A.,** McBryde, E. S., Adegboye, O. A. (2019). Delay effect and burden of weather-related tuberculosis cases in Rajshahi province, Bangladesh, 2007–2012. Applied Statistics and Policy Analysis conference, September 2019.

**Kuddus, M. A.,** Meehan, T. M., McBryde, E. S. (2017). Role of amplification in a TB model. TB research meeting, Australia Institute of Tropical Health and Medicine, James Cook University, Australia, September 2017.

**Kuddus, M. A.,** Meehan, T. M., McBryde, E. S. (2017). Role of amplification in a TB model. Infectious disease modelling, research and training, Mahidol University, Bangkok, Thailand, September 2017.

**Kuddus, M. A.,** Meehan, T. M., McBryde, E. S. (2017). A study on mathematical and economical modelling for transmission dynamics of tuberculosis (TB) in Bangladesh. Centre for Biodiscovery and Molecular Development of Therapeutics (CBMDT) and Center for Biosecurity of Tropical Infectious Diseases (CBTID) annual joint retreat, September 2017.

**Kuddus, M. A.,** Meehan, T. M., McBryde, E. S. (2017). Modelling the impact of novel tuberculosis treatments: from the microscopic to the global scale. Centre for Biodiscovery and Molecular Development of Therapeutics (CBMDT) and Center for Biosecurity of Tropical Infectious Diseases (CBTID) annual joint retreat, September 2017.

**Kuddus, M. A.,** Meehan, T. M., McBryde, E. S. (2017). Mathematical and cost-effective modelling for elimination of tuberculosis (TB) in Bangladesh. James Cook University Science Research Festival, September 2017.

**Kuddus, M. A.** (2017). Math's explains our world-epidemiology (workshop). Ayr State High School, Burdekin, Australia, August 2017.

**Kuddus, M. A.,** Meehan, T. M., McBryde, E. S. (2017). Modelling the impact of novel tuberculosis treatments: from the microscopic to the global scale. Policy relevant infectious disease simulation and mathematical modelling (PRISM) annual conference, August 2017.

**Kuddus, M. A.,** Meehan, T. M., McBryde, E. S. (2017). Epidemic models of tuberculosis in Bangladesh: mathematical and cost-effective analysis. Policy relevant infectious disease simulation and mathematical modelling (PRISM) annual conference, August 2017.

## POSTER PRESENTATIONS

**Kuddus, M. A.,** Meehan, T. M., McBryde, E. S. (2019). Mathematical analysis of a two-strain tuberculosis model in Bangladesh. Townsville Health Research Showcase, October 2019.

**Kuddus, M. A.,** Meehan, T. M., McBryde, E. S. (2018). Mathematical models of tuberculosis transmission in Bangladesh. PRISM international conference logistics and questions, Cairns, August 2018.

**Kuddus, M. A.,** Meehan, T. M., McBryde, E. S. (2017). A study on mathematical and economical modelling for transmission dynamics of tuberculosis (TB) in Bangladesh. Australasia Tropical Health conference, September 2017.

**Kuddus, M. A.,** Meehan, T. M., McBryde, E. S. (2017). A study on mathematical and economical modelling for transmission dynamics of tuberculosis (TB) in Bangladesh. James Cook University Science Research Festival, September 2017.

## SHORT COURSES

- Python programming language (James Cook University, Australia)
- Programming for everybody (Getting started with Python) (University of Michigan, USA)
- R programming (Johns Hopkins University, USA)
- Getting started with R and RStudio (James Cook University, Australia)
- Longitudinal and mixed model analysis (QCIF, Australia)
- Linear regression and modelling (Duke University, USA)
- Exploratory data analysis (Johns Hopkins University, USA)
- Bayesian statistics: from concept to data analysis (University of California, USA)
- Multiple regression analysis in public health (Johns Hopkins University, USA)
- Infectious disease modelling (PRISM - MAEMOD)
- Project management (e-Grad School, Australia)
- Public policy (e-Grad School, Australia)
- Research commercialisation (e-Grad School, Australia)
- Critical and creative thinking (e-Grad School, Australia)
- Skills for international postgraduates (SKIP) (James Cook University, Australia)
- Using R for data analysis and graphical presentation (James Cook University, Australia)
- An introduction to statistics using SPSS (James Cook University, Australia)
- Advanced statistics (SPSS) (James Cook University, Australia)
- Academic and thesis writing (James Cook University, Australia)
- Infection control training – COVID-19 (Department of Health, Australian Government)
- Infection prevention and control (IPC) for novel coronavirus (COVID-19) (World Health Organization)
- COVID-19: Operational planning guidelines and COVID-19 partner platform to support country preparedness and response (World Health Organization)
- Emerging respiratory viruses, including COVID-19: methods for detection, prevention, response and control (World Health Organization)
- Introduction to GO. Data – Field data collection, chains of transmission and contact follow-up (World Health Organization)
- All compulsory higher degree by research (HDR) JCU courses (James Cook University, Australia)

## LIST OF ABBREVIATIONS

BCG	: Bacille Calmette-Guerin
DOTS	: Directly Observed Treatment-Short Course
DS-TB	: Drug-susceptible Tuberculosis
DR-TB	: Drug-resistant Tuberculosis
HIV	: Human Immunodeficiency Virus
HIV/AIDS	: Human Immunodeficiency Virus/Acquired Immune Deficiency Syndrome
JCU	: James Cook University
IPT	: Isoniazid Preventive Therapy
LTBI	: Latent Tuberculosis Infection
MDR-TB	: Multidrug-Resistant Tuberculosis
NTP	: National TB Control Program (Bangladesh)
PMDT	: Programmatic Management of Multidrug-Resistant Tuberculosis
$R_0$	: Basic Reproduction Number
$R_{0s}$	: Basic Reproduction Number for Drug-Susceptible Tuberculosis
$R_{0r}$	: Basic Reproduction Number for Drug-resistant Tuberculosis
$R_{0m}$	: Basic Reproduction Number for Multidrug-Resistant Tuberculosis
SIR	: Susceptible-Infectious-Recovered
SIS	: Susceptible-Infectious-Susceptible
SLIR	: Susceptible-Latent-Infectious-Recovered
TB	: Tuberculosis
TST	: Tuberculin Skin Test
UN	: The United Nations
WHO	: World Health Organization
XDR-TB	: Extensively Drug-Resistant Tuberculosis

## TABLE OF CONTENTS

DECLARATION .....	iii
STATEMENT OF ACCESS.....	iv
DECLARATION ON ETHICS .....	v
ACKNOWLEDGEMENTS .....	vi
STATEMENT ON THE CONTRIBUTION OF OTHERS.....	vii
ABSTRACT.....	ix
KEYWORDS.....	xii
LIST OF PUBLICATIONS .....	xiii
OTHER PUBLICATIONS .....	xiv
COMMUNICATIONS .....	xv
SHORT COURSES .....	xvii
LIST OF ABBREVIATIONS.....	xviii
CHAPTER 1 .....	1
Introduction.....	1
1.1 Emergence of global and national problem .....	2
1.2 Aims of this thesis.....	4
1.3 Research objectives.....	5
1.4 Thesis structure .....	8
References.....	10
CHAPTER 2 .....	11
Background.....	11
Summary of this chapter .....	12
2.1 An overview of tuberculosis disease and its mode of transmission.....	13
2.2 The emergence of drug resistance.....	14
2.3 Current global statistics of TB and its risk factors .....	16
2.4 TB treatment and control strategies .....	21
2.5 Quantitative tools available for the control of TB .....	22
2.6 Health economics of TB .....	23
2.7 TB in Bangladesh and its current situation .....	24
2.8 Mathematical modelling of TB: An overview .....	27
2.8.1 Model diagram and equations .....	28
2.8.2 Basic reproduction number .....	30
2.8.3 Stability analysis of this system .....	34
2.8.4 TB model extensions.....	38

2.8.5 Multidrug-resistant (MDR) and extensively drug-resistant (XDR) TB models .....	47
2.8.6 Cost-effectiveness TB models .....	49
2.9 Conclusion .....	51
References.....	53
CHAPTER 3 .....	63
Delay effect and burden of weather-related tuberculosis cases in Rajshahi province, Bangladesh, 2007-2012 .....	63
Abstract.....	64
3.1 Introduction.....	65
3.2 Methods and material.....	66
3.2.1 Data sources .....	66
3.2.2 Statistical analysis .....	68
3.3 Results.....	72
3.3.1 Initial sequences of TB cases and weather factors.....	72
3.3.2 Association between TB and weather factors .....	72
3.3.3 Weather related burden of TB.....	78
3.4 Discussion .....	80
References.....	83
Supplementary materials.....	87
CHAPTER 4 .....	98
Mathematical analysis of a two-strain disease model with amplification.....	98
Abstract.....	99
4.1 Introduction.....	100
4.2 Model description and analysis.....	101
4.2.1 Model equations.....	101
4.2.2 Basic reproduction number .....	103
4.2.3 Strain replacement .....	105
4.2.4 System properties.....	105
4.3 Stability analysis .....	106
4.3.1 Infection-free equilibrium .....	106
4.3.2 Mono-existent endemic equilibrium .....	108
4.3.3 Co-existent endemic equilibrium .....	110
4.4 Sensitivity analysis.....	112
4.5 Numerical simulations .....	114
4.6 Discussion and conclusion.....	116
References.....	119
CHAPTER 5 .....	121
Mathematical analysis of a two-strain tuberculosis model in Bangladesh.....	121

Abstract.....	122
5.1 Introduction.....	123
5.2 Model description .....	124
5.2.1 Model equations.....	124
5.2.2 Basic reproduction number .....	127
5.2.3 System properties.....	129
5.3 Stability analysis .....	130
5.3.1 Disease-free equilibrium .....	130
5.3.2 Mono-existent endemic equilibrium .....	133
5.4 Estimation of model parameters .....	135
5.5 Sensitivity analysis.....	137
5.6 Numerical simulations .....	140
5.7 Discussion and conclusion.....	143
References.....	144
CHAPTER 6 .....	146
Modelling drug-resistant tuberculosis amplification rates and intervention strategies in Bangladesh .....	146
Abstract.....	147
6.1 Introduction.....	148
6.2 Material and methods.....	149
6.2.1 Bangladesh TB epidemiological data.....	149
6.2.2 Model description .....	150
6.2.3 Model calibration and control strategies .....	152
6.3 Results.....	154
6.3.1 Bangladesh TB prevalence rates .....	154
6.3.2 TB dynamical process in Bangladesh .....	155
6.3.3 Sensitivity analysis of model parameters.....	158
6.3.4 Optimal control strategies and cost-effectiveness analysis.....	161
6.4 Discussion and conclusion.....	175
References.....	178
Supplementary materials.....	180
CHAPTER 7 .....	219
Scenario analysis for programmatic tuberculosis control in Bangladesh: A mathematical modelling study.....	219
Abstract.....	220
7.1 Introduction.....	221
7.2 Model description .....	224
7.2.1 Basic reproduction numbers.....	226

7.3 Estimation of model parameters .....	229
7.4 Sensitivity analysis.....	231
7.5 Scenario development and analysis .....	234
7.6 Discussion and conclusion .....	243
References.....	245
CHAPTER 8 .....	248
Discussion and future directions .....	248
8.1 Discussion of main findings.....	249
8.2 Limitations .....	253
8.3 Significance and implications .....	254
8.4 Future directions .....	254
8.5 Conclusion .....	255
References.....	256

## List of Figures

Figure 2. 1 TB transmission cycle from person to person through the air.....	13
Figure 2. 2 The left side represents latent TB and the right side active TB.....	14
Figure 2. 3 Contributing factors related to TB disease outbreaks and their impact.....	21
Figure 2. 4 Nationwide number of TB case in Bangladesh from 2000 to 2019.....	26
Figure 2. 5 Flow Chart of the compartmental SEIR mathematical model showing the four states and the transition in and out of each state.....	29
Figure 2. 6 Numerical simulations of the model outcomes. ....	34
Figure 3. 1 Quarterly TB cases (black) during the study period, 2007-2012 with average (a) Temperature, (b) Humidity, and (c) Rainfall for the three districts (red). ....	67
Figure 3. 2 Exposure-lag-response association in the three districts. Left panel: Three dimensional association; Middle panel: Rainfall-TB association Right panel: Lag-TB association.....	73
Figure 3. 3 Exposure-lag-response association in the three districts. Left panel: Three dimensional association; Middle panel: Temperature-TB association Right panel: Lag-TB association. ....	74
Figure 3. 4 Exposure-lag-response association in the three districts. Left panel: Three dimensional association. Middle panel: Humidity-TB association. Right panel: Lag-TB association. ....	75
Figure 4. 1 Flow chart of the two-strain SIR model showing the four infection states, and the transition rates in and out of each state. ....	102
Figure 4. 2 PRCC values depicting the sensitivities of the model output $I_s$ with respect to the input parameters $\beta_s, \omega_s, \phi_s, \beta_m, \omega_m, \phi_m$ and $\rho$ , when $R_{0s} > \max[R_{0m}, 1]$ (i.e. co-existent endemic equilibrium $E^\dagger$ ).....	113
Figure 4. 3 PRCC values depicting the sensitivities of the model output $I_m$ with respect to the input parameters $\beta_s, \omega_s, \phi_s, \beta_m, \omega_m, \phi_m$ and $\rho$ , when $R_{0s} > \max[R_{0m}, 1]$ (i.e. co-existent endemic equilibrium $E^\dagger$ ).....	113
Figure 4. 4 PRCC values depicting the sensitivities of the model output $I_s + I_m$ with respect to the estimated parameters $\beta_s, \omega_s, \phi_s, \beta_m, \omega_m, \phi_m$ and $\rho$ , $R_{0s} > \max[R_{0m}, 1]$ (i.e. co-existent endemic equilibrium $E^\dagger$ ).....	113
Figure 4. 5 PRCC values depicting the sensitivities of the model output $I_m$ with respect to the estimated parameters $\beta_s, \omega_s, \phi_s, \beta_m, \omega_m, \phi_m$ and $\rho$ , when $R_{0m} > R_{0s}$ and $R_{0m} > 1$ (i.e. mono-existent endemic equilibrium $E^\#$ ). ....	113
Figure 4. 6 Co-existent endemic equilibrium: $R_{0s} > \max[R_{0m}, 1]$ . In this case both the drug-susceptible infection and drug-resistant infection persist in the population (black dot). All remaining parameter values assume their baseline values given in Table 4.1. ....	116

Figure 4. 7 Effect of amplification ( $\rho$ ) on the drug-susceptible ( $I_s$ ) prevalence and drug-resistant prevalence ( $I_m$ ). All remaining parameter values assume their baseline values given in Table 4.1. .... 116

Figure 4. 8 Effect of drug-susceptible treatment/recovery rate ( $\omega_s$ ) on the equilibrium level of total prevalence when both infectious rates ( $\beta_s, \beta_m$ ) are fixed. All remaining parameter values assume their baseline values given in Table 4.1. .... 116

Figure 4. 9 Effect of drug-susceptible treatment/recovery rate ( $\omega_s$ ) on the equilibrium level of the drug-resistant strain when both infectious rates ( $\beta_s, \beta_m$ ) are fixed. All remaining parameter values assume their baseline values given in Table 4.1. .... 116

Figure 5. 1 Flow chart of the TB compartmental mathematical model showing six states and the transitions in and out of each state in a closed population (no migration). .... 126

Figure 5. 2 Reported prevalence data (red dot) and the corresponding best fit (blue solid curve) of ( $I_s + I_r$ ). All remaining parameter values assume their baseline values given in Table 5.1.. 136

Figure 5. 3 Reported notification data (red dot) and the corresponding best fit (blue solid curve) of ( $\tau_s I_s + \tau_r I_r$ ). All remaining parameter values assume their baseline values given in Table 5.1. .... 136

Figure 5. 4 PRCC values depicting the sensitivities of the model output  $I_s$  with respect to the estimated parameters  $\beta_s, \alpha_s, \omega_s, \phi_s, \tau_s, \beta_r, \alpha_r, \omega_r, \phi_r, \tau_r$  and  $\rho$ , when  $R_{0s} > \max[R_{0r}, 1]$  (i.e. co-existent endemic equilibrium  $E^\dagger$ ). .... 139

Figure 5. 5 PRCC values depicting the sensitivities of the model output  $I_r$  with respect to the estimated parameters  $\beta_s, \alpha_s, \omega_s, \phi_s, \tau_s, \beta_r, \alpha_r, \omega_r, \phi_r, \tau_r$  and  $\rho$ , when  $R_{0s} > R_{0r}$  and  $R_{0s} > 1$  (i.e. co-existent endemic equilibrium  $E^\dagger$ ). .... 139

Figure 5. 6 PRCC values depicting the sensitivities of the model output  $I_s + I_r$  with respect to the estimated parameters  $\beta_s, \alpha_s, \omega_s, \phi_s, \tau_s, \beta_r, \alpha_r, \omega_r, \phi_r, \tau_r$  and  $\rho$ , when  $R_{0s} > \max[R_{0r}, 1]$  (i.e. co-existent endemic equilibrium  $E^\dagger$ ). .... 139

Figure 5. 7 PRCC values depicting the sensitivities of the model output  $I_r$  with respect to the estimated parameters  $\beta_s, \alpha_s, \omega_s, \phi_s, \tau_s, \beta_r, \alpha_r, \omega_r, \phi_r, \tau_r$  and  $\rho$ , when  $R_{0r} > R_{0s}$  and  $R_{0r} > 1$  (i.e. mono-existent endemic equilibrium  $E^\#$ ). .... 139

Figure 5. 8 Disease-free equilibrium:  $\max [R_{0s}, R_{0r}] \leq 1$ . The disease- free equilibrium is asymptotically stable, which means that the disease naturally dies out. Here we consider  $R_{0s} = 0.4$  and  $R_{0r} = 0.3$ . .... 142

Figure 5. 9 Mono-existent equilibrium:  $R_{0r} > \max[R_{0s}, 1]$ . In this case DS-TB dies out but the DR-TB persist in the population. Here we consider  $R_{0s} = 0.4$  and  $R_{0r} = 3$ . .... 142

Figure 5. 10 Co-existent equilibrium:  $R_{0s} > \max[R_{0r}, 1]$ . In this both DS-TB and DR-TB persist in the population. Here we consider  $R_{0s} = 5$  and  $R_{0r} = 3$ . .... 142

Figure 5. 11 Role of amplification. For  $R_{0r} < R_{0s}$ , we have co-existence. For  $R_{0r} > R_{0s}$ , DS-TB dies out but DR-TB increases with increasing  $R_{0r}$ . Notice, even for  $R_{0r} < R_{0s}$ , the DR-TB prevalence can exceed the DS-TB prevalence. All remaining parameter values assume their baseline values given in Table 5.1. .... 142

Figure 5. 12 . Effect of DS-TB treatment rate ( $\tau_s$ ) on equilibrium level of total prevalence when both infectious rates ( $\beta_s, \beta_r$ ) are fixed. All remaining parameter values assume their baseline values given in Table 5.1. .... 143

Figure 5. 13 Effect of DS-TB treatment rate ( $\tau_s$ ) on equilibrium level of DR-TB prevalence when both infectious rates ( $\beta_s, \beta_r$ ) are fixed. All remaining parameter values assume their baseline values given in Table 5.1. .... 143

Figure 6. 1 Schematic diagram of two-strain TB transmission model for Bangladesh TB setting..... 151

Figure 6. 2 Linear fit to Bangladesh TB prevalence data. .... 155

Figure 6. 3 The impacts of the strain specific basic reproduction number on the long-time dynamics of the TB model (6.2)..... 156

Figure 6. 4 A fit of model 3 to the Bangladesh TB cumulative incidence: (A) DS-TB and (B) MDR-TB. .... 157

Figure 6. 5 PRCC values depicting the sensitivities of the model output: (A)  $R_{0s}$  with respect to the estimated parameters  $\beta_s, \alpha_s, \delta_s, \omega_s, \phi_s$ , and  $\tau_s$ , and (B)  $R_{0m}$  with respect to the estimated parameters  $\beta_m, \alpha_m, \delta_m, \omega_m, \phi_m$ , and  $\tau_m$ . .... 159

Figure 6. 6 PRCC values depicting the sensitivities of the model DS, MDR and total TB prevalences. .... 160

Figure 6. 7 The single optimal control strategy: (A) The optimal distancing control strategy. (B) The benefits of using only distancing control strategy..... 164

Figure 6. 8 The double optimal control strategy: (A) The Distancing and latent case finding control strategy. (B) The benefits of using distancing and latent case finding control strategy..... 165

Figure 6. 9 The triple optimal control strategy: (A) The Distancing, latent case finding and case holding control strategy. (B) The benefits of using distancing, latent case finding and case holding control strategy. .... 166

Figure 6. 10 (A) The optimal quadruple control strategy; and (B) its effect on TB prevalence in Bangladesh..... 167

Figure 6. 11 Effects of varying the weighted cost ( $B_1$ ) on the distancing control ( $u_1$ ) (left Figure) and the objective functional (right Figure). .... 168

Figure 6. 12 The corresponding state variables associated with varying the weighted cost ( $B_1$ ) while applying the distancing control ( $u_1$ ). The state variables with and without controls are plotted by gray/blue dotted and black lines respectively. .... 169

Figure 6. 13 Combination of distancing control u1 and latent case finding control (u2) strategy, and considering distancing control u1 strategy as a function of time and weighted cost (B1). The weighted cost (B2) is set to the threshold values $B2=10^5=10^6=10^7$ . .....	170
Figure 6. 14 Combination of distancing control u1 and latent case finding control (u2) strategy, and considering latent case finding control u2 strategy as a function of time and weighted cost (B1). The weighted cost (B2) determined by three threshold values $B2=10^5=10^6=10^7$ . .....	170
Figure 6. 15 The corresponding state variables of the combination of distancing control (u1) and latent case finding control (u2) strategy and considering the weighted cost B1 is varied and $B2=10^5=10^6=10^7$ . The state variables with and without controls are plotted by grays/blue dotted and black lines respectively. ....	171
Figure 6. 16 Combination of distancing control u1 and latent case finding control (u2) strategy, and considering latent case finding u2 strategy as a function of time and weighted cost (B2). The weighted cost (B1) determined by three threshold values $B1=10^5=10^6=10^7$ . .....	172
Figure 6. 17 Combination of distancing control u1 and latent case finding (u2) control strategy, and considering distancing control u1 strategy as a function of time and weighted cost (B2). The weighted cost (B1) determined by three threshold values $B1=10^5=10^6=10^7$ . .....	173
Figure 6. 18 The corresponding state variables of the combination of distancing control (u1) and latent case finding control (u2) strategy and considering the weighted cost B2 is varied and $B1=10^5=10^6=10^7$ . The state variables with and without controls are plotted by grays/blue dotted and black lines respectively. ....	174
Figure 7. 1 Schematic diagram of TB model for Bangladesh TB setting. ....	226
Figure 7. 2 The effects of the strain-specific basic reproduction number on the dynamics of model (7.2). ....	229
Figure 7. 3 Reported Bangladesh TB annual incidence data as estimated The WHO (red dots) and the corresponding best fit (blue solid curve): (left) drug-susceptible (DS) TB and (right) multidrug-resistant (MDR) TB. ....	230
Figure 7. 4 PRCC values depicting the sensitivity of the drug-susceptible basic reproduction number $R_{0s}$ with respect to the parameters $\beta, \alpha, \phi, \delta, \gamma_s, \tau_s, \rho$ and $\eta_s$ . ....	232
Figure 7. 5 PRCC values depicting the sensitivity of the drug-resistant basic reproduction number $R_{0m}$ with respect to the parameters $\beta, \alpha, \phi, \delta, \gamma_m, \tau_m, \kappa, \eta_m$ and $c$ . ....	233
Figure 7. 6 Impact of the four single intervention strategies on TB burden. ....	237
Figure 7. 7 Impact of the four single intervention strategies on TB mortality. ....	238
Figure 7. 8 Combination intervention strategy and its effect on (A) DS-TB and (B) MDR-TB annual incidence cases in Bangladesh. ....	241

Figure 7. 9 Combination intervention strategy and its effect on (A) DS-TB and (B) MDR-TB annual mortality in Bangladesh. .... 242

## List of Table

Table 3. 1 Relative risks (with 95% eCI) of incidence at specific exposure-lag values. ....	77
Table 3. 2 Attributable fraction based on exponential covariance structure.....	79
Table 4. 1 Description of model parameters .....	114
Table 5. 1 Depiction and estimation of parameters.....	136
Table 5. 2 Sensitivity indices to parameters for the model (5.2)-(5.7) .....	140
Table 6. 1 Parameter description and estimates for Bangladesh TB model (6.2). ....	153
Table 6. 2 Fitting results .....	157
Table 6. 3 Sensitivity indices to parameters for the model (6.2) .....	161
Table 6. 4 Incremental cost-effective ratio of single control strategy.....	164
Table 6. 5 Incremental cost-effective ratio of coupled control strategy.....	165
Table 6. 6 Incremental cost-effectiveness ratio of each triple control strategy.....	166
Table 6. 7 Selecting best control strategy .....	167
Table 7. 1 List of parameters, symbols, plausible values, units and references.....	230
Table 7. 2 Sensitivity indices to parameters for the model (7.2). ....	233
Table 7. 3 Hypothetical single intervention strategy implemented in our proposed model of DS and MDR-TB control in Bangladesh, for the period 2020 – 2035. ....	238
Table 7. 4 Hypothetical combination intervention strategy implemented in our proposed model of DS and MDR-TB control in Bangladesh, for the period 2020 – 2035.....	242

# **CHAPTER 1**

## **Introduction**

## 1.1 Emergence of global and national problem

Tuberculosis (TB) is an airborne infectious disease that causes an estimated 1.2 million deaths worldwide each year [1]. *Mycobacterium tuberculosis (Mtb)* is the airborne pathogen transmitted from a diseased person to healthy person through expulsion of droplets from the infectious person and inhalation of droplets by the susceptible person when they come into contact each other. It is noted that a single inhalation or very short duration of contact may not lead to infection. Rather, it usually requires frequent or prolonged contact with an infectious person (hence household contacts or close contacts are most at risk) [1]. Once infected, the individual will first undergo a period without visible clinical symptoms, called latent TB infection (LTBI). The latent period is the timespan from the point of infection to the beginning of the state of infectiousness, which may last for weeks, months or the entire lifetime of the infected individual. The lifetime risk of progression to active TB for a person with LTBI has been estimated to be around 5-15%, depending on the age at infection [2].

In 2018, the World Health Organisation (WHO) estimated that 1.2 million people died from TB, and that an additional 10.0 million people became newly infected. Most of the new cases in 2018 occurred in Asia (44%) and Africa (24%) and 87% of TB deaths occurred in low- and middle-income countries [1]. The highest burden of TB is not surprisingly in regions where seasonal weather varies markedly and health systems are weak. For example, the incidence of TB has been shown to be highest during summer, thus, it was hypothesized that the disease infection may have been acquired during winter months. This could be attributed to reduction in vitamin D level in the winter season [3-7], winter indoor crowding activities [8, 9] and seasonal variation in immune function [10, 11].

In 2015, the WHO recognised 22 high-burden countries according to their actual number of TB cases [12]. Among these is Bangladesh, a country where poverty, high population density and malnutrition are commonplace, creating a favourable environment for TB outbreaks. Furthermore, TB treatment compliance is poor in Bangladesh – presumably as a result of the extensive period of therapy – leading to a rise in the number of multidrug-resistant (MDR) TB cases [13]. MDR-TB is defined as TB that is resistant to isoniazid and rifampicin (the two most effective and commonly used first-line drugs), with or without resistance to additional first-line drugs. There are two major ways of developing MDR-TB: one termed amplification, the other primary transmission; the latter term referring to MDR being passed directly from an MDR-TB infected person. Amplification refers to the change from DS-TB to MDR-TB in the same person through naturally-occurring mutations and the selection pressure of antibiotics (i.e. if a DS-TB patient has partial resistance or is inadequately treated with first line anti-TB drugs, sequential resistance can occur. Thus it is often called amplifier effect of chemotherapy and is in effect an iatrogenic phenomenon) [13].

Each year it is estimated that 70,000 people die of TB and 300,000 new cases arise in Bangladesh [14]. In 2014, the case notification rates per 100,000 population were 68 and 122 for new smear-positive cases (i.e. cases that are usually more infectious and have a higher mortality) and all forms of TB cases, respectively. In the same year, the number of all types of TB cases had increased due to increased migration to and from endemic countries – an alarming hypothesis given the high TB burden in neighbouring countries such as India and China [13].

In light of these alarming statistics, and similar figures emanating from regions all over the globe, in 2015 the WHO upgraded their Stop TB Strategy to the End TB Strategy, with the goal of eradicating TB from the human population (to reduce TB mortality by 95% and to cut incidence by 90%) by 2050 through improved case finding and treatment success rates. In order to achieve the global End TB targets of achieving at least 70% case finding and 85% treatment success, numerous strategies are used to control TB outbreaks at the national and global levels. Programmatic management of drug-resistant TB (PMDT) is one of the most effective strategies for the control and prevention of drug-resistant (DR) TB. PMDT activities include proper management of contacts by ensuring that optimal treatment, a reliable drug supply and adequate health facilities are available [15]. Among these strategies, Directly Observed Treatment-Short Course (DOTS) is a very important component in the internationally recommended policy package for TB control. During DOTS a qualified practitioner observes the patient ingesting their medication, which results in a demonstrable improvement in treatment rates and patient outcomes [16].

Prompt treatment and cure of infectious cases of TB cuts the chain of transmission of TB infection at the community level. Therefore, rapid identification of presumptive TB cases, rapid diagnosis, prompt commencement of treatment and successful completion of treatment are the most effective ways of eliminating TB [16]. Whilst treatment of DS-TB is relatively straightforward: combination therapy (isoniazid and rifampicin being the backbone of a four-drug regimen) taken for six months; treatment of DR-TB is more lengthy, e.g. treatment for MDR-TB takes approximately nine to twenty four months and typically incorporates a combination of both first- and second-line drugs. Moreover, DR-TB treatment regimens are also more toxic, have a higher cost of diagnosis and patients typically suffer higher mortality and failure rates [16].

Progress in TB control is constrained by the lack of effective new "tools" (diagnostics, drugs and vaccines). The lack of effective tools leads to the increase of new cases of DS-TB as well as MDR-TB. Many of the existing tools available for TB control are old and insufficient to address current TB epidemics – as evidenced by the 600,000 new cases of rifampicin resistant TB (RR-TB), of which 490,000 also met criteria for MDR-TB [16]. TB control programs in resource-poor countries have few

alternatives but to use a method of diagnosing the disease (sputum smear microscopy) that is 125 years old and detects only half of the cases [16].

Improvements in diagnostics and treatments are particularly needed in countries like Bangladesh, which is resource-poor and has a high TB burden. The only vaccine available (BCG) is effective in protecting children against severe forms of TB, but provides little protection in adults against developing the infectious form of TB [13]. Therefore, new treatment regimens are urgently needed. Current treatment regimens for DS-TB usually take approximately six months and for MDR-TB usually take approximately nine months in Bangladesh. The impact of these current treatment regimens need to be evaluated to investigate which one is optimal to a given scenario. While there are several randomized control trials (RCTs) for improved therapies with shorter durations and greater treatment success rates currently underway, these trials may take many years to complete, may be unable to ascertain the impact of more than one activity at a time and are extremely expensive [17]. Mathematical models offer an effective way to include more than one activity together at a time to investigate treatment efficacy and cost effectiveness [9, 18-22].

Statistics show that TB is one of the most pressing public health problems in Bangladesh [16]. However, the transmission dynamics and epidemiology of TB in Bangladesh remain poorly understood and no novel TB treatment therapies are in development. This means that right now there is an opportunity to develop a mathematical modelling framework for TB control efforts in Bangladesh. If delayed, the opportunity to identify the leading causes of DS-TB and MDR-TB epidemics will be lost. To my knowledge, no previous TB mathematical model structures exist for this country. Furthermore, no study has investigated the cost effectiveness of different TB intervention strategies specific to Bangladesh in order to identify the optimal approach given the limited resources.

## **1.2 Aims of this thesis**

The first aim of the thesis is to investigate the impact of weather variables on the TB epidemic over the period 2007 to 2012 in Bangladesh. I presented time series analysis using datasets including TB surveillance data aggregated at the district level and meteorological data recorded from 35 monitoring stations across the country to analyse the relationships between weather variables and the number of TB cases. The second aim of the thesis was to develop a mathematical model of the transmission dynamics of DS-TB and MDR-TB in Bangladesh and perform a rigorous analytical analysis of the system properties and solutions. I assessed specific intervention strategies to identify the most effective ways to control TB epidemics in this country.

### 1.3 Research objectives

The key objective of this project was to develop robust mathematical models that can be used to simulate the epidemic trajectory of TB in Bangladesh. Furthermore, economic models will be integrated to assess the efficacy, durability and cost-effectiveness of combinations of novel therapies.

Specific objectives are as follows:

**Objective 1:** To explore the association between weather variables and the number of TB cases in Rajshahi province, Bangladesh and investigate the risk of TB attributable to weather.

**Objective 2:** To investigate the dynamics of a two-strain disease model with amplification and explore the impact of poor quality treatment.

**Objective 3:** To investigate the dynamics of DS and DR-TB in Bangladesh and identify the most important parameters.

**Objective 4:** To develop an accurate economic forecasting model and identify the most cost-effective intervention strategies for reducing the burden of DS and MDR-TB in Bangladesh (and beyond).

**Objective 5:** To explore the TB dynamics in Bangladesh through different specific intervention scenarios.

I address each of these research objectives through published papers included as thesis chapters, as outlined below.

***Objective 1: To explore the association between weather variables and the number of TB cases in Rajshahi province, Bangladesh and investigate the risk of TB attributable to weather.***

In this chapter, I analyzed the number of TB cases from 2007 to 2012 using data sourced from the National TB Control Program (NTP) in Rajshahi province, Bangladesh. Weather variables including the maximum and minimum temperature, rainfall and relative humidity from 35 weather stations across Bangladesh were obtained from the climate division in Bangladesh as well as the National Oceanic and Atmospheric Administration (NOAA), and National Centers for Environmental Information (NCEI). I used generalised linear Poisson regression models to investigate the association between weather factors and TB cases reported to the Bangladesh NTP between 2007 and 2012 in three known endemic districts of North-East Bangladesh. The results highlight the high linearity of temporal lagged effects and magnitude of TB burden attributable to temperature, humidity, and rainfall. The results can hopefully advise the Bangladesh NTP and act as a practical reference for the early warning of TB cases particularly in the setting of extreme weather events or persistent weather changes.

***Objective 2: To investigate the dynamics of a two-strain disease model with amplification and explore the impact of poor quality treatment.***

I investigated a two-strain disease model (which was not disease specific) with amplification to simulate the prevalence of DS and DR disease strains. I modeled the emergence of drug resistance as a consequence of inadequate treatment, i.e. amplification. In this case, individuals infected with the DS strain acquire drug-resistant infection such that the strains are coupled. I perform a dynamical analysis of the resulting system and find that the model contains three equilibrium points (a solution to differential system of equations that does not change with time): a disease-free equilibrium; a mono-existent disease-endemic equilibrium in which only the DR strain exists; and a co-existent disease-endemic equilibrium where both the DS and DR strains persist. I conducted a local stability analysis of the system equilibrium points using the Routh-Hurwitz conditions and a global stability analysis using appropriate Lyapunov functions. Sensitivity analysis was used to identify the most important model parameters through the partial rank correlation coefficient (PRCC) method. I found that the contact rate of both strains had the largest influence on prevalence. I also investigated the impact of amplification and treatment/recovery rates of both strains on the equilibrium prevalence of infection; my results show that the longer the DS strain takes to recover, the more likely is coexistence and the higher the amplification rate, and longer the treatment process, the greater the relative abundance of resistant infections. This mechanism, I postulate, explains the relationship between poor quality treatment or incomplete therapy of infectious diseases and emergence of drug resistance.

***Objective 3: To investigate the dynamics of DS and DR-TB in Bangladesh and identify the most important parameters.***

In this component of the thesis, I developed a mathematical model of TB transmission dynamics over time. Taking advice from the recent review by [32] I selected the most parsimonious model structure capable of accurately reproducing observed TB epidemiology dynamics, particularly the prolonged latency period and the possibility of fast and slow progression to active TB. Then, I extended this model to incorporate two co-circulating TB strains: a DS-TB strain; and a DR-TB strain. An important feature of this model is the coupling between the two-strain representing the flow of infected individuals who acquire resistance during treatment.

I then performed a rigorous analytical analysis of the system properties and solutions to predict both the early- and late-time behaviour of the model. For each, I used the next generation matrix method to determine analytic expressions for the basic reproduction number,  $R_0$  of the different TB strains, where

$R_0$  is the expected number of secondary cases created by a single infectious case introduced into a totally susceptible population.  $R_0$  is often an important determinant of the system dynamics: when  $R_0 > 1$  an epidemic occurs (early-time behaviour) and the system settles towards an endemic state (late-time behaviour). The asymptotic behaviour of the system is predicted using the next-generation method and validated through stability analysis techniques such as the indirect Lyapunov method (i.e. linearisation).

To supplement and validate the analytical analysis, I used numerical techniques to solve the system equations and determine the epidemic trajectory for a range of possible parameter values and initial conditions.

Following this, I performed a sensitivity analysis to investigate the parameters that possess the greatest influence on the model outputs. In the first instance I obtained these parameters directly from inspection of the analytical expressions for  $R_0$ . I then performed a numerical analysis using the partial rank correlation coefficient technique to identify the most important model parameters. This analysis, performed in Matlab, provided information on the quantitative relationship between parameters and model outcomes, particularly over time. After completing my analysis of the system properties I fitted my model to the Bangladesh TB prevalence and notification data using least squares optimisation method (implemented in Matlab). I then compared my model outputs (e.g. TB prevalence and notification data) for supporting future policy and planning of TB control efforts in Bangladesh.

***Objective 4: To develop an accurate economic forecasting model and identify the most cost-effective intervention strategies for reducing the burden of DS and MDR-TB in Bangladesh (and beyond).***

In this component of the thesis, I considered a two-strain TB mathematical model that is fitted to DS- and MDR-TB incidence data to understand the transmission dynamics of TB in Bangladesh. Different control strategies including distancing, latent case finding, case holding, active case finding, and their combinations are investigated within the optimal control framework. Optimal control strategies are used for reducing the number of DS and MDR-TB patients with minimum intervention implementation costs. Results suggest that enhancing active case finding instead of case holding together with distancing and latent case finding is the most significant for reducing the spread of DS and MDR-TB in Bangladesh. This study provides an understanding of four different types of control strategies and will be presented to the NTP to inform their plan for controlling TB in Bangladesh.

***Objective 5: To explore the TB dynamics in Bangladesh through different specific intervention scenarios.***

In this study, I presented a two-strain mathematical modelling framework (modified version) to explore the dynamics of DS and MDR-TB in Bangladesh. Four hypothetical scenarios over the period from 2020 to 2035 were developed with the help of local staff. During this time, I incorporated four specific intervention strategies including improved detection proportion (the number of notified cases divided by the number of estimated incident cases for that year, expressed as a percentage), DS and MDR-TB treatment rates and drug-susceptibility testing rate to explore the impact of each intervention on DS and MDR-TB incidence and mortality. The results show that the scenario that combines improved detection proportion, drug-susceptibility testing, and DS and MDR-TB treatment is the most effective at rapidly reducing DS and MDR-TB incidence and mortality in Bangladesh. Alternative scenarios can be adopted to curb TB depending on the availability of resources and policymakers' decisions. My findings suggest that focusing on a single intervention including increasing the detection proportion turned out to be the most impactful strategy on the reduction of DS and MDR-TB incidence and mortality in Bangladesh but combine more interventions simultaneously are the most effective in decreasing the burden of DS and MDR-TB, which may help TB elimination policies and efforts and enable more effective control strategies in Bangladesh.

#### **1.4 Thesis structure**

This thesis is based on five published papers and three manuscripts under review addressing research objectives concerning the mathematical modelling and TB epidemiology in Bangladesh, along with background, discussion, and conclusions chapters. All papers were prepared during my doctoral candidature and reproduced with the permission of the publishing company and co-authors. The authors' contributions are detailed in the Appendix.

**Chapter 2** provides a summary of the epidemiology of TB globally and in Bangladesh and also provides background information on previous studies of mathematical modelling and TB. Further, cost-effectiveness modelling approaches are also provided at the end of this chapter.

In the paper presented in **Chapter 3**, I investigated the delay effect of weather variables on TB occurrences and estimate the burden of the disease that can be attributed to weather factors. Here, I used generalized linear Poisson regression models to investigate the association between weather factors and TB cases reported to the Bangladesh NTP between 2007 and 2012 in three known endemic districts of North-East Bangladesh.

In **Chapter 4**, I presented a paper regarding the disease unspecified two-strain model with amplification to simulate the prevalence of DS and DR disease strains. Here, I modeled the emergence of drug

resistance in, assuming it occurs in a fraction of treated cases (reflecting the assumption that a proportion of treatment courses are inadequate), i.e. amplification. I performed a dynamical analysis of the resulting system properties and solution coupled with numerical simulations, stability, and sensitivity analysis.

In the paper presented in **Chapter 5**, I developed a two-strain TB model of DS and DR strains and performed an analysis of the system properties and solutions. Here, I also performed the stability and sensitivity analysis through appropriate Lyapunov functions and partial rank correlation method respectively. Further, I investigated the impact of amplification and treatment rates of both strains on the equilibrium prevalence of infection; results suggest that poor quality treatment makes coexistence more likely but increases the relative proportion of DR-TB infections.

In **Chapter 6**, I presented a paper regarding the TB mathematical model that is fitted to the Bangladesh TB data to understand the transmission dynamics of DS and MDR-TB in this country. Several control strategies including distancing, latent case finding, case holding, active case finding, and combinations are examined within the optimal control outline. Optimal control strategies used for reducing the number of DS and MDR-TB patients with the lowest intervention execution costs.

In the paper presented in **Chapter 7**, I extend the TB mathematical model to fit with the DS and MDR-TB incidence data in Bangladesh. Here, I considered four specific intervention strategy including detection proportion, drug-susceptibility testing rate, DS and MDR-TB treatment rates during the time period from 2020 to 2035. Results suggest that combining more interventions simultaneously is the most effective way to decrease the burden of DS and MDR-TB incidence and mortality in Bangladesh.

A general discussion, recommendations, future directions and conclusions are presented in **Chapter 8**.

## References

1. WHO, *Global tuberculosis report. WHO/CDS/TB/2019.15, Geneva.* 2019.
2. Ai, J-W., et al., *Updates on the risk factors for latent tuberculosis reactivation and their managements.* Emerging Microbes & Infections, 2016. **5**(1): p. 1-8.
3. Fares, A., *Seasonality of tuberculosis.* Journal of Global Infectious Diseases, 2011. **3**(1): p. 46-55.
4. Talat, N., et al., *Vitamin D Deficiency and Tuberculosis Progression.* Emerging Infectious Diseases, 2010. **16**(5): p. 853-855.
5. Chan, T., *Vitamin D deficiency and susceptibility to tuberculosis.* Calcified Tissue International, 2000. **66**(6): p. 476-478.
6. Nnoaham, K. E. and Clarke, A., *Low serum vitamin D levels and tuberculosis: a systematic review and meta-analysis.* International Journal of Epidemiology, 2008. **37**(1): p. 113-119.
7. Wilkinson, R. J., et al., *Influence of vitamin D deficiency and vitamin D receptor polymorphisms on tuberculosis among Gujarati Asians in west London: a case-control study.* The Lancet, 2000. **355**(9204): p. 618-621.
8. Wubuli, A., et al., *Seasonality of active tuberculosis notification from 2005 to 2014 in Xinjiang, China.* PLoS One, 2017. **12**(7): p. e0180226.
9. Yang, Y., et al., *Seasonality impact on the transmission dynamics of tuberculosis.* Computational and Mathematical Methods in Medicine, 2016. **2016**.
10. Nelson, R. J., and Demas, G. E., *Seasonal changes in immune function.* The Quarterly Review of Biology, 1996. **71**(4): p. 511-548.
11. Nelson, R. J., *Seasonal immune function and sickness responses.* Trends in Immunology, 2004. **25**(4): p. 187-192.
12. WHO, *Global tuberculosis report 2015.* WHO/HTM/TB/2015.22, Switzerland, 2015.
13. NTP, *Tuberculosis control in Bangladesh. Annual report 2015.*
14. Zaman, K., et al., *Tuberculosis in Bangladesh: A 40-Year Review.* 11 ASCON. ICDDR,B. Scientific session, abstract book, 2007. **86**: p. 4-6.
15. Daley, C. L., *Global scale-up of the programmatic management of multidrug-resistant tuberculosis.* The Indian Journal of Tuberculosis, 2014. **61**(2): p. 108-15.
16. WHO, *Global tuberculosis report. WHO/HTM/TB/2017.23, Geneva,* 2017.
17. Bondemark, L., and Ruf, S., *Randomized controlled trial: the gold standard or an unobtainable fallacy?* European Journal of Orthodontics, 2015. **37**(5): p. 457-461.
18. Maude, R. J., et al., *The role of mathematical modelling in guiding the science and economics of malaria elimination.* International Health, 2010. **2**(4-6): p. 239-246.
19. Kim, S., et al., *What does a mathematical model tell about the impact of reinfection in korean tuberculosis infection?* Osong Public Health and Research Perspectives, 2014. **5**(1): p. 40-45.
20. Brooks-Pollock, E., Cohen, T., and Murray, M., *The impact of realistic age structure in simple models of tuberculosis transmission.* PLoS One, 2010. **5**(1): p. e8479.
21. Mishra, B. K. and Srivastava, J., *Mathematical model on pulmonary and multidrug-resistant tuberculosis patients with vaccination.* Journal of the Egyptian Mathematical Society, 2014. **22**(2): p. 311-316.
22. Trauer, J. M., Denholm, J. T., and McBryde, E.S., *Construction of a mathematical model for tuberculosis transmission in highly endemic regions of the Asia-Pacific.* Journal of Theoretical Biology, 2014. **358**: p. 74-84.

# CHAPTER 2

## Background

Partial contents of this chapter have been published, under review and copyrighted, as outlined below:

**Kuddus, M. A.,** Tynan, E., & McBryde, E. (2020). Urbanization: a problem for the rich and the poor? *Public Health Reviews*, 41(1), 1.

**Kuddus, M. A.,** Meehan, T. M., Doan, T., McBryde, E. S. (2021). The epidemiological presentation and management of tuberculosis: A literature review. *Antimicrobial Resistance & Infection Control* (under review).

**Kuddus, M. A.,** Meehan, T. M., Doan, T., McBryde, E. S. (2021). Tuberculosis in different setting and opportunity for modelling: A review. *Current Infectious Diseases Reports* (under review).

## **Summary of this chapter**

This chapter discusses the introduction and endemic establishment of TB, the mathematical and cost-effective modelling of TB, and the likelihood of future epidemics of severe TB in Bangladesh by synthesizing grey literature, academic published articles using Google Scholar, PubMed, NTP reports in Bangladesh, and the WHO library database. The search terms were “TB fever”, “TB transmission”, “TB incidence”, “TB prevalence”, “TB notification”, “TB mortality”, “TB risk factors”, “TB mathematical modelling”, “TB cost-effective modelling”, and “Bangladesh”. Numerous aspects of TB epidemiology in Bangladesh previously not synthesized are analysed in this description review paper. Diversity in TB epidemiology between Bangladesh and other high-burden countries is described. This chapter examines the possible causes of an apparent reduction in notified cases numbers, including control measures and population immunity, and whether bias in the Bangladesh NTP reporting system partially accounts for the reduction. The association between TB and its risk factors including health system factors, environmental factors, host factors, and sociological factors are also examined. Mathematical and cost-effective modelling approaches are also reviewed at the end of this chapter.

## 2.1 An overview of tuberculosis disease and its mode of transmission

Tuberculosis (TB) is a bacterial, potentially fatal, infectious disease that causes millions of deaths worldwide each year [1]. TB is an airborne disease caused by bacilli of the bacteria *Mycobacterium tuberculosis* (*Mtb*). The bacilli generally enter the body through the lungs, spreading to other parts of the body through the bloodstream, the lymphatic system, or through direct extension to additional organs (extra-pulmonary TB) [2, 3]. The mycobacterium measures approximately 1- 4  $\mu\text{m}$  long and 0.3-0.6  $\mu\text{m}$  in diameter, and grows very slowly, with cell division taking 12 to 20 hours [4].

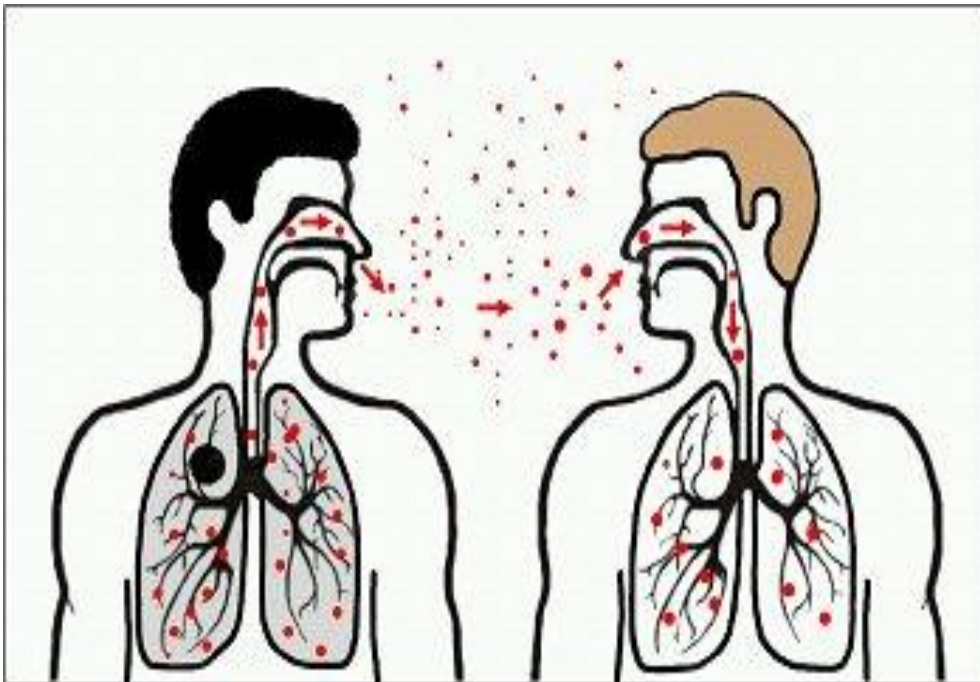


Figure 2. 1 TB transmission cycle from person to person through the air.

(<https://www.cdc.gov/tb/wwebcourses/tb101/page1699.html>)

Following an infectious person coughing, sneezing, speaking or singing, thousands or tens of thousands of droplet nuclei are exhaled [5]. These minute droplet nuclei can remain suspended in the air for several minutes to an hour, allowing spread to other persons through inhalation [5, 6]. The spread of *Mtb* from one individual to another depends on the number of droplet nuclei inhaled and the duration of exposure. This in turn is dependent on many factors, such as population crowding, the prevailing climatic conditions, the strain of TB, and the immune status of the individual [5, 6].

Once infected, the individual will first undergo a period without visible clinical symptoms, called latent TB infection (LTBI). The latent period is the timespan from the point of infection to the beginning of the state of infectiousness, which may last for weeks, months or the entire remaining life of the infected

individual. In fact, the lifetime risk of progression to active TB for a person with LTBI is around 5-15%, depending on the age at infection. For those who progress from LTBI to active TB, the majority will do so within the first two years of initial infection [7]. Figure 2.2 shows the difference between latent and active TB.

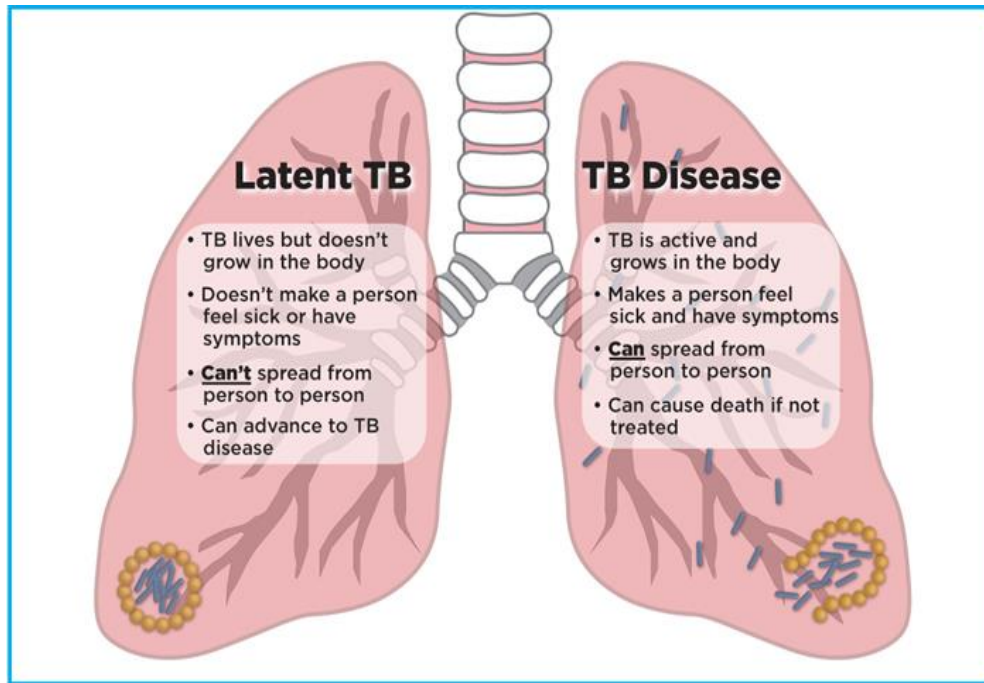


Figure 2. 2 The left side represents latent TB and the right side active TB.

(<https://aidsinfo.nih.gov/education-materials/fact-sheets/26/90/hiv-and-tuberculosis--tb->)

The World Health Organization (WHO) estimates that once infection has been activated and TB disease develops, a person with active but untreated TB may infect 10-15 (or more) other people per year [8]. Fortunately, the infected person is no longer a source of infection within 2 weeks of commencement of effective treatment [6]. Therefore, effective treatment not only protects TB infected persons, it also reduces exposure in the community and the likelihood of *Mtb* transmission. However, the risk is restored, and potentially increased, when the infected individual fails therapy, such as when the strain is drug-resistant (DR) TB or if the infected person does not have an adequate course of therapy.

## 2.2 The emergence of drug resistance

In recent years, antibiotic resistance to the most effective treatments (first line combination therapies) has emerged and spread [9]. This has led to a decline in the efficacy of antibiotics used to treat TB, with DR-TB patients experiencing much higher failure rates [10]. From a microbiological viewpoint, resistance first occurs by a genetic mutation in a micro-organism that renders a drug less effective. Typically, such resistance-conferring mutations exact a “fitness cost” whereby DR organisms reproduce

at a lower rate and are often less transmissible than their DS counterparts [11]. However, the selective pressure applied by antibiotic treatment permits DR mutants to become the dominant strain in a patient infected with TB on first-line therapy. Such selection is exacerbated by insufficient antibiotic courses or poor delivery of treatment to control TB outbreak. Acquisition of resistance (also referred to as amplification), i.e. when an individual's position changes from DS at initial presentation to resistant at follow-up, is the mode by which drug resistance first emerges in a population. Well-administered first-line treatment for DS-TB is the best way to prevent acquisition of resistance [12].

Once drug-resistant organisms have emerged in a population they can proliferate via primary (direct) transmission from an individual with DR-TB to susceptible individuals. Primary transmission is not expected to contribute significantly to the overall DR-TB burden due to the reduced fitness/transmissibility of drug-resistant organisms. However, subsequent evolution and compensatory mutations can restore fitness in the absence and/or presence of antimicrobials [13]. The WHO recommends that timely identification of DR-TB and adequate treatment regimens with second-line drugs administered early in the course of the disease, believing that these are essential to stop primary transmission [1]. Although its causes are microbial, clinical and programmatic, DR-TB is essentially a man-made phenomenon.

Currently, multidrug-resistant (MDR) TB is emerging as the greatest threat to TB control globally [14, 15]. MDR-TB is defined as TB that is resistant to isoniazid and rifampicin (the two most effective and commonly used first line drugs) with or without resistance to additional first line drugs [15]. Cohort studies within programs of TB treatment estimate that approximately 1% of a treated population who begin with a susceptible organism will develop MDR-TB [16]. Ongoing transmission of MDR-TB strains in a population may also contribute to new MDR-TB. MDR-TB is an emerging threat to success in TB control due to the higher cost of diagnosis and treatment. Therefore, control of MDR-TB requires prevention of both developed drug resistance and subsequent transmission, as well as effective diagnosis and treatment for those cases that do emerge [17].

Unfortunately, it does not stop there: inadequate treatment of MDR-TB may create even more resistance, with extensively drug-resistant tuberculosis (XDR-TB) strains beginning to emerge (XDR-TB is defined as MDR-TB with additional resistance to any fluoroquinolone and at least one of the three following injectable drugs: capreomycin, kanamycin, and amikacin). Although XDR-TB has been found in all areas of the world it is still relatively uncommon [18, 19]. However, wherever second line drugs are being used to treat MDR-TB, there is a risk of XDR-TB emerging. Therefore, the clinical significance of XDR-TB needs to be revised in light of new drugs including bedaquiline, delamanid and pretomanid and new information on the value of the injectable agents.

The emergence and spread of antibiotic resistance to the most effective treatments (first line combination therapies) has resulted in a decline in the efficacy of antibiotics in treating TB, with DR-TB patients experiencing much higher failure rates [1]. There were series of studies provide the following principles for addressing DR-TB:

1. The use of drug resistance diagnostics is critical because failure to rapidly and accurately diagnose DR-TB is contributing to the severity of the TB epidemic [20]. The gold standard drug resistance diagnostic is the use of culture in the presence of antibiotics to assess the resistant phenotype; however, genexpert is a rapid and cheap alternative [21, 22].
2. Treatment of MDR-TB is very complex and problematic. In regions in which MDR-TB is problematic, DOTS plus (treatment protocol) is recommended and includes second line anti-tuberculosis drugs (which are more toxic) [23, 24].
3. Prevention through rapid case detection, including contact tracing, and management. The most important component of rapid case detection is identification of symptomatic patients attending a health facility, either on their own initiative or through referral by another health facility, health worker, community volunteer, etc. [25, 26]. Patients diagnosed with any form of TB should always be asked whether there is anybody living in the same house who has a chronic cough and be encouraged to bring or send that person to the health facility for sputum examination.
4. Infection control, which includes prompt detection of infectious patients, airborne precautions and treatment of people who have supposed or confirmed TB [27, 28]. Standardised infection control procedures in all health services are also very important for prevention and contact tracing of DR-TB cases. The major goals of TB infection control are (i) to strengthen coordination for implementing appropriate TB infection control; (ii) to reduce the generation of aerosols and thereby the exposure to droplet nuclei; and (iii) to reduce concentrations of infectious particles, and (iv) to reduce inhalation of infectious particles [1, 27].

### **2.3 Current global statistics of TB and its risk factors**

TB kills more people each year than any other infectious disease, including HIV and malaria, and it is one of the primary global health problems [29, 30]. In 2018, the WHO estimated there were around 10.0 million new cases of TB, and 1.2 million died from TB disease. Most of the estimated cases in 2018 occurred in Asia (44%) and Africa (24%) and 87% of TB deaths occurred in low- and middle-

income countries [31]. A substantial proportion of cases occurred in the Western Pacific region (18%), with the Eastern Mediterranean region (8%), the European region (3%) and the Americas region (3%) also contributing [31]. Worldwide there is an imbalance in case notification between males (5.6 million new cases in 2010) and females (3.2 million new cases in 2010), which may have many causes, including missed cases. Childhood TB is often missed, as classical diagnosis with sputum smear is insensitive [32].

Numerous systemic risk factors can lead to an outbreak of TB disease. The risk factors include, but are not limited to, health system factors, environmental factors, host related factors and sociological factors [33-35]. Health System factors play a direct role in managing the impact of TB on a population [36]. For the purposes of this study, health system factors can be divided into three parts: 1) government support, including funding or lack thereof; 2) quality of service delivery at the basic measurement unit (BMU) level; and 3) a system for accessing, managing and delivering anti-bacterial medicines for each of the first-line drugs (for fully susceptible disease) and second line drugs (for MDR / XDR-TB). Each of these factors is interconnected.

Lack of government budget and service quality can increase TB disease. Prinja *et al.* (2015) stated that lack of government budget plays out strongly at the local and national levels from medicine selection, procurement, distribution, and prescription [37]. For drug procurement, adequate funds are essential. Without a reliable and efficient supply-chain management system, the allotted funds may not reach the intended beneficiaries. Weak institutions and poor governance are barriers to the timely supply of medicines to the whole country's population [38]. Therefore, ensuring that national or regional health systems are improved by strengthening the medicine supply-chain system is an important part of dealing with or controlling TB outbreaks [39]. In turn, this will ensure that the financial resources available for the procurement of pharmaceutical products are utilised efficiently to optimise households' access to medicines, for the government to achieve good value for money, and to accomplish transparency in the system [37].

Environmental factors impact the management of TB, particularly within developing countries. Research highlights major environmental factors to be urbanization, overcrowding and seasonality [40, 41]. Some of the major health problems resulting from urbanization include poor nutrition and pollution-related health conditions. These have direct impacts on individual quality of life, while straining public health systems and resources. Urbanization has a major negative impact on the nutritional health of poor populations. Because they have limited financial resources and the cost of food is higher in cities, the urban poor lack nutritious diets [42]. In addition, rapid urban expansion and migration might bring populations into contact with pathogenic cycles established in nearby rural areas.

Moreover, in urban slum areas, the poor live in overcrowded and congested conditions, with prolonged contact and polluted air; all leading to the spread of TB [43].

Seasonality is another major factor in TB incidence [44-46]. In cold regions, the incidence of TB is highest during winter, speculated to be owing to: vitamin D level decrease, an increase in indoor activities; and seasonal change in immune function [44]. A series of studies has supported the association between TB and deficiency in vitamin D, which has a known role in host immune responses specific to TB infection [47-50]. Therefore, all three environmental factors – urbanization, crowdedness, and seasonality – may work synergistically to increase the likelihood of a TB disease outbreak.

Host-related factors that lead to the spread of TB disease are nutrition status, age and comorbidity, including: low immunity; co-infections (e.g. HIV); and non-communicable diseases such as diabetes [51-54]. Malnutrition causes infection through its impact on immune system development and function. Malnourished children are more susceptible to infection and less likely to recover from TB [55]. Around 168 million children under five years of age are estimated to be malnourished and 76% of these children live in Asia [56].

A number of studies have also shown that improved nutrition status reduces the incidence of TB disease [57, 58]. Correction of malnutrition with nutritional supplementation can reduce suffering, cost and death, and increase treatment effectiveness by restoring host defences [57, 58]. Research also suggests that underweight patients are more likely to have clinical evidence of advanced disease and greater risk of side effects and deaths compared to patients with normal Body Mass Index (BMI) [59]. Another study implies that multiple-micronutrient (MMN) supplementation increased weight gain in TB patients [60]. Therefore, patients with under-nutrition should be considered a high risk group, and proper nutritional supplementation may be required as an adjunct to anti-TB therapy. Malnutrition is also an aggravating factor for progression of disease from latent TB infection and MDR-TB from conventional TB. Malnutrition can facilitate pathogen invasion and propagation to cause diseases, and diverse studies have demonstrated that malnutrition increases the risks of infection and death [61, 62].

As mentioned above, success of treatment is lower with MDR-TB than with DS-TB, hence restoring natural immunity is paramount. However, second line anti-TB drugs for MDR-TB decrease appetite, and lead to weight loss [63]. Consequently, more effort is required to analyze and identify the critical factors of developing MDR-TB disease, to improve diagnostic effectiveness and to limit the side effects of treatment of MDR-TB, in order to prevent deaths from MDR-TB.

HIV is the most significant known risk factor for reactivation of latent TB to active TB. For individuals with TB-HIV co-infection the lifetime risk of developing active TB is around 60% (compared with the 5 – 15% baseline figure quoted above) [64, 65]. HIV weakens the immune system particularly impairing macrophage and CD4<sup>+</sup> lymphocyte function and numbers [66]. The macrophage is the key effector cell in reaction to TB infection, and the CD4<sup>+</sup> cells are thought to play a major role in adaptive response to *Mtb* infection. In the presence of HIV infection, infected macrophages fail to present *Mtb* antigens to CD4<sup>+</sup> cells and therefore intracellular *Mtb* is more likely to survive [67].

Although less profound, the association between TB and diabetes may have been in play for many thousands of years, although the link was not documented until the 1950s [68]. In the early 20th century, it was assumed that people who developed diabetes usually died either from diabetes or TB [68, 69]. Later, because of the extensive use of insulin to treat diabetes and antibiotics for TB treatment, the relationship between these two life threatening diseases was underappreciated. Numerous epidemiological studies have proved that type 2 diabetes (T2D) (non-insulin dependent) is one of the strongest risk factors for TB vulnerability and its reactivation [70, 71]. T2D patients show 3 to 8 times more susceptibility to developing active TB compared with other patients [71, 72].

Sociological status, often indicated by education level, economic conditions with income and religious beliefs are additional risk factors that can affect the incidence of TB disease [73-75]. One way in which sociological factors impact directly on disease incidence, including TB, is through vaccination decisions. Some parents may object to immunization on religious or philosophical grounds, some may object to what seems to be a painful assault on their child, and others may believe that the benefits of immunization do not justify the risks to their child. Negative beliefs about vaccination have been shown to be correlated with low education levels [76]. Educated mothers throughout the world, including those in South Asia [77], are more likely to immunize their children compared with non-educated mothers [78]. Therefore, if people are educated, they are often better prepared to prevent TB via immunization [79]. Challenges even enter the realm of religion, as some religious teachings forbid followers to consume ingredients that form the vaccination itself [75, 80]. These factors are culturally sensitive, contributing to a worrisome problem in developing countries. Furthermore, vaccines have an indirect impact, reducing the number of infectious people, which in turn reduces exposure in the community. Consequently, lack of immunization increases both the risk to children who are denied the vaccine, and the risk of TB disease spreading throughout the community, as a result of reduced herd immunity. TB impacts poor populations more because lack of health facilities and services, poor nutrition, and housing together contribute to the spread of TB disease, its outcome in the individual and its effect upon the society [81].

TB exists throughout the world and its incidence is highly correlated with poverty at a national scale. In addition to the environmental factors already discussed, there are many potential reasons why poverty drives TB. For instance, access to high level care is impacted by income at a family level and also health system coverage at a national level, leading to late diagnosis and greatly increased TB transmission [82].

For numerous reasons, including violence or disturbance, nutritional shortages and inconsistent therapeutic arrangement, refugee children are at higher risk of TB [83]. According to estimates by the United Nations High Commissioner for Refugees, around 45 million persons are displaced worldwide, of whom 15 million are refugees, with approximately half below 18 years of age [84]. This vast heterogeneous population experiences significant health adversities. TB infected refugee populations are twice as likely to experience treatment failure compared to other immigrant populations, and the rates of TB infection in immigrant and refugee populations are highest within 5 years after immigration [85, 86]. This is due to pre-departure screening detection of active TB being uncommon in newly arriving refugees, and the rates of latent TB infection (LTBI) exceeding 40% in some populations. However, children under 5 years of age are capable of getting LTBI and children with LTBI also have greater rates of improved active TB infection [87].

Movement of TB infected people presents a challenge to public health officials and their governments. Humans have long gathered for the purpose of religious and sporting events. For example, every year during the times of the Hajj and Umrah pilgrimages, 10 million pilgrims from 184 countries are estimated to travel to the Kingdom of Saudi Arabia (KSA); a large majority come from high burden TB and MDR-TB areas and thus many may have undiagnosed active TB, sub-clinical TB and latent TB infection [88]. Furthermore, during the FIFA World Cup football competition, high TB and MDR-TB prevalence existed among the citizens of participating countries, with the potential to spread TB worldwide [89]. There was widespread concern among global public health authorities that this would lead to spread of TB between attendees and the exportation of MDR-TB [88]. Mass gatherings and overcrowding of individuals at these events raise the risk of importation, spatial spread and exportation of TB [88, 90].

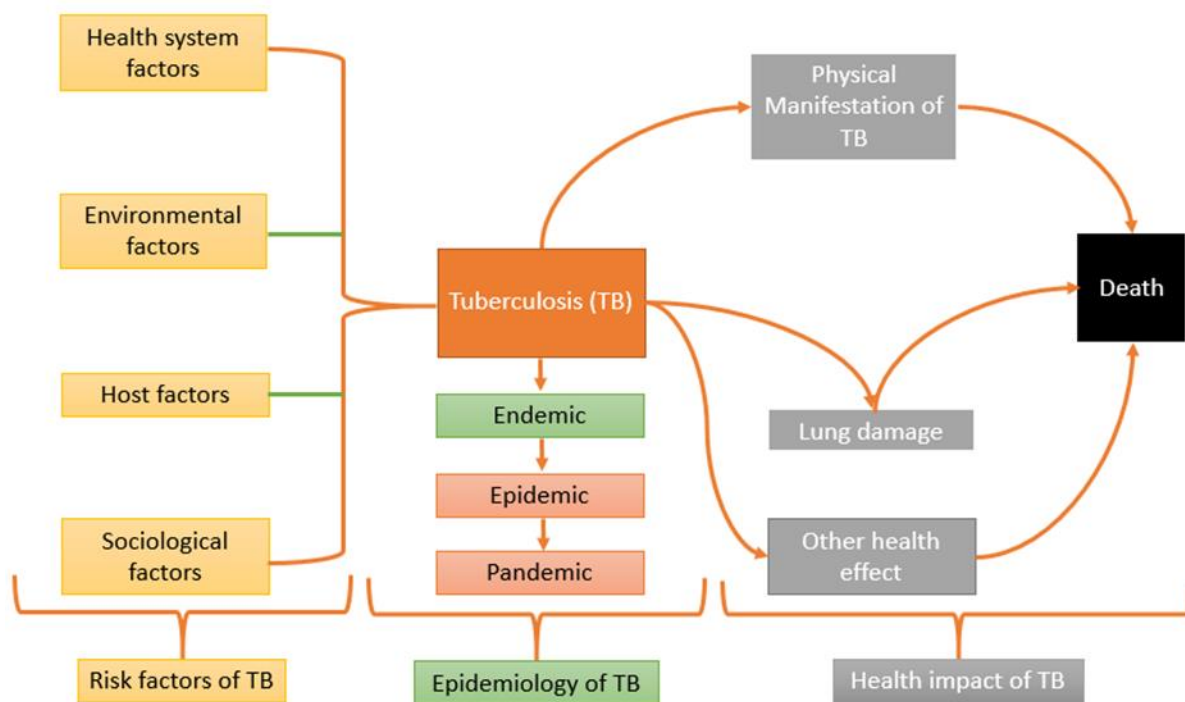


Figure 2. 3 Contributing factors related to TB disease outbreaks and their impact.

## 2.4 TB treatment and control strategies

Treatment of TB is lengthy and complex, usually incorporating a combination therapy taken for approximately six months for DS-TB and nine to 24 months for MDR-TB [91, 92]. Bacille Calmette-Guerin (BCG) vaccine, derived from an active attenuated strain, is recommended as soon as possible after birth to avoid life threatening TB diseases such as TB meningitis and miliary TB, however this vaccination is not lifelong and its efficacy varies from 50 to 80% in children and is lower in adults [93, 94]. Many of the existing tools available for TB control are old and insufficient to address current TB epidemics – evidenced by the 600,000 new cases of rifampicin (RR-TB) resistant TB estimated for 2016 [1]. TB control programs in resource-poor countries generally use a method of diagnosing the disease (sputum smear microscopy) that is 125 years old and detects only half the cases [95]. Several trials trying to reduce the treatment time for active DS-TB from six to four months have proven unsuccessful [96]. The nine month short-course regimen (Bangladesh regimen) for MDR-TB has been reported to be highly effective, with treatment success rates ranging from 84 to 88%, and better tolerance reported than the conventional MDR-TB regimens [1]. Furthermore, some studies have shown that bedaquiline (BDQ) has the potential to shorten MDR-TB treatment to less than six months when used in conjunction with standard anti-TB drugs [97]. Treating latent TB before it becomes active is another option [98]. The role of this strategy is not well defined and it is recommended in low-burden countries, whereas modelling studies suggest that higher burden countries are likely to benefit more

[99, 100]. Therefore, more effective and widely accessible tools are needed to make a greater impact on treatment regimens for DS and MDR-TB.

Prompt treatment and cure of infectious cases of TB cuts the chain of transmission of TB infection at the community level [101, 102]. Therefore, rapid identification of presumptive TB cases, rapid diagnosis, prompt commencement of treatment and successful completion of treatment are highly effective ways of preventing TB [1]. Patient compliance is key to treatment success. Lack of support (e.g. appropriate combinations of drugs, management and support of the patient) makes treatment adherence problematic and a proportion of patients stop treatment before completion [103]. This increases their risk of developing DR-TB and increases their duration of infectiousness, thus leading to enhanced transmission. To prevent this, and to improve patient outcomes, strict adherence to treatment is a pillar of the TB control strategy [102, 104].

To achieve the global WHO targets of achieving at least 70% case finding and 85% treatment success, numerous strategies are used to control TB outbreaks at the national and global levels. Programmatic management of drug-resistant TB (PMDT) is one of the most effective strategies for the control and prevention of DR-TB [105]. PMDT activities include proper management of contacts by ensuring that optimal treatment, a reliable drug supply and adequate health facilities are available [106]. Among these strategies, (DOTS) is an important component in the internationally recommended policy package for TB control. During DOTS, a qualified practitioner observes the patient ingest their medication, which results in a demonstrable improvement in treatment rates and patient outcomes [107].

## **2.5 Quantitative tools available for the control of TB**

Many areas of quantitative analysis can be used to improve the understanding of TB epidemiology, as well as the dynamics of disease spread, and explore the likely impact of interventions. These include:

**1. Decision theory:** Decision theory can guide a set of policies or give procedures on how or what we should do to make the best decisions for improving TB detection during a TB epidemic [108].

**2. Geographic Information System (GIS):** During a TB outbreak, GIS provides tools that speed the collection of precise field data, which helps support comprehensive decisions [109].

**3. Operational research:** Operational research can examine the knowledge for several interventions, policies, or tools that can improve the quality, usefulness, or coverage of each program's setting, especially in the areas that are experiencing high burdens of TB [110].

**4. *Mathematical modelling:*** Mathematical modelling can improve our understanding of the epidemiology of TB as well as those components that are significant to TB diagnosis and treatment. Mathematical modelling tools can be used to study a variety of influencing factors including e.g. poverty, host-related factors and population density, and to determine their relative importance in governing TB epidemics [111].

**5. *Health economics analysis:*** Health economic analysis can evaluate the economic effect on both patients and the health system considering factors such as schedule shortening for first line TB treatment and examining the unit cost for interventions. The results generated from the health economic analysis help identify interventions that are the most cost-effective [112].

Furthermore, real-time analysis of TB epidemics can support public health practitioners in re-examining continuing TB burdens with outbreaks and associated resource allocations, and thereby realign emergency plans. Electronic based communication systems including electronic signals became a priority to facilitate TB surveillance and outbreak investigation. These systems allow for much more rapid data collection, synthesis and analysis [113].

## **2.6 Health economics of TB**

TB has disruptive financial impacts on all ages but the greatest impacts occur during the most dynamic years of life, from 15 to 44 years of age. The community and family impacts on the individual of TB in this age group are worse as TB decreases the earning ability of an individual [114, 115]. Shortfalls in funding for TB prevention and response is a threat to TB control at the national and global levels. Currently, funding for TB care and prevention extended to US\$ 6.9 billion in 2017 in 118 low and middle-income countries compared to US\$ 6.3 billion in 2016 and more than double the US\$ 3.3 billion in 2006 [1]. In 2017, India's TB budget substantially increased to US\$ 525 million, almost double compared to 2016 [116]. In low-income countries, international donor (Global Fund, WHO, World Bank) funding exceeds national funding, and in the 25 high TB burden countries outside Brazil, the Russian Federation, India, China, and South Africa, national and international donor funding levels are similar. In 2017, an estimated total of US\$ 9.2 billion was required for TB diagnosis and treatment. This funding included US\$ 7.0 billion for DS-TB, US\$ 2.0 billion for MDR-TB and the remainder for TB-HIV interventions. The Global Fund delivers the largest international donor funding stream for TB control efforts [1]. However, the financial situation for TB control efforts in Bangladesh is not good. In 2017, US\$ 86 million was estimated to be needed for TB diagnosis and treatment, comprising 7% from domestic sources, 51% from international sources and 43% unfunded [1].

## **2.7 TB in Bangladesh and its current situation**

In 2015, the WHO classified 22 high TB burden countries among them Bangladesh has the 7<sup>th</sup> largest TB incidence globally. Further, for the MDR-TB Bangladesh ranked 10<sup>th</sup> of the 27 high MDR-TB burden countries [95]. Each year in Bangladesh an estimated 70,000 people die of TB and 300,000 new cases are projected making, TB one of the most important public health problems in Bangladesh [117]. Before 2014, the case notification rates per 100,000 population were 68 and 122 for new smear positive (usually more infectious and have a higher mortality) and all forms of TB cases respectively, but by the end of 2014 the number of all types of TB notifications had increased, with a substantial increase in the number of extra-pulmonary cases. This increase may be due to a substantial rise in migration to and from endemic countries. This is a worrying hypothesis, given the high TB burden in neighboring countries such as India and China.

In Bangladesh, the TB mortality rate is 43 per 100,000 per year, the incidence rate of all cases is 225 per 100,000 per year and the prevalence is 411 per 100,000 [118]. By way of comparison, in Thailand the tuberculosis death rate is 14 per 100,000 and the incidence rate is 150 per 100,000 people [119]. Thus, there is a great need to reduce incidence, prevalence, and mortality rates in Bangladesh [120]. Health care financing in Bangladesh primarily comes from three sources, namely the public exchequer, pocket payments by users and foreign aid [121]. The Bangladesh government is constitutionally obliged to supply basic medicine requirements to all community levels. However, a large number of rural people in Bangladesh have no or little access to health care services because of the inadequate health facilities [122]. Therefore, if people are infected by TB, they do not receive proper medication from the health care services. This poor quality of service to the poor population will have a negative health effect that can lead to TB disease outbreaks [123]. Furthermore, although the BCG vaccine is very effective for TB patients [1], a lack of access to BCG vaccines may be a contributing health factor and lead to outbreaks or spread of TB [124].

In Bangladesh, poverty, population density and malnutrition are common problems that create a favourable environment for developing TB [125]. Illiteracy and social stigmas are important factors that may lead to people failing to receive proper treatment [126]. Nationwide, more than five million people have diabetes; these people have a two to three times higher risk than other individuals of developing TB disease [127].

In Bangladesh, under the Ministry of Health and Family Welfare, the National TB Control Program (NTP) of the Directorate General of Health Services (DGHS) provides nationwide TB control services. These services include screening, case detection through diagnosis, treatment following the appropriate regimen, follow up and evaluation in all areas [63]. The goals of this program are to reduce illness,

death and transmission of TB, and to achieve universal high quality service for all people with active and latent TB [125]. More than 44 partner organizations (NGOs) also support the NTP in all areas, including advocacy, communication, and social mobilization (ACSM) activities. The NTP adopted the recent WHO recommended strategies -namely the DOTS Strategy-1993, the Stop TB Strategy-2006, and the End TB Strategy-2015 for TB control [63, 128].

Following the DOTS and End TB strategies, the NTP aims to sustain the global targets of achieving at least 70% case detection and 85% treatment success among new smear-positive TB cases for the whole country. The general progress in case finding was slow and steady until 2001 to reach case notification rates for new smear-positive cases of 31 per 100,000 population. From 2001 onwards, case notification increased to reach 46 per 100,000 in 2004 and further increased to 61 per 100,000 in 2005, 73 per 100,000 in 2006, and in 2009, the case notification reached 74 per 100,000 population for smear-positive cases. As a result of extra effort in special situations like smear-negative and child TB cases, as well as hard to reach areas with social support for poor groups, case notification reduced to 70 per 100,000 population in 2012 but in 2013 case notification increased to 119 per 100,000 and 122 per 100,000 population in 2014. During 2015, case notification further increased to 130 per 100,000 and in 2016 it was 138 per 100,000 population.

The NTP achieved its objectives in effective treatment, case detection and overall management through partnership, engaging all care providers (GO-NGOs) and making available free diagnostic and treatment support, particularly for DS-TB [63]. By 2003, the treatment success rate of this program reached the targeted 85% and has been maintained at 90% since 2005. In 2013, the program successfully treated 94% of notified new smear-positive cases such that by 2015 the number of all forms of TB cases fell to 225 per 100,000 population, with a case detection rate of approximately 58% [125]. In 2020, WHO estimated that 0.7% of new cases and 11% of previously treated cases are found to be positive for DR-TB, which has an incidence rate of 2.0 per 100,000 population [129]. Figure 2.4 shows the nationwide number of TB cases in Bangladesh over the year from 2000 to 2019 [129].

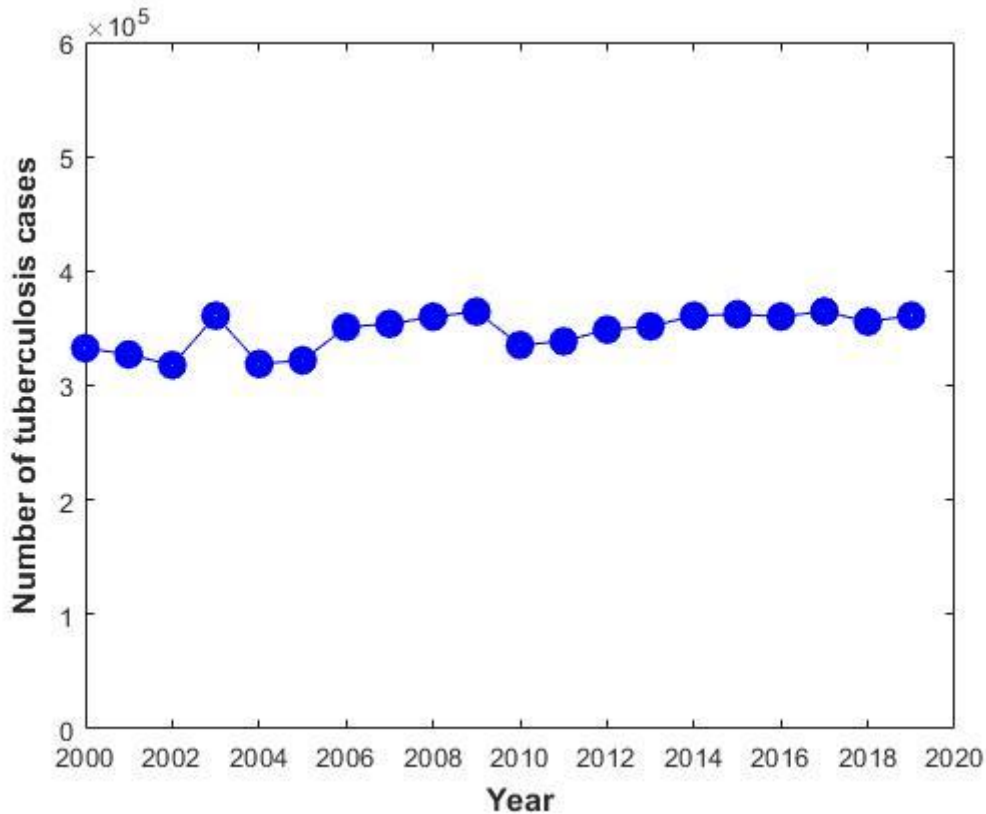


Figure 2. 4 Nationwide number of TB case in Bangladesh from 2000 to 2019.

In Bangladesh, several government hospitals, mainly chest disease hospitals, provide treatment to DS-TB patients and MDR-TB patients. They also provide conventional food supplementation three times a day [130]. Recently, Bangladesh introduced programmatic management of MDR-TB at the community level to reduce the high utilization of inpatient beds that resulted from MDR-TB treatment under standard regimens [131]. As the effectiveness of community-based short-course MDR-TB management (The Bangladesh regimen) was found to be significantly higher than hospital-based management, it is important to identify the factors responsible for effective MDR-TB management, including food and nutrition, awareness, and financial support from the treatment program, programmatic strengths, and emotional and psychological issues [125]. Although TB control in Bangladesh has significantly progressed – improved case finding, availability of free diagnostic and treatment services, involvement of multiple partners, newer diagnostic facilities, sufficient human resources, adequate capacity and guidelines – more effort is required. To reduce TB incidence and prevent deaths from TB in Bangladesh, we need to identify the critical factors for developing TB disease, improve diagnostic effectiveness, and reduce adverse drug reactions [63].

Bangladesh is a resource poor, high burden TB country, and the transmission dynamics and epidemiology of TB are poorly understood. The development pathway of novel TB treatment therapies is very slow. New treatment regimens are being developed that significantly shorten the duration of

therapy, improve patient outcomes, and are cheaper for patients and the health system. To date and to our knowledge, the transmission dynamics and epidemiology of TB in Bangladesh have not undergone rigorous and no mathematical model structure exists. The mathematical model can be used to predict quantitatively the period of an epidemic; its total size; peak height; peak time; and impact of infection control interventions including nonlinear interactions that happen when multiple interventions are implemented. Therefore, this project can refine our understanding of TB in Bangladesh and offer potential strategies to reduce overall disease burden. Furthermore, this project will also include a cost-effectiveness analysis to identify optimal TB treatment efficiency with satisfactory cost-effectiveness. The information that I generate from these analyses may contribute to improving the present situation in Bangladesh. Furthermore, it is also expected to benefit the administrators and policy makers who are concerned with the impact of DS and MDR-TB treatment in Bangladesh.

## **2.8 Mathematical modelling of TB: An overview**

Mathematical modelling is an abstraction of reality. This kind of modelling is a powerful tool for infectious disease control that can be used for both prediction and for understanding infectious disease dynamics [132]. Many researchers have implemented mathematical modelling frameworks to gain insights into different types of infectious diseases [111, 133-136]. Mathematical models can also improve our understanding of those components that are significant and suitable for infectious disease diagnosis and treatment [137-141]. Furthermore, health economic models, in particular cost-effectiveness models, are useful tools for evaluating the associated costs of an intervention incurred by patients, health systems and the wider community, relative to health benefits [112, 142].

From the information produced by mathematical model simulations, researchers and health workers can estimate different outputs such as incidence, prevalence, case notification and mortality that will help to develop health policies and disease monitoring plans [142]. Mathematical models can also be used to improve health policy and infectious disease monitoring plans by identifying thresholds which must be reached in order to achieve elimination. For example, analytical solutions, numerical solutions and stability analyses of mathematical models can identify regions in the parameter space where the various asymptotic states are stable or unstable, thus allowing us to predict the asymptotic (i.e. long-term) behaviour of the system [143]. Furthermore, sensitivity analyses of mathematical models allows us to discover the parameters (e.g. contact rate, progression rate, amplification rate, recovery rate, treatment rate, disease-induced death rate, rate of loss of immunity, etc.) that have the greatest influence on the model outputs (e.g. disease incidence, prevalence and mortality) [144]. Therefore, if we identify the parameters most responsible for the spread of disease, then respective governments can develop targeted policies to control any infectious disease outbreak.

An important threshold parameter whose analytical form can be identified through mathematical modelling is the basic reproduction number,  $R_0$  [145]. The basic reproduction number is the expected number of secondary cases generated by a single infectious case introduced into a totally susceptible population. If the basic reproduction number is greater than one, the number of infected individuals grows and an epidemic occurs. Conversely, if the basic reproduction number is less than one, the number of infective individuals typically tends to zero. The next generation matrix method can be used to calculate the basic reproduction number for compartmental transmission dynamic models (see below). To verify the asymptotic behaviour of the system we can use stability analysis and the direct Lyapunov method however, the threshold behaviour described above in terms of  $R_0$  is often a reliable indicator of the asymptotic dynamics [146].

Each year TB causes severe population loss in both developing and developed countries [1]. Therefore, novel tools have emerged for TB control in both developing and developed countries and human trials in the last few years after a long hiatus. Hence, it is crucial to deploy these judiciously and to examine ways in which any strategy will be most effective. Mathematical modelling of TB has been shown to be useful for understanding and mitigating this problem [147, 148]. Although models can range from very simple to highly complex, one of the commonest practices to improve understanding of infectious disease dynamics is a compartmental mathematical model [135]. One of the simplest mathematical models used in population-based infectious diseases modelling is the Susceptible-Exposed-Infected-Recovered (SEIR) compartmental model.

### **2.8.1 Model diagram and equations**

The compartmental modelling framework is composed of sets of interconnected state variables where each component of the compartmental model is considered to be homogeneous. A typical compartmental SEIR model is depicted in Figure 2.5, where S represents susceptible individuals, E represents exposed individuals who have not yet progressed to active infection, I represents individuals who are both infected and infectious, and R represents the removed/recovered population who were previously infected but successfully recovered.

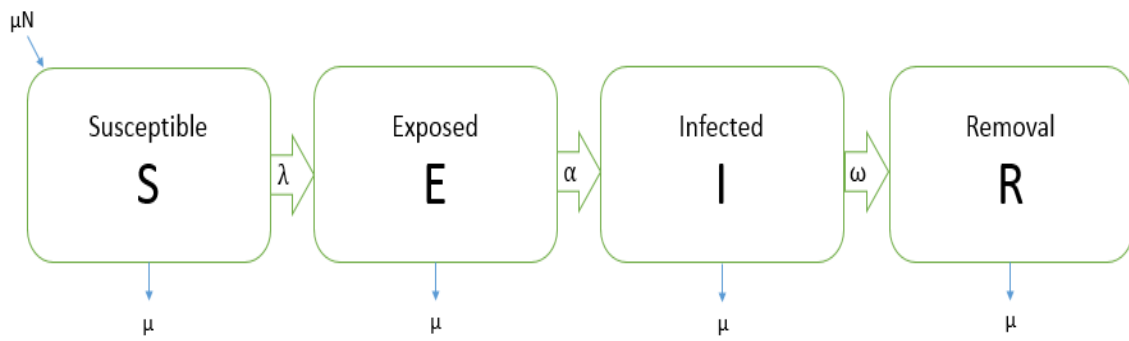


Figure 2. 5 Flow Chart of the compartmental SEIR mathematical model showing the four states and the transition in and out of each state.

Here,  $N$  = Total population,  $S$  = Susceptible population,  $E$  = Exposed population,  $I$  = Infected population,  $R$  = Removed/Recovered population,  $\mu$  = Birth rate/ Death rate,  $\lambda$  = Force of infection,  $\alpha$  = Progression rate to active disease,  $\omega$  = Recovery rate.

This model incorporates the following assumptions:

- The population is fixed. This means the births of susceptible persons exactly match the deaths in all groups (the birth rate and the death rate are assumed to be equal denoted by  $\mu$ ). Any net loss to the susceptible group occurs because a person becomes exposed to an infectious individual and becomes infected. Subsequently, the exposed population may activate and move to the infected group. The transition from the infected to the recovered group models recovery from disease. Once recovered, individuals are immune to further infection.
- Age, sex, social status and race do not affect any of the model parameters;
- There is no inherited immunity; and
- The members of the population mix homogeneously.

Let us consider a fixed homogeneously mixed group of  $N$  individuals consisting at any time  $t$  of  $S(t)$  susceptibles,  $E(t)$  exposed,  $I(t)$  infectives and  $R(t)$  removals. Therefore, the model can be formulated as:

$$S(t) + E(t) + I(t) + R(t) = N \text{ (Constant)}. \quad (2.1)$$

At the beginning of an epidemic, the value of  $R(t)$  is zero and  $S(0) = S_0 > 0$ ,  $E(0) > 0$ ,  $I(0) > 0$ , then we have:

$$S(0) + E(0) + I(0) = N. \quad (2.2)$$

Individuals enter the susceptible compartment at a constant rate  $\mu$  through birth and they may be infected with a circulating strain at a time dependent rate  $\lambda = \beta I(t)$ . Here,  $\beta$  is the rate at which susceptible individual is infected per infected individual per unit time. Individuals in the different compartments suffer from natural death at the same constant rate  $\mu$ , which is also the birth rate per person. All infected individuals move to the exposed infected compartment,  $E(t)$ . Those with exposed infection progress to active infection (the  $I$  compartment) as a result of reactivation of the latent infection at rate  $\alpha$ . A proportion of the infected individuals recover through treatment and natural recovery rate  $\omega$  and move into the recovered compartment  $R(t)$ . In this case the model can be expressed by the following four differential equations:

$$\frac{dS}{dt} = \mu N - \beta SI - \mu S. \quad (2.3)$$

$$\frac{dE}{dt} = \beta SI - \alpha E - \mu E. \quad (2.4)$$

$$\frac{dI}{dt} = \alpha E - \omega I - \mu I. \quad (2.5)$$

$$\frac{dR}{dt} = \omega I - \mu R. \quad (2.6)$$

The model we have just introduced has two equilibrium points: an infection-free equilibrium for which  $I = 0$ ; and an endemic equilibrium with  $I > 0$ . At the disease-free equilibrium,  $E = I = R = 0, S(0) = S_0$  and  $\frac{dS}{dt} = 0$ , which yields

$$\mu N - \mu S_0 = 0$$

$$\Rightarrow \mu N = \mu S_0$$

$$S_0 = N.$$

Hence, the disease-free equilibrium is  $(S(0), E, I, R) = (N, 0, 0, 0)$ . Here,  $S(0)$  refers to the value of  $S(t)$  when  $t = 0$ .

## 2.8.2 Basic reproduction number

### 2.8.2.1 Estimating the basic reproduction number of the pathogen

The basic reproduction number is well-defined as the expected number of secondary cases created by a single infectious case introduced into a totally susceptible population. The disease can spread in a population only if the basic reproduction number is greater than one. An epidemic occurs when an infection spreads through and infects a significant proportion of a population. A disease-free population is possible when the basic reproduction number is less than one, which means that the disease naturally fades-out [149, 150].

The system has two infected states, E and I, and two uninfected states, S and R, although there are four states in the system and the total population size is constant. At the infection-free steady state  $E = I = R = 0$ , hence  $S = N$ . The only occurrence of the variable S in equation (2.4) – (2.6), either directly or implicitly via N, is through the term  $\beta SI$ . Hence the equations (2.4) – (2.5) are closed, in that it does not involve the derivation of S from steady state value. Also R does not appear in equations (2.4) – (2.5), and for (E, I) we have the system.

$$\frac{dE}{dt} = \beta SI - \alpha E - \mu E. \quad (2.7)$$

$$\frac{dI}{dt} = \alpha E - \omega I - \mu I. \quad (2.8)$$

Here, the ODEs (2.7) and (2.8) are referred to as the infection subsystem, as they only describe the production of newly infected individuals and changes in the states of already infected individuals. By setting  $\mathbf{x}' = (E, I)'$ , where the prime denotes transpose, the infection subsystem can be written in the following form:

$$\dot{\mathbf{x}} = (\mathbf{T} + \mathbf{\Sigma})\mathbf{x}. \quad (2.9)$$

The matrix T corresponds to transmission (arrival of susceptibles into the infected compartments E and I) and the matrix  $\Sigma$  to transitions. Removal through death is included in the transition to keep the notation simple. All epidemiological events that lead to new infections are incorporated in the model via T and other events via  $\Sigma$ . If the infected states are indicated with i and j with  $i, j \in 1, 2$ , then the entry  $T_{ij}$  is the rate at which individuals in infected state j give rise to individuals in infected state i.

Regarding the subsystem (2.7) – (2.8) we obtain

$$\mathbf{T} = \begin{pmatrix} 0 & \beta S \\ 0 & 0 \end{pmatrix} = \begin{pmatrix} 0 & \beta N \\ 0 & 0 \end{pmatrix} \text{ and } \mathbf{\Sigma} = \begin{pmatrix} -\alpha - \mu & 0 \\ \alpha & -\omega - \mu \end{pmatrix}$$

$$-\mathbf{\Sigma}^{-1} = \begin{pmatrix} \frac{1}{(\alpha + \mu)} & 0 \\ \frac{\alpha}{(\alpha + \mu)(\omega + \mu)} & \frac{1}{(\omega + \mu)} \end{pmatrix}$$

Here, the element of  $(\mathbf{\Sigma}_{ij}^{-1})$  is the expected time spent in state i for an individual currently in state j during its entire future life.

Now,  $\frac{1}{(\alpha + \mu)}$  = life time of E compartment, 0 = time spent in E compartment starting from I

$\frac{\alpha}{(\alpha + \mu)(\omega + \mu)}$  = expected life of spent in I compartment starting from E compartment and the factor

$\frac{\alpha}{(\alpha + \mu)}$  = represent the probability of transitioning from compartment E to compartment I.

$\frac{1}{(\omega + \mu)}$  = time spend in I compartment starting from I.

### 2.8.2.2 Estimating the basic reproduction number using next generation matrix technique

The next generation matrix is a method used to evaluate the basic reproduction number for a compartmental model of the spread of infectious diseases. Two related matrices exist, which we define as the next generation matrix *with a large domain* and *small domain*. The next generation matrix with the large domain is always the matrix with the highest dimension, incorporating all infected states in the model. The small domain of the next generation matrix has the lower dimension and only incorporates states that are infectious. A small domain matrix will exist and can be used to define the next generation matrix if there are fewer states of infectiousness than states at infection [149].

Here, the next generation matrix (NGM) with large domain is denoted by  $K_L$ . An exposed state and infectious state are both infected states, but the variation from exposed to infectiousness does not contain a new infection happening, but rather an already established infection moving to a different infection stage. This has led to confusion as other researchers have tried to reconcile the appealing linear algebra approach [149]. To make the distinction clear and remove confusion we will call the matrix NGM ( $K_L$ ).

$$\text{NGM, } K_L = -T \Sigma^{-1} = T(-\Sigma^{-1}) = \begin{pmatrix} 0 & \beta N \\ 0 & 0 \end{pmatrix} \begin{pmatrix} \frac{1}{(\alpha+\mu)} & 0 \\ \frac{\alpha}{(\alpha+\mu)(\omega+\mu)} & \frac{1}{(\omega+\mu)} \end{pmatrix}$$

$$K_L = \begin{pmatrix} \frac{\beta N \alpha}{(\alpha+\mu)(\omega+\mu)} & \frac{\beta N}{(\omega+\mu)} \\ 0 & 0 \end{pmatrix}$$

### 2.8.2.3 Estimating the dominant eigenvalue of the matrix $K_L$

The dominant eigenvalue is the basic reproduction number of the disease. It represents the average number of infections produced by one infected individual.

Now the characteristic equation is  $|K_L - \lambda I| = 0$ , here  $I$  represents the identity matrix.

$$\Rightarrow \begin{vmatrix} \frac{\beta N \alpha}{(\alpha+\mu)(\omega+\mu)} - \lambda & \frac{\beta N}{(\omega+\mu)} \\ 0 & 0 - \lambda \end{vmatrix} = 0,$$

$$\Rightarrow \lambda \left( \frac{\beta N \alpha}{(\alpha+\mu)(\omega+\mu)} - \lambda \right) = 0,$$

$$\lambda_1 = 0 \text{ and } \lambda_2 = \frac{\beta N \alpha}{(\alpha+\mu)(\omega+\mu)}.$$

Hence, the basic reproduction number is  $R_0 = \frac{\beta N \alpha}{(\alpha+\mu)(\omega+\mu)}$ .

Now we break down the various components that make up the basic reproduction number of the model.

Here  $\beta$  = Transmission rate.

$\frac{\alpha}{(\alpha+\mu)}$  = Probability of becoming infectious once infected (i.e. the probability of transitioning from state E to state I).

$\frac{1}{(\omega+\mu)}$  = Mean infectious period.

### 2.8.2.4 Endemic equilibrium

Having defined the basic reproduction number, we now return to our analysis of the endemic equilibrium states of the system.

To determine the endemic equilibrium we set  $\frac{dS}{dt} = \frac{dE}{dt} = \frac{dI}{dt} = \frac{dR}{dt} = 0$ :

$$\mu N - \beta I^* S^* - \mu S^* = 0. \quad (2.10)$$

$$\beta I^* S^* - \alpha E^* - \mu E^* = 0. \quad (2.11)$$

$$\alpha E^* - \omega I^* - \mu I^* = 0. \quad (2.12)$$

$$\omega I^* - \mu R^* = 0. \quad (2.13)$$

Now from equation (2.11)

$$S^* I^* = \frac{(\alpha+\mu)}{\beta} E^*. \quad (2.14)$$

Now from (2.12)

$$I^* = \frac{\alpha}{(\omega+\mu)} E^*. \quad (2.15)$$

Putting the value of  $I^*$  in (2.14) we get,

$$S^* = \frac{N}{R_0}. \quad (2.16)$$

Now from (2.11)

$$E^* = \frac{\mu N (R_0 - 1)}{(\alpha + \mu) R_0}. \quad (2.17)$$

From (13)

$$R^* = \frac{\omega (R_0 - 1)}{\beta}. \quad (2.18)$$

Putting the value of  $S^*$ ,  $E^*$ , and  $R^*$  in (2.10) we get,

$$I^* = \frac{\mu (R_0 - 1)}{\beta}. \quad (2.19)$$

Hence, the endemic equilibrium is  $(S^*, E^*, I^*, R^*) = \left( \frac{N}{R_0}, \frac{\mu N (R_0 - 1)}{(\alpha + \mu) R_0}, \frac{\mu (R_0 - 1)}{\beta}, \frac{\omega (R_0 - 1)}{\beta} \right)$

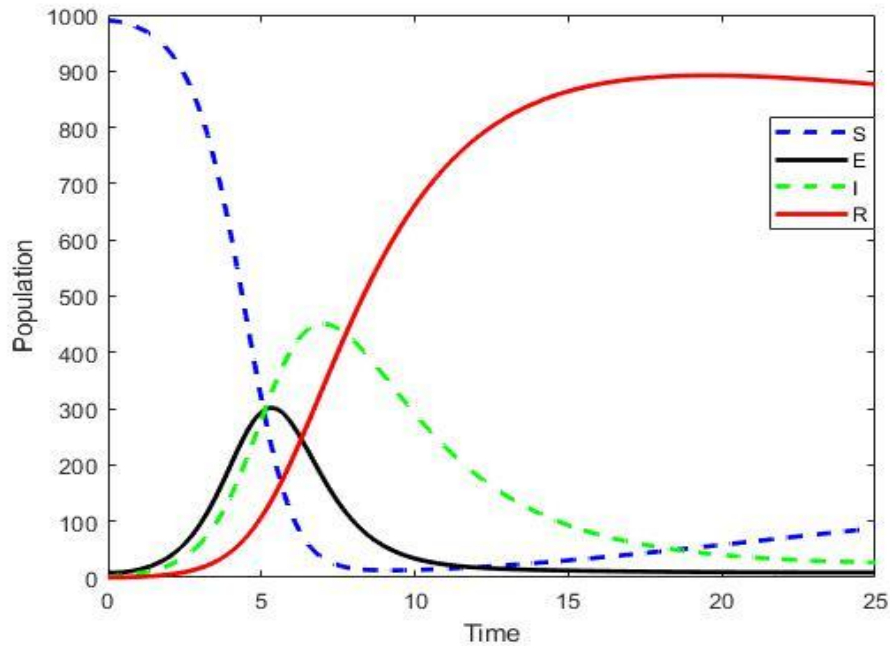


Figure 2. 6 Numerical simulations of the model outcomes.

Here the dotted blue line represents the dynamics of the susceptible population (S), the black line represents the exposed population (E), the dotted green line represents the infected population (I) and the red line represents the removal population (R).

In figure 2.6 we have provided a sample epidemic trajectory that is governed by the SEIR model. The susceptible (S), Exposed (E), Infected (I) and recovered (R) populations are considered in this model. In this example, the disease is highly contagious at the time of epidemic and almost all susceptibles move to the exposed class and then infected class. By setting a constant population (births = deaths), we can observe how many people will be in each class at a given period of time and how long an individual remains susceptible to the disease, and recovered from it. We start with everyone being susceptible to the disease and perturb the system by introducing one exposed person who then becomes infectious. The curve for the susceptible population (S) shows a very sharp decrease over time. In contrast, the number of exposed (E) and infected (I) populations firstly increases very dramatically and then decreases sharply and then remain stable during the rest of the time. Furthermore, the number of removal (R) population increasing rapidly and then remain stable. We justified numerical results of this model with analytical solutions which is same.

### 2.8.3 Stability analysis of this system

To investigate the behaviour of our model in the vicinity of the various equilibrium points, we linearize the system of equations (reference equation numbers) and analyze this simpler system. This type of stability analysis will identify regions in state space where the various asymptotic states are stable or

unstable and allow us to predict the asymptotic behaviour of the model. Further, the stability analysis of the equilibrium points will identify which conditions the disease will be eliminated or persist in the population based on the basic reproduction number.

Now the system (2.3)-(2.6) is written in the following form:

$$\frac{dS}{dt} = \mu N - \beta SI - \mu S = f_1 \quad (2.20)$$

$$\frac{dE}{dt} = \beta SI - \alpha E - \mu E = f_2 \quad (2.21)$$

$$\frac{dI}{dt} = \alpha E - \omega I - \mu I = f_3 \quad (2.22)$$

$$\frac{dR}{dt} = \omega I - \mu R = f_4 \quad (2.23)$$

Now the variation (Jacobian) matrix of the system (2.20)-(2.23) is given by:

$$J = \begin{pmatrix} \frac{\partial f_1}{\partial S} & \frac{\partial f_1}{\partial E} & \frac{\partial f_1}{\partial I} & \frac{\partial f_1}{\partial R} \\ \frac{\partial f_2}{\partial S} & \frac{\partial f_2}{\partial E} & \frac{\partial f_2}{\partial I} & \frac{\partial f_2}{\partial R} \\ \frac{\partial f_3}{\partial S} & \frac{\partial f_3}{\partial E} & \frac{\partial f_3}{\partial I} & \frac{\partial f_3}{\partial R} \\ \frac{\partial f_4}{\partial S} & \frac{\partial f_4}{\partial E} & \frac{\partial f_4}{\partial I} & \frac{\partial f_4}{\partial R} \end{pmatrix} = \begin{pmatrix} -\beta I - \mu & 0 & -\beta S & 0 \\ \beta I & -\alpha - \mu & \beta S & 0 \\ 0 & \alpha & -\omega - \mu & 0 \\ 0 & 0 & \omega & -\mu \end{pmatrix} \quad (2.24)$$

For the disease-free equilibrium,  $S_0 = N$ , and  $E = I = R = 0$ . Now from (2.24)

$$J = \begin{pmatrix} -\mu & 0 & -\beta N & 0 \\ 0 & -\alpha - \mu & \beta N & 0 \\ 0 & \alpha & -\omega - \mu & 0 \\ 0 & 0 & \omega & -\mu \end{pmatrix}$$

Now, the characteristic polynomial equation is,  $|J - \lambda I| = 0$

$$\Rightarrow \begin{vmatrix} -\mu - \lambda & 0 & -\beta N & 0 \\ 0 & -\alpha - \mu - \lambda & \beta N & 0 \\ 0 & \alpha & -\omega - \mu - \lambda & 0 \\ 0 & 0 & \omega & -\mu - \lambda \end{vmatrix} = 0$$

$$\Rightarrow (-\mu - \lambda)(-\mu - \lambda) \begin{vmatrix} -\alpha - \mu - \lambda & \beta N \\ \alpha & -\omega - \mu - \lambda \end{vmatrix} = 0$$

Here, we are searching for roots of the characteristic equation to discover whether the equilibrium is stable or unstable. If the real parts of all of the roots are negative then the equilibrium is not only stable but also asymptotically stable. If one of the roots is zero and the others are negative then the equilibrium is stable but not asymptotically stable. Further, if the real part of one of the roots is positive then the equilibrium is unstable.

$$\Rightarrow (-\mu - \lambda)(-\mu - \lambda) = 0 \text{ and } \begin{vmatrix} -\alpha - \mu - \lambda & \beta N \\ \alpha & -\omega - \mu - \lambda \end{vmatrix} = 0$$

$$\Rightarrow \lambda_1 = -\mu, \text{ and } \lambda_2 = -\mu$$

Rather than directly calculating the eigenvalues of the two by two matrix given above we can instead invoke several simple eigenvalue properties that will allow us to determine their sign. In particular, for a two by two matrix A, we have

$$\text{tr}(A) = \lambda_1 + \lambda_2, \quad \text{and}$$

$$\det(A) = \lambda_1 \lambda_2$$

where  $\text{tr}(A)$  and  $\det(A)$  are the trace and determinant of the matrix A respectively. Hence, for the matrix A to be considered stable, we require

$$\text{tr}(A) < 0, \text{ and}$$

$$\det(A) > 0.$$

$$\text{Now trace}(J) < 0: -\alpha - \mu - \omega - \mu < 0$$

$$\Rightarrow (\alpha + \mu) + (\omega + \mu) > 0 \tag{2.25}$$

$$\det(J) > 0: (\alpha + \mu)(\omega + \mu) - \alpha\beta N > 0$$

$$\Rightarrow (\alpha + \mu)(\omega + \mu) > \alpha\beta N$$

$$\Rightarrow \frac{\alpha\beta N}{(\alpha + \mu)(\omega + \mu)} < 1$$

$$\Rightarrow R_0 < 1 \tag{2.26}$$

Hence, the disease-free equilibrium of the basic model is locally asymptotically stable when  $R_0 < 1$ , which means that the disease will naturally die out in this case.

$$\text{For the disease endemic equilibrium, } S^* = \frac{N}{R_0}, E^* = \frac{\mu N(R_0 - 1)}{(\alpha + \mu)R_0}, I^* = \frac{\mu(R_0 - 1)}{\beta} \text{ and } R^* = \frac{\omega(R_0 - 1)}{\beta}$$

Now from (2.24)

$$J = \begin{pmatrix} -\beta I^* - \mu & 0 & -\beta S^* & 0 \\ \beta I^* & -\alpha - \mu & \beta S^* & 0 \\ 0 & \alpha & -\omega - \mu & 0 \\ 0 & 0 & \omega & -\mu \end{pmatrix}$$

$$\text{Now the Jacobian matrix is, } J = \begin{pmatrix} -\mu R_0 & 0 & -\frac{\beta N}{R_0} & 0 \\ \mu(R_0 - 1) & -\alpha - \mu & \frac{\beta N}{R_0} & 0 \\ 0 & \alpha & -\omega - \mu & 0 \\ 0 & 0 & \omega & -\mu \end{pmatrix}$$

Now  $\lambda_1 = -\mu$  which allows us to consider the following reduced Jacobian matrix:

$$\bar{J} = \begin{pmatrix} -\mu R_0 & 0 & -\frac{\beta N}{R_0} \\ \mu(R_0 - 1) & -\alpha - \mu & \frac{\beta N}{R_0} \\ 0 & \alpha & -\omega - \mu \end{pmatrix}$$

To determine the stability of this matrix we use the Routh-Hurwitz criteria. Specifically, all of the roots of the characteristic polynomial associated with a three by three matrix A are negative if  $A_1 > 0, A_2 > 0, A_3 > 0$ , and  $A_1 A_2 > A_3$ .

Here,  $A_1 = -\text{tr}(A)$ ,  $A_2$  represents the sum of the two by two principal minors of A and  $A_3 = -\det(A)$ .

For the matrix  $\bar{J}$  we then have  $-A_1 = -\mu R_0 - \alpha - \mu - \omega - \mu$

$$\Rightarrow A_1 = \alpha + 2\mu + \omega + \mu R_0$$

which will always be positive for positive (plausible) parameters values for  $\alpha, \beta, \omega$  and  $\mu$ .

$$A_2 = \begin{vmatrix} -\alpha - \mu & \frac{\beta N}{R_0} \\ \alpha & -\omega - \mu \end{vmatrix} + \begin{vmatrix} -\mu R_0 & -\frac{\beta N}{R_0} \\ 0 & -\omega - \mu \end{vmatrix} + \begin{vmatrix} -\mu R_0 & 0 \\ \mu(R_0 - 1) & -\alpha - \mu \end{vmatrix}$$

$$\Rightarrow A_2 = (\alpha + \mu)(\omega + \mu) - \frac{\alpha\beta N}{R_0} + \mu R_0(\omega + \mu) + \mu R_0(\alpha + \mu)$$

$$A_2 = (\alpha + \mu)(\omega + \mu) - \frac{\alpha\beta N}{R_0} + \mu R_0(\alpha + 2\mu + \omega)$$

$$\text{Again } -A_3 = \begin{vmatrix} -\mu R_0 & 0 & -\frac{\beta N}{R_0} \\ \mu(R_0 - 1) & -\alpha - \mu & \frac{\beta N}{R_0} \\ 0 & \alpha & -\omega - \mu \end{vmatrix}$$

$$\Rightarrow -A_3 = -\mu R_0 \left( (\alpha + \mu)(\omega + \mu) - \frac{\alpha\beta N}{R_0} \right) - \frac{\beta N}{R_0} (\alpha\mu(R_0 - 1))$$

$$\Rightarrow -A_3 = -\mu R_0(\alpha + \mu)(\omega + \mu) + \alpha\beta N\mu - \alpha\beta N\mu + \frac{\alpha\beta N\mu}{R_0}$$

$$\Rightarrow A_3 = \mu R_0(\alpha + \mu)(\omega + \mu) - \frac{\alpha\beta N\mu}{R_0}$$

$$\Rightarrow A_3 = \mu R_0(\alpha + \mu)(\omega + \mu) - \mu(\alpha + \mu)(\omega + \mu)$$

$$\Rightarrow A_3 = \mu(\alpha + \mu)(\omega + \mu)(R_0 - 1)$$

Now to satisfy the condition  $A_1 > 0$ , requires that  $\alpha + 2\mu + \omega + \mu R_0 > 0$

$A_2 > 0$ , requires that

$$\Rightarrow (\alpha + \mu)(\omega + \mu) - \frac{\alpha\beta N}{R_0} + \mu R_0(\alpha + 2\mu + \omega) > 0$$

$$\Rightarrow (\alpha + \mu)(\omega + \mu) - (\alpha + \mu)(\omega + \mu) + \mu R_0(\alpha + 2\mu + \omega) > 0$$

$$\Rightarrow \mu R_0(\alpha + 2\mu + \omega) > 0$$

which will always be positive for positive (plausible) parameters values for  $\alpha$ ,  $\beta$ ,  $\omega$  and  $\mu$ .

Similarly we require that  $A_3 > 0$  which implies

$$\Rightarrow \mu(\alpha + \mu)(\omega + \mu)(R_0 - 1) > 0$$

$$\Rightarrow \mu(\alpha + \mu)(\omega + \mu) > 0 \text{ and } R_0 > 1$$

Finally, for local stability of the steady state we require  $A_1A_2 > A_3$ , which implies

$$\Rightarrow \mu R_0(\alpha + 2\mu + \omega)(\alpha + 2\mu + \omega + \mu R_0) > \mu(\alpha + \mu)(\omega + \mu)(R_0 - 1)$$

$$\Rightarrow \mu R_0(\alpha + 2\mu + \omega)^2 + \mu^2 R_0^2(\alpha + 2\mu + \omega) + \mu(\alpha + \mu)(\omega + \mu) > \mu R_0(\alpha + \mu)(\omega + \mu)$$

which will always be positive for positive (plausible) parameters values for  $\alpha$ ,  $\beta$ ,  $\omega$  and  $\mu$ , and provided  $R_0 > 1$ .

Hence, the system satisfies the Routh-Hurwitz criteria, meaning that if  $R_0 > 1$ , the endemic equilibrium is stable and the disease persists in the population (in the compartmental model).

Various types of TB mathematical models extend the SEIR model to consider different types of contributing factors, which I will now discuss.

## 2.8.4 TB model extensions

### 2.8.4.1 Heterogeneity

As stated earlier, there are numerous contributing factors responsible for TB disease burden. The impact of demographic variables is well recognized to influence the incidence of TB disease. Hence, quite reasonably, there are a number of modelling efforts that consider heterogeneity in the population and individual level risk of developing TB. Murphy *et al.* (2002) used a modified Susceptible Exposed Infected (SEI) model to investigate the effects of genetic susceptibility and demographic factors on TB epidemiology in a heterogeneous population, and compared the prevalence and incidence in India and the United States of America (USA) [151]. Here, the authors investigated the impact of specific parameters related to genetic susceptibility on the levels of TB prevalence and incidence. The findings of this study showed that the variance of infectiousness has a greater impact on the genetically susceptible population and demographic factors including closed environments and access to health care strongly affect TB prevalence and incidence rates. One limitation was that the study did not take into account host related factors (nutrition status, existing illness and low immunity), migration and an over-populated environment. Nutritional status is a particularly potent disease modifier in TB [152].

#### **2.8.4.2 New data**

In low and high burden countries, TB control and eradication continues to be a challenge for public health policy makers and respective governments. New technological advantages and novel methods for case discovery, diagnosis and management are very important to include in models to investigate whether these should be incorporated into TB control programs and if so in what way they could optimally be deployed. Additionally, they need to be assessed for cost-effectiveness. This leads to improved understanding of TB epidemiology and the cost-effective analysis of different interventions. White and Abubakar (2016) developed a mathematical model of TB to understand the epidemiological situation and control strategies of TB as well as better manage public health intervention methods [153]. This model also extended the ability of collecting long term data and balanced experimental research with surveillance and observational studies. This study illustrated demographic and contact patterns, various work places, various living settings, and access to health care services for diagnosis and immigration that can affect transmission in a population. By combining high quality epidemiological data incorporating interaction tracing, detailed risk factor records and contact history, mathematical modelling can offer the prospect of new understandings [153].

#### **2.8.4.3 Social contact (infections network) structure**

Pienaar *et al.* (2010) developed a mathematical model with sociological factors [154]. In this model, the total city population consisted of four compartments: susceptible (S); latently infected (L); infectious (I); and recovered (R). The transmission dynamics model differentiates between three different social forms of contact / exposure: contact with commuters for the period of travel, continuous daytime communication, and family member exposure at night time. The major finding of this study was that large family size is responsible for more disease transmission than small family size, and daily travellers on public vehicles provide the ideal situation for the transmission of TB disease. Furthermore, the model also projected that improved treatment and diagnosis minimized the spread of TB disease.

#### **2.8.4.4 Investigating combinations of interventions**

Mathematical modelling has played a significant role in giving us some understanding of which combination of control processes would be more effective in decreasing the burden of active TB. Kim *et al.* (2014) developed a mathematical model for TB with exogenous reinfection and examined the current situation of active TB incidence in Korea [155]. In this study, the SEIR-style compartment model was deployed. The study showed active TB incidence can be calibrated to the observational data. The study showed that the case detection rate was the most important intervention for decreasing active TB cases. This study also observed that focus on treatment alone or case discovery alone will not

dramatically affect the decline in active TB incidence. In contrast, taking two or more key parameters simultaneously is the most effective way to decrease the burden of active TB cases.

#### **2.8.4.5 Accounting for seasonality**

Seasonality is a factor that can increase the outbreak of TB disease. Liu *et al.* (2010) developed a compartmental transmission dynamics TB model with seasonality to describe TB incidence rates with periodic properties in a mainland city of China [156]. This study showed the seasonal trend of new TB cases was highest in late spring to early summer, reaching the lowest point in late winter and early spring. This seasonal pattern may be linked to the Chinese Spring Festival because, at this time, entire families live in overcrowded, poorly ventilated rooms and have more frequent viral infections that can cause immunological vulnerability, hence, reactivation of or reinfection with *Mtb*. The model fitted very well with surveillance data according to the seasonal variation of the reported cases of active TB in China, and made predictions about incidence as well as prevalence.

Yang *et al.* (2016) developed another TB model with seasonality and determined that seasonality has high impact on TB related incidence, prevalence and mortality especially in the winter season [157]. The study observed that, during the winter season, indoor activities are much more frequent than during the summer season, which increases the probability of susceptible persons being exposed to *Mtb* from infectious persons because of reduced ventilation indoors. Furthermore, cold weather and lack of sunshine are common in the winter season which may decrease human immunity and lower vitamin D levels which may increase the reactivation of TB cases. In addition to Liu *et al.*, Yang *et al.* found that if the basic reproduction number of the seasonality model was less than one then the disease free equilibrium was globally asymptotically stable; if it is greater than one then TB disease persists in the population. Understanding the transmission dynamics of TB disease and predicting the disease patterns which may help health policy makers to implement supplementary defensive interventions in TB control throughout the period of greater threat of TB infection [156, 157]. Bangladesh has seasonal patterns and some data available to estimate humidity, temperature and rainfall. I used this data to investigate the degree of correlation between weather factors and TB incidence in Bangladesh in Chapter 3.

#### **2.8.4.6 Importation travel and exportation of TB infection**

Liu *et al.* (2018) deployed a two-patch SIS model with infection through transportation. This study examined two different categories of incidence rate: standard incidence within each patch and mass-action incidence through transportation [158]. The total population was divided into two compartments,

the susceptible population,  $S$ , and the infective population,  $I$ . The study demonstrated that if we set one travel rate, say  $m_{21}$  (the travel rate from patch 2 to patch 1) as a constant, then the infection level in the interior patch 1 will drop as  $m_{12}$  (the travel rate from patch 1 to patch 2) rises, and the infection level in the interior patch 2 will rise as  $m_{12}$  rises. An additional finding was that if the population mixed randomly over time, the entire population had a standard incidence rate in the interior of each patch. Furthermore, in the presence of travel for a given mass-action infection rate, there was a higher level of infection in each patch than would be predicted if no travel occurred [158].

#### **2.8.4.7 Demographic structure**

Age is an important influencing factor that can increase the occurrence of TB disease. Graciani *et al.* (2015) structured an agent-based model (ABM) to examine TB in the elderly [159]. The main idea of this model was to investigate how public health policies may affect the age prevalence of TB in a population. Graciani *et al.*'s TB model had two layers: an agent-based model and a biological elderly model. The first model simulated the spread of TB in a population, allowing the emergence of drug resistance, and the second model was a population computational model founded on cumulative changes in an individual's genome with age. Therefore, the combined model permitted the spread of TB in a scheme in which the population ages. The findings of this study showed that the prevalence of TB mostly in elders, for high efficacy treatments. Further, this study also performed that the model can be fitted to reproduce quantitative results, such as the spread of TB, with more accuracy including actual infectious networks.

Blaser *et al.* (2016) constructed a transmission dynamics TB model to observe the influence of age-structure (up to 50 years) in TB report rates [160]. The Cape Town, South Africa study results showed the first peak occurred in children, due to high transmission, and the second peak described the comparatively fast reactivation rate in early adulthood leading to a rise in incidence among 30 to 50 year olds. Sensitivity analysis showed age-pattern TB rates generally depend on the protection afforded by earlier latent infection. If there is no protective effect of previous latent infections, TB rates drop around the age of 25 years, disappear in early adulthood, until reappearing and persisting at high rates in late adulthood. Therefore, Blaser *et al.* recommended that TB interventions such as DOTS, Isoniazid Preventive Therapy (IPT), TB screening, and ART in HIV-infected TB patients must take age into account. IPT and rapid case discovery may be mainly significant in young adults considering the fast progression rates in early adulthood [160]. Kunkel *et al.* (2016) developed another mathematical model with IPT to observe the impact of IPT duration on the incidence of isoniazid-sensitive and isoniazid-resistant TB and found that continuous IPT on isoniazid-resistant TB incidence may erode its initial benefits [161]. They also found that a continuous IPT program was the most useful strategy for quickly dropping the burden of TB.

Guzzetta *et al.* (2011) developed an age-structured and socio-demographic individual-based time-dependent TB mathematical model [162]. This model considered social-contact factors such as households, workplaces and schools, casual contacts, and distance-dependent contacts. Results showed inclusion of age structure captures substantial amounts of the observed reactive TB cases. The socio-demographic structure provided a forecast of TB transmission rates of infection in household contacts, and the rate of relapse cases in household, school and workplace contacts. Therefore, the socio-demographic individual-based model is an ideal choice for assessment of current control policies, including contact network inquiry of index cases, and simulation of different circumstances for TB elimination goals [162-164].

Brooks *et al.* (2010) developed a TB mathematical model with survivorship to discover the impact of age structure on the prevalence of TB, the basic reproduction number, and the effect of control interventions [165]. This model emphasises the differences between constant and exponentially spread lifespans, and implements an individual-based model to examine the variety of behaviour arising from accurate distributions of survivorship. The model demonstrated natural mortality, and age structure plays an important role for transmission dynamics of TB. Three different age characterizations of survivorship were explored: constant life periods, exponential spread life periods, and hazard of mortality that rises exponentially. The results showed survivorship intensely affects steady state dynamics, parameter approximation, and forecasts about the usefulness of control interventions. For example, the constant life period assumption results in a greater prevalence of TB disease than exponential life periods.

TB in children is gradually being recognized as a major public health problem and a vital element of the total burden of TB [166]. TB transmission occurs via tiny aerosols (cough, sneeze) from someone with active pulmonary TB that contact a susceptible person. Children younger than around 10 years with TB of the lungs rarely infect other people because they have very few bacteria in their mucus secretions. However, young children with *Mtb* have a high risk of progressing to active TB. To determine the impact of TB in children, Dodd *et al.* (2016) developed a mathematical model of TB in children with different types of DR-TB to simulate regional, national, and global levels of DR-TB infection [167]. The model estimated that 850,000 children worldwide were infected with *Mtb* in 2014, 58,000 with isoniazid mono-resistant *Mtb*, 25,000 with multidrug-resistant *Mtb* and 12,000 with extensively drug-resistant *Mtb*. This study estimated that South-East Asia and Africa have the highest number of infections, while greater proportions of drug resistance exist in the European region. South-East Asia and the Western Pacific regions also contribute significantly to the burden of DR-TB. However, a potential limitation of Dodd *et al.*'s study was that drug resistance was not assigned a fitness cost. Moreover, the proportion of first-line drug-resistant *Mtb* in treatment naive patients should be

reflected in children and the authors did not include any uncertainty in relation to this parameter [167]. In contrast, Luciani *et al.* (2009) claimed that drug resistance is associated with treatment fitness cost [168]. The acquisition of resistance to antibiotics results in a longer duration of infection and may increase the duration of treatment as well as imposing a transmission fitness cost [168], two forces acting in opposite directions. Thus more studies are needed to investigate the likelihood of MDR dominating in a given situation, as I addressed in Chapter 4 and Chapter 5 of this thesis.

#### **2.8.4.8 TB model with different types of interventions**

For the possible eradication and control of TB, mathematical modelling allows simulation of the potential effect of interventions, and identifies areas where additional research is needed to improve realism of models and accuracy of inferences [169]. Mathematical modelling can provide credible evidence about the value of intervention programs and guide the improvement of interventions [170]. Models can estimate different risk factors of TB epidemiology under the influence of novel interventions. One of the most effective ways of describing interventions is their impact on the effective reproduction ratio [170]. Significantly, better communication between modellers and experimentalists or field staff will be needed to improve the questions, determine which data are significant and most immediately wanted, and to ensure that the analytical research leads to better strategies and better control [99].

##### **2.8.4.8.1 Modelling prevention of TB by treatment of latent *Mtb* infection**

According to many models, isoniazid preventive therapy (IPT) is the most effective TB treatment strategy to reduce TB incidence; however, this is not universally accepted at an implementation level and has been deployed in low-burden countries rather than high burden countries. To describe the relation between TB incidence and IPT effectiveness as a control strategy, Ragonnet *et al.* (2017) developed a transmission dynamic TB mathematical model and examined IPT impact under several epidemiological situations [171]. This study showed that to prevent one case of active TB, the lowest number needed to treat with IPT, and IPT effect, is highest at an intermediate incidence level, of around 800 per 100,000, and impact is reduced at both lower and higher incidence settings. The authors argued that TB burden is a serious issue and total disease burden should not prevent programmatic implementation of IPT.

Whang *et al.* (2011) constructed a time-dependent transmission dynamic SEIR TB model in South Korea [172]. Numerical techniques such as least-squares fitting were used for assessing the model parameters. Three strategies were used to reduce the future number of exposed and infectious TB individuals. Three control tools: expressive isolation (the evidence that persons have the ability to

isolate), case discovery and case holding efforts were considered. The isolation control strategy was modelled as a reduction in the transmission rate, hence a reduction in susceptible persons infected from infectious persons. The case finding control strategy represents the prevention of disease development with effective treatment for exposed persons or identification of active TB cases. The case holding control strategy was modelled as an initiative to reduce the relapse rate following treatment, such as improved care of TB patients up to complete treatment. This study showed if the model used single-control strategies, then the isolation control strategy was the most effective. Furthermore, this study also showed that the case holding strategy is more effective than the case finding strategy to decrease the number of exposed and infectious persons.

#### **2.8.4.8.2 Modelling completion of therapy rates**

The usefulness of the treatment policy depends on patients finishing proper treatment [1]. Incomplete treatment can leave patients infectious and symptomatic. Yang *et al.* (2010) developed two transmission dynamic compartmental TB models with incomplete treatment [173]. The first model incorporated incomplete treatment in a total population partitioned into four compartments: susceptible compartment (S), which indicates persons who have not yet been infected by TB; latent compartment (L), which means persons who have been infected but are not infectious; infectious compartment (I), which indicates persons are infectious but not being treated; and treatment compartment (T), which means persons who are being treated. When an infectious person is identified, he/she will enter the treatment compartment and be treated. However, in the second model, some TB susceptible persons may be affected by other chronic diseases, such as HIV and diabetes, which can decrease the capability of the immune system. Therefore, in persons without HIV and diabetes, the latent period of TB may be longer than that of persons with these diseases, and the latent compartment is divided into two stages. When an infectious individual is detected, he (she) will move to treatment compartment and be treated. After leaving the treatment compartment, an individual may enter infectious compartment due to the failure of treatment. The next generation matrix and Lyapunov function method [174] was used to determine the basic reproduction number and perform a stability analysis. The study showed that when the basic reproduction number is lower than unity, the disease eventually dies out. In contrast, when the basic reproduction number is greater than one, then the endemic equilibrium is unstable, which means that the disease persists in the population. Further, this study also revealed that reducing treatment failure is useful to reduce TB infection [173]. The realization of reducing treatment failure mainly depends on reducing the appearance of drug resistance. On the other hand, increasing the per-capita treatment rate has positive impact of TB control.

### **2.8.4.8.3 Models which address vaccination**

Statistics show that the BCG vaccine is very effective for young children to reduce the number of TB cases [175]. However, at an individual level BCG vaccination is only partly effective and this effect is thought to wane over time, but when modelled at a community level the impact is much higher. To evaluate the effect of vaccination, Mishra and Srivastava (2014) developed a transmission dynamic mathematical model to simulate the spread of TB disease in the human population of Jharkhand, India, for DS and MDR-TB cases with vaccination [176]. The main strategies of this model were vaccination, modelled by moving the susceptible population to the vaccination class, and quarantine (for MDR-TB only). The authors found that these two factors are interactive and synergistic for TB control. They also found that if the vaccination coverage rate is high then there would be a significant reduction of TB incidence. Other studies support the notion that BCG vaccination is very effective and is an important contributing factor for controlling TB worldwide because BCG vaccine develop body immunity against the disease [176-178].

### **2.8.4.8.4 Modelling increased case detection through raised awareness**

Okuonghae and Ikhimwin (2015) developed a realistic compartmental transmission dynamic TB model to investigate the impact of case detection rate [179]. According to the awareness level of the population, Okuonghae and Ikhimwin divided susceptible persons into two groups: the high risk group (low level of awareness), and low risk group (high level of awareness), and incorporated an active case discovery parameter. The authors stated that TB treatment alone may not significantly reduce TB burden at the community level but if we take two or more parameters together, such as treatment, awareness and active case finding, then it may be possible to reduce TB burden.

### **2.8.4.8.5 Modelling multiple interventions**

Multiple interventions modelling is essential to explore more substantial and sustained changes in behaviours related to TB prevention, detection and treatment than a single intervention. It is an important way of expanding our knowledge to assess the impact of multiple interventions outcomes at different levels on TB patients. A 10-compartmental TB model constructed by Trauer *et al.* (2014) modelled limited vaccine effectiveness, reinfection, MDR-TB, and de novo resistance through treatment [180]. This study showed that the model could not be standardized to the projected incidence rate without allowing for reinfection, modelled as a reversion to early latency, which has a higher rate of progression to disease compared with late latency. This model also imposes a fitness cost on drug resistance and estimates the importance of the basic reproduction number,  $R_0$ . Furthermore, the model found that the most significant influencing factor of TB disease is the detection rate and treatment

completion rates, whereas vaccination rate is less significant which may be possible due to the short term run of this model. In contrast, some studies argued that the vaccination coverage rate is very important to reduce TB incidence [176, 178].

Moualeu-Ngangue *et al.* (2015) constructed a compartmental transmission dynamics TB model in Cameroon [181]. This model incorporated lack of access to medical care, weak diagnosis capability, lack of evidence about the infected individual's location, role of traditional drugs, and considered the different dynamics using frequency versus density dependent transmission. For the density dependent transmission, the per capita contact rate between susceptible and infected persons depends on the population density. Therefore, transmission rates increase with population density. On the other hand, in frequency dependent transmission, the contact rate per person is assumed to be constant and not scale with density of the population [182]. Three infective subclass populations were considered: diagnosed infectious; undiagnosed infectious; and lost-sight individuals (active TB patients who have been diagnosed and started their treatment and are lost to follow-up). In developing countries throughout Asia and Sub-Saharan Africa, where the public health system is less developed, the undiagnosed and lost-sight subclasses are very significant for the burden of TB. Detailed sensitivity analysis was performed to identify the most important parameters for the outbreak of TB. Parameter estimation was performed with a subset of unknown parameters and the estimation process was repeated with the full set of parameters to check whether the new values of earlier unknown parameters affect values of the known ones. This procedure was repeated until convergence in the parameter values occurred. This study showed that varying parameters including treatment and diagnosis can significantly decrease the disease burden in the population. These parameters can be used to predict the impact of educational and diagnosis campaign activities that encourage TB screening. The authors recommended that this model be used for optimal control strategies in order to achieve the maximum decline of TB cases in the shortest time with minimum cost [181].

Okuonghae and Omosigho (2011) developed a qualitative and quantitative approach to a transmission dynamics TB mathematical model in Benin City, Nigeria [183]. The major purpose of this model was to identify some factors that could improve the case detection rate of TB. In this model, the susceptible population was separated into two groups depending on awareness of TB, with S1 representing high risk (low level of TB-consciousness) and S2 indicating low risk (high level of TB-consciousness). Infected people can enter the S1 or S2 group depending on the effectiveness of the education program. Four types of key factors increased the case detection rate: population consciousness; active cough identification; cost of treatment; and treatment effectiveness. A qualitative approach to calculating the basic reproduction number identified how the different control strategies could lead to a reduction in transmission under treatment. This study showed that developing a TB awareness program and increasing the active cough identification rate decreased the TB burden in the population, ultimately

bringing down the basic reproduction number under unity. Furthermore, mutually raising the TB consciousness program and lowering the cost of treatment in recognized cases can also decrease the basic reproduction number below unity [183].

To assess the influence of vaccination and treatment on the spread of TB disease, Liu and Zhang (2011) developed a compartmental transmission dynamics model [184]. In this model, the population was subdivided into five classes: the susceptible (S) population; the vaccinated (V) population; persons infected with TB in the latent stage (L); persons infected with TB in the active stage (I); and treated persons infected with TB (T). The model showed that if the basic reproduction number is less than one, then the disease-free equilibrium is globally asymptotically stable, and if the basic reproduction number is greater than one, then there is an endemic equilibrium and the disease continues. Furthermore, this model also recognized that the vaccination rate, vaccine efficacy and treatment rate also influence the effective reproduction rate, and showed that if the vaccination rate or the effectiveness or the treatment rates reach a particular threshold, then the spread of TB can be managed. Therefore, when one strategy, such as vaccination or treatment, fails to control the disease, then combination strategies will be the most effective way to eliminate TB disease transmission [184-186], as I addressed Chapter 6 and Chapter 7 of this thesis regarding multiple interventions strategies and showing that combination strategies are the most effective than single strategies.

### **2.8.5 Multidrug-resistant (MDR) and extensively drug-resistant (XDR) TB models**

In recent years, the emergence of resistance to the most effective treatment (combination therapies) has occurred in the Asia-Pacific region, and spread throughout the region, leading to a decline in the efficiency of antibiotics in treating infectious disease such as TB [187]. Resistance takes the form of delayed clearance of bacteria (or complete failure of clearance) under multi-drug treatment. Unfortunately, it does not stop there: inadequate treatment of MDR-TB may create even more resistance, with extensively drug-resistant tuberculosis (XDR-TB) strains beginning to emerge (XDR-TB is defined as MDR-TB with additional resistance to any fluoroquinolone and at least one of the three following injectable drugs: capreomycin, kanamycin, and amikacin) [188].

In 2008, Bhunu developed a three strain transmission dynamics SEIR TB model that included drug-sensitive, multidrug-resistant and extensively drug-resistant TB [189]. The centre manifold theory [190] was used to recognize the local stability of the endemic equilibrium, and it displayed the existence of backward bifurcation, with two steady-states when the basic reproduction number was lower than unity, although a single endemic equilibrium exists, and it is locally asymptotically stable when the basic reproduction number is larger than unity. However, the study showed that first-line treatment of *Mtb* strains will support a decrease in the spread of drug sensitive TB but, if these drugs are misused, then

MDR-TB cases will rise. Furthermore, MDR-TB treatment also supports a decrease in the MDR-TB burden but, if not appropriately used, then XDR-TB cases rise. Isolation of people with XDR-TB leads to a reduction in XDR-TB at a population level. In addition, numerical and analytical simulations recommend: implementing multiple control activities simultaneously; isolation of XDR cases plus treatment of drug sensitive TB cases, and MDR-TB cases, leading to a decrease in the spread of TB disease [189].

Trauer *et al.* (2016) developed a model for scenario analysis of programmatic TB control in Papua New Guinea (PNG). This model established five possible intervention scenarios [185]. The first scenario reproduced a continuation of the programmatic circumstances that had improved between 2011 and 2013. The programmatic factors used to calibrate the model to current activities were the 2013-level treatment completion rates, detection rates, and the modest capacity for treatment of MDR-TB. The second scenario involved a wide-ranging scale-up of DOTS-based programs (hence increased detection and successful completion rates). The third scenario incorporated the whole of the second scenario, with programmatic management of MDR-TB (PMDT), which included inpatient supervision during the intensive stage of treatment with parenteral antibiotics (hence increased capacity for MDR-TB treatment). The fourth scenario incorporated a modified third scenario using short course (9 month) for MDR-TB rather than what was conventional 22-month course. Finally, scenario five described a reversion of conditions to previous detection and success rates set at 2011 levels. This study showed that maintenance of current programmatic management strategies, overall TB incidence persisted at 555 per 100,000 population per year but the proportion of MDR-TB cases increased from 16% to 35%. Furthermore, wide-ranging establishment of current programs in the province decreased incidence to 353 per 100,000 population per year with 46% of existent cases being MDR-TB. In addition, including programmatic management of MDR-TB into these programs decreased incidence to 233 per 100,000 population with 14% of existent cases being MDR-TB. Moreover, this study also showed that to reduce the associated economic costs, community based treatments are very important [185].

Trauer *et al.* (2016) also developed another transmission dynamic model of TB to examine the effect of a short-course MDR-TB schedule in a high HIV prevalence area of Karakalpakstan, Uzbekistan, which had high rates of drug resistance, good availability of diagnostics, and a well-structured community based MDR-TB cure of around 400 patients [191]. This study found that if the treatment bottleneck is based on availability of places in an MDR-TB treatment program, then converting from a long-course to a short-course schedule increases the number of MDR-TB treatments. As a consequence, MDR-TB incidence is reduced from 15.2 to 9.7 cases per 100,000 population per year, and MDR-TB mortality from 3.0 to 1.7 deaths per 100,000 population per year. Moreover, a series of studies showed that short-course MDR-TB treatment schedules also promises to decrease transmission of a resistant strain for individual patients [191-193].

Different types of susceptibilities play a vital role in the transmission dynamics of TB. Okuonghae (2013) developed a mathematical model that separates various types of susceptibility among the population [194]. This study identified three groups of susceptible populations: susceptible with no resistance (S1); susceptible with partial resistance (S2); and susceptible with whole resistance (S3). The assumption of this model was that S3 persons never become infected. The same strategy was also applied for latently infected persons, divided into three groups: latently infected persons who rapidly develop active TB (E1); normal developers (E2); and none or very slow developers (E3). A further assumption was that E3 persons will have little or no reactivation rates throughout progression to active TB. Furthermore, I1 represented infectious persons from the rapid development compartment E1, and I2 represented the infectious persons from the normal development compartments E2 and E3. T1 indicated well-treated persons whose infections were produced by the rapid development compartment, and T2 indicated well-treated persons whose infections were produced from the normal or very slow development compartment. Assuming this model and estimating the fraction of people in each group, this study showed that the largest portion of susceptible persons had no or partial resistance to acquiring infection, and transfer into the normal development compartment. However, even in the worst case situation of having a high transmission rate, the disease can be controlled with effective and wide-ranging treatment. However, this study did not include the effect of vaccination, the effect of incomplete treatment, latent cases treatment, and migration of infected persons [194]. In contrast, numerous studies showed that those factors have high impact of TB related incidence, prevalence, and mortality [151, 176, 195].

### **2.8.6 Cost-effectiveness TB models**

Treatment of DS-TB is relatively straightforward: first-line combination therapy (isoniazid, rifampicin, ethambutol and pyrazinamide) taken for a minimum of six months [1]. Treatment of DR-TB is more lengthy and complex, e.g. treatment of MDR-TB takes approximately nine to 24 months, and typically incorporates a combination of both first and second line agents [1]. Several mathematical models measuring anti-TB drug activity are available but it is yet not clear which combination of agents leads to optimal DS and MDR-TB treatment efficiency with satisfactory cost-effectiveness [196-198]. Given the huge burden of MDR-TB and the paucity of data on combinations of regimens, there is a strong need for further research into drug combinations to identify novel, possibly powerful, anti-TB schedules and their conversion into clinical practice [199-201].

Novel shortened schedules have possible benefits, such as improving consequences through increased compliance, reduced time to cure, and reduced costs incurred by patients and the health system during treatment. While a number of randomised controlled trials for novel anti-mycobacterial agents are

underway, these are time consuming and costly and furthermore are limited to one or two combinations of therapies. Clearly there is a potential role for modelling to provide insights into candidate rational drug combinations. Gomez *et al.* (2016) established an individual-based model to measure the cost-effectiveness of a theoretical four-month schedule for first line treatment of TB and assumed non-inferiority to present schedules of a six-month period [202]. The individual-based model was populated using wide-ranging, empirically collected data to assess the economic effect on both patients and health systems' schedule shortening for first line TB treatment. This study found that dropping the period of first line treatment of TB has the possibility of considerable financial gains from the patient's perspective. The possible financial gains for health facilities may also be significant but depend on the proper pricing of any new schedule [203].

Aljayyoussi *et al.* (2017) developed a cost-effectiveness intra-host TB model and established that the kill-time of the intracellular *Mtb* sub-population is the critical factor for determining the clinical TB treatment period [204]. The model showed that greater doses of (35 mg/kg) rifampicin will decrease the treatment period. Aljayyoussi *et al.*'s model recommended a decision-making tool for the identification and prioritization of new therapies, to investigate the value and potential to decrease the TB treatment period.

In most countries, TB therapy has sub-optimal outcomes due to poor completion rates, reflective of the extensive duration of therapy [1]. With the rapid emergence of multidrug-resistant *Mtb* strains, the situation is further complicated. Therefore, TB control policy makers need to prioritise new drugs with important therapeutic activities against single or multiple drug-resistant strains of *Mtb* that permit a decrease in the period of treatment [205]. Jayaram *et al.* (2003) developed a model to identify reduction in therapy period for rifampicin [201]. This model estimated the association with bactericidal efficacy and rifampicin dose. This model predicted increasing rifampicin doses from 10 to 15 mg/kg reduces the duration of treatment by one-third to achieve a comparable concentration-time curve ratio.

The incidence of DS-TB has marginally decreased worldwide but the incidence of MDR-TB has increased due to poor treatment regimens. Diel *et al.* (2015) constructed a transmission dynamic stochastic and cohort-based Markov model for simulating the therapy costs and effectiveness parameters of newly diagnosed German MDR-TB patients (background regimen with and without the addition of Delamanid over a 10-year period) [206]. The first outcome of the model was incremental cost per quality-adjusted life year (QALY) gained: this is the net cost of achieving a rise of one QALY compared with the next less expensive intervention. The secondary outcome incorporated the incremental costs per disability-adjusted life years (DALYs) averted, which is usually used by the WHO for assessing effectiveness in developing countries. The results of this study showed that German Delamanid is usually cost-effective when compared to the background regimen alone. From a societal

perspective, Delamanid leads to greater benefit at lower costs compared to the background regimen in terms of incremental cost per QALY in 71% of wholly probabilistic expectations [206].

Although effective TB drug treatment prevents around 2 million deaths each year worldwide, in the case of MDR-TB, effective treatment in terms of response to second line drugs is complicated. Resch *et al.* (2006) constructed a dynamic state-transition model of TB to predict the health benefits and cost-effectiveness of drug susceptibility-testing and second line drugs in lower and middle income countries with high levels of MDR-TB [207]. This study showed standardized schedules could be cost-effective when a test for MDR-TB is used before enrolling previously treated patients into second line drug therapy. In addition, second line drug therapy was shown to be highly cost-effective for MDR-TB patients in lower and middle income countries. Furthermore, the attractiveness of policies using second line drugs depends on the MDR-TB burden, TB incidence, and the available budget, but individualized schedules would be cost-effective in an extensive range of circumstances [207].

During a treatment period, better supervision of DS cases can help to prevent the growth of drug resistance. An estimated 75% of MDR-TB cases occur in people who have been treated for TB before, and the spread of resistant strains within a population is the main problem [208]. Therefore, control of MDR-TB needs prevention of both developed drug resistance and transmission as well as effective diagnosis and treatment. In 2010, the WHO recommended that a healthcare intervention is extremely cost-effective if the cost per DALY averted is less than per capita GDP. Fitzpatrick and Floyd (2012) developed a cost-effectiveness model and found that in all sub regions, the cost per DALY averted for MDR-TB treatment could be less than per capita GDP [209]. Furthermore, the model indicated that outpatient models of care are more reasonable and cost-effective than models of care that depend on hospitalization for several months of treatment.

## **2.9 Conclusion**

TB is a well - recognized bacterial infectious disease worldwide. High level evidence through numerous randomized controlled trials shows that proper treatment and BCG vaccination are very effective for TB cure and prevention respectively. Nevertheless, TB continues to be the world's biggest infectious disease killer and the incidence rate varies dramatically, disproportionately impacting on developing countries. In developing countries such as Bangladesh, poverty and subsistent living lead to social and political obstructions that contribute to the problem. For example, people who are poor and live remote from major health centers are far less likely to seek early diagnosis, making them more likely to transmit *Mtb* to family and community. This contrasts with TB infected people in developed countries who have access to care without substantial impact on their livelihoods. In contrast, governments of developing countries may not provide sufficient funds and a number of downstream problems result including

inadequate vaccine delivery, drug stock outages in peripheral centers, poor logistics and high levels of centralization of services, poor outreach, and little awareness of TB disease [210, 211].

Challenges even exist in the realm of religion, as some religious instructions outlaw followers to consume certain elements incorporating vaccination as well [212]. In their world view,

*“Vaccination is an artificial invention made by man to alter immune function. The immune system, on the other hand, is a natural function given by God to protect us from disease. Trusting in manmade vaccination is like saying that we think God didn’t make us correctly and that we need artificial ‘boosting’ in order to survive”* [212].

These considerations are culturally sensitive, and contribute to a worrisome problem in developing countries in the Asia-Pacific region. Parents sometimes refuse vaccination against TB because of their religious beliefs and lack of knowledge [213], but if parents are educated by religious leaders who can explain both the effectiveness of vaccine and its acceptability from a religious point of view, TB disease outbreaks will be controlled [214].

Much can be learned and applied from developed to developing countries to promote resilience and recovery in those affected by the disease in developing countries. In most countries, the Ministry of Finance (MOF) controls the national budget [215] and sometimes does not understand the needs of the Ministry of Health and the negative consequences of underfunding or the economic importance of health, and that can lead to a lack of anti-bacterial medicines, and low quality services. Therefore, a good relationship between the Ministry of Health and Ministry of Finance is important for assuring sufficient budget allocation for the health sector. Additionally, good nutrition is essential for the human body. Healthy people are more alert, attentive, and healthy which protects the human body against any illness [216]. On the other hand, under-nutrition creates people who are quiet, withdrawn, and more susceptible to infection and illness. Thus, if people’s nutrition status is improved, then the incidence of TB disease may decrease.

During a TB outbreak, the host factors that influence emergence of new infections and their transmission have to be investigated and understood. Research based evidence must be developed to influence policy modification, including control plans. Mathematical modelling of TB is a way of incorporating understanding of health systems and practice, informed by accessible data to create predictions. The impacts of different policies can be estimated much more quickly than through trial in the field, which has in addition potential statistical error and sometimes feasibility problems and substantial costs. Mathematical modelling has numerous prospective tools to monitor and inform present eradication efforts such as incidence, prevalence, and case notification. Cost-effectiveness modelling considers costs against current or forecast benefits, to recommend optimum cost-effective

policies. Transmission dynamic mathematical and cost-effective modelling practices need to be joined to contribute maximum efficacy of different intervention strategies with satisfactory cost-effectiveness.

In this thesis, I performed a time series analysis to explore the association between weather variables and the number of TB cases in Bangladesh. I used a generalized linear Poisson regression models to identify quarterly changes in TB cases in three districts of Rajshahi province, in the North-West of Bangladesh (chapter 3). I also developed a mathematical model of the transmission dynamics of DS and DR-TB in Bangladesh (chapter 4 and 5) and performed a rigorous analytical analysis of the system properties and solutions. Finally, I also assessed specific intervention strategies (chapter 6 and 7) to identify the most effective ways to control DS and MDR-TB epidemics in this region – a study that, at present, remains relatively neglected in the literature.

## References

1. WHO, *Global tuberculosis report*. WHO/HTM/TB/2017.23, Geneva, 2017.
2. Koch, R. I., *Die Aetiologie der Tuberculose: Nach einem in der physiologischen Gesellschaft zu Berlin am 24. März cr. gehaltenen Vortrage*. Zentralblatt für Bakteriologie, Mikrobiologie und Hygiene. 1. Abt. Originale. A, Medizinische Mikrobiologie, Infektionskrankheiten und Parasitologie, 1982. **251**(3): p. 287-296.
3. Golden, M. P., and Vikram, R. H., *Extrapulmonary tuberculosis: an overview*. American Family Physician, 2005. **72**(9).
4. Ducati, R. G., et al., *The resumption of consumption: a review on tuberculosis*. Memórias do Instituto Oswaldo Cruz, 2006. **101**(7): p. 697-714.
5. Frieden, T. R., et al., *Tuberculosis*. Lancet, 2003. **362**(9387): p. 887-99.
6. Ahmed, N., and Hasnain, E. S., *Molecular epidemiology of tuberculosis in India: Moving forward with a systems biology approach*. Tuberculosis, 2011. **91**(5): p. 407-413.
7. Ai, J-W., et al., *Updates on the risk factors for latent tuberculosis reactivation and their managements*. Emerging Microbes & Infections, 2016. **5**(1): p. 1-8.
8. WHO, *Global tuberculosis report 2013*. . WHO/HTM/TB/2013.11, Switzerland, 2013.
9. Prestinaci, F., et al., *Antimicrobial resistance: a global multifaceted phenomenon*. Pathogens and Global Health, 2015. **109**(7): p. 309-318.
10. Ventola, C. L., *The antibiotic resistance crisis: part 1: causes and threats*. Pharmacy and Therapeutics, 2015. **40**(4): p. 277.
11. Munita, J. M., and Arias, C. A., *Mechanisms of antibiotic resistance*. Microbiology Spectrum, 2016. **4**(2): p. 10.1128/microbiolspec.VMBF-0016-2015.
12. Kendall, E. A., et al., *What will it take to eliminate drug-resistant tuberculosis?* The International Journal of Tuberculosis and Lung Disease, 2019. **23**(5): p. 535-546.
13. Brown, K. M., et al., *Compensatory mutations restore fitness during the evolution of dihydrofolate reductase*. Molecular Biology and Evolution, 2010. **27**(12): p. 2682-2690.
14. Zignol, M., et al., *Global incidence of multidrug-resistant tuberculosis*. The Journal of Infectious Diseases, 2006. **194**(4): p. 479-485.
15. Gandhi, N. R., et al., *Multidrug-resistant and extensively drug-resistant tuberculosis: a threat to global control of tuberculosis*. The Lancet, 2010. **375**(9728): p. 1830-1843.
16. Pai, M., et al., *Tuberculosis*. Nature Reviews Disease Primers, 2, 16076. 2016.
17. Davies, P. D., *Drug-resistant tuberculosis*. 2001, SAGE Publications Sage UK: London, England.
18. Bhunu, C., *Mathematical analysis of a three-strain tuberculosis transmission model*. Applied Mathematical Modelling, 2011. **35**(9): p. 4647-4660.

19. Jabbari, A., et al., *A two-strain TB model with multiple latent stages*. Mathematical Biosciences and Engineering, 2016. **13**(4): p. 741-785.
20. Seung, K. J., Keshavjee, S., and Rich, L. M., *Multidrug-resistant tuberculosis and extensively drug-resistant tuberculosis*. Cold Spring Harbor Perspectives in Medicine, 2015. **5**(9): p. a017863.
21. Claiborne, A. B., English, A. R., and Olson, S., *The Global Crisis of Drug-resistant Tuberculosis and Leadership of China and the BRICS: Challenges and Opportunities: Summary of a Joint Workshop by the Institute of Medicine and the Institute of Microbiology, Chinese Academy of Sciences*. 2014: National Academies Press.
22. O'Donnell, M. R., et al., *A novel reporter phage to detect tuberculosis and rifampin resistance in a high-HIV-burden population*. Journal of Clinical Microbiology, 2015. **53**(7): p. 2188-2194.
23. Caminero, J., *Management of multidrug-resistant tuberculosis and patients in retreatment*. European Respiratory Journal, 2005. **25**(5): p. 928-936.
24. Sterling, T. R., et al., *Impact of DOTS compared with DOTS-plus on multidrug resistant tuberculosis and tuberculosis deaths: decision analysis*. BMJ, 2003. **326**(7389): p. 574.
25. Golub, J. E., et al., *Active case finding of tuberculosis: historical perspective and future prospects*. The International Journal of Tuberculosis and Lung Disease, 2005. **9**(11): p. 1183-1203.
26. Yaesoubi, R., and Cohen, T., *Identifying dynamic tuberculosis case-finding policies for HIV/TB coepidemics*. Proceedings of the National Academy of Sciences, 2013. **110**(23): p. 9457-9462.
27. Coulter, C., *Infection control guidelines for the management of patients with suspected or confirmed pulmonary tuberculosis in healthcare settings*. Communicable Diseases Intelligence Quarterly Report, 2016. **40**(3): p. E360-E366.
28. Harte, J. A., *Standard and transmission-based precautions: an update for dentistry*. The Journal of the American Dental Association, 2010. **141**(5): p. 572-581.
29. Gupta and Bagarhatta, *Spectrum of abdominal findings In World's deadliest infectious disease: Tuberculosis*. 2020. European Congress of Radiology 2020.
30. Paulson, T., *Epidemiology: a mortal foe*. Nature, 2013. **502**(7470): p. S2-S3.
31. WHO, *Global tuberculosis report*. WHO/CDS/TB/2019.15, Geneva. 2019.
32. WHO, *Global tuberculosis report*. WHO/HTM/TB/2010.7, Switzerland, 2010.
33. Narasimhan, P., et al., *Risk Factors for Tuberculosis*. Pulmonary Medicine, 2013. **2013**: p. 828939.
34. Lee, S. J., et al., *Risk factors for latent tuberculosis infection in close contacts of active tuberculosis patients in South Korea: a prospective cohort study*. BMC Infectious Diseases, 2014. **14**(1): p. 566.
35. Carvalho, A. C., et al., *Transmission of Mycobacterium tuberculosis to contacts of HIV-infected tuberculosis patients*. American Journal of Respiratory and Critical Care Medicine, 2001. **164**(12): p. 2166-71.
36. Diez, M., et al., *Determinants of health system delay among confirmed tuberculosis cases in Spain*. European Journal of Public Health, 2005. **15**(4): p. 343-9.
37. Prinja, S., et al., *Availability of medicines in public sector health facilities of two North Indian States*. BMC Pharmacology & Toxicology, 2015. **16**: p. 43.
38. Amo-Adjei, J., *Views of health service providers on obstacles to tuberculosis control in Ghana*. Infectious Diseases of Poverty, 2013. **2**: p. 9-9.
39. Allos, B. M., Genshelmer, K. F., Bloch, A. B., Parrotte, D., Horan, J. M., Lewis, V., and Schaffner, W., *Management of an outbreak of tuberculosis in a small community*. Annals of Internal Medicine, 1996. **125**(2): p. 114-7.
40. WHO, *Why urban health matters*. 2010.
41. Somekh, E., et al., *The burden of uncomplicated cases of chickenpox in Israel*. The Journal of Infection, 2002. **45**(4): p. 233-6.
42. Harpham, T., and Stephens, C., *Urbanization and health in developing countries*. World Health Statistics Quarterly, 1991. **44**(2): p. 62-9.
43. Alirol, E., et al., *Urbanisation and infectious diseases in a globalised world*. The Lancet Infectious Diseases, 2011. **11**(2): p. 131-41.

44. Fares, A., *Seasonality of Tuberculosis*. Journal of Global Infectious Diseases, 2011. **3**(1): p. 46-55.
45. Chowdhury, R., et al., *Seasonality of tuberculosis in rural West Bengal: A time series analysis*. International Journal of Health & Allied Sciences, 2013. **2**(2): p. 95-98.
46. Yang, Y., et al., *Seasonality Impact on the Transmission Dynamics of Tuberculosis*. Computational and Mathematical Methods in Medicine, 2016. **2016**: p. 12.
47. Talat, N., et al., *Vitamin D Deficiency and Tuberculosis Progression*. Emerging Infectious Diseases, 2010. **16**(5): p. 853-855.
48. Onozuka, D., and Hagihara, A., *The association of extreme temperatures and the incidence of tuberculosis in Japan*. International Journal of Biometeorology, 2015. **59**(8): p. 1107-1114.
49. Leung, C. C., et al., *Seasonal pattern of tuberculosis in Hong Kong*. International Journal of Epidemiology, 2005. **34**(4): p. 924-930.
50. Kan, X., et al., *Indoor solid fuel use and tuberculosis in China: a matched case-control study*. BMC Public Health, 2011. **11**(1): p. 498.
51. Gupta, K. B., Gupta, R., Atreja, A., Verma, M., and Vishvkarma, S., *Tuberculosis and nutrition*. Lung India, 2009. **26**(1): p. 9-16.
52. Lienhardt, C., Bennett, S., Del Prete, G., Bah-Sow, O., Newport, M., Gustafson, P., Manneh, K., Gomes, V. Hill, A., and McAdam, K., *Investigation of environmental and host-related risk factors for tuberculosis in Africa. I. Methodological aspects of a combined design*. American Journal of Epidemiology, 2002. **155**(11): p. 1066-73.
53. Pawlowski, A., et al., *Tuberculosis and HIV Co-Infection*. PLoS Pathogens, 2012. **8**(2): p. e1002464.
54. Restrepo, B. I., *Diabetes and tuberculosis*. Microbiology spectrum, 2016. **4**(6): p. 10.1128/microbiolspec.TNMI7-0023-2016.
55. Macallan, D. C., *Malnutrition in tuberculosis*. Diagnostic Microbiology and Infectious Disease, 1999. **34**(2): p. 153-7.
56. Ahmed, F., et al., *Dietary pattern, nutrient intake and growth of adolescent school girls in urban Bangladesh*. Public Health Nutrition, 1998. **1**(2): p. 83-92.
57. Vijayakumar, M., Bhaskaram, P., and Hemalatha, P., *Malnutrition and childhood tuberculosis*. Journal of Tropical Pediatrics, 1990. **36**(6): p. 294-8.
58. Jaganath, D., and Mupere, E., *Childhood tuberculosis and malnutrition*. The Journal of Infectious Diseases, 2012. **206**(12): p. 1809-1815.
59. Podewils, L. J., et al., *Impact of malnutrition on clinical presentation, clinical course, and mortality in MDR-TB patients*. Epidemiology and Infection, 2011. **139**(1): p. 113-20.
60. Range, N., et al., *The effect of micronutrient supplementation on treatment outcome in patients with pulmonary tuberculosis: a randomized controlled trial in Mwanza, Tanzania*. Tropical Medicine and International Health, 2005. **10**(9): p. 826-32.
61. Santos, E.W., et al., *Hematological alterations in protein malnutrition*. Nutrition Reviews, 2017. **75**(11): p. 909-919.
62. Pelletier, D. L., and Frongillo, E. A., *Changes in child survival are strongly associated with changes in malnutrition in developing countries*. The Journal of Nutrition, 2003. **133**(1): p. 107-19.
63. DGHS, *National Tuberculosis Control Program (NTP). National guidelines and operational manual for tuberculosis control, 4th and 5th edition*. 2013.
64. Narasimhan, P., Wood, J., MacIntyre, C. R., and Mathai, D., *Risk factors for tuberculosis*. Pulmonary Medicine, 2013. **2013**: p. 828939.
65. Santos, M., et al., *The epidemiological dimension of TB/HIV co-infection*. Revista Latino-Americana De Enfermagem, 2009. **17**(5): p. 683-688.
66. Clayton, K. L., Garcia, J. V., Clements, J. E., and Walker, B. D., *HIV infection of macrophages: Implications for pathogenesis and cure*. Pathogens & Immunity, 2017. **2**(2): p. 179-192.
67. Jo, E. K., *Mycobacterial interaction with innate receptors: TLRs, C-type lectins, and NLRs*. Current Opinion in Infectious Diseases, 2008. **21**(3): p. 279-86.
68. Oscarsson, P. N., and Silwer, H., *Incidence of Pulmonary Tuberculosis among Diabetics*. Acta Medica Scandinavica, 1958. **161**: p. 23-48.

69. Root , H. F., *The Association of Diabetes and Tuberculosis*. New England Journal of Medicine, 1934. **210**(3): p. 127-147.
70. Kim, S.J., et al., *Incidence of pulmonary tuberculosis among diabetics*. Tubercle and Lung Disease 1995. **76**(6): p. 529-33.
71. Jeon, C.Y. and Murray, B. M., *Diabetes mellitus increases the risk of active tuberculosis: a systematic review of 13 observational studies*. PLoS Medicine, 2008. **5**(7): p. e152.
72. Restrepo, B. I., et al., *Type 2 diabetes and tuberculosis in a dynamic bi-national border population*. Epidemiology and Infection, 2007. **135**(3): p. 483-91.
73. Rasanathan, K., Sivasankara, K. A., Jaramillo, E., and Lonroth, K., *The social determinants of health: key to global tuberculosis control*. International Journal of Tuberculosis and Lung Disease 2011. **15 Suppl 2**: p. 30-36.
74. Sengupta, S., et al., *Social impact of tuberculosis in southern Thailand: views from patients, care providers and the community*. International Journal of Tuberculosis and Lung Disease, 2006. **10**(9): p. 1008-1012.
75. Strachan, D., et al., *Vegetarian diet as a risk factor for tuberculosis in immigrant south London Asians*. Thorax, 1995. **50**(2): p. 175-180.
76. Diekema , D. S., *Improving Childhood Vaccination Rates*. New England Journal of Medicine, 2012. **366**(5): p. 391-393.
77. World-Bank, *Engendering development. A World Bank policy research report*. . Oxford University press, 2001.
78. CGD, *Center for Global Development (CGD). Education and developing world*. 2002.
79. Vikram, K., Vanneman, R., and Desai, S., *Linkages between maternal education and childhood immunization in India*. Social Science and Medicine, 2012. **75**(2): p. 331-9.
80. Levin, J. S., *Religion and health: Is there an association, is it valid, and is it causal?* Social Science & Medicine, 1994. **38**(11): p. 1475-1482.
81. Katona, P., and Katona, A. J., *The Interaction between Nutrition and Infection*. Clinical Infectious Diseases, 2008. **46**(10): p. 1582-1588.
82. Somma, D., et al., *Gender and socio-cultural determinants of TB-related stigma in Bangladesh, India, Malawi and Colombia*. The International Journal of Tuberculosis and Lung Disease 2008. **12**(7): p. 856-66.
83. Renzaho, A. M. N., *Fat, rich and beautiful: changing socio-cultural paradigms associated with obesity risk, nutritional status and refugee children from sub-Saharan Africa*. Health & Place, 2004. **10**(1): p. 105-113.
84. UNHCR, *United Nations High Commissioner for Refugees global trends 2012*. Geneva, Switzerland. 2013.
85. Greenaway, C., et al., *Tuberculosis: evidence review for newly arriving immigrants and refugees*. Canadian Medical Association Journal, 2011. **183**(12): p. E939-51.
86. Barnett, E. D., *Infectious disease screening for refugees resettled in the United States*. Clinical Infectious Diseases, 2004. **39**(6): p. 833-41.
87. Stauffer, W. M., and Weinberg, M., *Emerging clinical issues in refugees*. Current Opinion in Infectious Diseases, 2009. **22**(5): p. 436-442.
88. Zumla, A., et al., *Tuberculosis and mass gatherings-opportunities for defining burden, transmission risk, and the optimal surveillance, prevention, and control measures at the annual Hajj pilgrimage*. International Journal of Infectious Diseases, 2016. **47**: p. 86-91.
89. Nsoesie, E. O., Kluberg, S. A., Mekaru, S. R., Majumder, M. S., Khan, K., Hay, S. I., and Brownstein, J. S., *New Digital Technologies for the Surveillance of Infectious Diseases at Mass Gathering Events*. Clinical Microbiology and Infection, 2015. **21**(2): p. 134-140.
90. Memish, Z. A., et al., *Hajj: infectious disease surveillance and control*. Lancet, 2014. **383**(9934): p. 2073-2082.
91. Shin, H. J., and Kwon, Y. S., *Treatment of drug susceptible pulmonary tuberculosis*. Tuberculosis and Respiratory Diseases, 2015. **78**(3): p. 161-167.
92. Brode, S. K., et al., *Multidrug-resistant tuberculosis: Treatment and outcomes of 93 patients*. Canadian Respiratory Journal : Journal of the Canadian Thoracic Society, 2015. **22**(2): p. 97-102.

93. Trunz, B. B., Fine, P., and Dye, C., *Effect of BCG vaccination on childhood tuberculous meningitis and miliary tuberculosis worldwide: a meta-analysis and assessment of cost-effectiveness*. *The Lancet*, 2006. **367**(9517): p. 1173-1180.
94. Roy, P., et al., *Potential effect of age of BCG vaccination on global paediatric tuberculosis mortality: a modelling study*. *The Lancet Global Health*, 2019. **7**(12): p. e1655-e1663.
95. WHO, *Global tuberculosis report 2015*. WHO/HTM/TB/2015.22, Switzerland, 2015.
96. Dutta, N. K., and Karakousis, P. C., *Can the duration of tuberculosis treatment be shortened with higher dosages of rifampicin?* *Frontiers in Microbiology*, 2015. **6**: p. 1117.
97. Irwin, S. M., et al., *Bedaquiline and Pyrazinamide Treatment Responses Are Affected by Pulmonary Lesion Heterogeneity in Mycobacterium tuberculosis Infected C3HeB/FeJ Mice*. *ACS Infectious Diseases*, 2016. **2**(4): p. 251-267.
98. Mariette, X., et al., *Influence of replacing tuberculin skin test with ex vivo interferon gamma release assays on decision to administer prophylactic antituberculosis antibiotics before anti-TNF therapy*. *Annals of the Rheumatic Diseases*, 2012. **71**(11): p. 1783-90.
99. Childs, L. M., et al., *Modelling challenges in context: lessons from malaria, HIV, and tuberculosis*. *Epidemics*, 2015. **10**: p. 102-7.
100. Yirdaw, K. D., et al., *Beneficial effect of isoniazid preventive therapy and antiretroviral therapy on the incidence of tuberculosis in people living with HIV in Ethiopia*. *PLoS One*, 2014. **9**(8): p. e104557.
101. Jo, K-W., *Preventing the transmission of tuberculosis in health care settings: administrative control*. *Tuberculosis and Respiratory Diseases*, 2017. **80**(1): p. 21-26.
102. Jensen, P. A., et al., *Guidelines for preventing the transmission of Mycobacterium tuberculosis in health-care settings, 2005*. 2005.
103. Shehzad, A., et al., *Challenges in the development of drugs for the treatment of tuberculosis*. *The Brazilian Journal of Infectious Diseases*, 2013. **17**(1): p. 74-81.
104. Alipanah, N., et al., *Adherence interventions and outcomes of tuberculosis treatment: A systematic review and meta-analysis of trials and observational studies*. *PLoS Medicine*, 2018. **15**(7): p. e1002595.
105. Mitnick, C. D., et al., *Programmatic management of drug-resistant tuberculosis: An updated research agenda*. *PLoS One*, 2016. **11**(5): p. e0155968.
106. Daley, C. L., *Global scale-up of the programmatic management of multidrug-resistant tuberculosis*. *The Indian Journal of Tuberculosis*, 2014. **61**(2): p. 108-15.
107. Sodt, D., and Ersted, S., *Directly Observed Therapy (DOT) for the Treatment of Tuberculosis-Minnesota Dept. of Health*. 2005.
108. Wagner, M. M., et al., *The emerging science of very early detection of disease outbreaks*. *Journal of Public Health Management and Practice*, 2001. **7**(6): p. 51-9.
109. Matt, A., *GIS for early detection and response to infectious disease*. E-book, ESRI, printed in the United States of America. , 2009.
110. Horstick, O., Sommerfeld, J., Kroeger, A., and Ridley, R., *Operational research in low-income countries*. *The Lancet Infectious Diseases*. **10**(6): p. 369-370.
111. Trauer, J. M., Ragonnet, R., Doan, T. N., and McBryde, E. S., *Modular programming for tuberculosis control, the "AuTuMN" platform*. *BMC Infectious Diseases*, 2017. **17**(1): p. 546.
112. Menzies, N. A., et al., *Cost-effectiveness and resource implications of aggressive action on tuberculosis in China, India, and South Africa: a combined analysis of nine models*. *The Lancet Global Health*, 2016. **4**(11): p. e816-e826.
113. Timimi, H., et al., *WHO guidance on electronic systems to manage data for tuberculosis care and control*. *Journal of the American Medical Informatics Association : JAMIA*, 2012. **19**(6): p. 939-941.
114. Tanimura, T., et al., *Financial burden for tuberculosis patients in low-and middle-income countries: a systematic review*. *European Respiratory Journal*, 2014. **43**(6): p. 1763-1775.
115. Hargreaves, J. R., et al., *The social determinants of tuberculosis: from evidence to action*. *American Journal of Public Health*, 2011. **101**(4): p. 654-662.
116. Chauhan, V., and Thakur, S., *State of the globe: The global battle for survival against Mycobacterium tuberculosis*. *Journal of Global Infectious Diseases*, 2017. **9**(4): p. 129-130.

117. Zaman, K., et al., *Tuberculosis in Bangladesh: A 40-Year Review*. 11 ASCON. ICDDR,B. Scientific session, abstract book, 2007. **86**: p. 4-6.
118. WHO, *Global tuberculosis report 2011*. WHO/HTM/TB/2011.16, Switzerland, 2011.
119. WDA, *Thailand tuberculosis incidence and death rates in 2019*. 2020.
120. Banu, S., et al., *Multidrug-resistant tuberculosis in Bangladesh: results from a sentinel surveillance system*. International Journal of Tuberculosis and Lung Disease 2017. **21**(1): p. 12-17.
121. Anwar, I., Ahsan, G.U., and Tuhin, B., *Health System Financing in Bangladesh: A Situation Analysis*. American Journal of Economics, Finance and Management, 2015. **1**(5): p. 494-502.
122. Islam, M. S., and Ullah, M. W., *People's Participation in Health Services: A Study of Bangladesh's Rural Health Complex*. SSRN:<http://dx.doi.org/10.2139/ssrn.1412874>, 2009.
123. Bulage, L., et al., *The Quality of tuberculosis services in health care centres in a rural district in Uganda: The providers' and clients' perspective*. Tuberculosis Research and Treatment, 2014. **2014**: p. 685982.
124. Eisenhut, M., et al., *BCG vaccination reduces risk of infection with Mycobacterium tuberculosis as detected by gamma interferon release assay*. Vaccine, 2009. **27**(44): p. 6116-6120.
125. NTP, *Tuberculosis control in Bangladesh*. Annual report 2015.
126. Chowdhury, M. R., et al., *Social Impact of Stigma Regarding Tuberculosis Hindering Adherence to Treatment: A Cross Sectional Study Involving Tuberculosis Patients in Rajshahi City, Bangladesh*. Japanese Journal of Infectious Diseases, 2015. **68**(6): p. 461-6.
127. Hossain, M. D., et al., *Bangladesh national guidelines on the management of tuberculosis and diabetes mellitus co-morbidity (summary)*. Indian Journal of Endocrinology and Metabolism, 2016. **20**(6): p. 853-857.
128. WHO, *The End TB Strategy*. 2015.
129. WHO, *Global tuberculosis report*. Geneva, 2020.
130. Banu, S., et al., *Multidrug-resistant tuberculosis in admitted patients at a tertiary referral hospital of Bangladesh*. PLoS One, 2012. **7**(7): p. e40545.
131. NTP, *National Guidelines and Operational Manual for Programmatic Management of Drug Resistant Tuberculosis, 2nd edition*. 2016.
132. Maude, R. J., et al., *The role of mathematical modelling in guiding the science and economics of malaria elimination*. International Health, 2010. **2**(4-6): p. 239-246.
133. White, L. J., Flegg, J. A., Phyo, A. P., Wiladpai-ngern, J. H., Bethell, D., Plowe, C., Anderson, T., Nkhoma, S., Nair, S., Tripura, R., Stepniewska, K., Pan-Ngum, W., Silamut, K., Cooper, B. S., Lubell, Y., Ashley, E. A., Nguon, C., Nosten, F., White, N. J., and Dondorp, A. M., *Defining the in vivo phenotype of artemisinin-resistant falciparum malaria: a modelling approach*. PLoS Medicine, 2015. **12**(4): p. e1001823.
134. Maude, R. J., Pontavornpinyo, W., Saralamba, S., Aguas, R., Yeung, S., Dondorp, A. M., Day, N. P., White, N. J., and White, L. J., *The last man standing is the most resistant: eliminating artemisinin-resistant malaria in Cambodia*. Malaria Journal, 2009. **8**: p. 31.
135. Ragonnet, R., Trauer, J. M., Denholm, J. T., Marais, B. J., and McBryde, E. S., *A user-friendly mathematical modelling web interface to assist local decision making in the fight against drug-resistant tuberculosis*. BMC Infectious Diseases, 2017. **17**(1): p. 374.
136. McBryde, E. S., Meehan, M. T., Doan, T. N., Ragonnet, R., Marais, B. J., Guernier, V., and Trauer, J. M., *The risk of global epidemic replacement with drug-resistant Mycobacterium tuberculosis strains*. International Journal of Infectious Diseases, 2017. **56**: p. 14-20.
137. Lubell, Y., Dondorp, A., Guérin, P. J., Drake, T., Meek, S., Ashley, E., Day, N. P., White, N. J., and White, L. J., *Artemisinin resistance – modelling the potential human and economic costs*. Malaria Journal, 2014. **13**(1): p. 452.
138. Doan, T. N., Eisen, D. P., Rose, M. T., Slack, A., Stearnes, G., and McBryde, E. S., *Interferon-gamma release assay for the diagnosis of latent tuberculosis infection: A latent-class analysis*. PLoS One, 2017. **12**(11): p. e0188631.
139. Ragonnet, R., Trauer, J. M., Denholm, J. T., Geard, N. L., Hellard, M., and McBryde, E. S., *Vaccination Programs for Endemic Infections: Modelling Real versus Apparent Impacts of Vaccine and Infection Characteristics*. Scientific Reports, 2015. **5**: p. 15468.

140. Zwerling, A., Shrestha, S., and Dowdy, D. W., *Mathematical Modelling and Tuberculosis: Advances in Diagnostics and Novel Therapies*. Advances in Medicine, 2015. **2015**: p. 10.
141. Denholm, J. T., and McBryde, E. S., *Can Australia eliminate TB? Modelling immigration strategies for reaching MDG targets in a low-transmission setting*. Australian and New Zealand Journal of Public Health, 2014. **38**(1): p. 78-82.
142. Bacaer, N., et al., *Modeling the joint epidemics of TB and HIV in a South African township*. Journal of Mathematical Biology, 2008. **57**(4): p. 557-93.
143. Cooke, K. L., *Stability analysis for a vector disease model*. The Rocky Mountain Journal of Mathematics, 1979. **9**(1): p. 31-42.
144. Wu, J., et al., *Sensitivity analysis of infectious disease models: methods, advances and their application*. Journal of the Royal Society Interface, 2013. **10**(86): p. 20121018.
145. Chitnis, N., Cushing, J. M., and Hyman, J., *Bifurcation analysis of a mathematical model for malaria transmission*. SIAM Journal on Applied Mathematics, 2006. **67**(1): p. 24-45.
146. Childs, L. M., et al., *Modelling challenges in context: lessons from malaria, HIV, and tuberculosis*. Epidemics, 2015. **10**: p. 102-107.
147. Wallis, R. S., *Mathematical models of tuberculosis reactivation and relapse*. Frontiers in Microbiology, 2016. **7**: p. 669.
148. Egonmwan, A. O., and Okuonghae, D., *Analysis of a mathematical model for tuberculosis with diagnosis*. Journal of Applied Mathematics and Computing, 2018.
149. Diekmann, O., Heesterbeek, J. A., and Roberts, M. G., *The construction of next-generation matrices for compartmental epidemic models*. Journal of the Royal Society Interface, 2010. **7**(47): p. 873-85.
150. Van, D. P., *Reproduction numbers of infectious disease models*. Infectious Disease Modelling, 2017. **2**(3): p. 288-303.
151. Murphy, B. M., et al., *Comparing epidemic tuberculosis in demographically distinct heterogeneous populations*. Mathematical Biosciences, 2002. **180**: p. 161-85.
152. Ozcaglar, C., et al., *Epidemiological models of Mycobacterium tuberculosis complex infections*. Mathematical Biosciences, 2012. **236**(2): p. 77-96.
153. White, P. J., and Abubakar, I., *Improving Control of Tuberculosis in Low-Burden Countries: Insights from Mathematical Modeling*. Front Microbiol, 2016. **7**: p. 394.
154. Pienaar, E., et al., *A Model of Tuberculosis Transmission and Intervention Strategies in an Urban Residential Area*. Computational Biology and Chemistry, 2010. **34**(2): p. 86-96.
155. Kim, S., et al., *What Does a Mathematical Model Tell About the Impact of Reinfection in Korean Tuberculosis Infection?* Osong Public Health and Research Perspectives, 2014. **5**(1): p. 40-45.
156. Liu, L., Zhao, X.Q., and Zhou, Y., *A tuberculosis model with seasonality*. Bulletin of Mathematical Biology, 2010. **72**(4): p. 931-952.
157. Yang, Y., et al., *Seasonality impact on the transmission dynamics of tuberculosis*. Computational and Mathematical Methods in Medicine, 2016. **2016**: p. 8713924.
158. Liu, J., Bai, Z., and Zhang, T., *A periodic two-patch SIS model with time delay and transport-related infection*. Journal of Theoretical Biology, 2018. **437**: p. 36-44.
159. Graciani R., Espíndola, C. C., Aquino, L., and Penna, T. J. P., *An agent-based computational model for tuberculosis spreading on age-structured populations*. Physica A: Statistical Mechanics and its Applications, 2015. **428**: p. 52-59.
160. Blaser, N., et al., *Tuberculosis in Cape Town: An age-structured transmission model*. Epidemics, 2016. **14**: p. 54-61.
161. Kunkel, A., et al., *Benefits of continuous isoniazid preventive therapy may outweigh resistance risks in a declining TB/HIV co-epidemic*. AIDS (London, England), 2016. **30**(17): p. 2715-2723.
162. Guzzetta, G., et al., *Modeling socio-demography to capture tuberculosis transmission dynamics in a low burden setting*. Journal of Theoretical Biology, 2011. **289**: p. 197-205.
163. Begun, M., et al., *Contact tracing of tuberculosis: a systematic review of transmission modelling studies*. PLoS One, 2013. **8**(9): p. e72470.

164. Prats, C., et al., *Individual-based modeling of tuberculosis in a user-friendly interface: understanding the epidemiological role of population heterogeneity in a City*. *Frontiers in Microbiology*, 2015. **6**: p. 1564.
165. Brooks, P. E., Cohen, T., and Murray, M., *The Impact of Realistic Age Structure in Simple Models of Tuberculosis Transmission*. *PLoS One*, 2010. **5**(1): p. e8479.
166. Zaman, K., *Tuberculosis: A Global Health Problem*. *Journal of Health, Population, and Nutrition*, 2010. **28**(2): p. 111-113.
167. Dodd, P. J., Sismanidis, C., and Seddon, J. A., *Global burden of drug-resistant tuberculosis in children: a mathematical modelling study*. *The Lancet Infectious Diseases*, 2016. **16**(10): p. 1193-1201.
168. Luciani, F., et al., *The epidemiological fitness cost of drug resistance in Mycobacterium tuberculosis*. *Proceedings of the National Academy of Sciences*, 2009. **106**(34): p. 14711-14715.
169. Murray, C. J. L., and Salomon, J. A., *Modeling the impact of global tuberculosis control strategies*. *Proceedings of the National Academy of Sciences of the United States of America*, 1998. **95**(23): p. 13881-13886.
170. Garnett, G. P., Cousens, S., Hallett, T. B., Steketee, R., and Walker, N., *Mathematical models in the evaluation of health programmes*. *The Lancet*, 2011. **378**(9790): p. 515-525.
171. Ragonnet, R., et al., *Is IPT more effective in high-burden settings? Modelling the effect of tuberculosis incidence on IPT impact*. *The International Journal of Tuberculosis and Lung Disease*, 2017. **21**(1): p. 60-66.
172. Whang, S., Choi, S., and Jung, E., *A dynamic model for tuberculosis transmission and optimal treatment strategies in South Korea*. *Journal of Theoretical Biology*, 2011. **279**(1): p. 120-131.
173. Yang, Y., et al., *Global stability of two models with incomplete treatment for tuberculosis*. *Chaos, Solitons & Fractals*, 2010. **43**(1-12): p. 79-85.
174. Korobeinikov, A., and Maini, K. P., *A Lyapunov function and global properties for SIR and SEIR epidemiological models with nonlinear incidence*. *Mathematical Biosciences & Engineering*, 2004. **1**(1): p. 57.
175. Trunz, B. B., Fine, P., and Dye, C., *Effect of BCG vaccination on childhood tuberculous meningitis and miliary tuberculosis worldwide: a meta-analysis and assessment of cost-effectiveness*. *The Lancet*, 2006. **367**(9517): p. 1173-1180.
176. Mishra, B. K., and Srivastava, J., *Mathematical model on pulmonary and multidrug-resistant tuberculosis patients with vaccination*. *Journal of the Egyptian Mathematical Society*, 2014. **22**(2): p. 311-316.
177. Young, D., and Dye, C., *The development and impact of tuberculosis vaccines*. *Cell*, 2006. **124**(4): p. 683-687.
178. Castillo, C., and Carlos, F. Z., *Global stability of an age-structure model for TB and its applications to optimal vaccination strategies*. *Mathematical Biosciences*, 1998. **151**(2): p. 135-154.
179. Okuonghae, D., and Ikhimwin, B. O., *Dynamics of a Mathematical Model for Tuberculosis with Variability in Susceptibility and Disease Progressions Due to Difference in Awareness Level*. *Frontiers in Microbiology*, 2015. **6**: p. 1530.
180. Trauer, J. M., Denholm, J. T., and McBryde, E. S., *Construction of a mathematical model for tuberculosis transmission in highly endemic regions of the Asia-Pacific*. *Journal of Theoretical Biology*, 2014. **358**: p. 74-84.
181. Moualeu-Ngangue, D. P., et al., *Parameter Identification in a Tuberculosis Model for Cameroon*. *PLoS One*, 2015. **10**(4): p. e0120607.
182. Ryder, J. J., et al., *Host-parasite population dynamics under combined frequency-and density-dependent transmission*. *Oikos*, 2007. **116**(12): p. 2017-2026.
183. Okuonghae, D., and Omosigho, S. E., *Analysis of a mathematical model for tuberculosis: What could be done to increase case detection*. *Journal of Theoretical Biology*, 2011. **269**(1): p. 31-45.
184. Liu, J., and Zhang, T., *Global stability for a tuberculosis model*. *Mathematical and Computer Modelling*, 2011. **54**(1): p. 836-845.

185. Trauer, J. M., et al., *Scenario Analysis for Programmatic Tuberculosis Control in Western Province, Papua New Guinea*. The American Journal of Epidemiology, 2016.
186. Kalu, A., and Inyama, S., *Mathematical Model of the Role of Vaccination and Treatment on the Transmission Dynamics of Tuberculosis*. Gen, 2012. **11**(1): p. 10-23.
187. Maude, R. J., et al., *The last man standing is the most resistant: eliminating artemisinin-resistant malaria in Cambodia*. Malaria Journal, 2009. **8**(1): p. 31.
188. Phyo, A. P., et al., *Emergence of artemisinin-resistant malaria on the western border of Thailand: a longitudinal study*. The Lancet. **379**(9830): p. 1960-1966.
189. Bhunu, C. P., et al., *Modelling the effects of pre-exposure and post-exposure vaccines in tuberculosis control*. Journal of Theoretical Biology, 2008. **254**(3): p. 633-49.
190. Hassard, B., and Wan, Y. H., *Bifurcation formulae derived from center manifold theory*. Journal of Mathematical Analysis and Applications, 1978. **63**(1): p. 297-312.
191. Trauer, J. M., et al., *Modelling the effect of short-course multidrug-resistant tuberculosis treatment in Karakalpakstan, Uzbekistan*. BMC Medicine, 2016. **14**(1): p. 187.
192. Kendall, E. A., Fojo, A. T., and Dowdy, D. W., *Expected effects of adopting a 9 month regimen for multidrug-resistant tuberculosis: a population modelling analysis*. The Lancet Respiratory Medicine, 2017. **5**(3): p. 191-199.
193. Moodley, R., and Godec, T. R., *Short-course treatment for multidrug-resistant tuberculosis: the STREAM trials*. European Respiratory Review, 2016. **25**(139): p. 29-35.
194. Okuonghae, D., *A mathematical model of tuberculosis transmission with heterogeneity in disease susceptibility and progression under a treatment regime for infectious cases*. Applied Mathematical Modelling, 2013. **37**(10): p. 6786-6808.
195. Yang, Y., *Global stability of two models with incomplete treatment for tuberculosis*. Chaos, Solitons & Fractals, 2010. **43**(1-12): p. 79-85.
196. Mistry, N., Tolani, M., and Osrin, D., *Drug-resistant tuberculosis in Mumbai, India: An agenda for operations research*. Operations Research for Health Care, 2012. **1**(2-3): p. 45-53.
197. Bastian, I., Stapledon, R., and Colebunders, R., *Current thinking on the management of tuberculosis*. Current Opinion in Pulmonary Medicine, 2003. **9**(3): p. 186-192.
198. Dowdy, D. W., et al., *The potential impact of enhanced diagnostic techniques for tuberculosis driven by HIV: a mathematical model*. Aids, 2006. **20**(5): p. 751-762.
199. Bhunu, C. P., *Mathematical analysis of a three-strain tuberculosis transmission model*. Applied Mathematical Modelling, 2011. **35**: p. 4647-4660.
200. Vaddady, P. K., Lee, R. E., and Meibohm, B., *In vitro pharmacokinetic/pharmacodynamic models in anti-infective drug development: focus on TB*. Future Medicinal Chemistry, 2010. **2**(8): p. 1355-1369.
201. Jayaram, R., et al., *Pharmacokinetics-Pharmacodynamics of Rifampin in an Aerosol Infection Model of Tuberculosis*. Antimicrobial Agents and Chemotherapy, 2003. **47**(7): p. 2118-2124.
202. Gomez, G. B., et al., *Cost and cost-effectiveness of tuberculosis treatment shortening: a model-based analysis*. BMC Infectious Diseases, 2016. **16**(1): p. 726.
203. Gomez, G. B., et al., *Cost and cost-effectiveness of tuberculosis treatment shortening: a model-based analysis*. BMC Infectious Diseases, 2016. **16**(1): p. 726.
204. Aljayyousi, G., et al., *Pharmacokinetic-Pharmacodynamic modelling of intracellular Mycobacterium tuberculosis growth and kill rates is predictive of clinical treatment duration*. Scientific Reports, 2017. **7**(1): p. 502.
205. Hoagland, D., et al., *New agents for the treatment of drug-resistant Mycobacterium tuberculosis*. Advanced Drug Delivery Reviews, 2016. **102**: p. 55-72.
206. Diel, R., Hittel, N., and Schaberg, T., *Cost effectiveness of treating multi-drug resistant tuberculosis by adding Deltyba to background regimens in Germany*. Respiratory Medicine, 2015. **109**(5): p. 632-41.
207. Resch, S. C., et al., *Cost-Effectiveness of Treating Multidrug-Resistant Tuberculosis*. PLoS Medicine, 2006. **3**(7): p. e241.
208. Nathanson, E., et al., *MDR tuberculosis--critical steps for prevention and control*. The New England Journal of Medicine, 2010. **363**(11): p. 1050-8.
209. Fitzpatrick, C., and Floyd, K., *A Systematic Review of the Cost and Cost Effectiveness of Treatment for Multidrug-Resistant Tuberculosis*. Pharmacoeconomics, 2012. **30**(1): p. 63-80.

210. WHO, *Removing obstacles to healthy development: report on infectious diseases*. 1999.
211. Murray, C. J., Styblo, K., and Rouillon, A., *Tuberculosis in developing countries*. Morbidity and Mortality Weekly Report, 1990. **39**(33): p. 561-569.
212. Pelčić, G., et al., *Religious exception for vaccination or religious excuses for avoiding vaccination*. Croatian Medical Journal, 2016. **57**(5): p. 516-521.
213. Fredrickson, D. D., et al., *Childhood immunization refusal: provider and parent perceptions*. Family Medicine Kansas City, 2004. **36**: p. 431-439.
214. Wallace, A. S., et al., *Experiences with provider and parental attitudes and practices regarding the administration of multiple injections during infant vaccination visits: lessons for vaccine introduction*. Vaccine, 2014. **32**(41): p. 5301-5310.
215. Alam, M., *Budgetary process in uncertain contexts: a study of state-owned enterprises in Bangladesh*. Management Accounting Research, 1997. **8**(2): p. 147-167.
216. Ludy, D., Christine, R., and Perry, B. D., *The role of healthy relational interactions in buffering the impact of childhood trauma*. Working with children to heal interpersonal trauma: The power of play, 2010: p. 26-43.

# CHAPTER 3

---

## **Delay effect and burden of weather-related tuberculosis cases in Rajshahi province, Bangladesh, 2007-2012**

---

### **Statement of joint authorship**

**Md Abdul Kuddus** wrote the manuscript, constructed the dataset, developed the model, analysed the data, and wrote code for model.

**Emma S. McBryde** initiated the concept for the manuscript, assisted with the proof read and critically reviewed the manuscript.

**Oyelola A. Adegboye** assisted with the development of the model, analysed the data, code for model extensions, proof read and critically reviewed the manuscript.

**Kuddus, M. A., McBryde, E. S., Adegboye, O. A. (2019).** Delay effect and burden of weather-related tuberculosis cases in Rajshahi province, Bangladesh, 2007–2012. *Scientific Reports*, 9(1), 1-13.

## **Abstract**

Tuberculosis (TB) is a potentially fatal infectious disease that continues to be a public health problem in Bangladesh. Each year in Bangladesh an estimated 70,000 people die of TB and 300,000 new cases are projected. It is important to understand the association between TB incidence and weather factors in Bangladesh in order to develop proper intervention programs. In this study, we examine the delayed effect of weather variables on TB occurrence and estimate the burden of the disease that can be attributed to weather factors. We used generalized linear Poisson regression models to investigate the association between weather factors and TB cases reported to the Bangladesh National TB control program between 2007 and 2012 in three known endemic districts of North-East Bangladesh. The associated risk of TB in the three districts increases with prolonged exposure to temperature and rainfall, and persisted at lag periods beyond 6 quarters. The association between humidity and TB is strong and immediate at low humidity, but the risk decreases with increasing lag. Using the optimum weather values corresponding to the lowest risk of infection, the risk of TB is highest at low temperature, low humidity and low rainfall. Measures of the risk attributable to weather variables revealed that weather-TB cases attributed to humidity is higher than that of temperature and rainfall in each of the three districts. Our results highlight the high linearity of temporal lagged effects and magnitudes of the burden attributable to temperature, humidity, and rainfall on TB endemics. The results will provide important information to advise the Bangladesh National TB control program and act as a practical reference for the early warning of TB cases.

**Keywords:** Tuberculosis, Bangladesh, Distributed lag models, Weather

### 3.1 Introduction

Tuberculosis (TB) kills millions of people each year and is one of the major global health problems identified by the World Health Organization [1]. It is an airborne infectious disease caused by infection with the bacteria *Mycobacterium tuberculosis* (*Mtb*) [2]. The *Mtb* spreads easily from a person with active TB to another person when the infectious person coughs, sneezes, speaks or sings and the susceptible person comes into physical contact with fluid from droplets via body entrance cavities [3]. The incidence of TB disease is increasing and it is estimated that globally there were around 10.4 million new cases of TB, and 1.7 million died from the TB disease. Most of the estimated cases in 2017 occurred in Asia (45%) and Africa (25%) and 87% of TB deaths occurred in low- and middle- income countries [1]. TB is therefore a major challenge to public health that has only been exacerbated by urbanization, population movement and climate change [4-6].

Previous studies have shown that environmental factors exhibit important effects on the distribution of TB disease, vectors and host [4, 7-12]. For example, the incidence of TB has been shown to be highest during summer, thus, it was hypothesized that the disease may have been acquired during winter months. This could be attributed to reduction in vitamin D level in the winter season [5, 7, 13-15], winter indoor crowding activities [16, 17] and seasonal change in immune function [18, 19]. Similarly, air quality is affected by atmospheric pollution, where carbon monoxide promotes bacillary reactivation and increases the risk of TB outbreaks [20].

TB is one of the major public health problems in Bangladesh [21-23]. Many areas of quantitative analysis can be used to improve the understanding of infectious diseases epidemiology as well as its dynamics. Time series analysis has been extensively used to explore exposure-response relationships of diseases. For example, Onozuka *et al.* applied generalized linear Poisson models in combination with autoregressive model to investigate the effect of weekly mean temperature and humidity on the incidence of mycoplasma pneumonia in Japan [24], Adegboye *et al.* used a spatial time-series regression model to investigate the influence of temperature and rainfall on malaria and leishmaniasis in Afghanistan [25-27], and Xiao *et al.* applied a distributed lag non-linear model to study the effects of multiple meteorological variables on monthly incidence of TB in Southwest China [28].

Overall, the transmission dynamics and epidemiology of TB in Rajshahi are poorly understood. No available study has concurrently discussed the impact of weather factors on TB incidence and attributable burden of the disease in Bangladesh. Therefore, this study will fill this gap in the literature by investigating the distributed lag effects of weather on TB incidence. We also aimed to identify the

influence of multiple weather indicators and the burden of TB attributable to weather variables in the North-West region of Bangladesh using consecutive surveillance data collected over 6 years.

We applied distributed lag models (DLMs) to explore simultaneously the exposure-lag-response impact of selected weather factors (i.e. temperature, humidity and rainfall) on TB incidence. The DLM is a novel and flexible modelling structure for dealing with lagged relations between or among time series structures. It will efficiently capture and control the behaviour of study variables in the exposure range and time dimension. The findings in this study will contribute to a better understanding of the TB incidence related to weather factors including temperature, rainfall and humidity and provide more evidence to support the Bangladesh National TB control program (NTP) decision-making and to prevent and control future TB outbreaks.

## **3.2 Methods and material**

### **3.2.1 Data sources**

#### **3.2.1.1 TB case notifications**

Bangladesh is a TB disease endemic country in South-East Asia [1]. Control of TB in such a resource-scare country should be informed by an in-depth epidemiological understanding of the disease. This study is based on reported quarterly TB cases in three districts of Rajshahi province, in the North-West of Bangladesh (Figure 3.1) obtained from the NTP in Bangladesh. The diagnosis of TB cases was based on the clinical criteria established in the NTP guide published by the Ministry of Health in Bangladesh [29]. At time of data collection, individuals are told of their diagnosis (of tuberculosis) and informed that it is a notifiable disease [29].

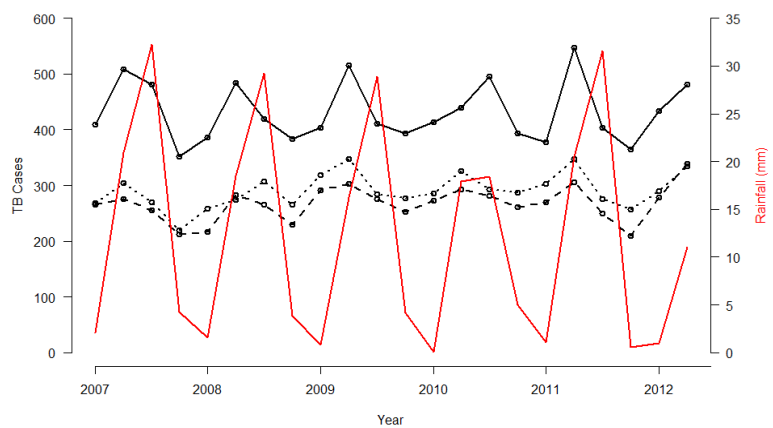
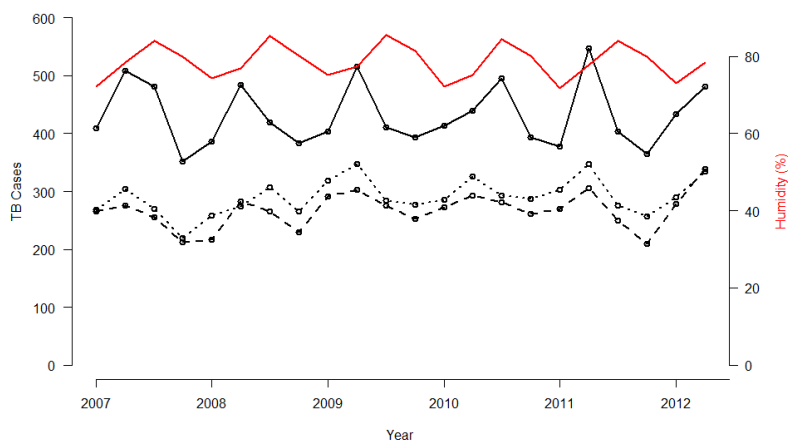
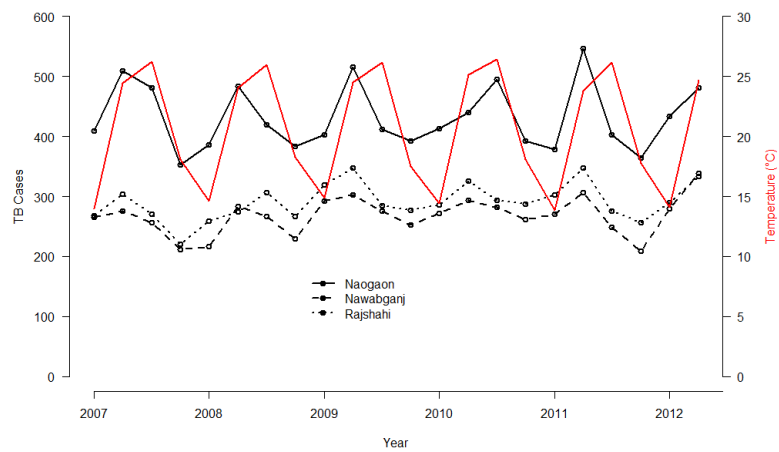


Figure 3. 1 Quarterly TB cases (black) during the study period, 2007-2012 with average (a) Temperature, (b) Humidity, and (c) Rainfall for the three districts (red).

### 3.2.1.2 Weather variables

Weather data from 35 weather stations across Bangladesh were obtained from the National Oceanic and Atmospheric Administration (NOAA), National Centers for Environmental Information (NCEI) (Figure 3.1). However, none of the weather stations is located in the study region, that is, the location of the weather stations do not match the study areas (misaligned data) (Figure 3.1). Misalignment in spatial analysis occurs when samples taken at different spatial scales are not linked [30-32]. Therefore, interpolation (Kriging) of the weather data is required [33, 34]. Here we use a Bayesian Kriging method [32] to estimate the daily weather variables in each of the study districts within the range of known weather stations shown in Figure 3.1.

The general formula for Kriging is,

$$\vec{Z}(S_0) = \sum_{i=1}^N \lambda_i Z(S_i) \quad (3.1)$$

Where

$Z(S_i)$  is the measured value at the  $i$  th location

$\lambda_i$  is an unknown weight for the measured value at the  $i$  th location

$S_0$  represents the predicted location

$N$  is the number of measured values

Here,  $\lambda_i$  depends on the measured points, distance to the prediction location and the spatial relationship among the measured values around the prediction location.

We used variogram to create covariance function to evaluate the spatial dependence [33-35].

$$\gamma_h = 0.5 * \text{average values} (\text{location}_i - \text{location}_j)^2 \quad (3.2)$$

where  $i, j = 1, 2, 3, \dots, N$ .

The empirical semivariogram is a graph of the averaged semivariogram values of the y axis and the distance on the x axis and it's provides information on the spatial autocorrelation of datasets. Three mathematical models- spherical, exponential and marten functions [36] were explored to estimate  $\gamma_h$  used for interpolation.

The Bayesian Kriging was implemented in the R package for geostatistical analysis "geoR" [37]. The estimated daily weather variables: mean temperature (°C); mean rainfall (mm); and mean relative humidity (%) were aggregated to quarterly data (See Figure S3.1).

### 3.2.2 Statistical analysis

### 3.2.2.1 Weather -TB association

The association between weather variables and the number of TB cases was investigated using distributed lag models (DLMs) [38, 39] via a quasi-Poisson regression model adjusting for population, seasonality and long-term trend.

The quarterly counts of TB cases,  $Y_t$  at time  $t$  may be explained in terms of past weather exposures  $x_{t-\ell}$ , up to  $\ell$  lag.

$$Y_t \sim \text{quasiPoisson}(\mu_t)$$

$$\log(\mu_t) = \alpha + \text{offset}(\text{Population}) + s(\text{Time}) + s_j(x_{t-\ell,j} \beta_{l,j}) \quad (3.3)$$

where  $\mu_t \equiv E(Y_t)$ , and  $Y_t$  is assumed to arise from an over-dispersed Poisson distribution. Population was entered as a fixed effect and a smoothing function of time was used to model the trend and seasonality. The functions  $s_j$  specify the relationship between the weather variable,  $x_j$ , and the exposure-lag-response curve, defined by the parameter vectors  $\beta_{l,j}$ .

The functions  $s_j$  defines the relationship along the two dimensions: exposure and lag and is computed as the approximate integral of the exposure-lag-response function over the lag dimension, representing the cumulated risk over the lag period.

$$S_j = \int_{l_0}^L f. w(x_{t-l}, l) dl \\ \approx \sum_{l=l_0}^L f. w(x_{t-l}, l) = w_{x,t}^T \quad (3.4)$$

The parameterization in the final step of the equation (3.4) is obtained through a cross-basis function involving a tensor product between the basis chosen for  $f(x)$  and  $w(l)$ . The cross-basis function specified with a reference value  $x_0$  used later as a centering point for the function  $f(x)$ , which is used to define the counterfactual condition [40-42].

### 3.2.2.2 Model assessment

We explored several structures of *exposure-lag-response function*,  $s_j(x_{t-\ell,j} \beta_{l,j})$ ; linear and quadratic spline functions were explored for exposure-response relationship while constant, linear and quadratic splines were explored for lag-response relationship. To examine the lag effects, various lag models should be compared because few models may lead to misleading conclusions. Adding more lag variables may lead to a greater loss of accuracy with a minimal benefit in lag effect detection [43]. In exposure and lag functions, different lags (up to 6 quarters) and knot positions (equally spaced and

mean) were investigated. A natural cubic spline of time was used to model the trend and seasonality exploring 0 to 7 degrees of freedom.

A collection of 64 candidate models were developed based on the number of knot positions, number of lags, number of degrees of freedom (df) and smoothing functions for each exposure-lag-response function (See Table S3.1 and S3.2 for details). Each of these choices will depend on the objectives of the analysis as well as the best model fit. In general, simpler models (e.g. linear) have the advantage of being easy to interpret and are particularly attractive in multicity studies in which one seeks to compare associations across cities. However, more complex models (e.g. Quadratic B-Spline) may produce better fits to the data and are useful in exploratory single-city studies as well as to indicate to what extent there are weather effects [44]. The choice of specific model may also be informed by model fit criteria including deviance, modified Akaike and Bayesian information criteria for models with over dispersed data, Quasi-AIC and Quasi-BIC [45, 46]. However, when using model-fit principles to inform model choice, we must keep in mind that relative performance of each of the model depends on their model formulation. Finally, considering the choice of a preferred model, it is also required to consider sensitivity of model choice not only in relation to the weather factors, but also to season and other specific factors [44, 47].

Therefore, in this study, we carried out an extensive model search using QAIC, QBIC and visualization of weather-TB association. Tables S3.1 present the model description. The models selected by QAIC and QBIC are complex model and contain a high number of degrees of freedom spent to describe the weather-TB overall effect (more than 20 df for a 22 time series observations per districts) (Tables S3.2). Previous studies have suggested that information criteria tends to select under fit models when sample size and effect size are small [43, 48]. A simpler model providing relative risk (RR) estimates without bias and with smaller variance may be preferred [43, 49]. Therefore, taking these considerations into account and motivated by several previous studies [43-45, 47, 48, 50], we consider linear-linear (exposure-lag-response) models to assess the relationship between three weather variables: temperature; rainfall; and relative humidity, and the number of TB cases in three districts of Bangladesh. The final model selected described both the weather-TB and lag-TB relationships by a linear function for up to 6 quarter lags and 7 degrees of freedom for long-term trends.

### **3.2.2.3 Attributable risk associated with weather variables**

The attributable fraction (AF) and attributed number (AN) are indicators of weather-related health burdens that take into account weather-associated risk as well as the lags on which that risk is observed [51]. Results from the final model were used to derive estimates of weather-TB overall associations,

reported as relative risks (RRs), cumulating the risk during the lag period. The number of TB cases attributable to weather variables using optimum weather values (which is the weather value corresponding to a minimum number of TB cases) as reference was used to derive the attributable measures.

We used both backward and forward perspective to estimate the attributable measures depending on the interpretation of the term,  $\beta_{x,l}$  for each intensity,  $x_t$ . The terms  $\beta_{x,l}$  are the contributions from the exposure  $x_t$  occurring at time  $t$  to the risk at respective periods [51, 52]. From a forward viewpoint, looking from current exposure to future risks, the terms  $\beta_{x,l}$  are the contributions from the exposure  $x_t$  occurring at time  $t$  to the risk at time  $t + l_0, \dots, t + L$  given by the equation below:

$$f - AF_{x,t} = 1 - e^{-\sum_{l=l_0}^L \beta_{x,t,l}}$$

$$f - AN_{x,t} = f - AF_{x,t} \sum_{l=l_0}^L \frac{n_{t+l}}{L-l_0+1} \quad (3.5)$$

Where  $f - AF_{x,t}$  and  $f - AN_{x,t}$  can be interpreted as the fraction and number of future cases in the period  $t + l_0, \dots, t + L$  attributable to the single exposure  $x$  occurring at time  $t$  to  $x_0$  [40].

The backward perspective assumed that the risk at time  $t$  is attributable to a series of exposure events  $x_t$  in the past, described as:

$$b - AF_{x,t} = 1 - e^{-\sum_{l=l_0}^L \beta_{x_{t-l},l}}$$

$$b - AN_{x,t} = b - AF_{x,t} \cdot n_t \quad (3.6)$$

The terms  $\beta_{x,l}$  are the contributions to the risk at time  $t$  from exposure  $x_{t-l_0}, \dots, x_{t-L}$  experienced at  $t - l_0, \dots, t - L$ . In this study, the attributable risk at each quarter was treated as a result of previous exposures up to the maximum lag, 6 quarters in the past.  $n_t$  is the number of cases at time  $t$ ;  $b - AN_{x,t}$  and ;  $b - AF_{x,t}$  are interpreted as the number of cases and the related fraction at time  $t$  attributable to past exposures to  $x$  in the period  $t - l_0, \dots, t - L$ , compared to a constant exposure  $x_0$  within the same period [40].

### 3.2.2.4 Sensitivity analysis

We carried out sensitivity analysis to assess whether our model parameters and attributable risk measures were robust. The effects of our estimates due to the choice of covariance structures for weather prediction were also investigated. We changed the covariance structure used in our Bayesian Kriging analysis from spherical, to exponential and Matern, and used the new weather predictions in our DLMS (See Table S3.3 and S3.4). Furthermore, we assessed the interplay between all three weather parameters looking at exposure to individual weather parameters and up to three-way interactions (Figure S3.2).

All analyses were done using the package DLM [38] in the R 3.4.2 statistical software [53].

### **3.3 Results**

#### **3.3.1 Initial sequences of TB cases and weather factors**

There were 6394, 5896 and 9498 TB cases reported in the three districts considered in this study, Naogaon, Nawabganj and Rajshahi from 2007 to 2012. The time-series distribution of quarterly TB cases and average quarterly temperature, relative humidity and rainfall during the study period are presented in Figure 3.1. Variations of the three weather factors with time presented a recognizable cyclic pattern.

#### **3.3.2 Association between TB and weather factors**

The associations between TB and average quarterly temperature, relative humidity and rainfall from the final model are illustrated in Figures 3.2-3.4. The left panel of the plots displays the three-dimensional plots of the relationships between weather variables and TB cases along the lags, while the middle and the right panels display the exposure-response and lag-response associations, respectively. The TB-temperature and TB-rainfall plots suggest that the slope of relations is steeper at the lower end of the temperature and rainfall scale in all the three districts. These associations are delayed and increase at lag periods up to 6 quarters. Significant negative associations were found between temperature/rainfall and the risk of TB at lag 0-6 (Figures 3.2-3.3). The association between relative humidity and TB was immediate at low humidity, and the risk decreases with increasing lag. The effect of relative humidity was significant for lag periods up to 6 quarters (Figure 3.4).

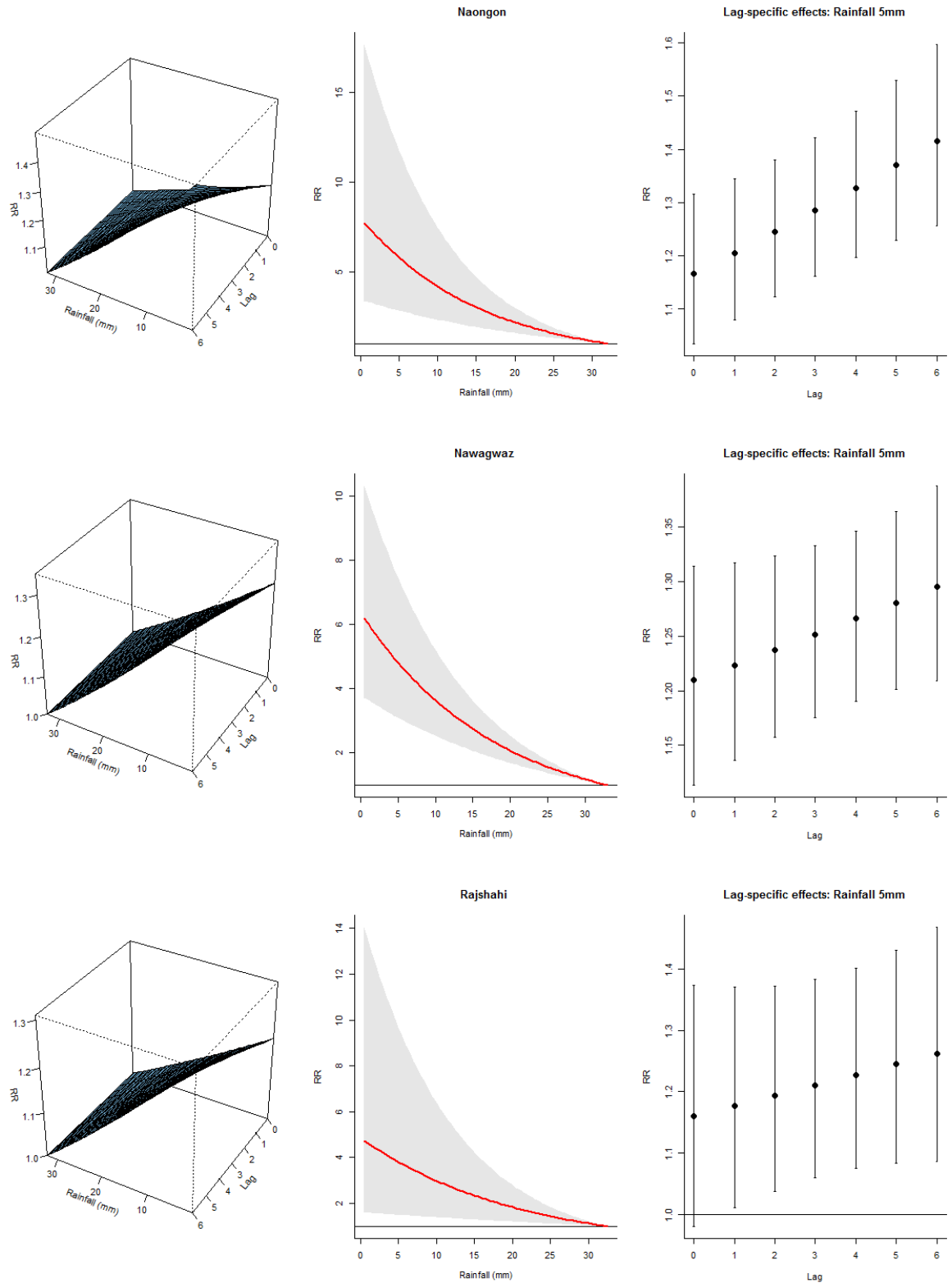


Figure 3. 2 Exposure-lag-response association in the three districts. Left panel: Three dimensional association; Middle panel: Rainfall-TB association Right panel: Lag-TB association.

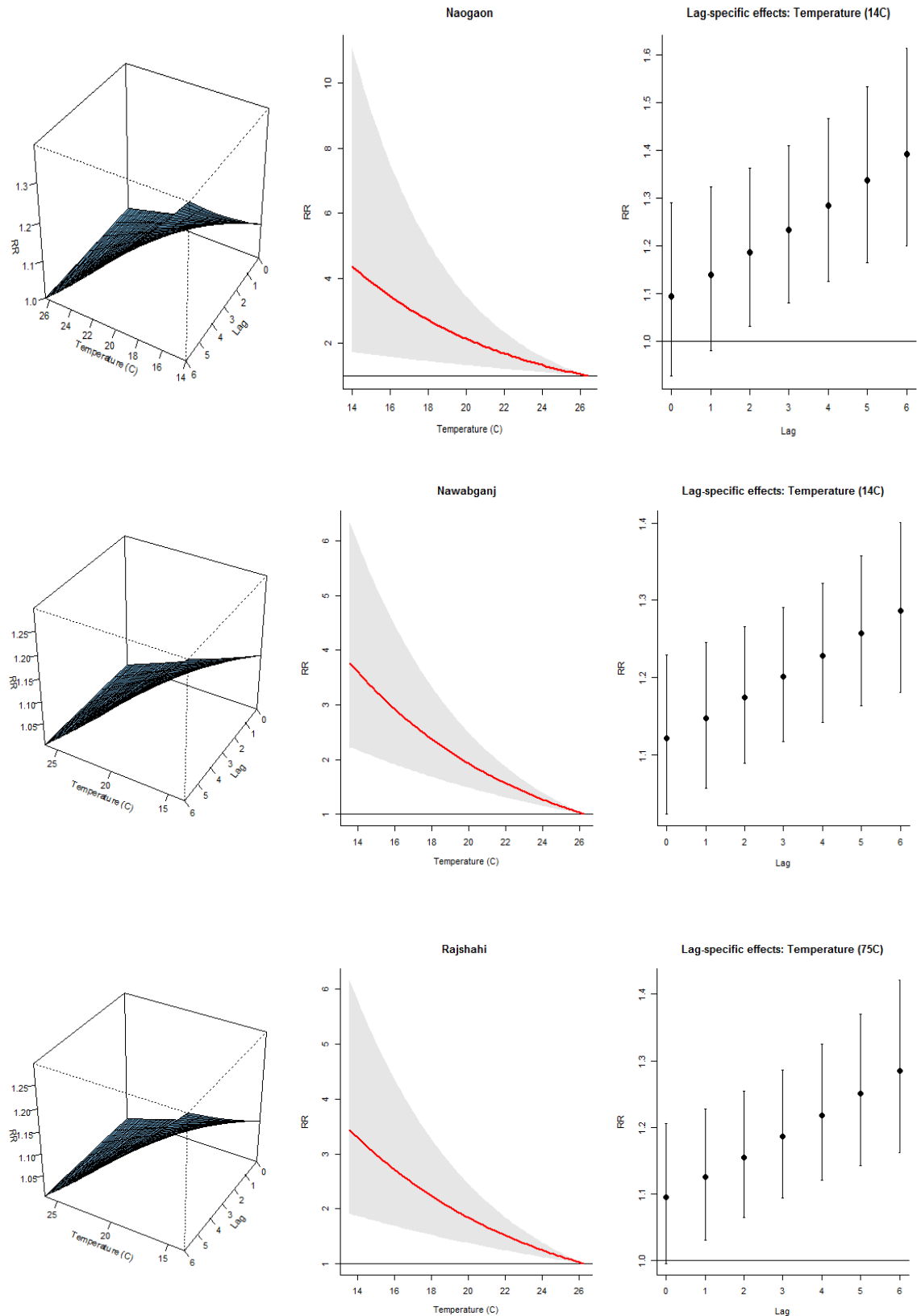


Figure 3. 3 Exposure-lag-response association in the three districts. Left panel: Three dimensional association; Middle panel: Temperature-TB association Right panel: Lag-TB association.

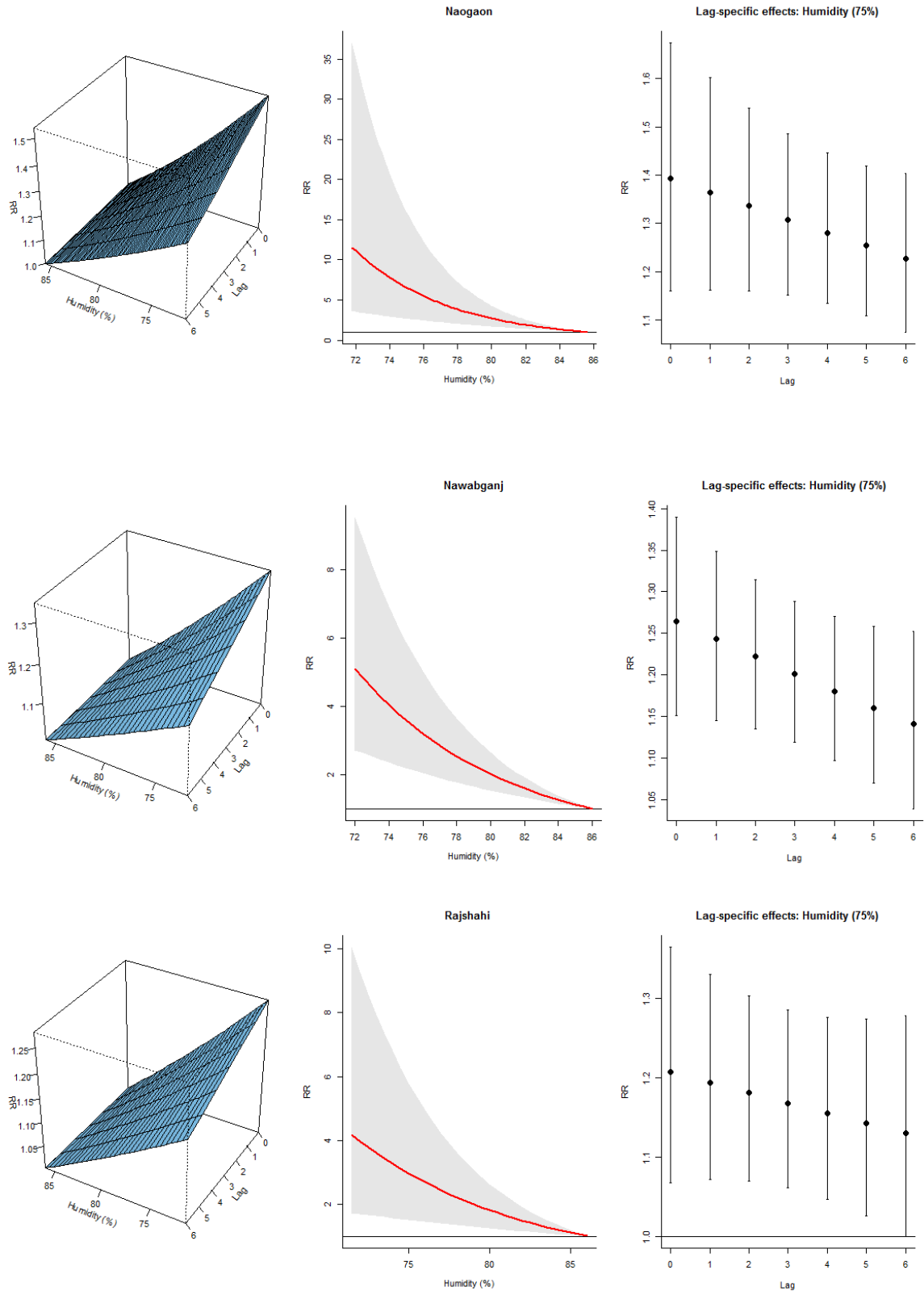


Figure 3. 4 Exposure-lag-response association in the three districts. Left panel: Three dimensional association. Middle panel: Humidity-TB association. Right panel: Lag-TB association.

In the three districts, the predicted lag-specific effects suggested an increasing effect of temperature and rainfall over lag 0-6 especially at low values but an immediate effect of humidity (Figure S3.3-S3.5 right panel). Similarly, the multiple plot of projected effects along temperature, humidity and rainfall at specific lags and the corresponding lag-specific effects (Figure S3.3-S3.5 right panel) illustrates the variability of the effects of high and low- temperatures, humidity and rainfall on TB cases. A very strong and delayed association with low temperature and low rainfall was observed in the three districts and an immediate effect of low humidity on the TB cases.

Table 3.1 showed the relative risks (RRs) of TB cases for overall cumulative effect (lag 0-6) and at different lag exposures (0 to 6) estimated at 10th, 50th and 90th percentiles of temperature, relative humidity, and rainfall values for each specific district. In all districts, the weather effect RRs were highest at the lowest value.

Table 3. 1 Relative risks (with 95% eCI) of incidence at specific exposure-lag values.

	Districts		Overall: Lag 0 – 6	Lag 0	Lag 1	Lag 2	Lag 3	Lag 4	Lag 5	Lag 6
Temperature	Naogaon	10 <sup>th</sup> (14.1)	4.31 (1.71 – 10.83)	1.09 (0.93 – 1.29)	1.14 (0.98 – 1.32)	1.18 (1.03 – 1.36)	1.23 (1.08 – 1.41)	1.28 (1.12 – 1.46)	1.33 (1.16 – 1.53)	1.39 (1.20 – 1.61)
		50 <sup>th</sup> (21.0)	1.89 (1.26 – 2.83)	1.04 (0.97 – 1.12)	1.06 (0.97 – 1.13)	1.08 (1.01 – 1.14)	1.10 (1.03 – 1.16)	1.11 (1.05 – 1.18)	1.13 (1.07 – 1.20)	1.15 (1.08 – 1.23)
		90 <sup>th</sup> (26.2)	1.03 (1.01 – 1.04)	1.00 (0.99 – 1.00)	1.00 (1.00 – 1.00)	1.00 (1.00 – 1.01)	1.00 (1.00 – 1.01)	1.00 (1.00 – 1.01)	1.00 (1.00 – 1.01)	1.00 (1.00 – 1.01)
Humidity	Naogaon	10 <sup>th</sup> (72.3)	10.63 (3.45 – 32.74)	1.52 (1.21 – 1.91)	1.48 (1.21 – 1.81)	1.44 (1.20 – 1.72)	1.40 (1.19 – 1.65)	1.36 (1.17 – 1.59)	1.33 (1.14 – 1.55)	1.29 (1.09 – 1.53)
		50 <sup>th</sup> (78.4)	3.58 (1.95 – 6.57)	1.25 (1.11 – 1.42)	1.23 (1.11 – 1.38)	1.22 (1.11 – 1.34)	1.20 (1.10 – 1.31)	1.18 (1.10 – 1.28)	1.17 (1.07 – 1.27)	1.15 (1.05 – 1.26)
		90 <sup>th</sup> (84.5)	1.22 (1.11 – 1.35)	1.04 (1.02 – 1.06)	1.03 (1.02 – 1.05)	1.03 (1.02 – 1.05)	1.03 (1.02 – 1.04)	1.03 (1.01 – 1.04)	1.02 (1.01 – 1.04)	1.02 (1.01 – 1.04)
Rainfall	Naogaon	10 <sup>th</sup> (0.87)	7.6 (3.34 – 17.05)	1.19 (1.04 – 1.37)	1.24 (1.09 – 1.41)	1.29 (1.14 – 1.45)	1.33 (1.19 – 1.50)	1.39 (1.23 – 1.56)	1.44 (1.27 – 1.63)	1.49 (1.30 – 1.71)
		50 <sup>th</sup> (8.01)	4.8 (2.54 – 8.93)	1.15 (1.03 – 1.28)	1.18 (1.07 – 1.30)	1.21 (1.11 – 1.33)	1.25 (1.14 – 1.37)	1.29 (1.17 – 1.41)	1.32 (1.20 – 1.46)	1.36 (1.22 – 1.52)
		90 <sup>th</sup> (29.18)	1.21 (1.12 – 1.31)	1.02 (1.00 – 1.03)	1.02 (1.01 – 1.03)	1.02 (1.01 – 1.04)	1.03 (1.02 – 1.04)	1.03 (1.02 – 1.04)	1.04 (1.02 – 1.05)	1.04 (1.03 – 1.05)
Temperature	Nawabganj	10 <sup>th</sup> (14.0)	3.59 (2.17 – 5.94)	1.12 (1.02 – 1.23)	1.15 (1.06 – 1.24)	1.17 (1.10 – 1.26)	1.20 (1.12 – 1.29)	1.23 (1.14 – 1.32)	1.26 (1.16 – 1.36)	1.28 (1.18 – 1.40)
		50 <sup>th</sup> (21.1)	1.72 (1.39 – 2.13)	1.05 (1.01 – 1.10)	1.06 (1.02 – 1.10)	1.07 (1.04 – 1.11)	1.08 (1.05 – 1.11)	1.09 (1.06 – 1.13)	1.10 (1.07 – 1.14)	1.11 (1.18 – 1.15)
		90 <sup>th</sup> (26.2)	1.01 (1.01 – 1.02)	1.00 (1.00 – 1.00)	1.00 (1.00 – 1.00)	1.00 (1.00 – 1.00)	1.00 (1.00 – 1.00)	1.00 (1.00 – 1.00)	1.00 (1.00 – 1.00)	1.00 (1.00 – 1.00)
Humidity	Nawabganj	10 <sup>th</sup> (72.4)	4.87 (2.65 – 8.95)	1.34 (1.19 – 1.50)	1.31 (1.18 – 1.45)	1.28 (1.17 – 1.40)	1.25 (1.15 – 1.37)	1.23 (1.12 – 1.34)	1.20 (1.09 – 1.33)	1.18 (1.05 – 1.32)
		50 <sup>th</sup> (78.5)	2.40 (1.71 – 3.36)	1.17 (1.10 – 1.25)	1.16 (1.10 – 1.23)	1.15 (1.09 – 1.21)	1.13 (1.08 – 1.19)	1.12 (1.07 – 1.18)	1.11 (1.05 – 1.17)	1.09 (1.03 – 1.17)
		90 <sup>th</sup> (84.8)	1.16 (1.09 – 1.22)	1.03 (1.02 – 1.04)	1.02 (1.02 – 1.03)	1.02 (1.01 – 1.03)	1.02 (1.01 – 1.03)	1.02 (1.01 – 1.03)	1.02 (1.01 – 1.03)	1.01 (1.00 – 1.03)
Rainfall	Nawabganj	10 <sup>th</sup> (0.97)	6.03 (3.65 – 9.96)	1.24 (1.13 – 1.37)	1.26 (1.16 – 1.37)	1.28 (1.18 – 1.38)	1.29 (1.20 – 1.39)	1.31 (1.22 – 1.41)	1.33 (1.23 – 1.43)	1.34 (1.24 – 1.45)
		50 <sup>th</sup> (7.72)	4.13 (2.78 – 6.14)	1.19 (1.10 – 1.28)	1.20 (1.12 – 1.28)	1.21 (1.14 – 1.29)	1.22 (1.14 – 1.30)	1.24 (1.17 – 1.31)	1.25 (1.18 – 1.32)	1.26 (1.19 – 1.34)
		90 <sup>th</sup> (29.82)	1.20 (1.14 – 1.26)	1.02 (1.01 – 1.03)	1.02 (1.01 – 1.03)	1.02 (1.02 – 1.03)	1.03 (1.02 – 1.03)	1.03 (1.02 – 1.03)	1.03 (1.02 – 1.04)	1.03 (1.02 – 1.04)
Temperature	Rajshahi	10 <sup>th</sup> (14.0)	3.31 (1.88 – 5.83)	1.10 (0.99 – 1.21)	1.12 (1.03 – 1.23)	1.56 (1.06 – 1.25)	1.89 (1.09 – 1.28)	1.22 (1.12 – 1.31)	1.25 (1.14 – 1.37)	1.28 (1.16 – 1.42)
		50 <sup>th</sup> (21.0)	1.67 (1.31 – 2.14)	1.04 (1.00 – 1.08)	1.05 (1.01 – 1.09)	1.06 (1.03 – 1.10)	1.07 (1.04 – 1.11)	1.10 (1.05 – 1.13)	1.10 (1.06 – 1.15)	1.11 (1.07 – 1.16)
		90 <sup>th</sup> (26.1)	1.02 (1.01 – 1.03)	1.00 (1.00 – 1.00)	1.00 (1.00 – 1.00)	1.00 (1.00 – 1.00)	1.00 (1.00 – 1.00)	1.00 (1.00 – 1.00)	1.00 (1.00 – 1.00)	1.00 (1.00 – 1.01)
Humidity	Rajshahi	10 <sup>th</sup> (72.2)	3.89 (1.69 – 8.94)	1.26 (1.09 – 1.47)	1.25 (1.09 – 1.43)	1.23 (1.09 – 1.39)	1.21 (1.08 – 1.37)	1.20 (1.06 – 1.35)	1.18 (1.03 – 1.35)	1.17 (1.00 – 1.36)
		50 <sup>th</sup> (78.2)	2.18 (1.35 – 3.51)	1.14 (1.05 – 1.25)	1.14 (1.05 – 1.23)	1.23 (1.05 – 1.21)	1.12 (1.04 – 1.20)	1.11 (1.03 – 1.19)	1.10 (1.02 – 1.19)	1.09 (1.00 – 1.19)
		90 <sup>th</sup> (85.1)	1.11 (1.04 – 1.19)	1.02 (1.01 – 1.03)	1.02 (1.01 – 1.03)	1.02 (1.01 – 1.03)	1.02 (1.01 – 1.02)	1.01 (1.00 – 1.02)	1.01 (1.00 – 1.02)	1.01 (1.00 – 1.02)
Rainfall	Rajshahi	10 <sup>th</sup> (1.0)	4.62 (1.59 – 13.45)	1.19 (0.98 – 1.44)	1.20 (1.01 – 1.43)	1.22 (1.04 – 1.44)	1.24 (1.07 – 1.45)	1.26 (1.09 – 1.47)	1.29 (1.10 – 1.51)	1.31 (1.10 – 1.55)
		50 <sup>th</sup> (7.0)	3.45 (1.45 – 8.21)	1.15 (0.98 – 1.34)	1.16 (1.01 – 1.34)	1.18 (1.03 – 1.34)	1.19 (1.05 – 1.35)	1.21 (1.07 – 1.37)	1.23 (1.08 – 1.39)	1.24 (1.08 – 1.43)
		90 <sup>th</sup> (27.3)	1.28 (1.08 – 1.53)	1.03 (1.00 – 1.06)	1.03 (1.00 – 1.06)	1.03 (1.01 – 1.06)	1.04 (1.01 – 1.06)	1.04 (1.01 – 1.07)	1.04 (1.02 – 1.07)	1.04 (1.02 – 1.07)

In particular, Naogaon district showed the highest cumulative risk associated with humidity at the 10th percentile (72.3%), (RR=10.63, 95% CI 3.45 – 32.74). The risk decreases with increasing percentile: 50th (78.4%) and 90th (84.5%), (RR: 3.58 vs 1.22). Exploring the immediate effect of humidity at lag

0, there was an increase risk at the 10th percentile (72.3%), (RR = 1.52, 95% CI 1.21 – 1.91). The risk decrease at the 50th and 90th percentiles (78.4% and 84.5%, respectively) but remains significant (RR = 1.25, 95% CI 1.11 – 1.42) vs (RR = 1.04, 95% CI 1.02 – 1.06). Similarly, we found a significant relationship with the 10th percentile temperature of 14.1 °C, (RR = 4.31, 95% CI 1.71 – 10.83), 50th percentile temperature of 21.0 °C, (RR = 1.89, 95% CI 1.89 – 2.83), and 90th percentile temperature of 26.2 °C, (RR = 1.03, 95% CI 1.01 – 1.04) at lag 0-6. For rainfall, we found the highest relationship with 0.87 mm, (RR=1.49, 95% CI 1.30 – 1.71), 8.01 mm, (RR=1.36, 95% CI 1.22 – 1.52), and 29.18 mm, (RR=1.04, 95% CI 1.03 – 1.05) at lag 6 quarterly.

The overall temperature effect in Nawabganj district at the 10th percentile (14 °C) was (RR=3.59, 95% CI: 2.17 – 5.94). At a specific lag, the temperature-TB association was highest at lag 6 and inversely related. For example at the 10th percentile temperature (14 °C), RR was 1.28, (95% CI: 1.18 – 1.40), at the 50th percentile, 21.1 °C, (RR=1.15, 95% CI: 1.11 – 1.28), and at the 90th percentile, 26.2 °C, (RR=1.00, 95% CI: 1.00 – 1.00). For humidity, we found the highest relationship at a humidity level of 72.4%, (RR=1.34, 95% CI: 1.19 – 1.50) at lag 0. For rainfall, we observed an increased risk at lower rainfall at lag 6: 0.97 mm, (RR = 1.34, 95% CI: 1.24 – 1.45), 7.72 mm, (RR = 1.26, 95% CI: 1.19 – 1.34), and 29.82 mm, (RR = 1.03, 95% CI: 1.02 – 1.04).

Finally, Rajshahi district showed the overall highest cumulative risk associated with rainfall at the 10th percentile of 1.0 mm: (RR=4.62, 95% CI: 1.59 – 13.45). The risk decreases at increased percentiles: 50th (7.0mm) and 90th (27.3mm), (RR: 3.45 vs 1.28). At a specific lag, increased risks were observed for the rainfall-TB association at lag 6 and at lower rainfall: 1.0 mm, (RR = 1.31, 95% CI 1.10 – 1.55), 7.0 mm, (RR = 1.24, 95% CI 1.08 – 1.43), and 27.3 mm, (RR = 1.04, 95% CI 1.02 – 1.07). For temperature, highest association was observed at lag 6 and at lower temperature: 14 °C, (RR=1.28, 95% CI 1.16 – 1.42), 21 °C, (RR=1.11, 95% CI 1.107 – 1.16 ), and 26.1 °C, (RR=1.00, 95% CI 1.00 – 1.01). For humidity, we observed the highest relationship at 72.2%, (RR = 1.26, 95% CI 1.09 – 1.47), 78.2%, (RR = 1.14, 95% CI 1.05 – 1.25), and 85.1%, (RR = 1.02, 95% CI 1.01 – 1.03) at lag 6.

### 3.3.3 Weather related burden of TB

Table 3.2 shows the estimated attributable fractions due to total, low and high weather variables in each district with 95% empirical confidence intervals (eCIs). Based on the backward perceptible the overall proportions of TB attributable to temperature in Naogaon, Nawabganj, and Rajshahi districts were 49.0%, 44.0% and 42.3%, respectively. Similarly, the burden of TB attributable to relative humidity is higher than temperature with 69.8%, 56.4%, and 51.5% of TB cases attributed to relative humidity in Naogaon, Nawabganj, and Rajshahi districts respectively. Finally, the overall attributable risk of TB

cases due to rainfall is higher than that of temperature and relative humidity: 71.9% in Naogaon; 68.3% in Nawabganj; and 64.6% in Rajshahi districts.

Table 3. 2 Attributable fraction based on exponential covariance structure

Variables	Districts	Cases		Overall	Extreme low temperature (< 10 <sup>th</sup> percentile)	Extreme high temperature (> 90 <sup>th</sup> percentile)
Temperature	Naogaon	5,896	Forw	40.5 (20.4 – 51.4)	4.9 (2.7 – 5.8)	0.26 (0.10 – 0.42)
			Back	49.0 (22.3 – 66.4)	9.4 (2.6 – 14.9)	0.21 (0.09 – 0.32)
	Nawabganj	9,498	Forw	36.3 (26.4 – 43.6)	4.2 (3.1 – 4.8)	0.10 (0.06 – 0.14)
			Back	44.0 (29.4 – 55.8)	8.8 (5.3 – 12.0)	0.07 (0.05 – 0.10)
	Rajshahi	6,394	Forw	35.5 (22.4 – 44.4)	4.1 (2.8 – 4.9)	0.05 (0.03 – 0.07)
			Back	42.3 (24.9 – 55.5)	8.1 (4.2 – 11.7)	0.07 (0.4 – 0.1)
				Overall	Extreme low rainfall (< 10 <sup>th</sup> percentile)	Extreme high rainfall (> 90 <sup>th</sup> percentile)
Humidity	Naogaon	5,896	Forw	59.8 (42.5 – 68.9)	11.5 (9.2 – 12.3)	1.4 (0.8 – 1.9)
			Back	69.8 (47.6 – 82.9)	24.2 (14.0 – 32.1)	1.5 (0.8 – 2.1)
	Nawabganj	9,498	Forw	49.7 (36.9 – 58.7)	9.8 (7.7 – 10.9)	1.3 (0.8 – 1.7)
			Back	56.4 (40.3 – 68.3)	17.3 (11.2 – 22.8)	1.3 (0.8 – 1.8)
	Rajshahi	6,394	Forw	45.7 (22.6 – 58.6)	9.3 (5.1 – 11.0)	0.8 (0.3 – 1.3)
			Back	51.5 (24.7 – 68.7)	15.2 (6.5 – 22.5)	0.9 (0.3 – 1.4)
				Overall	Extreme low humidity (< 10 <sup>th</sup> percentile)	Extreme high humidity (> 90 <sup>th</sup> percentile)
Rainfall	Naogaon	5,896	Forw	63.5 (48.7 – 72.0)	11.1 (9.1 – 12.1)	1.1 (0.7 – 1.5)
			Back	71.9 (53.5 – 83.1)	25.0 (15.6 – 33.1)	1.3 (0.7 – 1.8)
	Nawabganj	9,498	Forw	60.9 (51.4 – 67.7)	10.9 (9.5 – 11.7)	0.7 (0.5 – 0.9)
			Back	68.3 (56.6 – 76.8)	23.1 (17.2 – 28.6)	1.3 (0.9 – 1.6)
	Rajshahi	6,394	Forw	59.3 (27.1 - 74.2)	5.1 (2.5 – 6.0)	1.4 (0.4 – 2.1)
			Back	64.6 (27.0 – 83.1)	17.9 (5.3 – 27.4)	1.9 (0.6 – 3.2)

The attributable risks were then separated into two components (Table 3.2); extreme low (less than the 10th percentile); and extreme high (more than the 90th percentile) weather values. The comparison of the two contributions clearly indicates that extreme low temperatures are responsible for most of the TB incidence with attributable proportions of 9.4%, 8.8% and 8.1%, compared to 0.21%, 0.07% and 0.07% for extreme high temperatures in Naogaon, Nawabganj, and Rajshahi districts, respectively. Similarly, extreme low relative humidity is responsible for most of the TB cases attributable to humidity with 24.2%, 17.3% and 15.2%, compared to 1.5%, 1.3% and 0.9% for extreme high relative humidity in Naogaon, Nawabganj, and Rajshahi districts, respectively. Finally, extreme low rainfall is also responsible for most of the TB incidence attributable to rainfall 25.0%, 23.1% and 17.9%, compared to

1.3%, 1.3% and 1.9% for extreme high rainfall, in Naogaon, Nawabganj, and Rajshahi districts, respectively.

The exposure-lag-response association and the estimation of the attributable fraction may be sensitive to the choices of covariance model used for predicting the weather variables. Therefore, we tested the robustness associated with using different covariance models: Exponential, Spherical and Matern. Changing the covariance model to spherical or Matern yielded similar results as presented in Tables S3.3-S3.4. Similarly, we estimated the attributable fraction using a forward perspective [51] and we compared the results with those estimated with the backward perspective. We observed slight, but not substantial differences in the estimated attributable fraction using both methods. This is not unexpected, Gasparrini et al., 2014 [51] reported that attributable fractions computed forward are affected by a certain degree of negative bias associated with the averaging of future events within the lag period.

We present the results from investigating the interplay between the weather parameters in Figure S3.1. The figure displayed the weather-TB associations expressed as logarithm of relative risk (due to large values) for three single and six adjusted weather parameters in the three districts. All the single weather parameter models indicates significant risk estimates for weather exposure except rainfall. The risks associated with temperature increased after adjusting for humidity in the three districts but decreased subsequently when adjusted for rainfall. In the districts the effect of single-weather parameter, humidity on TB cases decreased after adjusting for temperature and rainfall. Rainfall showed the lowest association with TB among the single parameter models. After adjusting for temperature, the effect of rainfall increased slightly but decreases when adjusted for humidity.

### **3.4 Discussion**

In this study, we quantified the lagged and cumulative effects of temperature, rainfall, and humidity on the risk of TB in three districts using a distributed lag model. After controlling for long-term trend, results showed that weather factors may play an important role in the epidemic of TB incidence. We found a strong association between three climate variables and TB incidence in Rajshahi province, Bangladesh. Low temperature, low humidity and low rainfall are all associated with higher incidence of TB in this study, however, the lag differs with each weather variable. Temperature and rainfall effects were delayed and increases over the lag period while humidity was immediate and the risk decreases with longer exposure. This suggests that temperature may govern transmission and humidity may govern reactivation (incubation period); previous studies have also yielded similar results [54, 55].

In recent years, TB has been recognized as a significant infectious disease related to climate change [56-58]. An increased risk of TB incidence following weather factors has been reported all over the world [5, 59, 60]. A study in China showed that the seasonal rate of new TB cases was highest in late spring to early summer, reaching the lowest point in late winter and early spring [61]. Similarly, Yang *et al.* [8] showed that weather factors were significantly associated with an increased risk of TB incidence [8]. A previous Cameroon study, estimated that more TB cases were reported in the rainy seasons, with a significant difference as compared to the other seasons [62]. Furthermore, relative low humidity also was thought to play an important role in increasing the magnitude of the TB outbreak [63].

While our study and those cited above measure association and cannot be concluded to indicate causality, it is interesting to consider the potential mechanisms of the association. Weather factors may play an important role in TB transmission by influencing mycobacterial growth or its survival. Alternatively, weather can impact human behaviour and human susceptibility. Cold temperature and lack of sunshine have been shown to decrease human immunity and lower vitamin D levels which may increase the reactivation of TB cases [61, 64]. Also, in cold environments with low humidity, the conditions in the upper airways of host populations may be favourable to *Mtb* due to the higher speed of entry [65].

It is also clear from epidemiological studies that close and prolonged contact is responsible for the spread of *Mtb* from infected persons to uninfected persons [66]. In winter and at times of low humidity, indoor activities are much more frequent than in the summer season, which increases crowding and reduces ventilation – two factors known to be associated with the transmission of *Mtb* [8]. Such conditions also increase the frequency of viral infections that can cause immunological vulnerability [67], hence, may render people more vulnerable to infection with *Mtb*.

Several limitations of this study should be noted. Firstly, our time series analysis was based on quarterly time series observations. Measurements based on such long time intervals may be too coarse, and therefore the risk of bias cannot be excluded. Secondly, we could only adjust for a few important weather variables in the model. Many of the other important risk factors for TB were unavailable including: human activities; population density; and other environmental factors. Thirdly, weather variables based on fixed monitoring sites are not completely accurate exposure observations for each individual. Therefore, more accurate data and additional risk factors of TB could be adjusted in the models to confirm their associations and mechanism of TB cases and continuing climate change.

To our knowledge, this is the first study to explore the effects of weather variation (temperature, humidity, and rainfall) on TB at a long time scale using DLMS in Bangladesh. The lag effects of weather factors on TB cases observed in this study can help the NTP in Bangladesh with preparedness activities including forward planning, and implementing public health interventions for the prevention and control of TB. Each year, an estimated 70,000 people die of TB and 300,000 new cases are projected in Bangladesh [68]. Although this study is based on data from Rajshahi province only, the real impact of TB incidence in Bangladesh due to weather factors might be much greater, given the large population of big cities (e.g. Dhaka) at risk.

In this study, we found significant interactions between weather parameters. We observed changes in the estimated risk of single weather variables on TB after adjusting for additional weather parameter. Weather parameters are often highly correlated and difficult to isolate [69]. For example, skilling found [70] relative humidity changes when temperature changes because warm air can hold more water vapor than cool air, this may have significant impact on incidence of TB. Furthermore, humidity and rainfall have strong connection because evaporation cool the air and increase absolute moisture [71]. This implies that average relative humidity decrease through rainfall, which may increase the outbreak of TB cases.

The assessment of weather-TB associations in the North-West region of Bangladesh has provided new insight into the burden of the disease that can be attributed to varying weather conditions. Our findings identified statistically significant associations between weather variables (temperature, humidity, and rainfall) and TB cases in Rajshahi province using DLMS methods. The effects of low temperature, humidity, and rainfall on TB were immediate and strong. These results suggest that there is an important link between TB and weather variables and that such knowledge could be considered in the design of policy to support NTP in Bangladesh for controlling TB cases.

### **Ethics approval**

This study is based on aggregated TB surveillance data in Rajshahi province provided by the Bangladesh National TB control program. No confidential information was included because analyses were performed at the aggregate level. All of the methods were conducted in accordance with the approved research protocol. The research protocol was approved by the James Cook University human ethics approval board, H7300.

### **Acknowledgements**

The first author was funded by the College of Medicine and Dentistry at James Cook University, Australia PhD programme (JCU-QLD-866531). The authors would also like to thank the National TB control program of Bangladesh and climate division in Bangladesh for providing TB and weather data.

## References

1. WHO, *Global tuberculosis report 2017*. WHO/HTM/TB/2017.23, Geneva, 2017.
2. Kumar, V., and Cotran, R. S., *Robbins' basic pathology*. Archives of Pathology and Laboratory Medicine, 1994. **118**(2): p. 203-203.
3. Frieden, T. R., et al., *Tuberculosis*. Lancet, 2003. **362**(9387): p. 887-99.
4. Alirol, E., et al., *Urbanisation and infectious diseases in a globalised world*. The Lancet Infectious Diseases, 2011. **11**(2): p. 131-41.
5. Fares, A., *Seasonality of tuberculosis*. Journal of Global Infectious Diseases, 2011. **3**(1): p. 46-55.
6. Chowdhury, R., et al., *Seasonality of tuberculosis in rural West Bengal: A time series analysis*. International Journal of Health and Allied Sciences, 2013. **2**(2): p. 95-98.
7. Talat, N., et al., *Vitamin D Deficiency and Tuberculosis Progression*. Emerging Infectious Diseases, 2010. **16**(5): p. 853-855.
8. Yang, Y., et al., *Seasonality impact on the transmission dynamics of tuberculosis*. Computational and Mathematical Methods in Medicine, 2016. **2016**: p. 8713924.
9. Bennett, S., et al., *Investigation of environmental and host-related risk factors for tuberculosis in Africa. II. Investigation of host genetic factors*. American Journal of Epidemiology, 2002. **155**(11): p. 1074-1079.
10. Griffin, J. M., et al., *The association of cattle husbandry practices, environmental factors and farmer characteristics with the occurrence of chronic bovine tuberculosis in dairy herds in the Republic of Ireland*. Preventive Veterinary Medicine, 1993. **17**(3-4): p. 145-160.
11. Narasimhan, P., et al., *Risk factors for tuberculosis*. Pulmonary Medicine, 2013. **2013**.
12. Tornee, S., et al., *The association between environmental factors and tuberculosis infection among household contacts*. Southeast Asian Journal of Tropical Medicine & Public Health, 2005. **36**: p. 221-224.
13. Chan, T., *Vitamin D deficiency and susceptibility to tuberculosis*. Calcified Tissue International, 2000. **66**(6): p. 476-478.
14. Nnoaham, K. E., and Clarke, A., *Low serum vitamin D levels and tuberculosis: a systematic review and meta-analysis*. International Journal of Epidemiology, 2008. **37**(1): p. 113-119.
15. Wilkinson, R. J., et al., *Influence of vitamin D deficiency and vitamin D receptor polymorphisms on tuberculosis among Gujarati Asians in west London: a case-control study*. The Lancet, 2000. **355**(9204): p. 618-621.
16. Wubuli, A., et al., *Seasonality of active tuberculosis notification from 2005 to 2014 in Xinjiang, China*. PLoS One, 2017. **12**(7): p. e0180226.
17. Yang, Y., et al., *Seasonality impact on the transmission dynamics of tuberculosis*. Computational and Mathematical Methods in Medicine, 2016. **2016**.
18. Nelson, R. J., and Demas, E. G., *Seasonal changes in immune function*. The Quarterly Review of Biology, 1996. **71**(4): p. 511-548.
19. Nelson, R. J., *Seasonal immune function and sickness responses*. Trends in Immunology, 2004. **25**(4): p. 187-192.
20. Fernandes, F. M. D. C., et al., *Relationship between climatic factors and air quality with tuberculosis in the Federal District, Brazil, 2003-2012*. Brazilian Journal of Infectious Diseases, 2017. **21**(4): p. 369-375.

21. Begum, V., et al., *Tuberculosis and patient gender in Bangladesh: sex differences in diagnosis and treatment outcome*. The International Journal of Tuberculosis and Lung Disease, 2001. **5**(7): p. 604-610.
22. Mondal, M. N. I., Chowdhury, K. R. M., and Sayem, A. M., *Associated Factors of Pulmonary Tuberculosis in Rajshahi City of Bangladesh*. Journal of Human Ecology, 2014. **45**(1): p. 61-68.
23. Rahmatullah, M., et al., *Medicinal plants and formulations used by the Soren clan of the Santal tribe in Rajshahi district, Bangladesh for treatment of various ailments*. African Journal of Traditional, Complementary and Alternative Medicines, 2012. **9**(3): p. 350-359.
24. Onozuka, D., Hashizume, M., and Hagihara, A., *Impact of weather factors on Mycoplasma pneumoniae pneumonia*. Thorax, 2009. **64**(6): p. 507-511.
25. Adegboye, O., and Adegboye, M., *Spatially correlated time series and ecological niche analysis of cutaneous leishmaniasis in Afghanistan*. International Journal of Environmental Research and Public Health, 2017. **14**(3): p. 309.
26. Adegboye, O., Al-Saghir, M., and Leung, H. D., *Joint spatial time-series epidemiological analysis of malaria and cutaneous leishmaniasis infection*. Epidemiology & Infection, 2017. **145**(4): p. 685-700.
27. Adegboye, M. A., et al., *Effects of time-lagged meteorological variables on attributable risk of leishmaniasis in central region of Afghanistan*. Science of The Total Environment, 2019. **685**: p. 533-541.
28. Xiao, Y., et al., *The influence of meteorological factors on tuberculosis incidence in Southwest China from 2006 to 2015*. Scientific Reports, 2018. **8**.
29. NTP, *Tuberculosis control in Bangladesh*. Annual report, 2017.
30. Gotway, C. A., and Young, J. L., *Combining incompatible spatial data*. Journal of the American Statistical Association, 2002. **97**(458): p. 632-648.
31. Adegboye, O., and Kotze, D., *Epidemiological analysis of spatially misaligned data: a case of highly pathogenic avian influenza virus outbreak in Nigeria*. Epidemiology & Infection, 2014. **142**(5): p. 940-949.
32. Lawson, A. B., *Bayesian disease mapping: hierarchical modeling in spatial epidemiology*. 2013: Chapman and Hall/CRC.
33. Adegboye, O. A., and Kotze, D., *Epidemiological analysis of spatially misaligned data: a case of highly pathogenic avian influenza virus outbreak in Nigeria*. Epidemiology & Infection, 2014. **142**(5): p. 940-949.
34. Oliver, M. A., and Webster, R., *Kriging: a method of interpolation for geographical information systems*. International Journal of Geographical Information System, 1990. **4**(3): p. 313-332.
35. Mitas, L., and Mitasova, H., *Spatial interpolation*. Geographical information systems: principles, techniques, management and applications, 1999. **1**(2).
36. Bivand, R. S., Pebesma, J. E., and Gomez-Rubio, V., *Interpolation and geostatistics*. Applied spatial data analysis with R, 2008: p. 191-235.
37. Ribeiro Jr, P., and Diggle, P., *geoR: a package for geostatistical analysis*. R-NEWS. 2001; **1** (2): 15–18. View Article PubMed/NCBI Google Scholar, 2009.
38. Gasparrini, A., *Distributed Lag Linear and Non-Linear Models in R: The Package dlnm*. Journal of Statistical Software, 2011. **43**(8): p. 1-20.
39. Gasparrini, A., *Modeling exposure–lag–response associations with distributed lag non-linear models*. Statistics in Medicine, 2014. **33**(5): p. 881-899.
40. Gasparrini, A., and Leone, M., *Attributable risk from distributed lag models*. BMC Medical Research Methodology, 2014. **14**(1): p. 55.
41. Gasparrini, A., *Distributed lag linear and non-linear models for time series data*. Document Is Available at R Project: <https://cran.R-project.org/web/packages/dlnm/> (Accessed: 4 May 2015) <http://143107.2013>, 2013. **212**.
42. Baek, J., et al., *Distributed lag models: examining associations between the built environment and health*. Epidemiology (Cambridge, Mass.), 2016. **27**(1): p. 116.

43. Kim, H., and Lee, T. J., *Spatial variation in lag structure in the short-term effects of air pollution on mortality in seven major South Korean cities, 2006–2013*. Environment International, 2019.
44. Armstrong, B., *Models for the relationship between ambient temperature and daily mortality*. Epidemiology, 2006: p. 624-631.
45. Wagenmakers, E. J., and Farrell, S., *AIC model selection using Akaike weights*. Psychonomic Bulletin & Review, 2004. **11**(1): p. 192-196.
46. Gasparrini, A., Armstrong, B., and Kenward, G. M., *Distributed lag non-linear models*. Statistics in Medicine, 2010. **29**(21): p. 2224-2234.
47. Sillmann, J., et al., *Understanding, modeling and predicting weather and climate extremes: Challenges and opportunities*. Weather and Climate Extremes, 2017. **18**: p. 65-74.
48. Kim, H., and Lee, T. J., *On inferences about lag effects using lag models in air pollution time-series studies*. Environmental Research, 2019. **171**: p. 134-144.
49. Dziak, J. J., et al., *Sensitivity and specificity of information criteria*. bioRxiv, 2019: p. 449751.
50. Shrestha, S.L., Shrestha, L. I., and Shrestha, N., *Region-wise effects of climate sensitive variables on some specific disease burdens in Nepal*. The Open Atmospheric Science Journal, 2016. **10**(1).
51. Gasparrini, A., and Leone, M., *Attributable risk from distributed lag models*. BMC Medical Research Methodology, 2014. **14**(1): p. 55-55.
52. Gasparrini, A., et al., *Mortality risk attributable to high and low ambient temperature: a multicountry observational study*. The Lancet, 2015. **386**(9991): p. 369-375.
53. R Core Team, *R: A language and environment for statistical computing*. R Foundation for Statistical Computing, Vienna, Austria. 2017.
54. Zhang, Q., Yan, L., and He, J., *Time series analysis of correlativity between pulmonary tuberculosis and seasonal meteorological factors based on theory of Human-Environmental Inter Relation*. Journal of Traditional Chinese Medical Sciences, 2018. **5**(2): p. 119-127.
55. Narula, P., et al., *Analyzing seasonality of tuberculosis across Indian states and union territories*. Journal of Epidemiology and Global Health, 2015. **5**(4): p. 337-346.
56. Wingfield, T., et al., *The seasonality of tuberculosis, sunlight, vitamin D, and household crowding*. The Journal of Infectious Diseases, 2014. **210**(5): p. 774-783.
57. Tam, C. M., et al., *Seasonal pattern of tuberculosis in Hong Kong*. International Journal of Epidemiology, 2005. **34**(4): p. 924-930.
58. Willis, M. D., et al., *Seasonality of tuberculosis in the United States, 1993–2008*. Clinical Infectious Diseases, 2012. **54**(11): p. 1553-1560.
59. Luquero, F., et al., *Trend and seasonality of tuberculosis in Spain, 1996–2004*. The International Journal of Tuberculosis and Lung Disease, 2008. **12**(2): p. 221-224.
60. Mason, P. H., and Degeling, C., *Beyond biomedicine: Relationships and care in tuberculosis prevention*. Journal of Bioethical Inquiry, 2016. **13**(1): p. 31-34.
61. Liu, L., Zhao, X. Q., and Zhou, Y., *A tuberculosis model with seasonality*. Bulletin of Mathematical Biology, 2010. **72**(4): p. 931-952.
62. Ane-Anyangwe, I. N., et al., *Seasonal variation and prevalence of tuberculosis among health seekers in the South Western Cameroon*. East African Medical Journal, 2006. **83**(11): p. 588-95.
63. Pérez-Padilla, R., and Franco-Marina, F., *The impact of altitude on mortality from tuberculosis and pneumonia*. The International Journal of Tuberculosis and Lung Disease, 2004. **8**(11): p. 1315-1320.
64. Ali, S., and Bakhshi, S. S., *Does vitamin d deficiency account for ethnic differences in tuberculosis seasonality in the UK? AU - Douglas, A. Stuart*. Ethnicity & Health, 1998. **3**(4): p. 247-253.
65. Hoppentocht, M., et al., *Developments and strategies for inhaled antibiotic drugs in tuberculosis therapy: A critical evaluation*. European Journal of Pharmaceutics and Biopharmaceutics, 2014. **86**(1): p. 23-30.
66. Driver, C. R., et al., *Transmission of Mycobacterium tuberculosis associated with air travel*. JAMA, 1994. **272**(13): p. 1031-1035.

67. Mäkinen, T. M., et al., *Cold temperature and low humidity are associated with increased occurrence of respiratory tract infections*. *Respiratory Medicine*, 2009. **103**(3): p. 456-462.
68. Zaman, K., et al., *Tuberculosis in Bangladesh: A 40-Year Review*. 11 ASCON. ICDDR,B. Scientific session, abstract book, 2007. **86**: p. 4-6.
69. Vanos, J., et al., *Association of weather and air pollution interactions on daily mortality in 12 Canadian cities*. *Air Quality, Atmosphere & Health*, 2015. **8**(3): p. 307-320.
70. Skilling, T., *The relationship between relative humidity, temperature and dew point*. Chicago Tribune, 2009.
71. Davis, R. E., McGregor, R. G., and Enfield, B. K., *Humidity: A review and primer on atmospheric moisture and human health*. *Environmental Research*, 2016. **144**: p. 106-116.

## Supplementary materials

Table S3.1: Model specification

Models	Exposure-response	Lag-response
Model 1	Linear	Constant
Model 2	Quadratic B-Spline <sup>a</sup>	Constant
Model 3	Quadratic B-Spline <sup>b</sup>	Constant
Model 4	Quadratic B-Spline <sup>c</sup>	Constant
Model 5	Linear	Linear
Model 6	Quadratic B-Spline <sup>a</sup>	Linear
Model 7	Quadratic B-Spline <sup>b</sup>	Linear
Model 8	Quadratic B-Spline <sup>c</sup>	Linear
Model 9	Linear	Quadratic B-Spline <sup>d</sup>
Model 10	Quadratic B-Spline <sup>a</sup>	Quadratic B-Spline <sup>d</sup>
Model 11	Quadratic B-Spline <sup>b</sup>	Quadratic B-Spline <sup>d</sup>
Model 12	Quadratic B-Spline <sup>c</sup>	Quadratic B-Spline <sup>d</sup>
Model 13	Linear	Quadratic B-Spline <sup>e</sup>
Model 14	Quadratic B-Spline <sup>a</sup>	Quadratic B-Spline <sup>e</sup>
Model 15	Quadratic B-Spline <sup>b</sup>	Quadratic B-Spline <sup>e</sup>
Model 16	Quadratic B-Spline <sup>c</sup>	Quadratic B-Spline <sup>e</sup>

For each of the meteorological variables, Temperature, Relative humidity and Rainfall:

<sup>a</sup>Knot is placed at median value

<sup>b</sup>Knot is placed at 2 equally spaced distance

<sup>c</sup>Knot is placed at 3 equally spaced distance

For each of the lag-quarter specifications, Lag 0-2, Lag 0-3, Lag 0-4, Lag 0-5 and Lag 0-6:

<sup>d</sup>Knot is placed at mean position with intercept

<sup>e</sup>Knot is placed at mean position without intercept

Table S3.2: Summary of models selection criteria- QAIC and QBIC using data from the three districts.

Weather variable	LAG 0-1						LAG 0-2						LAG 0-3					
	Best Model	Total df	QAIC value	Best Model	Total df	QBIC value	Best Model	Total df	QAIC value	Best Model	Total df	QBIC value	Best Model	Total df	QAIC value	Best Model	Total df	QBIC value
Temperature	2	13	1075.8	12	20	923.2	2	13	992.1	3	13	859	12	20	743.2	8	10	859.8
	3	13	1006.7	12	20	919.8	3	13	1012.9	3	13	862.8	12	20	697.7	12	20	831.2
	4	13	1156.2	12	20	959.4	4	13	1070.9	3	13	862	12	20	702.9	12	20	843.4
	5	8	933.1	8	10	901.5	5	8	1012.7	3	13	859	8	10	766.1	12	20	857.9
	6	8	998.5	12	20	872.6	6	8	944	3	13	838.2	12	20	675.5	10	12	777.1
	7	12	1063.2	10	12	883.2	7	12	999	5	4	808.2	10	12	647.3	10	12	737.9
	8	4	1119.1	10	12	920.2	8	4	1060.6	5	4	802.9	10	12	645.9	10	12	738.8
	9	4	999.7	10	12	881.5	9	4	1034.7	5	4	803.9	10	12	652.1	10	12	751.8
	Rainfall	2	13	1031.5	13	3	870.1	2	13	960.9	2	5	848.2	13	3	800.7	13	3
3		5	1152.3	9	4	956.1	3	5	1151.5	2	5	832.5	9	4	774	13	3	852.2
4		13	1255.5	9	4	1001.8	4	13	1238.5	2	5	838.3	9	4	781.5	13	3	865.7
5		13	1057.4	9	4	983.6	5	13	1260.2	2	5	847.8	9	4	790.7	13	3	884.1
6		13	1005.5	16	15	859	6	13	937.2	2	5	857	16	15	793.2	9	4	910.4
7		13	1147.4	12	20	918.3	7	13	1069.9	3	13	861.8	12	20	777	13	3	919.4
8		13	1198.5	12	20	952.3	8	13	1135.1	2	5	863.6	12	20	790.9	9	4	933,7
9		5	1270.2	16	15	956.4	9	5	1175.1	3	13	866.4	16	15	797.8	9	4	952
Humidity		2	13	933.1	13	3	925.2	2	13	874.6	3	13	881.7	13	3	816.5	13	3
	3	1	867.3	9	4	920.8	3	1	966	1	1	850.2	9	4	811.1	13	3	895.5
	4	1	971.5	9	4	965.1	4	1	1009.3	1	1	845.2	9	4	805.5	9	4	901.7
	5	1	802.9	9	4	913	5	1	992	1	1	853.8	9	4	813.7	13	3	915.5
	6	1	868.2	13	3	870.9	6	1	862.8	1	1	860.2	13	3	814	13	3	921.1
	7	1	888.9	13	3	892.9	7	1	925.3	1	1	850.2	13	3	810.9	13	3	925.1
	8	1	922	13	3	930.3	8	1	960	1	1	844.3	13	3	819.2	13	3	944.2
	9	1	825.4	6	6	891.7	9	1	971.1	1	1	851.5	6	6	818.6	13	3	969.3

Table A3.2: continued

Weather variable	LAG 0-4						LAG 0-5						LAG 0-6					
	Best Model	Total df	QAIC value	Best Model	Total df	QBIC value	Best Model	Total df	QAIC value	Best Model	Total df	QBIC value	Best Model	Total df	QAIC value	Best Model	Total df	QBIC value
Temperature	12	20	697.2	12	20	832.1	12	20	642.5	12	20	749.7	12	20	697.2	12	20	832.1
	12	20	644.4	12	20	750.8	12	20	633.1	12	20	737.6	12	20	644.4	12	20	750.8
	12	20	633.3	12	20	750.8	12	20	634.5	12	20	742.8	12	20	633.3	5	4	750.8
	16	15	661.2	12	20	749.8	12	20	645.6	12	20	764	16	15	661.2	12	20	749.8
	12	20	644.3	12	20	759.3	12	20	632	8	10	734.3	12	20	644.3	12	20	759.3
	10	12	637.2	12	20	725.5	12	20	616	8	10	702.6	5	4	637.2	12	20	725.5
	10	12	632.2	8	10	736.1	12	20	620.2	10	12	728	10	12	632.2	8	10	736.1
	10	12	635.4	12	20	750	12	20	621.9	8	10	714.9	10	12	635.4	12	20	750
Rainfall	13	3	784.2	13	3	851.8	13	3	771.1	12	20	838	13	3	788.4	13	3	881.1
	9	4	753.3	9	4	830	6	6	743.3	13	3	822.2	12	20	783.5	9	4	883.3
	9	4	759.9	13	3	844.2	6	6	754.1	13	3	834.3	12	20	699.1	11	16	826.4
	9	4	769.1	13	3	861.9	13	3	761.8	13	3	851.4	11	16	709.5	11	16	846.9
	16	15	763.7	13	3	875	13	3	763.3	13	3	861.2	11	16	706.4	11	16	846.4
	16	15	771.7	2	3	893.3	12	20	720.9	2	3	882.7	5	4	714	11	16	861.9
	16	15	777.5	2	3	895.7	12	20	742.3	2	3	892.6	11	16	722.1	11	16	880.4
	4	5	793.4	2	3	917.2	12	20	735.2	2	3	910.4	11	16	728.5	11	16	895
Humidity	12	20	788.4	13	3	881.1	12	20	753.6	11	16	907.7	12	20	642.5	12	20	697.2
	12	20	783.5	9	4	883.3	11	16	772.1	11	16	939	12	20	633.1	12	20	644.4
	11	16	699.1	11	16	826.4	12	20	723.2	11	16	826	12	20	634.5	12	20	633.3
	11	16	709.5	11	16	846.9	11	16	692	10	12	814.9	10	12	645.6	16	15	661.2
	11	16	706.4	11	16	846.4	10	12	688.6	14	9	803.5	8	10	632	12	20	644.3
	11	16	714	11	16	861.9	11	16	685	14	9	808.2	12	20	616	5	4	637.2
	11	16	722.1	11	16	880.4	10	12	674.3	10	12	792.6	12	20	620.2	10	12	632.2
	11	16	728.5	11	16	895	10	12	679.4	10	12	804.7	5	4	621.9	10	12	635.4

Table S3.3: Attributable fraction based on Matern covariance structure

Variables	Districts	Cases		Overall	Extreme low Temperature (<10 <sup>th</sup> percentile)	Extreme high temperature (> 90 <sup>th</sup> percentile)
Temperature	Naogaon	5,896	Forw	40.3 (20.2 – 51.0)	4.9 (2.7 – 5.8)	0.2 (0.1 – 0.4)
			Back	48.9 (22.8 – 66.3)	9.4 (3.0 – 14.8)	0.18 (0.1 – 0.3)
	Nawabganj	9,498	Forw	37.2 (26.6 – 44.4)	4.2 (3.2 – 4.9)	0.15 (0.1 – 0.2)
			Back	44.9 (30.2 – 56.1)	8.9 (5.5 – 12.0)	0.12 (0.1 – 0.2)
	Rajshahi	6,394	Forw	34.3 (21.4 – 42.8)	4.1 (2.7 – 4.9)	0.07 (0.03 – 0.10)
			Back	41.1 (23.8 – 54.2)	8.0 (3.9 – 11.5)	0.05 (0.03 – 0.07)
				Overall	Extreme low humidity (< 10 <sup>th</sup> percentile)	Extreme high humidity (> 90 <sup>th</sup> percentile)
Humidity	Naogaon	5,896	Forw	59.5 (41.5 – 68.8)	11.53 (9.1 – 12.3)	1.1 (0.6 – 1.6)
			Back	69.7 (47.0 – 82.8)	24.1 (13.9 – 32.0)	1.2 (0.6 – 1.8)
	Nawabganj	9,498	Forw	49.3 (36.1 – 58.3)	9.8 (7.6 – 10.9)	1.1 (0.7 – 1.5)
			Back	56.0 (39.7 – 67.5)	17.2 (11.2 – 22.5)	1.1 (0.7 – 1.5)
	Rajshahi	6,394	Forw	45.7 (21.9 – 59.1)	9.3 (5.2 – 11.1)	0.9 (0.4 – 1.4)
			Back	51.6 (24.4 – 69.3)	15.2 (6.1 – 22.6)	0.9 (0.4 – 1.5)
				Overall	Extreme low rainfall (< 10 <sup>th</sup> percentile)	Extreme high rainfall (> 90 <sup>th</sup> percentile)
Rainfall	Naogaon	5,896	Forw	63.1 (48.5 – 71.4)	11.1 (9.0 – 12.1)	1.1 (0.7 – 1.4)

			Back	71.8 (53.6 – 82.8)	25.1 (15.5 – 33.3)	1.1 (0.7 – 1.5)
	Nawabganj	9,498	Forw	60.6 (51.0 – 67.6)	10.8 (9.4 – 11.7)	0.7 (0.5 – 0.9)
			Back	68.0 (55.9 – 76.7)	23.0 (16.9 – 28.3)	1.3 (0.9 – 1.6)
	Rajshahi	6,394	Forw	59.3 (26.6 – 74.5)	5.1 (2.4 – 6.1)	1.4 (0.5 – 2.2)
			Back	64.5 (26.3 – 82.9)	17.9 (5.3 – 27.3)	1.95 (0.6 – 3.3)

Table S3.4: Attributable fraction based on spherical covariance structure

Variables	Districts	Cases		Overall	Extreme low temperature (< 10 <sup>th</sup> percentile)	Extreme high temperature (> 90 <sup>th</sup> percentile)
Temperature	Naogaon	5,896	Forw	40.5 (20.3 – 51.3)	4.9 (2.6 – 5.7)	0.11 (0.04 – 0.18)
			Back	49.0 (21.4 – 66.3)	9.4 (3.0 – 14.9)	0.12 (0.04 – 0.21)
	Nawabganj	9,498	Forw	37.6 (27.4 – 44.9)	4.2 (3.3 – 4.9)	0.08 (0.05 – 0.11)
			Back	45.2 (30.6 – 56.2)	8.9 (5.4 – 12.1)	0.10 (0.06 – 0.14)
	Rajshahi	6,394	Forw	34.4 (21.4 – 43.1)	4.1 (2.7 – 4.9)	0.09 (0.05 – 0.14)
			Back	41.1 (23.8 – 54.5)	8.0 (3.9 – 11.5)	0.07 (0.04 – 0.10)
				Overall	Extreme low humidity (< 10 <sup>th</sup> percentile)	Extreme high humidity (> 90 <sup>th</sup> percentile)
Humidity	Naogaon	5,896	Forw	60.7 (43.9 – 70.1)	11.6 (9.3 – 12.4)	1.8 (1.0 – 2.50)
			Back	70.7 (47.5 – 83.1)	24.3 (14.4 – 32.3)	1.9 (1.0 – 2.8)

	Nawabganj	9,498	Forw	50.4 (37.3 – 59.6)	9.8 (7.6 – 10.9)	1.6 (1.0 – 2.1)
			Back	56.9 (40.8 – 68.8)	17.2 (11.4 – 22.5)	1.7 (1.0 – 2.3)
	Rajshahi	6,394	Forw	45.9 (22.7 – 58.8)	9.3 (5.2 – 11.1)	1.1 (0.4 – 1.7)
			Back	51.6 (23.6 – 68.6)	15.1 (6.6 – 22.5)	1.1 (0.4 – 1.8)
				Overall	Extreme low rainfall (< 10 <sup>th</sup> percentile)	Extreme high rainfall (> 90 <sup>th</sup> percentile)
Rainfall	Naogaon	5,896	Forw	62.7 (48.0 – 71.2)	11.1 (9.1 – 12.0)	1.0 (0.6 – 1.3)
			Back	71.2 (52.8 – 82.6)	24.8 (15.5 – 32.7)	1.1 (0.6 – 1.5)
	Nawabganj	9,498	Forw	60.6 (50.1 – 67.5)	10.9 (9.5 – 11.7)	0.7 (0.5 – 0.9)
			Back	68.0 (55.9 – 76.7)	23.0 (17.0 – 28.3)	1.3 (0.9 – 1.7)
	Rajshahi	6,394	Forw	59.4 (26.0 – 74.1)	5.1 (2.5 – 6.0)	1.4 (0.4 – 2.1)
			Back	64.6 (25.4 – 82.7)	17.9 (5.1 – 27.8)	1.9 (0.5 – 3.2)

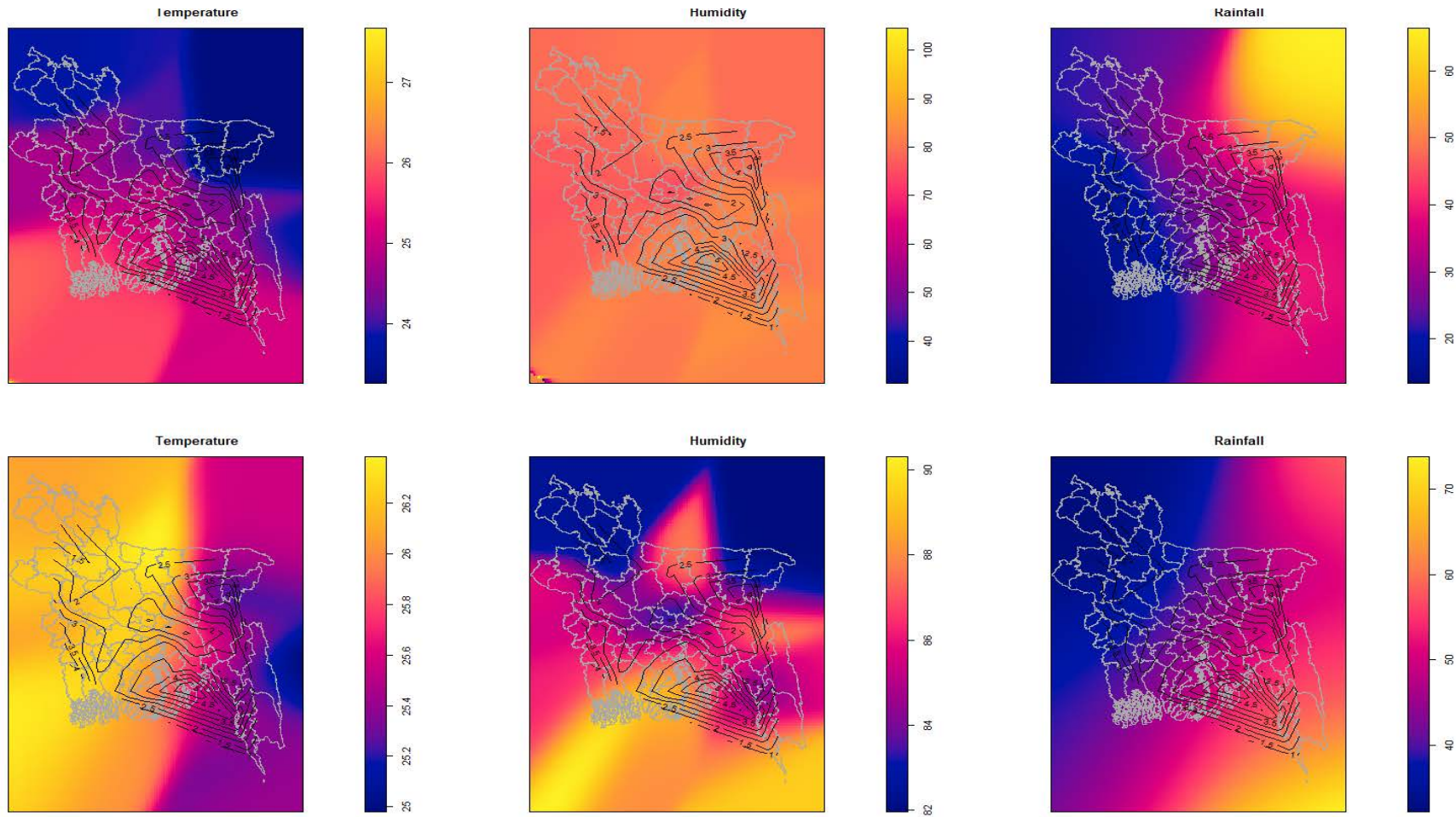


Figure S3.1: Distribution of weather parameters after Bayesian Kriging. (Top panel) First Quarter 2007. (Bottom panel) Second Quarter 2007.

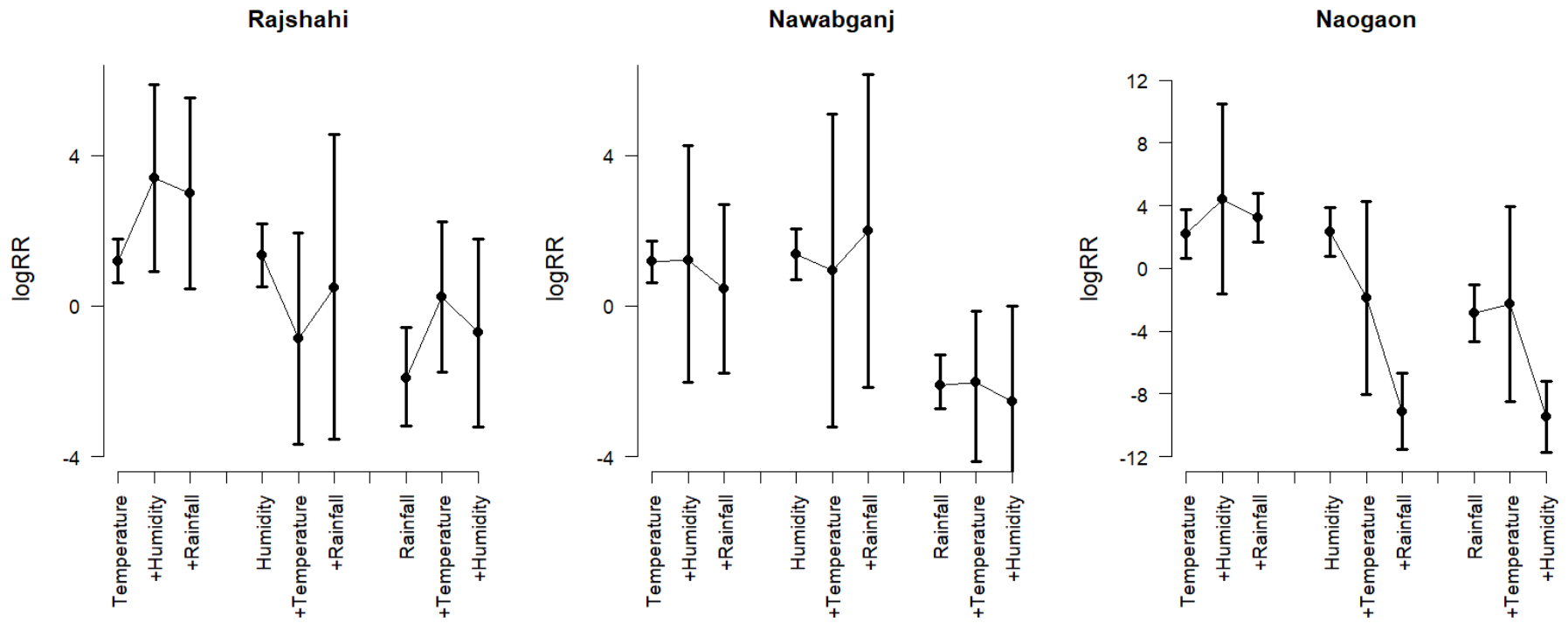


Figure S3.2: Weather-TB association (log relative risks) with 95% CI for an exposure to 10<sup>th</sup> percentile weather parameters for single exposure and adjusted logRR for the remaining weather parameters.

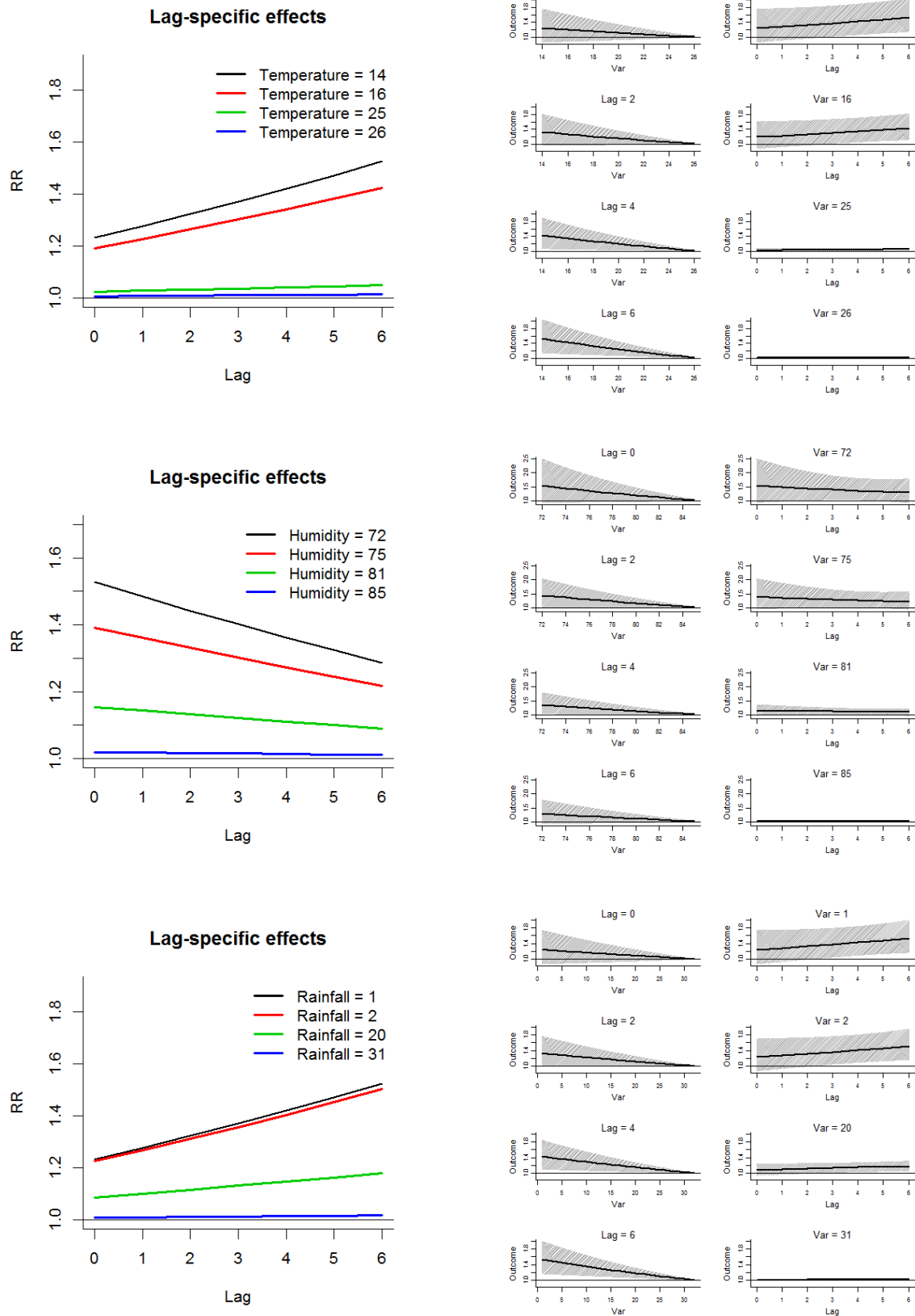


Figure S3.3: Lag-specific effects at different temperature exposures (top panel) and temperature-specific effects at different lags (left column in bottom panel) on TB in Naogaon District.

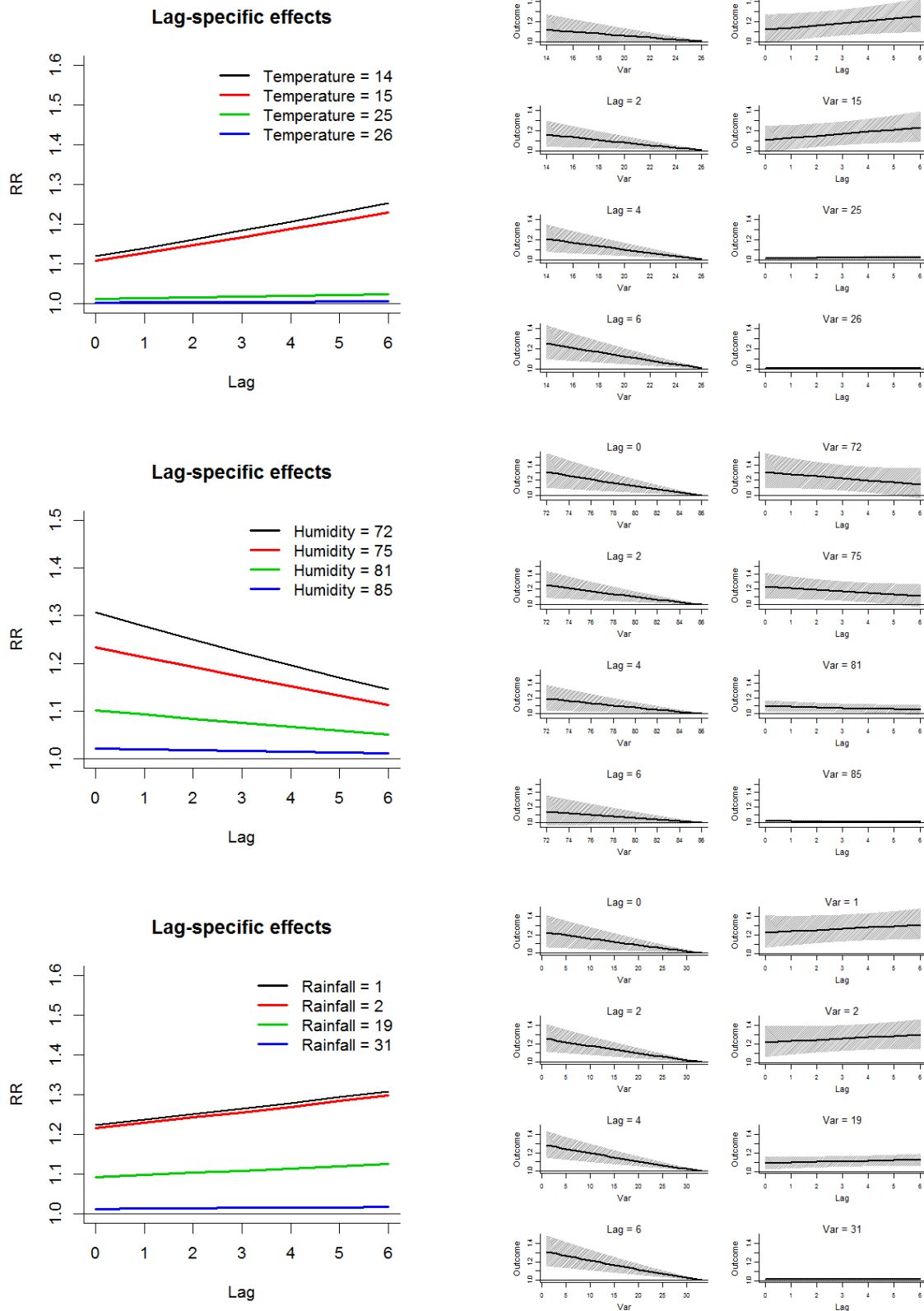


Figure S3.4: Lag-specific effects at different temperature exposures (top panel) and temperature-specific effects at different lags (left column in bottom panel) on TB in Nawabganj District.

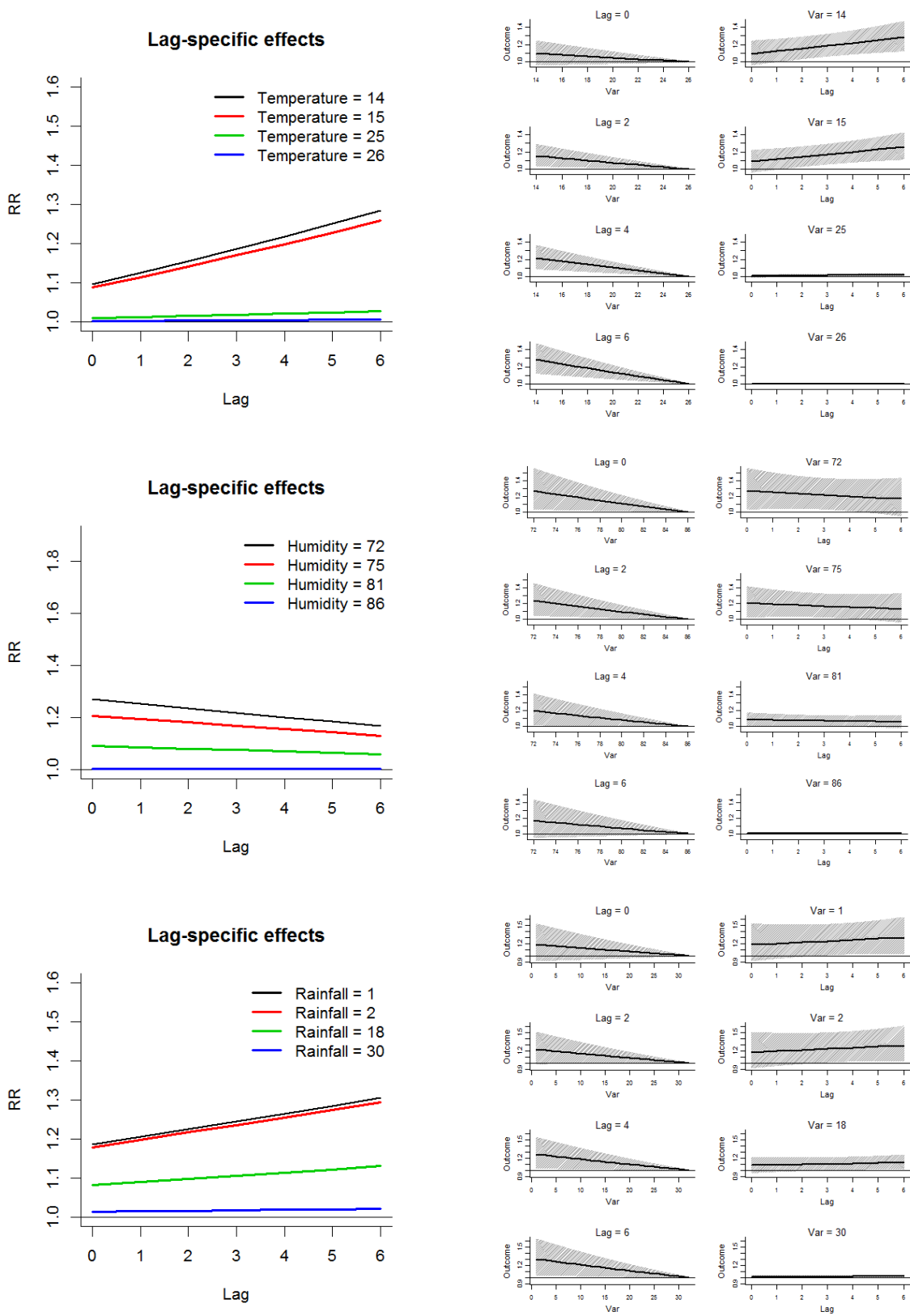


Figure S3.5: Lag-specific effects at different temperature exposures (top panel) and temperature-specific effects at different lags (left column in bottom panel) on TB in Rajshahi District.

# CHAPTER 4

---

## Mathematical analysis of a two-strain disease model with amplification

---

### Statement of joint authorship

**Md Abdul Kuddus** initiated the concept of the study, wrote the manuscript, developed the model, analysed the data, wrote code for model, and acted as corresponding author.

**Emma S. McBryde** assisted with the development of the model, proof read and critically reviewed the manuscript.

**Adeshina I. Adekunle** critically reviewed the manuscript.

**Lisa J. White** proof read and critically reviewed the manuscript.

**Michael T. Meehan** assisted with the development of the model, analysed the data, proof read and critically reviewed the manuscript.

**Kuddus, M. A.,** McBryde, E. S., Adekunle, I. A., White, J. L., Meehan, T. M. (2021). Mathematical analysis of a two-strain disease model with amplification. *Journal of Chaos, Soliton's & Fractals*, 143 (2021), 110594.

## Abstract

We investigate a two-strain disease model with amplification to simulate the prevalence of drug-susceptible (s) and drug-resistant (m) disease strains. Drug resistance first emerges when drug-susceptible strains mutate and become drug-resistant, possibly as a consequence of inadequate treatment, i.e. amplification. In this case, the drug-susceptible and drug-resistant strains are coupled. We perform a dynamical analysis of the resulting system and find that the model contains three equilibrium points: a disease-free equilibrium; a mono-existent disease-endemic equilibrium at which only the drug-resistant strain persists; and a co-existent disease-endemic equilibrium where both the drug-susceptible and drug-resistant strains persist. We found two basic reproduction numbers: one associated with the drug-susceptible strain ( $R_{0s}$ ); the other with the drug-resistant strain ( $R_{0m}$ ), and showed that at least one of the strains can spread in a population if  $\max[R_{0s}, R_{0m}] > 1$ . Furthermore, we also showed that if  $R_{0m} > \max[R_{0s}, 1]$ , the drug-susceptible strain dies out but the drug-resistant strain persists in the population (mono-existent equilibrium); however if  $R_{0s} > \max[R_{0m}, 1]$ , then both the drug-susceptible and drug-resistant strains persist in the population (co-existent equilibrium). We conducted a local stability analysis of the system equilibrium points using the Routh-Hurwitz conditions and a global stability analysis using appropriate Lyapunov functions. Sensitivity analysis was used to identify the key model parameters that drive transmission through calculation of the partial rank correlation coefficients (PRCCs). We found that the contact rate of both strains had the largest influence on prevalence. We also investigated the impact of amplification and treatment/recovery rates of both strains on the equilibrium prevalence of infection; results suggest that poor quality treatment/recovery makes coexistence more likely and increases the relative abundance of resistant infections.

**Keywords:** drug resistance, multi-strain, stability analysis

## 4.1 Introduction

Many pathogens have several circulating strains. The presence of drug-resistant strains of a pathogen often follows soon after a new treatment becomes available. This can be due to sub-therapeutic drug levels which may efficiently kill drug-susceptible pathogens whilst allowing drug-resistant sub-populations to grow [1]. This acquired resistance, which can result from incorrect treatment, poor adherence or malabsorption, is called amplification [2-4]. One of the major challenges in preventing the spread of infectious diseases is to control the genetic variations of pathogens through proper treatment regimens [5, 6].

Mathematical models can improve our understanding of genetic variations of infectious pathogens as well as those components that are significant to infectious disease diagnosis, and treatment [7-13]. Mathematical models can also be used to improve health policy and infectious disease monitoring plans by identifying thresholds which must be reached in order to achieve elimination [13-15]. For example, analytical solutions, numerical solutions and stability analyses of mathematical models can identify regions in the parameter space where the various asymptotic states are stable or unstable, thus allowing us to predict the long-term behaviour of the system [13, 14, 16]. Further, sensitivity analysis of a mathematical model allows us to discover the parameters that have the greatest influence on the model outputs [14, 17].

The growing threat of drug-resistant pathogen strains presents a significant challenge throughout the world, particularly in developing countries and those with lower socio-economic status [18]. Once drug-resistant strains have emerged in a population, primary transmission of these strains may also contribute to the disease burden (in addition to amplification) [19]. Recent studies [20-24] have shown that drug-resistant strains can in some cases possess higher virulence to transmit disease than drug-susceptible strains, and those individuals infected with a drug-resistant strain have the highest mortality rate, e.g. tuberculosis and HIV [25, 26].

To examine the threat posed by genetic variations of pathogens, we present a two-strain (drug-susceptible, and drug-resistant) Susceptible-Infected-Recovered (SIR) epidemic model with coupled infectious compartments and use it to investigate the emergence and spread of mutated strains of infectious diseases. We consider the possibility that an individual's position changes from drug-susceptible at initial presentation to resistant at follow-up. This is the mode by which drug resistance first emerges in a population and is designed to reproduce the phenotypic phenomenon of amplification. The model can be applied to investigate the co-existent or competitive exclusive phenomena among the strains. We choose the SIR model in this study in order to model the many diseases that have a protracted infectious period with treatment – including hepatitis C and HIV. Here the removed compartment “R”

is to be applied broadly to those people who are neither infectious nor susceptible, including people in treatment, isolation, no longer contacting others or dead. In this way, we believe that our model captures many of the infectious agents that are traditionally modelled by Susceptible (S) to Infected (I) models.

Explicitly, in this paper we perform a rigorous analytical and numerical analysis of the proposed two-strain model properties and solutions from both the mathematical and biological viewpoints. For each, we use the next-generation matrix method to determine analytic expressions for the basic reproduction numbers of the drug-susceptible and drug-resistant strains and find that these are important determinants for regulating system dynamics. With a focus on the early and late-time behaviour of the system, we outline the required conditions for disease fade-out, infection mono-existence, and co-existence.

To supplement and validate the analytic analysis, we use numerical techniques to solve the model equations and explore the epidemic trajectory for a range of possible parameter values and initial conditions. The local stability of the three system equilibria is examined using the Routh-Hurwitz conditions and the global stability of the disease-free equilibrium and mono-existent disease-endemic equilibrium is examined using appropriate Lyapunov functions. Following this, we perform a sensitivity analysis to investigate the model parameters that have the greatest influence on disease prevalence.

The remainder of this paper is constructed as follows: in section 4.2 we present the two-strain SIR model with differential infectivity and amplification, and verify the boundedness and positivity of solutions as well as the existence of several equilibria. Local and global stability analyses of the equilibria are presented in section 4.3. In section 4.4 we discuss a sensitivity analysis of the model outputs. We then provide numerical simulations to support analytic results in section 4.5. Finally, in section 4.6, we provide a summary of our outcomes, discuss their importance for public health policy and propose guidelines for future disease management efforts.

## **4.2 Model description and analysis**

### **4.2.1 Model equations**

We developed a dynamic two-strain SIR model for the transmission of drug-susceptible and drug-resistant infections, where the total population is divided into four subclasses: S –susceptible individuals;  $I_s$  – individuals infected with the drug-susceptible strain;  $I_m$  – individuals infected with the drug-resistant strain; and R – recovered individuals, who are assumed to have immunity against both strains. Thus the total population number  $N(t)$  at time  $t$  is

$$N(t) = S(t) + I_s(t) + I_m(t) + R(t). \tag{4.1}$$

We also introduced the following parameters:  $\Lambda$  – constant recruitment rate into the susceptible class through birth or immigration<sup>1</sup>;  $\mu$  – natural per-capita death rate across the entire population;  $\beta_s$  ( $\beta_m$ ) – effective contact rate between individuals with drug-susceptible (drug-resistant) infection and susceptibles;  $\omega_s$  ( $\omega_m$ ) – per-capita treatment/recovery rate for drug-susceptible (drug-resistant) infected individuals;  $\phi_s$  ( $\phi_m$ ) – disease-related per-capita death rate for drug-susceptible (drug-resistant) infected individuals;  $\rho$  – proportion of individuals who amplify from the drug-susceptible strain to the drug-resistant strain during treatment/recovery. We assumed the proportion of individuals who amplify – due to incomplete treatment or lack of compliance in the use of first-line drugs – move directly from the drug-susceptible compartment  $I_s$  into the drug-resistant compartment  $I_m$ . The model structure is illustrated in Figure 4.1.

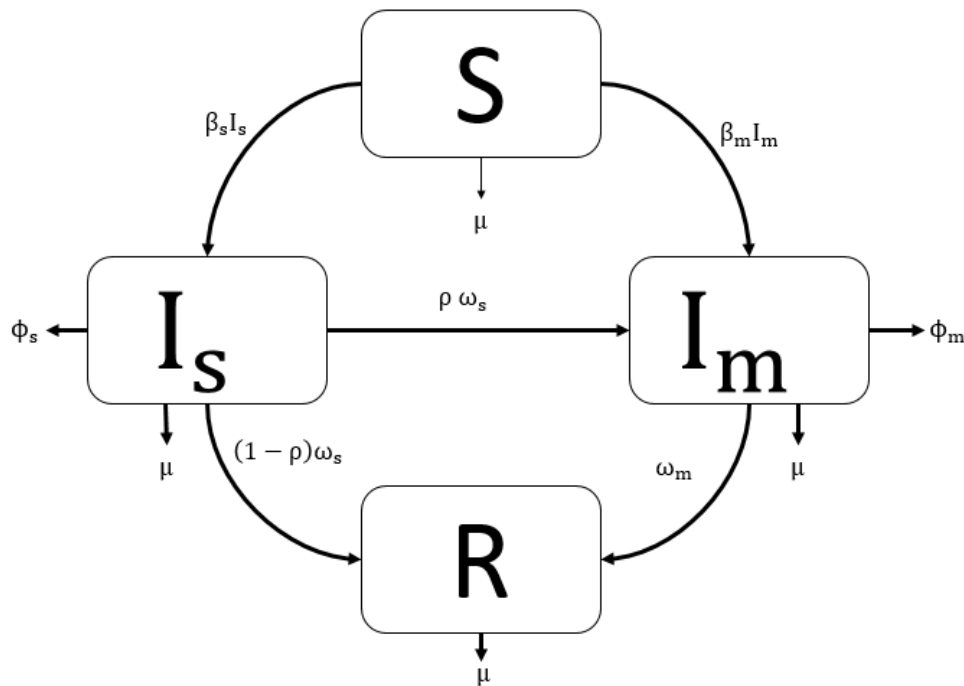


Figure 4. 1 Flow chart of the two-strain SIR model showing the four infection states, and the transition rates in and out of each state.

(Not shown: the constant recruitment rate  $\Lambda$  into the susceptible compartment S). Subscripts s and m denote drug-susceptible and drug-resistant quantities respectively.

From the aforementioned, the populations in each disease state are determined by the following system of nonlinear ordinary differential equations:

$$\dot{S} = \Lambda - \mu S - \beta_s I_s S - \beta_m I_m S, \quad (4.2)$$

$$\dot{I}_s = \beta_s I_s S - (\omega_s + \phi_s + \mu) I_s, \quad (4.3)$$

<sup>1</sup> Data strongly suggest that the absolute number of births globally has been approximately constant for the last 30 years and is predicted to remain constant for the next 30 years. Therefore, within the timescale of an SIR-type infection it is reasonable to assume a constant growth rate (<https://population.un.org/wpp/Graphs/900>).

$$\dot{I}_m = \rho\omega_s I_s + \beta_m I_m S - (\omega_m + \phi_m + \mu)I_m, \quad (4.4)$$

$$\dot{R} = (1 - \rho)\omega_s I_s + \omega_m I_m - \mu R. \quad (4.5)$$

Given non-negative initial conditions for the system above, it is straightforward to show that each of the state variables remain non-negative for all  $t > 0$ . Moreover, summing equations (4.2) – (4.5) we find that the size of the total population,  $N(t)$ , satisfies

$$\dot{N}(t) \leq \Lambda - \mu N(t).$$

Integrating this inequality we find

$$N(t) \leq \frac{\Lambda}{\mu} + N(0)e^{-\mu t}.$$

This shows that the total population size  $N(t)$  is bounded in this case and that it naturally follows that each of the compartment states ( $S, I_s, I_m, R$ ) are also bounded.

Note that equations (4.2) – (4.4) are independent of the size of the recovered population  $R(t)$ ; therefore, if we only wish to track disease incidence and prevalence, we can focus our attention on the following reduced system (4.6) – (4.8):

$$\dot{S} = \Lambda - \mu S - \beta_s I_s S - \beta_m I_m S, \quad (4.6)$$

$$\dot{I}_s = (\beta_s S - \chi_s)I_s, \quad (4.7)$$

$$\dot{I}_m = \rho\omega_s I_s + \beta_m I_m S - \chi_m I_m \quad (4.8)$$

where  $\chi_s = \omega_s + \phi_s + \mu$  and  $\chi_m = \omega_m + \phi_m + \mu$  represent the total removal rates from the respective infectious compartments.

Given the positivity and boundedness of the system solutions, we find that the feasible region for equations (4.6) – (4.8) is given by

$$D = \left\{ (S, I_s, I_m) \in \mathbb{R}_+^3 : S + I_s + I_m \leq \frac{\Lambda}{\mu} \right\} \quad (4.c)$$

where  $D$  is positively invariant. Therefore, in this study we consider the system of equations (4.6) – (4.8) in the set  $D$ .

#### 4.2.2 Basic reproduction number

Here we estimate the basic reproduction number of the model (4.6) – (4.8). In an epidemic model, the basic reproduction number is the expected number of secondary cases created by a single infectious case introduced into a totally susceptible population. If the basic reproduction number is greater than one, the number of infected individuals grows and the infection typically shows persistent behaviour. Conversely, if the basic reproduction number is less than one, the number of infective individuals

typically tends to zero [12, 27, 28]. Here we use the next-generation matrix technique to estimate the basic reproduction number(s) of our system [28].

The reduced model (4.6) – (4.8) has two infected states:  $I_s$ ; and  $I_m$ , and one uninfected state:  $S$ . At the infection-free steady state  $I_s^* = I_m^* = 0$ . Hence, from (4.6), in the absence of infection  $S^* = \frac{\Lambda}{\mu}$ .

Linearizing the system about the infection-free equilibrium, we find that equations (4.3) – (4.4) are closed, such that the linearized infection sub-model becomes

$$\dot{I}_s = (\beta_s S^* - \chi_s) I_s, \quad (4.9)$$

$$\dot{I}_m = \rho \omega_s I_s + \beta_m I_m S^* - \chi_m I_m. \quad (4.10)$$

Here, the ODEs (4.9) and (4.10) describe the production of newly infected individuals and changes in the states of already infected individuals.

By setting  $\mathbf{x}^T = (I_s, I_m)^T$ , where  $T$  denotes transpose, the infection subsystem can be written in the following form:

$$\dot{\mathbf{x}} = (T + \Sigma)\mathbf{x}. \quad (4.11)$$

The matrix  $T$  contains the transmission component of equations (4.9) and (4.10) (i.e. the arrival of susceptible individuals into the infected compartments  $I_s$  and  $I_m$ ) and the matrix  $\Sigma$  contains transitions between, and out of the infected states (i.e. recovery, amplification and death).

For the subsystem (4.9) – (4.10), these components are given respectively by

$$T = \begin{pmatrix} \beta_s S^* & 0 \\ 0 & \beta_m S^* \end{pmatrix} \text{ and } \Sigma = \begin{pmatrix} -\chi_s & 0 \\ \rho \omega_s & -\chi_m \end{pmatrix}.$$

The next-generation matrix,  $K$ , is then given by [27]

$$K = -T\Sigma^{-1} = \begin{pmatrix} \frac{S^* \beta_s}{\chi_s} & 0 \\ \frac{S^* \beta_m \omega_s \rho}{\chi_s \chi_m} & \frac{S^* \beta_m}{\chi_m} \end{pmatrix}.$$

The dominant eigenvalues of  $K$  are the basic reproduction numbers for the drug-susceptible and drug-resistant strains; they represent the average number of new infections from each strain produced by one infected individual. The lower triangular structure of  $K$  allows us to immediately read off the basic reproduction numbers for the drug-susceptible and drug-resistant strains respectively as:

$$R_{0s} = \frac{S^* \beta_s}{\chi_s} = \frac{\Lambda \beta_s}{\mu \chi_s} \quad (4.a)$$

and

$$R_{0m} = \frac{S^* \beta_m}{\chi_m} = \frac{\Lambda \beta_m}{\mu \chi_m}. \quad (4.b)$$

Interestingly we find that the basic reproduction numbers  $R_{0s}$  and  $R_{0m}$  are both independent of the amplification rate  $\rho$  [29].

### 4.2.3 Strain replacement

To investigate the relative magnitude of  $R_{0s}$  and  $R_{0m}$ , which is anticipated to strongly influence the system dynamics (see below), we introduce the parameters  $c$  and  $\epsilon$  which we respectively define as the fitness cost exacted on the transmissibility of strain  $m$  relative to that of strain  $s$ , and the reduction in treatment rate of strain  $m$  relative to that of strain  $s$ . More specifically, we let

$$\beta_m = (1 - c)\beta_s$$

and

$$\omega_m = (1 - \epsilon)\omega_s.$$

If we assume that both  $R_{0s}$  and  $R_{0m}$  are greater than 1, then the condition for resistant infections to replace sensitive infections is given by,

$$R_{0m} > R_{0s}.$$

Substituting the formulae (4.a) and (4.b) for the basic reproduction numbers gives:

$$\frac{\beta_m}{\omega_m + \phi_m + \mu} > \frac{\beta_s}{\omega_s + \phi_s + \mu}.$$

Assuming that  $\mu \approx 0$  (since it is very slow compared to the other rates) and that  $\phi_m \approx \phi_s$  yields the condition

$$\frac{(1-c)\beta_s}{(1-\epsilon)\omega_s + \phi_s} > \frac{\beta_s}{\omega_s + \phi_s},$$

which we can rearrange to obtain

$$\epsilon > \frac{c(\omega_s + \phi_s)}{\omega_s}.$$

The above relation shows that the resistant strain can outcompete the susceptible strain if the resistance level  $\epsilon$  is high (which may be the case for drug-resistant individuals). Alternatively, the resistant strain will be fitter than the susceptible one if the fitness cost  $c$  is sufficiently low.

### 4.2.4 System properties

#### 4.2.4.1. Existence of equilibria

It is clear from equations (4.6) – (4.8) that a disease-free equilibrium (denoted by  $E^*$ ) always exists:

$$E^* = (S^*, I_s^*, I_m^*) = \left( \frac{\Lambda}{\mu}, 0, 0 \right). \quad (4.12)$$

From equation (4.6) – (4.8) we can also derive the mono-existent endemic equilibrium point (denoted by  $E^\#$ ) at which the drug-resistant strain persists and the drug-susceptible strain dies out:

$$E^\# = (S^\#, 0, I_m^\#),$$

where

$$S^\# = \frac{S^*}{R_{0m}} = \frac{\Lambda}{\mu R_{0m}},$$

$$I_s^\# = 0,$$

$$I_m^\# = \frac{\mu(R_{0m}-1)}{\beta_m}. \quad (4.13)$$

Inspecting (4.13) we see that the mono-existent endemic equilibrium  $E^\# = (S^\#, 0, I_m^\#) \in D$  (i.e. exists) if, and only if  $R_{0m} \geq 1$ . Finally, the co-existent endemic equilibrium of the system (4.6) – (4.8)

(denoted by  $E^\dagger$ ) is given by

$$E^\dagger = (S^\dagger, I_s^\dagger, I_m^\dagger),$$

where

$$S^\dagger = \frac{\Lambda}{\mu R_{0s}} = \frac{S^*}{R_{0s}},$$

$$I_s^\dagger = \frac{\mu(R_{0s}-1)}{\beta_s} \Psi,$$

$$\begin{aligned} I_m^\dagger &= \frac{\rho R_{0s} \omega_s \mu (R_{0s}-1)}{\beta_s \chi_m (R_{0s}-R_{0m}) + \rho R_{0s} \omega_s \beta_m}, \\ &= \frac{\rho \omega_s R_{0s}}{\chi_m (R_{0s}-R_{0m})} \frac{\mu (R_{0s}-1)}{\beta_s} \Psi. \end{aligned} \quad (4.14)$$

The variable  $\Psi$  in equation (4.14) is defined as

$$\Psi = \left( 1 + \frac{\rho \omega_s R_{0s} \beta_m}{\beta_s \chi_m (R_{0s}-R_{0m})} \right)^{-1} = \left( 1 + \frac{\rho \omega_s R_{0m}}{\chi_s (R_{0s}-R_{0m})} \right)^{-1}, \quad (4.d)$$

and  $0 < \Psi < 1$  for  $R_{0s} > R_{0m}$ . Therefore, equation (4.14) shows that the co-existent endemic equilibrium  $E^\dagger = (S^\dagger, I_s^\dagger, I_m^\dagger) \in D$  (i.e. exists) if, and only if  $R_{0s} > \max[R_{0m}, 1]$ .

### 4.3 Stability analysis

Since equations (4.2) – (4.4) are independent of equation (4.5) (i.e. the evolution of  $S$ ,  $I_s$  and  $I_m$  are independent of  $R(t)$ ), we can focus our attention on the reduced system (4.6) – (4.8) to study the persistence of the infection. To investigate stability of the equilibria of equations (4.6) – (4.8), the following results are established:

#### 4.3.1 Infection-free equilibrium

**Lemma 1:** If  $R_0 = \max[R_{0s}, R_{0m}] < 1$ , the disease-free equilibrium  $E^*$  of (4.6) – (4.8) is locally and globally asymptotically stable; if, however,  $R_0 = \max[R_{0s}, R_{0m}] > 1$ ,  $E^*$  is unstable.

**Proof:** We consider the Jacobian of the system (4.6) – (4.8) which is given by

$$J = \begin{pmatrix} -\beta_s I_s - \beta_m I_m - \mu & -\beta_s S & -\beta_m S \\ \beta_s I_s & \beta_s S - \chi_s & 0 \\ \beta_m I_m & \rho \omega_s & \beta_m S - \chi_m \end{pmatrix}.$$

At the infection-free equilibrium point,  $E^*$ , this reduces to

$$J^* = \begin{pmatrix} -\mu & -\beta_s S^* & -\beta_m S^* \\ 0 & \chi_s(R_{0s} - 1) & 0 \\ 0 & \rho \omega_s & \chi_m(R_{0m} - 1) \end{pmatrix}.$$

The structure of  $J^*$  allows us to immediately read off the three eigenvalues,  $\lambda_i$ , as

$$\lambda_1 = -\mu, \lambda_2 = \chi_s(R_{0s} - 1) \text{ and } \lambda_3 = \chi_m(R_{0m} - 1). \quad (4.15)$$

It is easy to verify that all the eigenvalues (4.15) have negative real parts for  $R_{0s} < 1$  and  $R_{0m} < 1$ . Hence, the disease-free equilibrium  $E^*$  of (4.6) – (4.8) is locally asymptotically stable for  $R_{0s} < 1$  and  $R_{0m} < 1$ . If  $R_{0s} > 1$  or  $R_{0m} > 1$ , at least one of the eigenvalues (4.15) has a positive real part and  $E^*$  is unstable.

Now the global stability of the disease-free equilibrium  $E^*$  for  $R_{0s} < 1$  and  $R_{0m} < 1$  can be investigated. First, from equation (4.7), we have

$$\dot{I}_s = (\beta_s S - \chi_s) I_s,$$

which can be integrated to give

$$I_s(t) = I_s(0) e^{\int_0^t \beta_s S(\tau) d\tau - \chi_s t} \quad (4.16)$$

for all  $t \geq 0$ .

Substituting in the upper bound  $S(t) \leq \frac{\Lambda}{\mu} = S^*$ , which follows immediately from the definition of  $D$

(equation (4.c)), we obtain

$$\begin{aligned} I_s(t) &\leq I_s(0) e^{(\beta_s S^* - \chi_s)t}, \\ &\leq I_s(0) e^{\chi_s(R_{0s} - 1)t}. \end{aligned}$$

It follows then that if  $R_{0s} < 1$  we have  $I_s(t) \rightarrow 0$  as  $t \rightarrow \infty$ .

Hence the hyperplane  $I_s = 0$  attracts all solutions of (4.6) – (4.8) originating in  $D$  whenever  $R_{0s} < 1$ .

Since  $I_s(t) \rightarrow 0$  as  $t \rightarrow \infty$  for  $R_{0s} < 1$ , it follows that  $\rho \omega_s I_s(t) \rightarrow 0$  such that equation (4.8) reduces to

$$\dot{I}_m = \beta_m I_m S - \chi_m I_m.$$

Following the same strategy for  $I_m$  as we used above for  $I_s$  yields

$$I_m(t) \leq I_m(0) e^{\chi_m(R_{0m} - 1)t}.$$

Similarly, if  $R_{0m} < 1$ ,  $I_m(t) \rightarrow 0$  as  $t \rightarrow \infty$  and the hyperplane  $I_m = 0$  attracts all solutions of (4.6) – (4.8) originating in  $D$ . Finally, it is straightforward to show that if  $I_s \rightarrow 0$ , and  $I_m \rightarrow 0$ , then  $S \rightarrow S^*$ . Therefore  $E^*$  is globally asymptotically stable when  $R_0 = \max[R_{0s}, R_{0m}] < 1$ .

### 4.3.2 Mono-existent endemic equilibrium

**Lemma 2:** If the boundary equilibrium  $E^\# = (S^\#, 0, I_m^\#)$  of the equations (4.6)–(4.8) exists and  $R_{0m} > \max[1, R_{0s}]$ ,  $E^\#$  is locally and globally asymptotically stable.

**Proof:** We consider the Jacobian of the system (4.6)–(4.8) at the mono-existent endemic equilibrium point  $E^\#$  which is given by

$$J^\# = \begin{pmatrix} -\beta_m I_m^\# - \mu & -\beta_s S^\# & -\beta_m S^\# \\ 0 & -\frac{\chi_s(R_{0m} - R_{0s})}{R_{0m}} & 0 \\ \beta_m I_m^\# & \rho\omega_s & 0 \end{pmatrix}.$$

The structure of  $J^\#$  allows us to immediately read off the first eigenvalue,  $\lambda_1 = -\chi_s \frac{(R_{0m} - R_{0s})}{R_{0m}}$  which is negative whenever  $R_{0m} > R_{0s}$ . The remaining eigenvalues can be calculated as the roots of the following equation

$$(\lambda^2 + a_1\lambda + a_2) = 0 \tag{4.17}$$

where

$$a_1 = \beta_m I_m^\# + \mu = \mu R_{0m},$$

$$a_2 = \beta_m^2 I_m^\# S^\# = \mu \chi_m (R_{0m} - 1).$$

For local stability we must ensure that the Routh-Hurwitz criteria [30] are satisfied:

$$a_1 > 0, \text{ and}$$

$$a_2 > 0, \text{ which holds whenever } R_{0m} > 1.$$

Thus, by the Routh-Hurwitz criteria, the boundary equilibrium  $E^\#$  is locally asymptotically stable whenever  $R_{0m} > \max[1, R_{0s}]$ . Conversely, for  $E^\# \in D$ , it is unstable when  $R_{0m} < R_{0s}$ .

Now we prove  $E^\#$  is globally asymptotically stable if  $R_{0m} > \max[1, R_{0s}]$ . Considering equation (4.7) and (4.8), we have

$$\dot{I}_s = (\beta_s S - \chi_s) I_s, \tag{4.18}$$

$$\dot{I}_m = \rho\omega_s I_s + \beta_m I_m S - \chi_m I_m. \tag{4.19}$$

Following [31], first we divide equation (4.18) and (4.19) through by  $I_s$  and  $I_m$  respectively to obtain

$$\frac{d \log I_s}{dt} = \beta_s S - \chi_s, \quad (4.20)$$

$$\frac{d \log I_m}{dt} = \beta_m S - \chi_m + \rho \omega_s \frac{I_s}{I_m}. \quad (4.21)$$

Rearranging equations (4.20) and (4.21) to solve for S we get

$$S = \frac{1}{\beta_s} \frac{d \log I_s}{dt} + \frac{\chi_s}{\beta_s} = \frac{1}{\beta_m} \frac{d \log I_m}{dt} + \frac{\chi_m}{\beta_m} - \frac{\rho \omega_s}{\beta_m} \frac{I_s}{I_m} \quad (4.22)$$

which immediately leads to the following inequality:

$$\frac{1}{\beta_s} \frac{d \log I_s}{dt} + \frac{\chi_s}{\beta_s} \leq \frac{1}{\beta_m} \frac{d \log I_m}{dt} + \frac{\chi_m}{\beta_m}.$$

Integrating both sides of the equation above gives

$$\left( \frac{I_s(t)}{I_s(0)} \right)^{\frac{1}{\beta_s}} e^{\frac{\chi_s t}{\beta_s}} \leq \left( \frac{I_m(t)}{I_m(0)} \right)^{\frac{1}{\beta_m}} e^{\frac{\chi_m t}{\beta_m}}$$

which we can rearrange to obtain

$$\left( \frac{I_s(t)}{I_s(0)} \right)^{\frac{1}{\beta_s}} \leq \left( \frac{I_m(t)}{I_m(0)} \right)^{\frac{1}{\beta_m}} e^{\left( \frac{\chi_m}{\beta_m} - \frac{\chi_s}{\beta_s} \right) t}.$$

Next, we use equations (4.a) and (4.b) for the basic reproduction numbers, to rewrite this inequality as

$$\left( \frac{I_s(t)}{I_s(0)} \right)^{\frac{1}{\beta_s}} \leq \left( \frac{I_m(t)}{I_m(0)} \right)^{\frac{1}{\beta_m}} e^{S^* \left( \frac{1}{R_{0m}} - \frac{1}{R_{0s}} \right) t}.$$

Finally, since both  $I_s(t)$  and  $I_m(t)$  are bounded, as we take the limit as  $t \rightarrow \infty$  we find:

$$\lim_{t \rightarrow \infty} \left( \frac{I_s(t)}{I_s(0)} \right)^{\frac{1}{\beta_s}} \leq \lim_{t \rightarrow \infty} \left( \frac{I_m(t)}{I_m(0)} \right)^{\frac{1}{\beta_m}} e^{S^* \left( \frac{1}{R_{0m}} - \frac{1}{R_{0s}} \right) t} \rightarrow 0 \text{ for } R_{0m} > R_{0s}.$$

Hence the hyperplane  $I_s = 0$  attracts all solutions of (4.6) – (4.8) when  $R_{0m} > R_{0s}$ .

To complete the global stability proof, we show the endemic equilibrium  $E^\#$  is globally asymptotically stable on the hyperplane  $I_s = 0$  by constructing the following Lyapunov function [32]:

$$V^\# = S - S^\# \ln S + I_m - I_m^\# \ln I_m + C$$

where

$$C = -(S^\# - S^\# \ln S^\# + I_m^\# - I_m^\# \ln I_m^\#).$$

Taking the derivative of  $V^\#(t)$  along system trajectories yields

$$\begin{aligned} \dot{V}^\# &= \left( 1 - \frac{S^\#}{S} \right) \dot{S} + \left( 1 - \frac{I_m^\#}{I_m} \right) \dot{I}_m, \\ &= \left( 1 - \frac{S^\#}{S} \right) (\Lambda - \mu S - \beta_m I_m S) + \left( 1 - \frac{I_m^\#}{I_m} \right) (\beta_m I_m S - \chi_m I_m), \\ &= \Lambda - \mu S - \beta_m I_m S - \Lambda \frac{S^\#}{S} + \mu S^\# + \beta_m I_m S^\# + \beta_m I_m S - \chi_m I_m - \beta_m I_m^\# S + \chi_m I_m^\#. \end{aligned}$$

First, we substitute in the identity

$$\Lambda = \mu S^\# + \beta_m I_m^\# S^\#,$$

to obtain

$$\begin{aligned} \dot{V}^\# &= \mu S^\# + \beta_m I_m^\# S^\# - \mu S - \mu S^\# \frac{S^\#}{S} - \beta_m I_m^\# S^\# \frac{S^\#}{S} + \mu S^\# + \beta_m I_m S^\# - \chi_m I_m - \beta_m I_m^\# S + \chi_m I_m^\#, \\ &= \mu S^\# \left( 2 - \frac{S}{S^\#} - \frac{S^\#}{S} \right) + \beta_m I_m^\# S^\# - \beta_m I_m^\# S^\# \frac{S^\#}{S} + \beta_m I_m S^\# - \chi_m I_m - \beta_m I_m^\# S + \chi_m I_m^\#. \end{aligned}$$

We can simplify this expression further by substituting in the identity

$$\beta_m S^\# = \chi_m$$

to get

$$\begin{aligned} \dot{V}^\# &= \mu S^\# \left( 2 - \frac{S}{S^\#} - \frac{S^\#}{S} \right) + \chi_m I_m^\# - \chi_m I_m^\# \frac{S^\#}{S} + \chi_m I_m - \chi_m I_m - \chi_m I_m^\# \frac{S}{S^\#} + \chi_m I_m^\#, \\ &= \mu S^\# \left( 2 - \frac{S}{S^\#} - \frac{S^\#}{S} \right) + \chi_m I_m^\# \left( 2 - \frac{S}{S^\#} - \frac{S^\#}{S} \right), \\ &= (\mu S^\# + \chi_m I_m^\#) \left( 2 - \frac{S}{S^\#} - \frac{S^\#}{S} \right). \end{aligned}$$

Since the arithmetic mean is greater than or equal to the geometric mean, we obtain  $\dot{V}^\# \leq 0$ .

Therefore, the mono-existent endemic equilibrium  $E^\#$  is globally asymptotically stable if  $R_{0m} > 1$ .

### 4.3.3 Co-existent endemic equilibrium

We now show the stability analysis of the co-existent endemic equilibrium  $E^\dagger = (S^\dagger, I_s^\dagger, I_m^\dagger)$ .

**Lemma 3:** If the endemic equilibrium  $E^\dagger = (S^\dagger, I_s^\dagger, I_m^\dagger)$  of equations (4.6)—(4.8) exists,  $E^\dagger$  is locally asymptotically stable.

**Proof:** We consider the Jacobian of the system (4.6)—(4.8) at the co-existent endemic equilibrium point  $E^\dagger$  which is given by

$$J^\dagger = \begin{pmatrix} -\beta_s I_s^\dagger - \beta_m I_m^\dagger - \mu & -\beta_s S^\dagger & -\beta_m S^\dagger \\ \beta_s I_s^\dagger & \beta_s S^\dagger - \chi_s & 0 \\ \beta_m I_m^\dagger & \rho \omega_s & \beta_m S^\dagger - \chi_m \end{pmatrix}.$$

To simplify this expression, we use the following identities

$$-\beta_s I_s^\dagger - \beta_m I_m^\dagger - \mu = -\mu R_{0s},$$

$$-\beta_s S^\dagger = -\frac{R_{0s} \chi_s}{S^*} \frac{S^*}{R_{0s}} = -\chi_s,$$

$$-\beta_m S^\dagger = -\frac{R_{0m} \chi_m}{S^*} \frac{S^*}{R_{0s}} = -\chi_m \frac{R_{0m}}{R_{0s}},$$

$$\beta_s I_s^\dagger = \beta_s \frac{\mu (R_{0s} - 1)}{\beta_s} \Psi = \mu (R_{0s} - 1) \Psi,$$

$$\beta_m I_m^\dagger = \frac{\rho \omega_s}{\chi_s} \frac{R_{0m}}{(R_{0s} - R_{0m})} \mu (R_{0s} - 1) \Psi,$$

$$\beta_s S^\dagger - \chi_s = \chi_s \left( \frac{\beta_s S^*}{R_{0s} \chi_s} - 1 \right) = \chi_s \left( \frac{R_{0s}}{R_{0s}} - 1 \right) = \chi_s (1 - 1) = 0,$$

$$\beta_m S^\dagger - \chi_m = \chi_m \left( \frac{\beta_m S^*}{\chi_m R_{0s}} - 1 \right) = \frac{\chi_m}{R_{0s}} (R_{0m} - R_{0s})$$

where in the fourth line we have substituted in the definition of  $\Psi$  given in equation (4.d). This allows us to rewrite the matrix  $J^\dagger$  in the following form:

$$J^\dagger = \begin{pmatrix} -\mu R_{0s} & -\chi_s & -\chi_m \frac{R_{0m}}{R_{0s}} \\ \mu (R_{0s} - 1) \Psi & 0 & 0 \\ \mu (R_{0s} - 1)(1 - \Psi) & \rho \omega_s & \chi_m \frac{(R_{0m} - R_{0s})}{R_{0s}} \end{pmatrix}.$$

To determine the stability of this matrix we use the Routh-Hurwitz criteria, which state that the real parts of the roots of the characteristic polynomial associated with a three by three matrix  $J^\dagger$  are negative if  $A_1 > 0$ ,  $A_2 > 0$ ,  $A_3 > 0$ , and  $A_1 A_2 > A_3$ , where  $A_1 = -\text{trace}(J^\dagger)$ ,  $A_2$  represents the sum of the two by two principal minors of  $J^\dagger$  and  $A_3 = -\det(J^\dagger)$ .

**Condition 1:** For the matrix  $J^\dagger$ , we have

$$A_1 = -\text{trace}(J^\dagger) = \mu R_{0s} + \frac{\chi_m (R_{0s} - R_{0m})}{R_{0s}}.$$

Hence,  $A_1 > 0$  if  $R_{0s} > R_{0m}$ .

**Condition 2:**

$$A_2 = \begin{vmatrix} 0 & 0 \\ \rho \omega_s & \frac{\chi_m (R_{0m} - R_{0s})}{R_{0s}} \end{vmatrix} + \begin{vmatrix} -\mu R_{0s} & -\chi_m \frac{R_{0m}}{R_{0s}} \\ \mu (R_{0s} - 1)(1 - \Psi) & \chi_m \frac{(R_{0m} - R_{0s})}{R_{0s}} \end{vmatrix}$$

$$= \mu \chi_m (R_{0s} - R_{0m}) + \mu \chi_m \frac{R_{0m}}{R_{0s}} (R_{0s} - 1)(1 - \Psi) + \mu \chi_s (R_{0s} - 1) \Psi.$$

Recalling that  $0 < \Psi < 1$  for  $R_{0s} > R_{0m}$ , we see that  $A_2 > 0$  is satisfied whenever  $R_{0s} > 1$  and  $R_{0s} > R_{0m}$ .

**Condition 3:**

$$A_3 = \det(J^\dagger),$$

$$= -\mu (R_{0s} - 1) \Psi \begin{vmatrix} -\chi_s & \chi_m \frac{R_{0m}}{R_{0s}} \\ \rho \omega_s & \chi_m \frac{(R_{0m} - R_{0s})}{R_{0s}} \end{vmatrix},$$

$$= -\mu (R_{0s} - 1) \Psi \left[ \frac{\chi_s \chi_m (R_{0s} - R_{0m})}{R_{0s}} + \frac{\rho \omega_s \chi_m R_{0m}}{R_{0s}} \right],$$

$$\begin{aligned}
&= -\mu (R_{0s} - 1) \Psi \frac{\chi_s \chi_m (R_{0s} - R_{0m})}{R_{0s}} \left[ 1 + \frac{\rho \omega_s R_{0m}}{\chi_s (R_{0s} - R_{0m})} \right], \\
&= -\mu (R_{0s} - 1) \frac{\chi_s \chi_m (R_{0s} - R_{0m})}{R_{0s}} \frac{\Psi}{\Psi'}, \\
&= \frac{\mu \chi_s \chi_m}{R_{0s}} (R_{0s} - 1) (R_{0s} - R_{0m})
\end{aligned}$$

where in the fifth line we have substituted in the definition of  $\Psi$  given in equation (4.d). The condition  $A_3 > 0$  is true if  $R_{0s} > 1$  and  $R_{0s} > R_{0m}$ .

Finally, if we multiply the expressions for  $A_1$  and  $A_2$  it is straightforward to show that the condition  $A_1 A_2 > A_3$  is satisfied when  $R_{0s} > 1$  and  $R_{0s} > R_{0m}$ . Thus, by the Routh-Hurwitz criteria, the co-existent endemic equilibrium  $E^\dagger$  is locally asymptotically stable when  $R_{0s} > 1$  and  $R_{0s} > R_{0m}$ .

#### 4.4 Sensitivity analysis

Recognizing the relative importance of the various risk factors responsible for the transmission of infectious diseases is essential. The progression of the drug-resistant strain and its incidence and prevalence must be understood in order to determine how best to decrease disease burden. For this purpose, we calculated the partial rank correlation coefficients (PRCCs) – which is a global sensitivity analysis technique using Latin Hypercube Sampling (LHS) – of several key output variables. In each case we assigned a uniform distribution from 0 to 3 times the baseline value for each input parameter to generate a total of 100,000,000 computations of each output variable of interest. Here the model outputs we consider are the number of infectious individuals  $I_s$  and  $I_m$  and their total sum ( $I_s + I_m$ ) at equilibrium. Note that PRCC values lie between -1 and +1. Positive (negative) values imply a positive (negative) correlation to the model parameter and outcomes. The bigger (smaller) the absolute value of the PRCC, the greater (lesser) the correlation of the parameter to the model outcome.

Figures 4.2-4.4 display the correlation between  $I_s$ ,  $I_m$  and ( $I_s + I_m$ ) and the corresponding parameters  $\beta_s$ ,  $\omega_s$ ,  $\phi_s$ ,  $\beta_m$ ,  $\omega_m$ ,  $\phi_m$  and  $\rho$  when  $R_{0s} > \max[R_{0m}, 1]$ , that is, at the co-existent endemic equilibrium. From Figures 4.2-4.4, it is easy to perceive that  $I_s$  and ( $I_s + I_m$ ) have a strong positive correlation with  $\beta_s$  and  $I_m$  has a weaker positive correlation with  $\beta_s$ , implying that a positive change of  $\beta_s$  will increase  $I_s$ , ( $I_s + I_m$ ) and  $I_m$ . Parameters  $\omega_s$  and  $\phi_s$  have a negative correlation with  $I_s$ ,  $I_m$  and ( $I_s + I_m$ ). In addition  $\beta_m$  has a negative correlation with  $I_s$  and ( $I_s + I_m$ ) but a strong positive correlation with  $I_m$ . Parameters  $\omega_m$  and  $\phi_m$  have a positive correlation with  $I_s$  and ( $I_s + I_m$ ) but strong negative correlation with  $I_m$ .

Further, parameter  $\rho$  has a negative correlation with  $I_s$  and  $(I_s + I_m)$  but a strong positive correlation with  $I_m$ . Figure 4.5 represents the correlation between the equilibrium value of  $I_m$  and the corresponding model parameters  $\beta_s, \omega_s, \phi_s, \beta_m, \omega_m, \phi_m$  and  $\rho$  when  $R_{0m} > R_{0s}$  and  $R_{0m} > 1$  (i.e. at the mono-existent endemic equilibrium). Parameters  $\beta_s, \beta_m$  and  $\rho$  (small value not showing) have positive PRCC values, implying that a positive change in these parameters will increase  $I_m$ . In contrast,  $\omega_s, \phi_s, \omega_m$  and  $\phi_m$  have negative PRCC values and, thus, increasing these parameters will consequently decrease  $I_m$ .

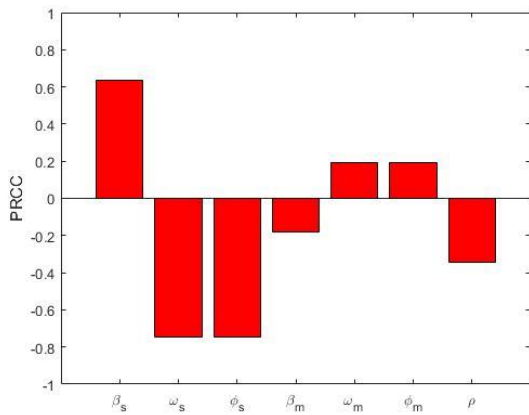


Figure 4. 2 PRCC values depicting the sensitivities of the model output  $I_s$  with respect to the input parameters  $\beta_s, \omega_s, \phi_s, \beta_m, \omega_m, \phi_m$  and  $\rho$ , when  $R_{0s} > \max[R_{0m}, 1]$  (i.e. co-existent endemic equilibrium  $E^\dagger$ ).

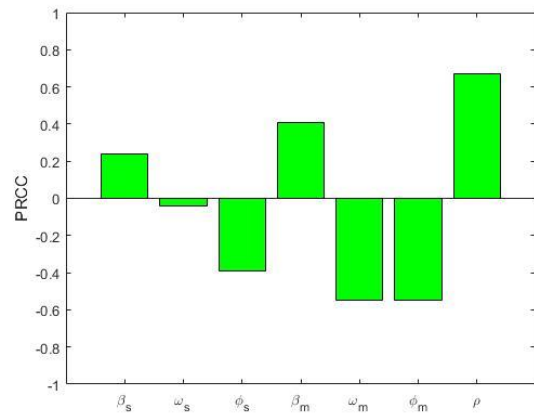


Figure 4. 3 PRCC values depicting the sensitivities of the model output  $I_m$  with respect to the input parameters  $\beta_s, \omega_s, \phi_s, \beta_m, \omega_m, \phi_m$  and  $\rho$ , when  $R_{0s} > \max[R_{0m}, 1]$  (i.e. co-existent endemic equilibrium  $E^\dagger$ ).

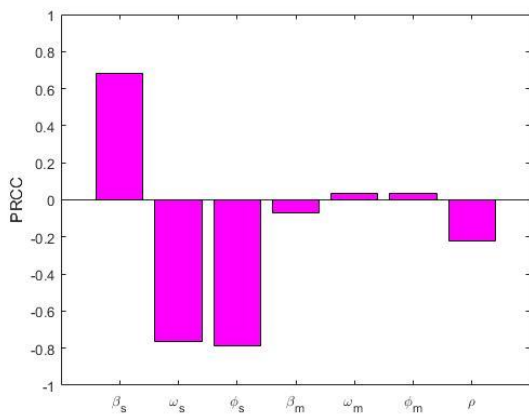


Figure 4. 4 PRCC values depicting the sensitivities of the model output  $I_s + I_m$  with respect to the estimated parameters  $\beta_s, \omega_s, \phi_s, \beta_m, \omega_m, \phi_m$  and  $\rho$ ,  $R_{0s} > \max[R_{0m}, 1]$  (i.e. co-existent endemic equilibrium  $E^\dagger$ ).

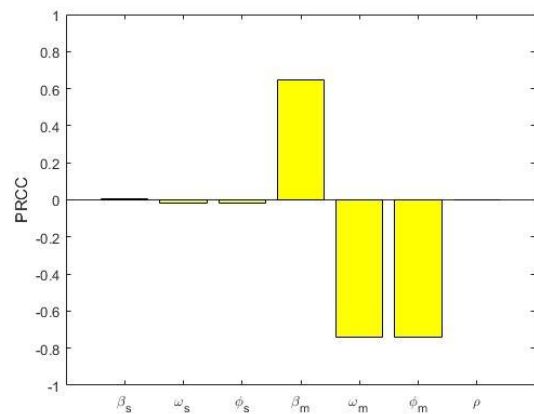


Figure 4. 5 PRCC values depicting the sensitivities of the model output  $I_m$  with respect to the estimated parameters  $\beta_s, \omega_s, \phi_s, \beta_m, \omega_m, \phi_m$  and  $\rho$ , when  $R_{0m} > R_{0s}$  and  $R_{0m} > 1$  (i.e. mono-existent endemic equilibrium  $E^\#$ ).

## 4.5 Numerical simulations

In this section, we carry out detailed numerical simulations (using the Matlab programming language) to support the analytic results and to assess the impact of amplification and the drug-susceptible treatment/recovery rate on equilibrium levels of total prevalence and drug-resistant prevalence. For illustration we have chosen baseline parameter values consistent with tuberculosis infection and transmission [33-35]. In accordance with the analytic results we found three equilibrium points: the disease-free equilibrium  $E^*$ ; a mono-existent endemic equilibrium  $E^\#$ ; and a co-existent endemic equilibrium  $E^\dagger$ . We used different initial conditions for both strains of all populations and found that if both basic reproduction numbers are less than one (i.e.  $\max[R_{0s}, R_{0m}] < 1$ ) then the disease-free equilibrium is locally and globally asymptotically stable. If  $R_{0m} > \max[R_{0s}, 1]$ , the drug-susceptible strain dies out but the drug-resistant strain persists in the population. Furthermore, if  $R_{0s} > \max[R_{0m}, 1]$ , then both the drug-susceptible and drug-resistant strains persist in the population.

Table 4. 1 Description of model parameters

Parameters	Description	Estimated value	References
$\Lambda$	A demographic parameter which represents the recruitment rate into the population	1	
$\mu$	Per-capita death rate	$\frac{1}{70}$ per year	[33]
$\beta_s$	The effective contact rate per unit time between susceptible and drug-susceptible infective individuals	variable	--
$\beta_m$	The effective contact rate per unit time between susceptible and drug-resistant infective individuals	variable	--
$\omega_s$	The per-capita rate at which the drug-susceptible infected population progress to the recovery stage per unit time as a result of treatment	0.290 per year	[34]
$\omega_m$	The per-capita rate at which the drug-resistant infected population progress to the recovery stage per unit time as a result of treatment	0.145 per year	Assume
$\rho$	The proportion of amplification due to treatment default on first-line drug therapy	0.035	[35]
$\varphi_s$	The per-capita rate at which the drug-susceptible infected population die from infection per unit time	0.37 over 3 years	[35]
$\varphi_m$	The per-capita rate at which the drug-resistant infected population die from infection per unit time	0.37 over 3 years	[35]

Figure 4.6 illustrates the stability of the co-existent endemic equilibrium (i.e. when  $R_{0s} > \max[R_{0m}, 1]$ ) by depicting system trajectories through the  $I_s$  vs  $I_m$  plane originating from different initial conditions. In this system both strains ( $I_s$  and  $I_m$ ) persist because of the amplification pathway from the drug-susceptible strain to the drug-resistant strain. Figure 4.7 depicts the effect of amplification ( $\rho$ ) on equilibrium levels of drug-susceptible prevalence and drug-resistant prevalence and shows that in the first region ( $\rho \lesssim 0.6$ ) the drug-susceptible prevalence is initially dominant but that the drug-resistant prevalence rises with increasing  $\rho$ . Eventually, for  $\rho \gtrsim 0.6$ , the drug-resistant strain becomes dominant courtesy of the amplification pathway.

Figure 4.8, and Figure 4.9 show the effect of the drug-susceptible strain treatment/recovery rate on the equilibrium level of total prevalence, and drug-resistant prevalence when both infection rates ( $\beta_s, \beta_m$ ) are fixed. If we increase the proportion of amplification, both the total prevalence and drug-resistant prevalence also increase.

However, Figure 4.9 shows that for high amplification, the drug-resistant prevalence increased when the treatment/recovery rate of the drug-susceptible strain moved from zero to around 0.25 to 0.30, then declined to a common point. For lower amplification values, the drug-resistant proportion only increased up to the common point. This point is the drug-resistant only equilibrium and occurs when the effective reproduction number of the drug-susceptible strain becomes lower than the basic reproduction number of drug-resistant strain. Numerical simulations show that for sufficiently high amplification, the prevalence of the drug-resistant strain will exceed that of its inherent equilibrium value (that is, the resistant-only equilibrium) when the drug-susceptible strain exists and is being treated.

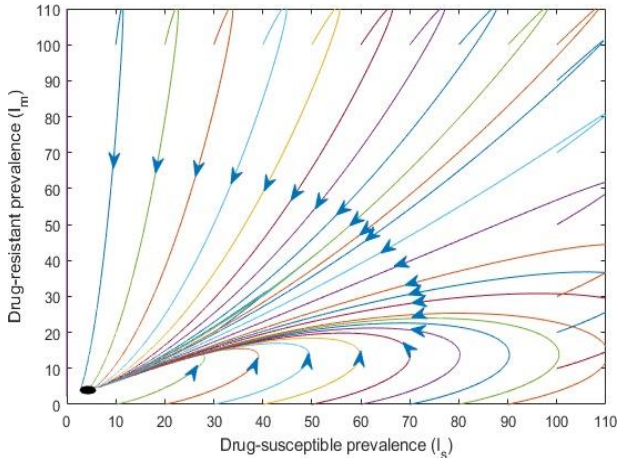


Figure 4. 6 Co-existent endemic equilibrium:  $R_{0S} > \max[R_{0m}, 1]$ . In this case both the drug-susceptible infection and drug-resistant infection persist in the population (black dot). All remaining parameter values assume their baseline values given in Table 4.1.

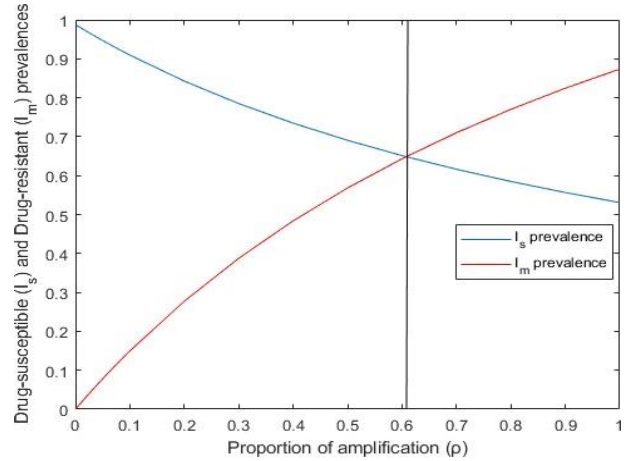


Figure 4. 7 Effect of amplification ( $\rho$ ) on the drug-susceptible ( $I_s$ ) prevalence and drug-resistant prevalence ( $I_m$ ). All remaining parameter values assume their baseline values given in Table 4.1.

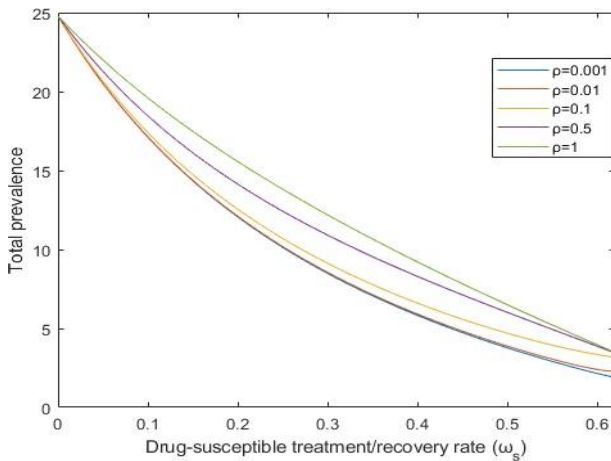


Figure 4. 8 Effect of drug-susceptible treatment/recovery rate ( $\omega_s$ ) on the equilibrium level of total prevalence when both infectious rates ( $\beta_s, \beta_m$ ) are fixed. All remaining parameter values assume their baseline values given in Table 4.1.

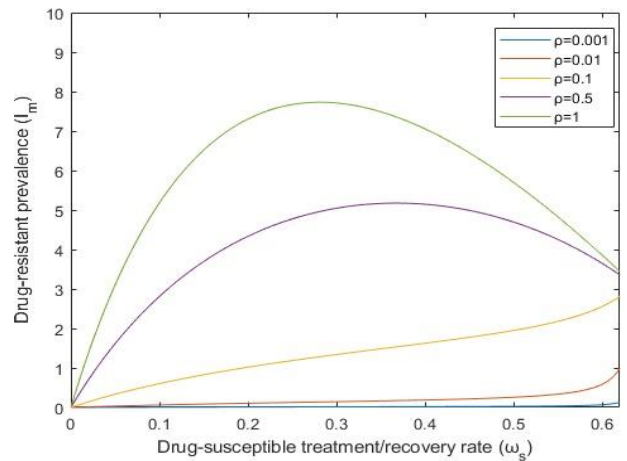


Figure 4. 9 Effect of drug-susceptible treatment/recovery rate ( $\omega_s$ ) on the equilibrium level of the drug-resistant strain when both infectious rates ( $\beta_s, \beta_m$ ) are fixed. All remaining parameter values assume their baseline values given in Table 4.1.

#### 4.6 Discussion and conclusion

In this study, we formulated a two-strain SIR non-constant population model with amplification and investigated its dynamic behaviour. We considered amplification as the process by which an individual infected with a drug-susceptible strain acquires infection with a drug-resistant strain. Using the next-

generation matrix, we obtained the basic reproduction number of each strain, namely  $R_{0s}$  for drug-susceptible cases and  $R_{0m}$  for drug-resistant cases. We found that the basic reproduction numbers determine the equilibrium states of the system and their stability. Specifically if  $R_{0m}$  is greater than  $R_{0s}$  and unity, only the drug-resistant strain will remain, whereas if  $R_{0s}$  is larger than  $R_{0m}$  and unity, a coexistence is likely. We also found that both basic reproduction numbers are independent of the amplification rate, which indicates that the reproductive capacity of each strain is autonomous of the amplification rate between them.

We also found that the drug-susceptible strain is not necessarily the most prevalent at equilibrium even if it has the highest basic reproduction number. This is a consequence of the fact that the drug-susceptible strain persists purely on direct transmission whereas the drug-resistant strain prevalence is driven by a combination of direct transmission and amplification. These results explain in part the rise in drug-resistant strain prevalence when the drug-susceptible strain is treated.

Lastly, we explored the effect of the drug-susceptible treatment rate on the equilibrium level of total prevalence and drug-resistant prevalence. We found that if we increase the drug-susceptible treatment rate, the total prevalence will decline. However, the response of the drug-resistant strain prevalence is non-monotonic, increasing for a certain period and then declining at a particular threshold point. This finding has important implications for choosing the proper intervention or treatment strategies. From a microbiological viewpoint, resistance first occurs by a genetic mutation in a micro-organism that leads to resistance to a treatment, modelled by reducing the treatment rate. Therefore, one could question whether it is prudent to risk the emergence of drug-resistant strains by increasing the treatment rate of the drug-susceptible strain. However, at least initially, such resistance-conferring mutations typically exact a “fitness cost” whereby drug-resistant organisms reproduce at a lower rate and are often less transmissible than their drug-susceptible counterparts [36]. Nevertheless, the selective pressure applied by antibiotic treatment permits drug-resistant mutants to become the dominant strain in a patient infected with disease on first-line therapy and allows for further mutations with selection for fitness. Therefore, increasing drug-susceptible treatment rates may increase the likelihood of emergence of an even more prolific strain which also has drug resistance.

In conclusion, this study has concentrated on a two-strain coupled SIR epidemic model and performed a rigorous analytical analysis of the system properties and solutions, for understanding infectious disease genetic variation and the rising threat of antibiotic resistance or inadequate treatment. These results help inform the practice of drug treatment in the setting of drug resistance and emergent strains, such as is occurring in tuberculosis and other bacterial pathogens. This work shows theoretically that treatment of drug-susceptible strains of an infectious disease can drive the emergence of the drug-

resistant strain, even if that strain has reduced fitness, such that the reproduction number is less than one. Further, under these circumstances, our analysis shows that this emergence of drug resistance will be overcome if the treatment rate is sufficient to eliminate the drug-susceptible strain from the population. Hence, we recommend that for problematic drug-resistant pathogens, estimates of the reproduction numbers of the susceptible and resistant strains be made along with the risk of amplification, to ensure optimal levels of treatment be used to minimise the risk of emergence of the resistant strains. Future modelling studies could focus on specific pathogens (and their associated parameters) and whether treatment may lead to unintended threats to infection control such as an increase in resistant strains.

#### **Declarations of competing interest**

None

#### **Funding**

This work was conducted as a part of a PhD programme of the first authors and funded by the College of Medicine and Dentistry at the James Cook University, Australia (JCU-QLD-835481).

#### **Acknowledgements**

The authors would like to thank Dr. Elizabeth Tynan, James Cook University, for her assistance in preparing this article.

## References

1. Gumbo, T., et al., *Redefining multidrug-resistant tuberculosis based on clinical response to combination therapy*. Antimicrobial Agents and Chemotherapy, 2014. **58**(10): p. 6111-6115.
2. Fofana, M. O., et al., *A multistrain mathematical model to investigate the role of pyrazinamide in the emergence of extensively drug-resistant tuberculosis*. Antimicrobial Agents and Chemotherapy, 2017. **61**(3): p. 00498-16.
3. Sharomi, O., and Gumel, A., *Dynamical analysis of a multi-strain model of HIV in the presence of anti-retroviral drugs*. Journal of Biological Dynamics, 2008. **2**(3): p. 323-345.
4. Aguiar, M., and Stollenwerk, N., *Mathematical models of dengue fever epidemiology: multi-strain dynamics, immunological aspects associated to disease severity and vaccines*. Communication in Biomathematical Sciences, 2017. **1**(1): p. 1-12.
5. May, R. M., and Nowak, A. M., *Coinfection and the evolution of parasite virulence*. Proceedings of the Royal Society of London. Series B: Biological Sciences, 1995. **261**(1361): p. 209-215.
6. Parton, R., Hall, E., and Wardlaw, A., *Responses to Bordetella pertussis mutant strains and to vaccination in the coughing rat model of pertussis*. Journal of Medical Microbiology, 1994. **40**(5): p. 307-312.
7. Zwering, A., Shrestha, S., and Dowdy, W. D., *Mathematical Modelling and Tuberculosis: Advances in Diagnostics and Novel Therapies*. Advances in Medicine, 2015. **2015**: p. 10.
8. Bacaër, N., et al., *Modeling the joint epidemics of TB and HIV in a South African township*. Journal of Mathematical Biology, 2008. **57**(4): p. 557.
9. Liu, L., Zhao, Q. X., and Zhou, Y., *A Tuberculosis Model with Seasonality*. Bulletin of Mathematical Biology, 2010. **72**(4): p. 931-952.
10. Blaser, N., et al., *Tuberculosis in Cape Town: An age-structured transmission model*. Epidemics, 2016. **14**: p. 54-61.
11. Guzzetta, G., et al., *Modeling socio-demography to capture tuberculosis transmission dynamics in a low burden setting*. Journal of Theoretical Biology, 2011. **289**: p. 197-205.
12. Childs, L. M., et al., *Modelling challenges in context: Lessons from malaria, HIV, and tuberculosis*. Epidemics, 2015. **10**: p. 102-107.
13. Jajarmi, A., et al., *A new fractional HRSV model and its optimal control: a non-singular operator approach*. Physica A: Statistical Mechanics and its Applications, 2020. **547**: p. 123860.
14. Mustapha, U. T., et al., *Fractional modeling for the spread of Hookworm infection under Caputo operator*. Chaos, Solitons & Fractals, 2020. **137**: p. 109878.
15. Kuddus, M. A., et al., *Modeling drug-resistant tuberculosis amplification rates and intervention strategies in Bangladesh*. PLoS One, 2020. **15**(7): p. e0236112.
16. Cooke, K. L., *Stability analysis for a vector disease model*. The Rocky Mountain Journal of Mathematics, 1979. **9**(1): p. 31-42.
17. Kim, S., Aurelio, A., and Jung, E., *Mathematical model and intervention strategies for mitigating tuberculosis in the Philippines*. Journal of Theoretical Biology, 2018. **443**: p. 100-112.
18. Laxminarayan, R., et al., *Antibiotic resistance—the need for global solutions*. The Lancet Infectious Diseases, 2013. **13**(12): p. 1057-1098.
19. Gandhi, N. R., et al., *Multidrug-resistant and extensively drug-resistant tuberculosis: a threat to global control of tuberculosis*. The Lancet, 2010. **375**(9728): p. 1830-1843.
20. Dodd, P. J., Sismanidis, C., and Seddon, A. J., *Global burden of drug-resistant tuberculosis in children: a mathematical modelling study*. The Lancet Infectious Diseases, 2016. **16**(10): p. 1193-1201.
21. Mistry, N., Tolani, M., and Osrin, D., *Drug-resistant tuberculosis in Mumbai, India: An agenda for operations research*. Operations Research for Health Care, 2012. **1**(2-3): p. 45-53.
22. McBryde, E. S., et al., *The risk of global epidemic replacement with drug-resistant Mycobacterium tuberculosis strains*. International Journal of Infectious Diseases, 2017. **56**: p. 14-20.

23. Davies, P. D. O., *Drug-resistant tuberculosis*. Journal of the Royal Society of Medicine, 2001. **94**(6): p. 261-263.
24. Stengel, R. F., *Mutation and control of the human immunodeficiency virus*. Mathematical Biosciences, 2008. **213**(2): p. 93-102.
25. Kurz, S. G., Furin, J. J., and Bark, M. C., *Drug-resistant tuberculosis: challenges and progress*. Infectious Disease Clinics, 2016. **30**(2): p. 509-522.
26. Xuan, Q., et al., *High prevalence of HIV-1 transmitted drug resistance among therapy-naïve Burmese entering travelers at Dehong ports in Yunnan, China*. BMC infectious diseases, 2018. **18**(1): p. 211.
27. Diekmann, O., Heesterbeek, J., and Roberts, G. M., *The construction of next-generation matrices for compartmental epidemic models*. Journal of the Royal Society Interface, 2009. **7**(47): p. 873-885.
28. Van Den Driessche, P., *Reproduction numbers of infectious disease models*. Infectious Disease Modelling, 2017. **2**(3): p. 288-303.
29. Meehan, M. T., et al., *Coupled, multi-strain epidemic models of mutating pathogens*. Mathematical Biosciences, 2018. **296**: p. 82-92.
30. DeJesus, E. X., and Kaufman, C., *Routh-Hurwitz criterion in the examination of eigenvalues of a system of nonlinear ordinary differential equations*. Physical Review A, 1987. **35**(12): p. 5288.
31. Bremermann, H. J., and Thieme, H., *A competitive exclusion principle for pathogen virulence*. Journal of Mathematical Biology, 1989. **27**(2): p. 179-190.
32. Korobeinikov, A., and Maini, K. P., *A Lyapunov function and global properties for SIR and SEIR epidemiological models with nonlinear incidence*. Mathematical Biosciences and Engineering, 2004. **1**(1): p. 57-60.
33. Yang, Y., et al., *Global stability of two models with incomplete treatment for tuberculosis*. Chaos, Solitons & Fractals, 2010. **43**(1-12): p. 79-85.
34. Ullah, S., et al., *Modeling and analysis of Tuberculosis (TB) in Khyber Pakhtunkhwa, Pakistan*. Mathematics and Computers in Simulation, 2019.
35. Trauer, J. M., Denholm, T. J., and McBryde, E. S., *Construction of a mathematical model for tuberculosis transmission in highly endemic regions of the Asia-Pacific*. Journal of Theoretical Biology, 2014. **358**: p. 74-84.
36. Munita, J. M., and Arias, C. A., *Mechanisms of antibiotic resistance*. Microbiology Spectrum, 2016. **4**(2).

# CHAPTER 5

---

## Mathematical analysis of a two-strain tuberculosis model in Bangladesh

---

### Statement of joint authorship

**Md Abdul Kuddus** initiated the concept of the study, wrote the manuscript, developed the model, analysed the data, wrote code for model, and acted as corresponding author.

**Emma S. McBryde** assisted with the development of the model, proof read and critically reviewed the manuscript.

**Adeshina I. Adekunle** critically reviewed the manuscript.

**Lisa J. White** critically reviewed the manuscript.

**Michael T. Meehan** assisted with the development of the model, analysed the data, proof read and critically reviewed the manuscript.

**Kuddus, M. A., McBryde, E. S., Adekunle, I. A., White, J. L., Meehan, T. M.** (2021). Mathematical analysis of a two-strain tuberculosis model in Bangladesh. *Journal of Applied Mathematics and Computation* (under review).

## Abstract

Tuberculosis (TB) is an airborne infectious disease that causes millions of deaths worldwide each year (1.7 million people died in 2017). Alarming, several strains of the causative agent, *Mycobacterium tuberculosis* (*Mtb*) – including drug-susceptible (DS) and drug-resistant (DR) variants – already circulate throughout most developing and developed countries, particularly in Bangladesh, with increasingly drug-resistant strains continuing to emerge. In this study we develop a two-strain DS and DR-TB transmission model and perform an analysis of the system properties and solutions. Both analytical and numerical results show that the prevalence of drug-resistant infection increases with increasing drug use through amplification. Similarly, both analytic results and numerical simulations suggest that if the basic reproduction numbers of both DS ( $R_{0s}$ ) and DR ( $R_{0r}$ ) TB are less than one, i.e.  $\max[R_{0s}, R_{0r}] < 1$ , the disease-free equilibrium is asymptotically stable, meaning that the disease naturally dies out. Furthermore, if  $R_{0r} > \max[R_{0s}, 1]$ , then DS-TB dies out but DR-TB persists in the population, and if  $R_{0s} > \max[R_{0r}, 1]$  both DS-TB and DR-TB persist in the population. Further, sensitivity analysis of the model parameters found that the contact rate of both strains had the largest influence on DS and DR-TB prevalence. We also investigate the impact of amplification and treatment rates of both strains on the equilibrium prevalence of infection; results suggest that poor quality treatment makes co-existence more likely and increases the relative abundance of DR-TB infections.

**Keywords:** Tuberculosis model; drug-resistant TB; stability and sensitivity analysis

## 5.1 Introduction

Tuberculosis (TB) is a bacterial infectious disease that causes millions of deaths worldwide each year. In 2017, the World Health Organization (WHO) estimated there were approximately 10.4 million new cases of TB, and 1.7 million individuals died from TB disease [1]. Most of the estimated cases in 2017 occurred in Asia (45%), Africa (25%), and 87% of TB deaths occurred in low- and middle-income countries [1].

TB is an airborne disease caused by bacilli of the bacteria *Mycobacterium tuberculosis* (*Mtb*) [2]. Once infected, the individual will first undergo a period without visible clinical symptoms, called latent TB infection (LTBI) [3]. The latent period is the timespan from the point of infection to the beginning of the state of infectiousness, which may last for weeks, months or the entire life of the infected individual [4]. The lifetime risk of progression to active TB for a person with LTBI is around 5-15%, depending on the age at infection; for those who do progress from LTBI to active TB, the majority will do so within the first two years of initial infection [4].

Currently, multidrug-resistant (MDR) TB is emerging as the greatest threat to TB control globally [1]. MDR-TB is defined as TB that is resistant to isoniazid and rifampicin (the two most effective and commonly used first line drugs), with or without resistance to additional first line drugs [1]. The higher costs, and the longer and more toxic regimens associated with MDR-TB treatment place substantial stress on health systems [5]. Inadequate treatment of DR-TB may create even more resistance to the drug used; this has been termed the amplification effect of short-course combination therapy [6]. Ongoing transmission of DR-TB strains in a population also generates new DR-TB cases [7].

Mathematical modelling is an important tool to explore the dynamics of TB and can provide useful insights into the performance of various TB control strategies [8-10]. In the last few decades, several mathematicians, statisticians and biologists have developed different transmission dynamic models of TB. For instance, Murphy *et al.* (2002) used a modified Susceptible Exposed Infected (SEI) model to investigate the effects of genetic susceptibility and demographic factors on TB epidemiology in a heterogeneous population, comparing the prevalence and incidence in India and the United States of America (USA) [11]. Kim *et al.* (2014) developed a mathematical model for TB with exogenous reinfection, examining the current situation of active TB incidence in Korea [12]. Liu *et al.* (2010) developed a TB model with seasonality to describe TB incidence rates with periodic properties in a mainland city of China [13]. A 10-compartment TB model constructed by Trauer *et al.* (2014) modelled limited vaccine effectiveness, reinfection, DR-TB, and de novo resistance through treatment [14]. This study showed that the model could not be calibrated to the projected incidence rate without allowing

for reinfection, which was modelled as a reversion to early latency, which has a higher rate of progression to disease compared with late latency.

To examine the threat of genetic variations of DS and DR-TB strains, we present a two-strain (DS and DR-TB) SLIRS epidemic model with coupled infectious compartments and use it to investigate the emergence and spread of DR-TB. We consider the possibility that an individual's position changes from DS-TB at initial presentation to DR-TB at follow-up. This is the mode by which DR-TB first emerges in a population and is designed to reproduce the phenotypic phenomenon of acquired drug resistance, known as amplification. The model can be used to investigate the co-existent or competitive exclusive phenomena among DS and DR-TB strains.

In this study we perform an analytical and numerical analysis of our novel two-strain TB model properties and solutions from both the mathematical and biological viewpoints. For each, we use the next generation matrix method to determine analytic expressions for the basic reproduction numbers of the DS-TB and DR-TB strains and find that these are important determinates for regulating system dynamics. With a focus on the early and late time behaviour of the system, we outline the required conditions for the stability of the infection-free state, infection mono-existence and co-existence of two-strain.

To supplement and validate the analytical analysis, we use numerical techniques to solve the model equations and explore the dynamic epidemic trajectory for a range of possible parameter values and initial conditions. From the analytical and numerical viewpoints, the local and global stability of the disease-free equilibrium and mono-existent disease endemic equilibrium are examined through Routh-Hurwitz conditions and appropriate Lyapunov functions. The co-existent disease endemic equilibrium is also examined numerically. Following this, we perform a sensitivity analysis to investigate the model parameters that have the greatest influence on DS, DR and total TB prevalence.

This paper is structured as follows: Section 5.2 describes the model. Stability analysis, model calibration and sensitivity analysis are performed in sections 5.3, 5.4 and 5.5. In section 5.6, we provide numerical simulations to support analytic results. A brief discussion and concluding remarks finalize the paper.

## **5.2 Model description**

### **5.2.1 Model equations**

We developed a deterministic mathematical model of the transmission of DS and DR-TB strains between the following mutually exclusive compartments: susceptible  $S(t)$ , uninfected individuals who

are susceptible to TB infection; those exposed to TB that become latently infected  $L_i(t)$  (where the subscript  $i = s, r$  refers to quantities associated with drug-susceptible,  $s$ , and drug-resistant,  $r$ , TB infection, representing those who are infected and have not yet developed active TB; infectives  $I_i(t)$ , comprising individuals with active TB; the recovered  $R(t)$ , who were previously infected and successfully treated and assumed to be temporarily immune to reinfection. The subscripts  $s$  and  $r$  are used to denote quantities associated with the DS strain and DR strain respectively. We assume that the DR strain is initially generated through inadequate and poor treatment of DS-TB and could subsequently be transmitted to other individuals. Individuals may also return to the susceptible compartment following recovery at the constant per-capita rate  $\gamma$  due to the loss of immunity. The total population size  $N(t)$ , is given by

$$N(t) = S(t) + L_s(t) + I_s(t) + L_r(t) + I_r(t) + R(t). \quad (5.1)$$

Individuals in the different compartments suffer from natural death at the same constant rate  $\mu$  and active TB cases in  $I_i (i = s, r)$  experience disease-related death at a rate  $\phi_i (i = s, r)$ . To ensure the population size remains constant, we replace all deaths as newborns in the susceptible compartment. Individuals in the  $S$  compartment may be infected with a circulating *Mtb* strain  $i (i = s, r)$  at a time dependent rate  $\lambda_i(t) = \beta_i I_i(t)$  where  $\beta_i$  is the transmission rate between infected and susceptible individuals. Once infected with strain  $I_i$ , individuals move to the latently infected compartment  $L_i$ . A proportion of those with latent infections progress to active TB as a result of endogenous reactivation of the latent bacilli at rate  $\alpha_i$ . Individuals with drug sensitive and DR active TB  $I_i$  may eventually be detected and treated at rates  $\tau_s$  and  $\tau_r$  respectively. A proportion  $(1 - \rho)$  of the treated DS active TB recover to move into the recovered compartment  $R$ , and the complementary proportion  $\rho$  develop drug resistance due to incomplete treatment or lack of strict compliance in the use of first-line drugs (drugs used to treat the DS forms of TB) to move into compartment  $I_r$ . Furthermore, individuals recover naturally at a rate  $\omega_i$ , moving from  $I_i$  to  $R$ . The model flow diagram is presented in Figure 5.1.

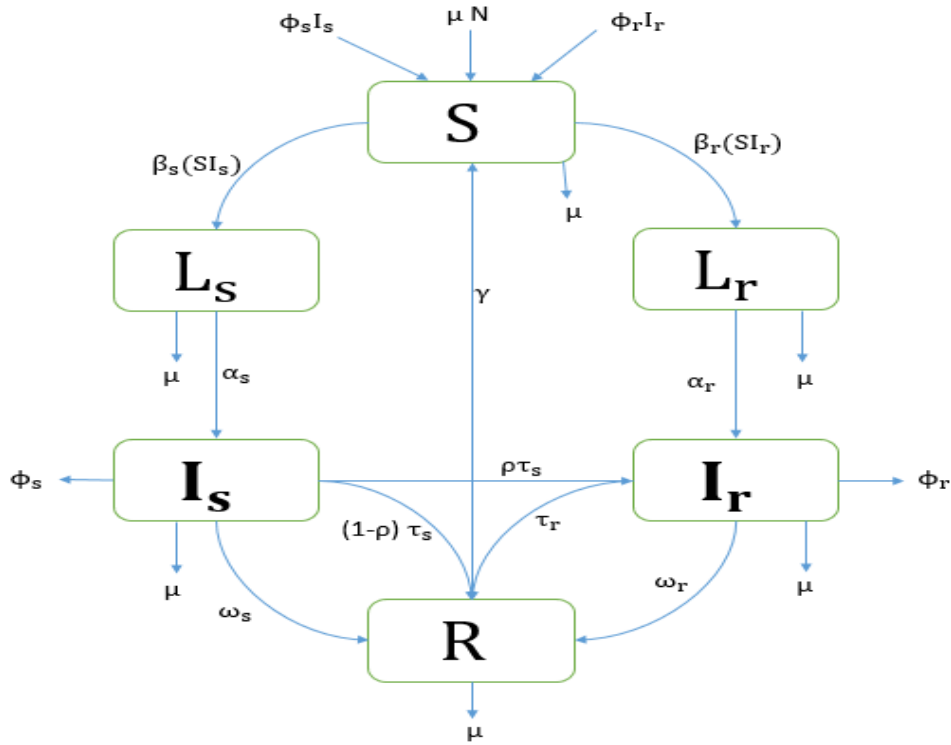


Figure 5. 1 Flow chart of the TB compartmental mathematical model showing six states and the transitions in and out of each state in a closed population (no migration).

Here,  $N$  = Total population,  $S$  = Susceptible population,  $L$  = Latent population,  $I$  = Infected population,  $R$  = Recovered population,  $\mu$  = Birth rate / Death rate,  $\beta$  = Contact rate/Transmission rate,  $\alpha$  = Progression rate,  $\phi$  = Disease-related death rate,  $\tau$  = Treatment rate,  $\omega$  = Recovery rate,  $\rho$  = Proportion of amplification and  $\gamma$  = Rate of losing immunity. Subscripts  $s$  and  $r$  denote DS and DR quantities, respectively.

From the aforementioned, the transmission of DS and DR-TB is given by the following deterministic system of nonlinear ordinary differential equations that describe the model:

$$\frac{dS}{dt} = \mu N - \beta_S I_S S - \beta_R I_R S - \mu S + \gamma R + \phi_S I_S + \phi_R I_R, \quad (5.2)$$

$$\frac{dL_S}{dt} = \beta_S I_S S - \alpha_S L_S - \mu L_S, \quad (5.3)$$

$$\frac{dI_S}{dt} = \alpha_S L_S - \omega_S I_S - \mu I_S - \tau_S I_S - \phi_S I_S, \quad (5.4)$$

$$\frac{dL_R}{dt} = \beta_R I_R S - \alpha_R L_R - \mu L_R, \quad (5.5)$$

$$\frac{dI_R}{dt} = \alpha_R L_R - \omega_R I_R - \mu I_R + \rho \tau_S I_S - \phi_R I_R - \tau_R I_R, \quad (5.6)$$

$$\frac{dR}{dt} = \omega_S I_S + \omega_R I_R - \gamma R - \mu R + (1 - \rho) \tau_S I_S + \tau_R I_R. \quad (5.7)$$

Given non-negative initial conditions for the system above, it is straightforward to show that each of the state variables remain non-negative for all  $t > 0$ . Moreover, summing equations (5.2) – (5.7) we find that the size of the total population,  $N(t)$  satisfies

$N(t) = \text{constant}$ .

Given the constant population size and positivity of solutions it naturally follows that each of the compartment states  $S, L, I$ , etc are bounded. Therefore, we find that the feasible region for equations (5.2) – (5.7) is given by

$$D = \{ (S, L_s, I_s, L_r, I_r, R) \in \mathbb{R}_+^6 : S + L_s + I_s + L_r + I_r + R = N \}. \quad (5.c)$$

## 5.2.2 Basic reproduction number

The model has four infected states,  $L_s, I_s, L_r, I_r$ , and two uninfected states,  $S$  and  $R$ . At the infection-free steady state,  $L_s^* = I_s^* = L_r^* = I_r^* = R^* = 0$ , hence  $S^* = N$ . To calculate the basic reproduction numbers of the DS and DR-TB strains we follow [15] and focus on the linearized infection subsystem derived from equations (5.2) - (5.7):

$$\frac{dL_s}{dt} = \beta_s I_s N - \alpha_s L_s - \mu L_s, \quad (5.8)$$

$$\frac{dI_s}{dt} = \alpha_s L_s - \chi_s I_s, \quad (5.9)$$

$$\frac{dL_r}{dt} = \beta_r I_r N - \alpha_r L_r - \mu L_r, \quad (5.10)$$

$$\frac{dI_r}{dt} = \alpha_r L_r - \chi_r I_r + \rho \tau_s I_s, \quad (5.11)$$

where,  $\chi_s = \omega_s + \phi_s + \tau_s + \mu$  and  $\chi_m = \omega_r + \phi_r + \tau_r + \mu$  are the total removal rates from the DS and DR active TB infection states respectively.

Here, the ODEs (5.8) – (5.11) describe the production of new infected and changes in the states of already infected individuals about the infection-free equilibrium.

By setting  $\mathbf{X}^T = (L_s, I_s, L_r, I_r)^T$ , where  $T$  denotes transpose, we now want to write the infection subsystem in the form

$$\dot{\mathbf{X}} = (T + \Sigma)\mathbf{X}. \quad (5.12)$$

The matrix  $T$  corresponds to transmissions and the matrix  $\Sigma$  to transitions. They are obtained from system (5.8) – (5.11) by separating the transmission events from other events. If we refer to the infected states with indices  $i$  and  $j$ , with  $i, j \in 1, 2, 3, 4$ , then entry  $T_{ij}$  is the rate at which individuals in infected state  $j$  give rise to individuals in infected state  $i$  in the system. Hence, for the subsystem (5.8) – (5.11) we obtain

$$T = \begin{pmatrix} 0 & \beta_s N & 0 & 0 \\ 0 & 0 & 0 & 0 \\ 0 & 0 & 0 & \beta_r N \\ 0 & 0 & 0 & 0 \end{pmatrix} \text{ and } \Sigma = \begin{pmatrix} -(\alpha_s + \mu) & 0 & 0 & 0 \\ \alpha_s & -\chi_s & 0 & 0 \\ 0 & 0 & -(\alpha_r + \mu) & 0 \\ 0 & \rho \tau_s & \alpha_r & -\chi_r \end{pmatrix}.$$

The next generation matrix,  $K$ , is given by [16] (note the essential minus sign)

$$K = -T\Sigma^{-1} = T(-\Sigma^{-1})$$

$$= \begin{pmatrix} \frac{N\alpha_s\beta_s}{(\alpha_s + \mu)\chi_s} & \frac{N\beta_s}{\chi_s} & 0 & 0 \\ 0 & 0 & 0 & 0 \\ \frac{N\alpha_s\beta_r\rho\tau_s}{(\alpha_s + \mu)\chi_s\chi_r} & \frac{N\beta_r\rho\tau_s}{\chi_s\chi_r} & \frac{N\alpha_r\beta_r}{(\alpha_r + \mu)\chi_r} & \frac{N\beta_r}{\chi_r} \\ 0 & 0 & 0 & 0 \end{pmatrix}.$$

The dominant eigenvalues of  $K$  are the basic reproduction numbers for DS and DR-TB; they represent the average number of new infections produced by one infected individual. Hence the basic reproduction number for DS and DR-TB are:

$$R_{0s} = \frac{N\alpha_s\beta_s}{(\alpha_s + \mu)\chi_s}, \quad (5.a)$$

and

$$R_{0r} = \frac{N\alpha_r\beta_r}{(\alpha_r + \mu)\chi_r}. \quad (5.b)$$

Here,  $\frac{\alpha_s}{(\alpha_s + \mu)}$  and  $\frac{\alpha_r}{(\alpha_r + \mu)}$  are the probability of transitioning from the latent compartment to the infectious compartment of the DS and DR strains respectively. Further,  $\frac{1}{\chi_s}$  and  $\frac{1}{\chi_r}$  represent the time spent by infectious individuals in states  $I_s$  and  $I_r$  respectively.

Interestingly we find that both the basic reproduction numbers  $R_{0s}$  and  $R_{0r}$  are purely a function of the epidemiological parameters of the DS and DR-TB respectively, i.e. both are independent of the amplification rate  $\rho$  [17].

Given these expressions (5.a) – (5.b) for the DS and DR-TB basic reproduction numbers, we can now investigate the relationship between the fitness cost,  $c$ , exacted on the transmissibility of DR-TB and its resistance to treatment,  $\epsilon$ , on the relative fitness of DS and DR-TB.

If we assume that both  $R_{0s}$  and  $R_{0r}$  are greater than 1, then the condition for resistant infections to replace sensitive infections is given by,

$$R_{0r} > R_{0s}.$$

Substituting the formulae (5.a) – (5.b) for the basic reproduction numbers gives:

$$\frac{\alpha_r\beta_r}{(\alpha_r + \mu)\chi_r} > \frac{\alpha_s\beta_s}{(\alpha_s + \mu)\chi_s}.$$

If we consider that resistance exacts a fitness cost,  $c$ , on the transmissibility of the DR-TB, it follows that

$$\beta_r = (1 - c)\beta_s.$$

Further, if we assume that DR-TB has a level of resistance,  $\epsilon$ , to treatment we have

$$\tau_r = (1 - \varepsilon)\tau_s.$$

Lastly, assuming that  $\mu \approx 0$  (since it is very slow compared to the other rates) and that  $\phi_r = \phi_s$ , and  $\omega_r = \omega_s$  yields the condition for resistant infections to replace sensitive infections,

$$\varepsilon > \frac{c(\omega_s + \phi_s + \tau_s)}{\tau_s}.$$

The above relation shows that DR-TB can outcompete DS-TB if the resistance level  $\varepsilon$  is high, which may occur due to poor quality treatment. Alternatively, DR-TB will be fitter than DS-TB if the fitness cost  $c$  is sufficiently low.

### 5.2.3 System properties

In this section we provide the basic properties of the proposed TB model (5.2) – (5.7) equilibria.

#### 5.2.3.1 Existence of equilibria

Three types of equilibrium solutions appear in this system: the disease-free equilibrium, which is reached when both basic reproduction numbers are less than one i.e.  $\max[R_{0s}, R_{0r}] < 1$ ; the mono-existent endemic equilibrium, which is reached when the basic reproduction number of DR-TB is greater than the basic reproduction number of DS-TB and one i.e.  $R_{0r} > \max[R_{0s}, 1]$ ; and the co-existent endemic equilibrium, which is reached when the basic reproduction number of DS-TB is greater than that of DR-TB and one i.e.  $R_{0s} > \max[R_{0r}, 1]$ . We discuss these in order below.

Clearly, equations (5.2) – (5.7) always have a disease-free equilibrium

$$E^* = (S^*, L_s^*, I_s^*, L_r^*, I_r^*, R^*) = (N, 0, 0, 0, 0, 0).$$

From equations (5.2)-(5.7) we can also derive the mono-existent endemic equilibrium point

$$E^\# = (S^\#, 0, 0, L_r^\#, I_r^\#, R^\#) \text{ at which the DR strain persists and the DS strain dies out:}$$

$$S^\# = \frac{N}{R_{0r}},$$

$$L_s^\# = 0,$$

$$I_s^\# = 0,$$

$$I_r^\# = \frac{\mu (R_{0r} - 1)}{\beta_r \sigma},$$

$$L_r^\# = \frac{\chi_r}{\alpha_r} I_r^\#,$$

$$R^\# = \frac{(\tau_r + \omega_r)}{(\gamma + \mu)} I_r^\#, \tag{5.13}$$

where  $\sigma = \frac{\left(\gamma\left(1 - \frac{\alpha_r(\omega_r + \phi_r + \tau_r)}{(\alpha_r + \mu)(\omega_r + \phi_r + \tau_r + \mu)}\right) + \mu\left(1 - \frac{\alpha_r \phi_r}{(\alpha_r + \mu)\chi_r}\right)\right)}{\gamma + \mu} \Rightarrow 0 < \sigma < 1$ . From (5.13) if  $R_{0r} > 1$ , equations

(5.2) – (5.7) have a unique boundary equilibrium  $E^\# = (S^\#, 0, 0, L_r^\#, I_r^\#, R^\#) \in D$ .

Next, the co-existent endemic equilibrium of the system is examined. If

$E^\dagger = (S^\dagger, L_s^\dagger, I_s^\dagger, L_r^\dagger, I_r^\dagger, R^\dagger)$  is any co-existent endemic equilibrium, from equations (5.2) - (5.7), we obtain

$$\begin{aligned} S^\dagger &= \frac{N}{R_{0s}}, \\ L_s^\dagger &= \frac{\chi_s}{\alpha_s} I_s^\dagger, \\ L_r^\dagger &= \frac{\rho \tau_s R_{0r}}{\alpha_r} I_s^\dagger, \\ I_r^\dagger &= \frac{\rho R_{0s} \tau_s}{\chi_r (R_{0s} - R_{0r})} I_s^\dagger, \\ R^\dagger &= \frac{1}{(\gamma + \mu)} \left( ((1 - \rho)\tau_s + \omega_s) + \frac{\rho \tau_s R_{0s} (\omega_r + \tau_r)}{\chi_r (R_{0s} - R_{0r})} \right) I_s^\dagger, \end{aligned} \quad (5.14)$$

To check if  $E^\dagger \in D$ , it remains to determine the sign of state variable  $I_s^\dagger$ . This is most easily done using the total population conservation equation:

$$\begin{aligned} N &= S^\dagger + L_s^\dagger + I_s^\dagger + L_r^\dagger + I_r^\dagger + R^\dagger, \\ I_s^\dagger &= N \left( 1 - \frac{1}{R_{0s}} \right) \eta \end{aligned} \quad (5.15)$$

where  $\eta = \left( 1 + \frac{\chi_s}{\alpha_s} + \frac{\rho \tau_s R_{0r}}{\alpha_r} + \frac{\rho R_{0s} \tau_s}{\chi_r (R_{0s} - R_{0r})} + \frac{(1 - \rho)\tau_s + \omega_s}{(\gamma + \mu)} + \frac{(\omega_r + \tau_r)}{(\gamma + \mu)} \frac{\rho R_{0s} \tau_s}{\chi_r (R_{0s} - R_{0r})} \right)^{-1} > 0$  for  $R_{0s} > R_{0r}$ .

We then have

$$\text{sign}(I_s^\dagger) = \text{sign}\left(1 - \frac{1}{R_{0s}}\right) \Rightarrow R_{0s} > 1 \Rightarrow I_s^\dagger > 0.$$

From (5.14), for the co-existent region in which the condition  $I_s^\dagger > 0$  is required, a necessary and sufficient condition for the endemic population  $I_s^\dagger$  to be non-negative is to have both  $R_{0s} > 1$  and  $R_{0s} > R_{0r}$ . That is, if  $R_{0s} > \max[R_{0m}, 1]$  then (5.2) – (5.7) have a co-existent endemic equilibrium  $E^\dagger = (S^\dagger, L_s^\dagger, I_s^\dagger, L_r^\dagger, I_r^\dagger, R^\dagger) \in D$ .

### 5.3 Stability analysis

To investigate the stability of the equilibria of equations (5.2) – (5.7), the following results are established:

#### 5.3.1 Disease-free equilibrium

**Lemma 1:** The disease-free equilibrium of the model is locally and globally asymptotically stable if  $\max[R_{0s}, R_{0r}] < 1$  and unstable if  $\max[R_{0s}, R_{0r}] > 1$ .

**Proof:** We consider the Jacobian of the system (5.2) – (5.7) which is given by

$$J = \begin{pmatrix} -(\beta_s I_s + \beta_r I_r + \mu) & 0 & -\beta_s S + \phi_s & 0 & -\beta_r S + \phi_r & \gamma \\ \beta_s I_s & -(\alpha_s + \mu) & \beta_s S & 0 & 0 & 0 \\ 0 & \alpha_s & -(\omega_s + \phi_s + \tau_s + \mu) & 0 & 0 & 0 \\ \beta_r I_r & 0 & 0 & -(\alpha_r + \mu) & \beta_r S & 0 \\ 0 & 0 & \rho \tau_s & \alpha_r & -(\omega_r + \phi_r + \tau_r + \mu) & 0 \\ 0 & 0 & (1 - \rho)\tau_s + \omega_s & 0 & (\omega_r + \tau_r) & -(\gamma + \mu) \end{pmatrix}$$

which, at the disease-free equilibrium point,  $E^*$ , reduces to

$$J^* = \begin{pmatrix} -\mu & 0 & -\beta_s N + \phi_s & 0 & -\beta_r N + \phi_r & \gamma \\ 0 & -(\alpha_s + \mu) & \beta_s N & 0 & 0 & 0 \\ 0 & \alpha_s & -(\omega_s + \phi_s + \tau_s + \mu) & 0 & 0 & 0 \\ 0 & 0 & 0 & -(\alpha_r + \mu) & \beta_r N & 0 \\ 0 & 0 & \rho \tau_s & \alpha_r & -(\omega_r + \phi_r + \tau_r + \mu) & 0 \\ 0 & 0 & (1 - \rho)\tau_s + \omega_s & 0 & (\omega_r + \tau_r) & -(\gamma + \mu) \end{pmatrix}.$$

The structure of  $J^*$  allows us to immediately read off two eigenvalues,  $\lambda_1 = -\mu$  and  $\lambda_2 = -(\gamma + \mu)$ .

The remaining eigenvalues can be calculated from the following reduced matrix

$$\bar{J}^* = \begin{pmatrix} -(\alpha_s + \mu) & \beta_s N & 0 & 0 \\ \alpha_s & -(\omega_s + \phi_s + \tau_s + \mu) & 0 & 0 \\ 0 & 0 & -(\alpha_r + \mu) & \beta_r N \\ 0 & \rho \tau_s & \alpha_r & -(\omega_r + \phi_r + \tau_r + \mu) \end{pmatrix}.$$

This matrix can be written in block form as

$$\bar{J}^* = \begin{pmatrix} A & B \\ C & D \end{pmatrix}$$

where,  $A = \begin{pmatrix} -\alpha_s - \mu & \beta_s N \\ \alpha_s & -\omega_s - \phi_s - \tau_s - \mu \end{pmatrix}$ ,  $B = \begin{pmatrix} 0 & 0 \\ 0 & 0 \end{pmatrix}$ ,  $C = \begin{pmatrix} 0 & 0 \\ 0 & \rho \tau_s \end{pmatrix}$  and

$$D = \begin{pmatrix} -\alpha_r - \mu & \beta_r N \\ \alpha_r & -\omega_r - \phi_r - \tau_r - \mu \end{pmatrix}.$$

Here the matrix A corresponds to DS-TB dynamics, the matrix D represents DR-TB dynamics, and matrix C gives the flow between DS and DR-TB.

The characteristic equation of the two-by-two block matrix  $\bar{J}^*$  is

$$\det(A - \lambda I) \det((D - \lambda I) - C(A - \lambda I)^{-1}B) = 0.$$

Since  $B = \begin{pmatrix} 0 & 0 \\ 0 & 0 \end{pmatrix}$  this reduces to

$$\det(A - \lambda I) \det(D - \lambda I) = 0.$$

This relation implies that we can apply the Routh-Hurwitz criteria for stability to matrices A and D directly, and independently. We then have

$$\text{trace}(A) = -(\alpha_s + \mu) + (-\omega_s - \phi_s - \tau_s - \mu) < 0,$$

and

$$\det(A) = (\alpha_s + \mu)(\omega_s + \phi_s + \tau_s + \mu) - \alpha_s \beta_s N > 0,$$

which we can reformulate as

$$R_{0s} < 1. \tag{5.16}$$

Now for DR-TB cases (i.e. matrix D)

$$\text{trace}(D) = -(\alpha_r + \mu) + (-\omega_r - \phi_r - \tau_r - \mu) < 0,$$

and

$$\det(D) = (\alpha_r + \mu)(\omega_r + \phi_r + \tau_r + \mu) - \alpha_r \beta_r N > 0,$$

which can similarly be rewritten as

$$R_{0r} < 1. \tag{5.17}$$

Hence, the disease-free equilibrium  $E^*$  of (5.16) and (5.17) is locally asymptotically stable for  $R_{0s} < 1$  and  $R_{0r} < 1$ . If either  $R_{0s} > 1$  or  $R_{0r} > 1$ , at least one of the roots of the characteristic equation has a positive real part and  $E^*$  is unstable.

Now the global stability of the disease-free equilibrium  $E^*$  for  $R_{0s} < 1$  and  $R_{0r} < 1$  can be investigated. To do this, we first show that the infected subpopulations  $L_s$  and  $I_s$  approach zero for  $R_{0s} < 1$  using an appropriate Lyapunov function:

$$V_s(t) = L_s(t) + \frac{(\alpha_s + \mu)}{\alpha_s} I_s(t).$$

Taking the derivative of  $V_s(t)$  along system trajectories yields

$$\begin{aligned} \dot{V}_s &= \dot{L}_s + \frac{(\alpha_s + \mu)}{\alpha_s} \dot{I}_s, \\ &= \beta_s I_s S - (\alpha_s + \mu) L_s + (\alpha_s + \mu) L_s - \frac{\chi_s (\alpha_s + \mu)}{\alpha_s} I_s, \\ &= \beta_s I_s S - \frac{\chi_s (\alpha_s + \mu)}{\alpha_s} I_s, \\ &= \frac{\chi_s (\alpha_s + \mu)}{\alpha_s} \left( \frac{\alpha_s \beta_s S}{(\alpha_s + \mu) \chi_s} - 1 \right) I_s, \\ &\leq \frac{\chi_s (\alpha_s + \mu)}{\alpha_s} (R_{0s} - 1) I_s(t) \end{aligned}$$

where in the last line we have invoked the inequality  $S \leq N$ . It follows then that if  $R_{0s} < 1$  we have  $L_s(t), I_s(t) \rightarrow 0$  as  $t \rightarrow \infty$ . Hence the hyperplane  $L_s = I_s = 0$  attracts all solutions of (5.2) – (5.7) whenever  $R_{0s} < 1$ .

Since  $L_s(t) = I_s(t) \rightarrow 0$  as  $t \rightarrow \infty$  for  $R_{0s} < 1$ , it follows that  $\rho\omega_s I_s \rightarrow 0$ , such that equation (5.6) reduces to

$$\dot{I}_r = \alpha_r L_r - \chi_r I_r.$$

Following the same strategy for DR-TB ( $L_r$  and  $I_r$ ) as we used above for DS-TB ( $L_s$  and  $I_s$ ) and introducing the Lyapunov function

$$V_r(t) = L_r(t) + I_r(t)$$

yields

$$\dot{V}_r(t) \leq \frac{\chi_r(\alpha_r + \mu)}{\alpha_r} (R_{0r} - 1)I_r(t).$$

Therefore if  $R_{0r} < 1$  we have  $L_r(t), I_r(t) \rightarrow 0$  as  $t \rightarrow \infty$  and the hyperplane  $L_r = I_r = 0$  attracts all solutions of (5.2) – (5.7). It follows then that  $R \rightarrow 0$  and  $S \rightarrow N$  such that  $E^*$  is globally asymptotically stable when  $\max[R_{0s}, R_{0r}] < 1$ .

Epidemiologically it can be implied that TB can be eliminated from the community when both the basic reproduction numbers are less than one, i.e.  $\max[R_{0s}, R_{0r}] < 1$ . If  $\max[R_{0s}, R_{0r}] < 1$  then this means the average infected individual produces less than one new infected individual over the course of the infectious period and the infection dies out.

### 5.3.2 Mono-existent endemic equilibrium

**Lemma 2:** If the boundary equilibrium  $E^\# = (S^\#, 0, 0, L_r^\#, I_r^\#, R^\#)$  of the equations (5.2)–(5.7) exists (i.e.  $R_{0r} > \max[1, R_{0s}]$ ) then  $E^\#$  is locally asymptotically stable.

**Proof:** For simplicity, we use the condition  $R = N - S - L_s - I_s - L_r - I_r$  to eliminate the  $R$  equation from the full system given in (5.2) and consider the Jacobian of the system (5.2)–(5.6) at the mono-existent endemic equilibrium point  $E^\#$ , which is given by

$$J^\# = \begin{pmatrix} -(\beta_r I_r^\# + \mu + \gamma) & -\gamma & -\beta_s S^\# + \phi_s - \gamma & -\gamma & -\beta_r S^\# + \phi_r - \gamma \\ 0 & -(\alpha_s + \mu) & \beta_s S^\# & 0 & 0 \\ 0 & \alpha_s & -(\omega_s + \phi_s + \tau_s + \mu) & 0 & 0 \\ \beta_r I_r^\# & 0 & 0 & -(\alpha_r + \mu) & \beta_r S^\# \\ 0 & 0 & \rho\tau_s & \alpha_r & -(\omega_r + \phi_r + \tau_r + \mu) \end{pmatrix}.$$

Simultaneously interchanging rows and columns of the matrix  $J^\#$  we obtain the equivalent Jacobian

$$J^\# = \begin{pmatrix} -(\beta_r I_r^\# + \mu + \gamma) & -\gamma & -\beta_r S^\# + \phi_r - \gamma & -\gamma & -\beta_s S^\# + \phi_s - \gamma \\ \beta_r I_r^\# & -(\alpha_r + \mu) & \beta_r S^\# & 0 & 0 \\ 0 & \alpha_r & -(\omega_r + \phi_r + \tau_r + \mu) & 0 & \rho\tau_s \\ 0 & 0 & 0 & -(\alpha_s + \mu) & \beta_s S^\# \\ 0 & 0 & 0 & \alpha_s & -(\omega_s + \phi_s + \tau_s + \mu) \end{pmatrix}$$

which can be written in block form as

$$J^\# = \begin{pmatrix} A_1 & A_2 \\ A_3 & A_4 \end{pmatrix}$$

$$\text{where } A_1 = \begin{pmatrix} -(\beta_r I_r^\# + \mu + \gamma) & -\gamma & -\beta_r S^\# + \phi_r - \gamma \\ \beta_r I_r^\# & -(\alpha_r + \mu) & \beta_r S^\# \\ 0 & \alpha_r & -(\omega_r + \phi_r + \tau_r + \mu) \end{pmatrix},$$

$$A_2 = \begin{pmatrix} -\gamma & -\beta_s S^\# + \phi_s - \mu \\ 0 & 0 \\ 0 & \rho \tau_s \end{pmatrix}, A_3 = \begin{pmatrix} 0 & 0 & 0 \\ 0 & 0 & 0 \end{pmatrix}, A_4 = \begin{pmatrix} -(\alpha_s + \mu) & \beta_s S^\# \\ \alpha_s & -(\omega_s + \phi_s + \tau_s + \mu) \end{pmatrix}.$$

The characteristic equation of  $J^\#$  is

$$\det(J^\# - \lambda I) = \det \begin{pmatrix} A_1 - \lambda I & A_2 \\ A_3 & A_4 - \lambda I \end{pmatrix} = 0,$$

$$\Rightarrow \det(A_1 - \lambda I) \det((A_4 - \lambda I) - A_3(A_1 - \lambda I)^{-1}A_2) = 0,$$

Since  $A_3 = \begin{pmatrix} 0 & 0 & 0 \\ 0 & 0 & 0 \end{pmatrix}$ , then we obtain

$$\det(A_1 - \lambda I) \det(A_4 - \lambda I) = 0.$$

Again this allows us to apply the Routh-Hurwitz stability conditions separately to the matrices  $A_1$  and  $A_4$ .

According to the Routh-Hurwitz stability conditions we obtain from matrix  $A_1$

**Condition 1:**

$$\text{trace}(A_1) < 0,$$

$$-(\beta_r I_r^\# + \mu + \gamma) - (\alpha_r + \mu) - (\omega_r + \phi_r + \tau_r + \mu) < 0,$$

**Condition 2:**

$$\begin{vmatrix} -(\alpha_r + \mu) & \beta_r S^\# \\ \alpha_r & -(\omega_r + \phi_r + \tau_r + \mu) \end{vmatrix} + \begin{vmatrix} -(\beta_r I_r^\# + \mu + \gamma) & -\beta_r S^\# + \phi_r - \gamma \\ 0 & -(\omega_r + \phi_r + \tau_r + \mu) \end{vmatrix} + \begin{vmatrix} -(\beta_r I_r^\# + \mu + \gamma) & -\gamma \\ \beta_r I_r^\# & -(\alpha_r + \mu) \end{vmatrix} > 0.$$

Which gives

$$\begin{aligned} & ((\alpha_r + \mu)(\omega_r + \phi_r + \tau_r + \mu) - \alpha_r \beta_r S^\#) + (\omega_r + \phi_r + \tau_r + \mu)(\beta_r I_r^\# + \mu + \gamma) \\ & + (\alpha_r + \mu)(\beta_r I_r^\# + \mu + \gamma) + \beta_r I_r^\# \gamma > 0, \end{aligned}$$

Substituting in the analytical solution for  $S^\#$  and the expression for  $R_{0s}$  we find that the first bracketed term cancels, which yields

$$(\omega_r + \phi_r + \tau_r + \mu)(\beta_r I_r^\# + \mu + \gamma) + (\alpha_r + \mu)(\beta_r I_r^\# + \mu + \gamma) + \beta_r I_r^\# \gamma > 0.$$

**Condition 3:**

$$\det(A_1) < 0,$$

$$(-\beta_r I_r^\# - \mu - \gamma) \left( (\alpha_r + \mu)(\omega_r + \phi_r + \tau_r + \mu) - \alpha_r \beta_r S^\# \right) + \gamma(-(\omega_r + \phi_r + \tau_r + \mu)) \beta_r I_r^\# \\ + (-\beta_r S^\# + \phi_r - \gamma) \alpha_r \beta_r I_r^\# < 0,$$

Once again we find that the first term cancels and the remaining terms can be rearranged to obtain (note that we have divided through by  $(\alpha_r + \mu)(\omega_r + \phi_r + \tau_r + \mu)$  and substituted in  $S^\# = \frac{N}{R_{0r}}$  and  $R_{0r} = \frac{N\alpha_r\beta_r}{(\alpha_r + \mu)\chi_r}$

$$\left( \frac{\gamma\beta_r}{(\alpha_r + \mu)} + \frac{\alpha_r\beta_r(\beta_r S^\# + \gamma)}{(\alpha_r + \mu)(\omega_r + \phi_r + \tau_r + \mu)} - \frac{\alpha_r\beta_r\phi_r}{(\alpha_r + \mu)(\omega_r + \phi_r + \tau_r + \mu)} \right) I_r^\# > 0.$$

$$\text{since } I_r^\# = \frac{\mu}{\beta_r} (R_{0r} - 1) \frac{(\gamma + \mu)}{\sigma} > 0.$$

Recalling the definition of  $\sigma$  (equation (5.13)), which is positive, we see that this condition is satisfied whenever  $R_{0r} > 1$ .

and

$$\left( \frac{\gamma\beta_r}{(\alpha_r + \mu)} + \frac{\alpha_r\beta_r(\beta_r S^\# + \gamma)}{(\alpha_r + \mu)(\omega_r + \phi_r + \tau_r + \mu)} - \frac{\alpha_r\beta_r\phi_r}{(\alpha_r + \mu)(\omega_r + \phi_r + \tau_r + \mu)} \right) > 0,$$

which gives,

$$\frac{\gamma\beta_r}{(\alpha_r + \mu)} + \frac{R_{0r}\gamma}{N} + \frac{\mu R_{0r}\phi_r}{N} + \frac{R_{0r}(\alpha_r + \mu)(\omega_r + \tau_r + \mu)}{N} > 0.$$

Now from matrix  $A_4$

$$\text{trace}(A_4) < 0,$$

$$-(\alpha_s + \mu) - (\omega_s + \phi_s + \tau_s + \mu) < 0,$$

$$(\alpha_s + \mu) + (\omega_s + \phi_s + \tau_s + \mu) > 0.$$

and

$$\det(A_4) > 0,$$

$$(\alpha_s + \mu)(\omega_s + \phi_s + \tau_s + \mu) - \alpha_s \beta_s S^\# > 0,$$

Which gives

$$\frac{\alpha_s \beta_s N}{(\alpha_s + \mu)(\omega_s + \phi_s + \tau_s + \mu) R_{0r}} < 1,$$

which becomes

$$R_{0r} > R_{0s}.$$

Hence, the Routh-Hurwitz conditions are satisfied when  $R_{0r} > \max[1, R_{0s}]$ . Therefore, the mono-existent endemic equilibrium  $E^\#$  is locally asymptotically stable if  $R_{0r} > \max[1, R_{0s}]$ , which means that DS-TB dies out but DR-TB persists in the population.

## 5.4 Estimation of model parameters

In this section we estimate the model parameters based on the actual TB prevalence and notification data in Bangladesh taken from the WHO report from 2005 to 2015. In order to parameterise the TB model (5.2) – (5.7), we obtained some of the parameter values from the literature (Table 5.1), whilst others were estimated or fitted to the data (Figure 5.2 and Figure. 5.3). The best fitted parameter values were obtained by minimizing the squared error between the actual TB prevalence and notification data and the solution of the proposed model (5.2) – (5.7). The objective function used in the parameter estimation is as follows

$$\hat{\theta} = \operatorname{argmin} \sum_{i=1}^n \left( (I_{st_i} + I_{rt_i}) - \text{data}_{t_{ip}} \right)^2, \text{ and}$$

$$\hat{\theta}_1 = \operatorname{argmin} \sum_{i=1}^n \left( (\tau_s I_{st_i} + \tau_r I_{rt_i}) - \text{data}_{t_{iq}} \right)^2,$$

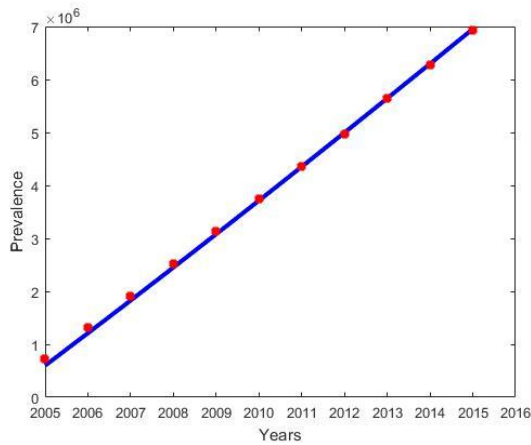


Figure 5. 2 Reported prevalence data (red dot) and the corresponding best fit (blue solid curve) of  $(I_s + I_r)$ . All remaining parameter values assume their baseline values given in Table 5.1.

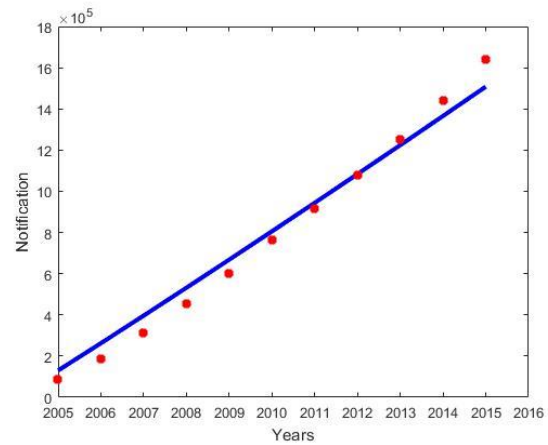


Figure 5. 3 Reported notification data (red dot) and the corresponding best fit (blue solid curve) of  $(\tau_s I_s + \tau_r I_r)$ . All remaining parameter values assume their baseline values given in Table 5.1.

Table 5. 1 Depiction and estimation of parameters

Parameters	Description	Estimated value	References
N	Population in 2015	159,000,000	[18]
$\mu$	Birth/death rate	$\frac{1}{70} \text{ yr}^{-1}$	[19]
$\beta_s$	Transmission rate for DS-TB	Variable	--
$\beta_r$	Transmission rate for DR-TB	Variable	--
$\alpha_s$	Progression rate from $L_s$ to $I_s$	0.129	[20]
$\alpha_r$	Progression rate from $L_r$ to $I_r$	0.129	[20]

$\omega_s$	Recovery rate for DS-TB	0.2873	[21]
$\omega_r$	Recovery rate for DR-TB	0.12	assumed
$\rho$	Proportion of treated patients who amplify	0.035	[20]
$\phi_s$	Disease related death rate for DS-TB	0.37 over 3 years	[20]
$\phi_r$	Disease related death rate for DR-TB	0.37 over 3 years	[20]
$\tau_s$	Treatment rate for DS-TB	2 per year	[20]
$\tau_r$	Treatment rate for DR-TB	0.5 per year	[20]
$\gamma$	Rate of losing immunity	0.10	[22]

where  $\text{data}_{t_{ip}}$  and  $\text{data}_{t_{iq}}$  denotes the actual TB prevalence and notifications respectively and  $(I_{st_i} + I_{rt_i})$  and  $(\tau_s I_{st_i} + \tau_r I_{rt_i})$  are the corresponding model solutions at time  $t_i$  respectively,  $n$  is the number of available data points. The associated state variable and parameters of the model (5.2) – (5.7) are tabulated in Table 5.1. We also plot our model predictions using the fitted parameter values and compare the results with the observed TB prevalence and notification cases in Bangladesh for the years 2005 – 2015 (Figure 5.2 and Figure 5.3). We consider the initial condition for the state variables are,  $S(0) = 152,699,417$ ,  $L_s(0) = 6,121,094$ ,  $I_s(0) = 129,007$ ,  $L_r(0) = 49,440$ ,  $I_r(0) = 1,042$ , and  $R(0) = 0$ .

## 5.5 Sensitivity analysis

It is essential to recognize the relative importance of the various risk factors responsible for TB transmission. The progression of DR-TB and its prevalence determine how best to decrease TB burden. Here, we calculated the Partial Rank Correlation Coefficients (PRCCs), which is a global sensitivity analysis technique using Latin Hypercube Sampling (LHS). Specifically, a uniform distribution is assigned for each model parameter and a total of 10,000,000 random draws are taken for each. The model is then simulated for each of the 10,000,000 parameter sets and relevant outputs such as disease prevalence and incidence are recorded. Here the model outputs we considered were DS-TB ( $I_s$ ), DR-TB ( $I_r$ ) and total TB ( $I_s + I_r$ ) prevalence at equilibrium. Positive (negative) PRCC values refer to a positive (negative) correlation of the model parameter and model outcome. The bigger (smaller) the absolute value of the PRCC, the greater (lesser) the correlation of the parameter with the model outcome [23].

Figure 5.4 displays the correlation between the co-existent equilibrium value of DS-TB prevalence ( $I_s$ ) and corresponding parameters  $\beta_s, \alpha_s, \omega_s, \phi_s, \tau_s, \beta_r, \alpha_r, \omega_r, \phi_r, \tau_r, \rho$  and  $\gamma$ , when  $R_{0s} > \max[R_{0r}, 1]$ . From Figure 5.4 it is easy to perceive that DS-TB prevalence ( $I_s$ ) has a positive correlation with  $\beta_s, \alpha_s, \beta_r, \alpha_r$ , and  $\gamma$ , implying that a positive change in any of these parameters will increase the DS-TB prevalence ( $I_s$ ). We also observe that the transmission rate  $\beta_s$  has the highest impact on DS-TB prevalence ( $I_s$ ). Therefore, from a public health perspective it is very important to protect susceptible individuals from TB exposure by effectively reducing the contact rate between susceptible and infectious individuals. In contrast, parameters  $\omega_s, \phi_s, \tau_s, \omega_r, \phi_r, \tau_r$  and  $\rho$  have a negative correlation with DS-TB prevalence ( $I_s$ ), which means that increasing these parameters values will consequently decrease the  $I_s$  prevalence. Our finding is consistent with observations, because if we implement different intervention strategies including screening of high-risk exposed individuals, preventing the failure of treatment in infectious individuals, latent TB treatment and active TB treatment then the recovery rate will be increased, and as a result DS-TB prevalence will be reduced. Further, amplification has a negative impact on DS-TB prevalence because some of the DS-TB infected individuals move to the DR-TB infected state due to incorrect treatment. Figure 5.5 represents the correlation between the DR-TB prevalence and corresponding model parameters  $\beta_s, \alpha_s, \omega_s, \phi_s, \tau_s, \beta_r, \alpha_r, \omega_r, \phi_r, \tau_r, \rho$  and  $\gamma$  when  $R_{0s} > \max[R_{0r}, 1]$ . Parameters  $\beta_s, \alpha_s, \beta_r, \alpha_r, \rho$  and  $\gamma$  have positive PRCC values and parameters  $\omega_s, \phi_s, \tau_s, \omega_r, \phi_r$  and  $\tau_r$  have negative PRCC values. Our finding is in line with reality, because due to poor quality treatment of DS-TB, the progression rate ( $\alpha_s$ ) and transmission rate ( $\beta_s$ ) have a positive impact on DR-TB prevalence at the co-existent equilibrium.

Figure 5.6 displays the correlation between total TB prevalence ( $I_s + I_r$ ) and corresponding parameters  $\beta_s, \alpha_s, \omega_s, \phi_s, \tau_s, \beta_r, \alpha_r, \omega_r, \phi_r, \tau_r, \rho$  and  $\gamma$ , when  $R_{0s} > \max[R_{0r}, 1]$ . From Figure 5.6 it is easy to see that total TB prevalence has a positive correlation with  $\beta_s, \alpha_s, \beta_r, \alpha_r$  and  $\gamma$ , implying that positive changes in these parameters will increase the total TB prevalence. In contrast, parameters  $\omega_s, \phi_s, \tau_s, \omega_r, \phi_r, \tau_r$  and  $\rho$  have a negative correlation with total TB prevalence, which means increasing these parameters values will consequently decrease the total TB prevalence.

Finally, Figure 5.7 represents the correlation between the DR-TB prevalence and corresponding model parameters  $\beta_s, \alpha_s, \omega_s, \phi_s, \tau_s, \beta_r, \alpha_r, \omega_r, \phi_r, \tau_r, \rho$  and  $\gamma$  when  $R_{0r} > R_{0s}$  and  $R_{0r} > 1$ , i.e. at the mono-existent endemic equilibrium. Parameters  $\beta_s, \alpha_s, \beta_r, \alpha_r, \rho$  and  $\gamma$  have positive PRCC values and parameters  $\omega_s, \phi_s, \tau_s, \omega_r, \phi_r$  and  $\tau_r$  have negative PRCC values. Although the parameters values  $\omega_s, \phi_s$  and  $\tau_s$  are negative, they are negligible because in the mono-existent equilibrium, DS-TB dies out and the parameters have insignificant impact on DR-TB prevalence.

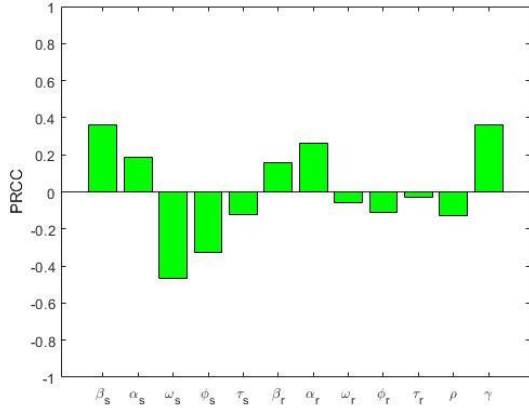


Figure 5. 4 PRCC values depicting the sensitivities of the model output  $I_s$  with respect to the estimated parameters  $\beta_s, \alpha_s, \omega_s, \phi_s, \tau_s, \beta_r, \alpha_r, \omega_r, \phi_r, \tau_r$  and  $\rho$ , when  $R_{0s} > \max[R_{0r}, 1]$  (i.e. co-existent endemic equilibrium  $E^\dagger$ ).

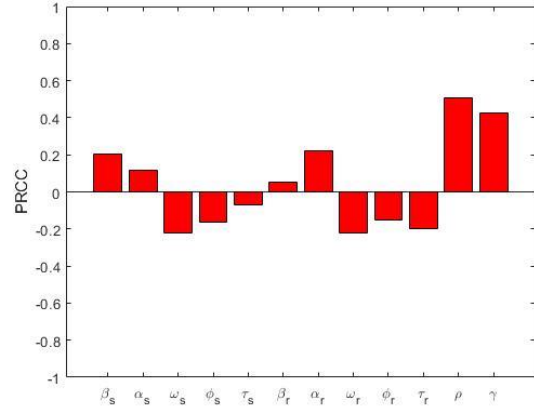


Figure 5. 5 PRCC values depicting the sensitivities of the model output  $I_r$  with respect to the estimated parameters  $\beta_s, \alpha_s, \omega_s, \phi_s, \tau_s, \beta_r, \alpha_r, \omega_r, \phi_r, \tau_r$  and  $\rho$ , when  $R_{0s} > R_{0r}$  and  $R_{0s} > 1$  (i.e. co-existent endemic equilibrium  $E^\dagger$ ).

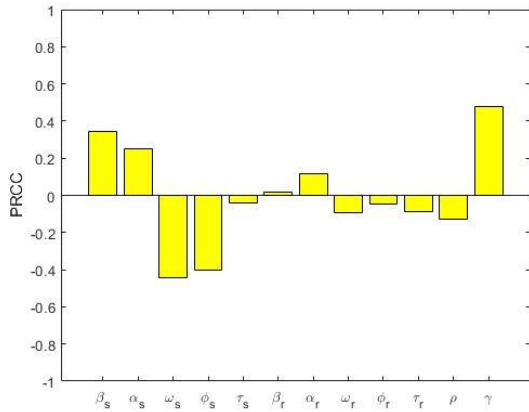


Figure 5. 6 PRCC values depicting the sensitivities of the model output  $I_s + I_r$  with respect to the estimated parameters  $\beta_s, \alpha_s, \omega_s, \phi_s, \tau_s, \beta_r, \alpha_r, \omega_r, \phi_r, \tau_r$  and  $\rho$ , when  $R_{0s} > \max[R_{0r}, 1]$  (i.e. co-existent endemic equilibrium  $E^\dagger$ ).

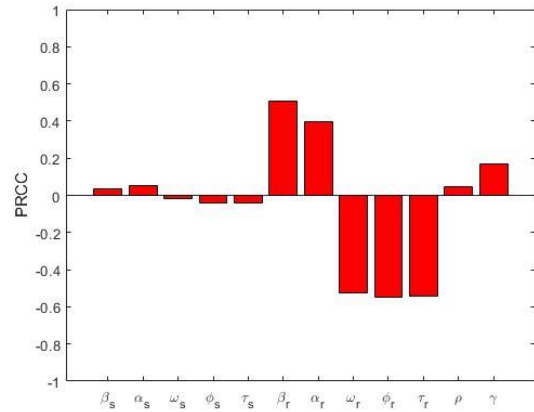


Figure 5. 7 PRCC values depicting the sensitivities of the model output  $I_r$  with respect to the estimated parameters  $\beta_s, \alpha_s, \omega_s, \phi_s, \tau_s, \beta_r, \alpha_r, \omega_r, \phi_r, \tau_r$  and  $\rho$ , when  $R_{0r} > R_{0s}$  and  $R_{0r} > 1$  (i.e. mono-existent endemic equilibrium  $E^\#$ ).

From the explicit formula for  $R_{0s}$  and  $R_{0r}$  given in equation (5.a)-(5.b), analytical expressions for the sensitivity indices  $\Upsilon_j^i$  can be derived following the method in [24] to each of the model parameters. For example, for  $\beta_s$  we have:

$$\Upsilon_{\beta_s}^{R_{0s}} = \frac{\partial R_{0s}}{\partial \beta_s} \times \frac{\beta_s}{R_{0s}}.$$

Now using the parameter values in Table 5.1, we have the following results (Table 5.2).

Table 5. 2 Sensitivity indices to parameters for the model (5.2)-(5.7)

Parameter	Sensitivity index ( $R_{0s}$ )	Parameter	Sensitivity index ( $R_{0r}$ )
$\beta_s$	+ 1.000	$\beta_r$	+1.000
$\alpha_s$	+0.100	$\alpha_r$	+0.100
$\omega_s$	- 0.108	$\omega_r$	- 0.120
$\phi_s$	- 0.139	$\phi_r$	- 0.368
$\tau_s$	-0.749	$\tau_r$	- 0.498

In the sensitivity indices of  $R_{0s}$  and  $R_{0r}$ , the most sensitive parameters are the effective contact rates of DS-TB,  $\beta_s$  and DR-TB,  $\beta_r$ . Since  $\Upsilon_{\beta_s}^{R_{0s}} = 1$ , and  $\Upsilon_{\beta_r}^{R_{0r}} = 1$ , increasing (or decreasing) the effective contact rates,  $\beta_s$  and  $\beta_r$  of DS-TB and DR-TB by 100%, increases (or decreases) the reproduction numbers  $R_{0s}$  and  $R_{0r}$  by 100%.

## 5.6 Numerical simulations

In this section, we carry out detailed numerical simulations (using the Matlab programming language) to support the analytic results and to assess the impact of amplification and the DS-TB treatment rate on equilibrium levels of total prevalence and DR prevalence. We used different initial conditions for both strains of all populations and obtained the stability results for the model equilibria, finding TB disease will eventually die out from the population when the condition  $\max[R_{0s}, R_{0r}] < 1$ , holds. The condition  $R_{0r} > \max[R_{0s}, 1]$  implies that DS-TB dies out but DR-TB persists in the population. Furthermore, the condition  $R_{0s} > \max[R_{0r}, 1]$  implies that both DS-TB and DR-TB persist in the population.

Figure 5.8 depicts system trajectories in the  $I_s$  vs  $I_r$  plane with different initial conditions using parameter values for which the disease-free equilibrium is asymptotically stable. In this system both strains ( $I_s$  and  $I_r$ ) die out, this is because the basic reproduction numbers for the strains were both less than one ( $\max[R_{0s}, R_{0r}] < 1$ ). Figure 5.9 depicts system trajectories in the  $I_s$  vs  $I_r$  plane with different initial conditions using parameter values for which the mono-existent equilibrium is asymptotically stable. In this system the DS-TB strain ( $I_s$ ) dies out but DR-TB strain ( $I_r$ ) persists in the population ( $R_{0r} > \max[R_{0s}, 1]$ ).

Figure 5.10 depicts system trajectories in the  $I_s$  vs  $I_r$  plane with different initial conditions using parameter values for which the co-existent equilibrium is asymptotically stable ( $R_{0s} > \max[R_{0r}, 1]$ ). In this system both strains ( $I_s$  and  $I_r$ ) persist; this is because the basic reproduction number  $R_{0s}$  of DS-TB is greater than one and there was an amplification pathway from DS-TB to DR-TB. Figure 5.11 depicts the effect of amplification ( $\rho$ ) on the equilibrium levels of DS-TB and DR-TB prevalence showing that in the first region ( $\rho \lesssim 0.6$ ), DS-TB initially dominated and DR-TB also rose but for  $\rho \gtrsim 0.6$ , the DR strain becomes dominant courtesy of the amplification pathway.

Figure 5.12 and Figure 5.13 show the effect of the DS-TB treatment rate ( $\tau_s$ ) and amplification on the equilibrium level of total TB and DR-TB prevalence, when both infectious rates ( $\beta_s, \beta_r$ ) are fixed. If we increase the proportion of amplification, the total TB and DR-TB prevalence also increase. However, Figure 5.13 shows that for high amplification, DR-TB prevalence increased when the DS-TB treatment rate moved from zero to around 0.8 to 0.9 and then declined to a common point. For lower amplification values, the DR-TB proportion only increased up to the common point. This point is the DR-TB-only equilibrium and occurs when the effective reproduction number of DS-TB becomes lower than the basic reproduction ratio of DR-TB. Numerical simulations show that for sufficiently high amplification, the prevalence of the DR-TB will exceed that of its inherent equilibrium value (that is, the DR-only equilibrium) when the DS-TB is in existence and is being treated.

From the above numerical analysis, it is clear that proper treatment is very important for DS-TB patients otherwise it will lead to the creation of new cases of DR-TB. Therefore, well-administered first-line treatment for DS-TB is the best way to prevent acquisition of resistance (referred to as amplification). Timely identification of DR-TB and adequate treatment regimens with second-line drugs administered are essential to prevent rises in DR-TB prevalence.

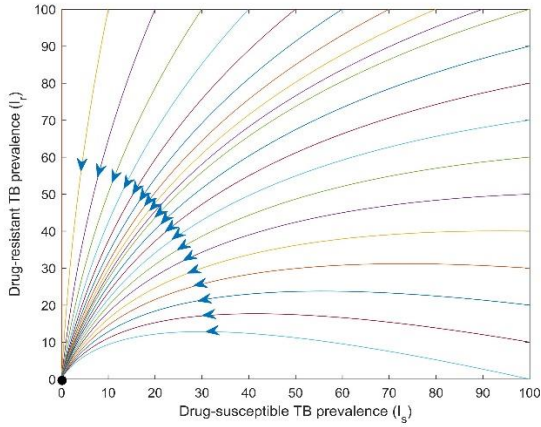


Figure 5. 8 Disease-free equilibrium:  $\max [R_{0s}, R_{0r}] \leq 1$ . The disease-free equilibrium is asymptotically stable, which means that the disease naturally dies out. Here we consider  $R_{0s} = 0.4$  and  $R_{0r} = 0.3$ .

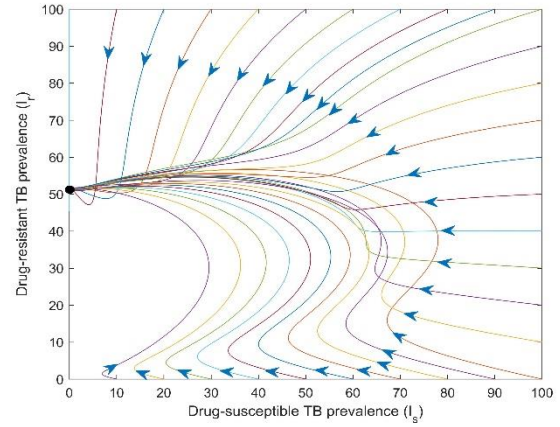


Figure 5. 9 Mono-existent equilibrium:  $R_{0r} > \max[R_{0s}, 1]$ . In this case DS-TB dies out but the DR-TB persist in the population. Here we consider  $R_{0s} = 0.4$  and  $R_{0r} = 3$ .

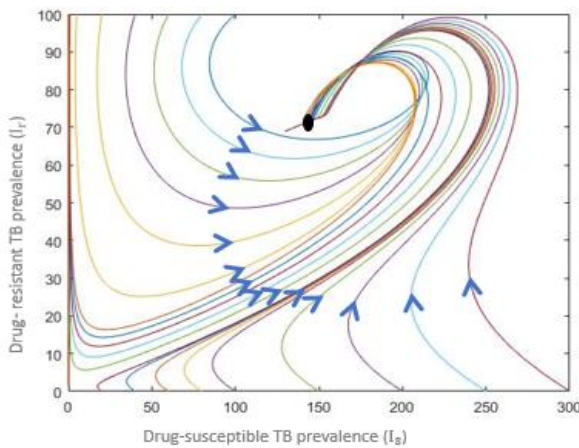


Figure 5. 10 Co-existent equilibrium:  $R_{0s} > \max[R_{0r}, 1]$ . In this both DS-TB and DR-TB persist in the population. Here we consider  $R_{0s} = 5$  and  $R_{0r} = 3$ .

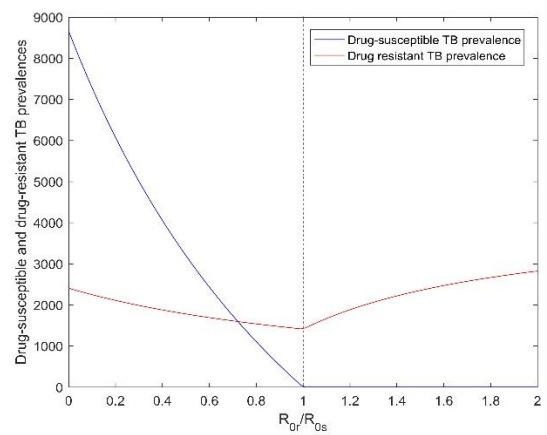


Figure 5. 11 Role of amplification. For  $R_{0r} < R_{0s}$ , we have co-existence. For  $R_{0r} > R_{0s}$ , DS-TB dies out but DR-TB increases with increasing  $R_{0r}$ . Notice, even for  $R_{0r} < R_{0s}$ , the DR-TB prevalence can exceed the DS-TB prevalence. All remaining parameter values assume their baseline values given in Table 5.1.

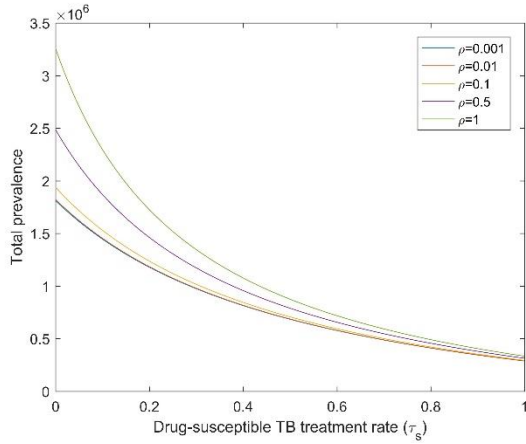


Figure 5. 12 . Effect of DS-TB treatment rate ( $\tau_s$ ) on equilibrium level of total prevalence when both infectious rates ( $\beta_s, \beta_r$ ) are fixed. All remaining parameter values assume their baseline values given in Table 5.1.

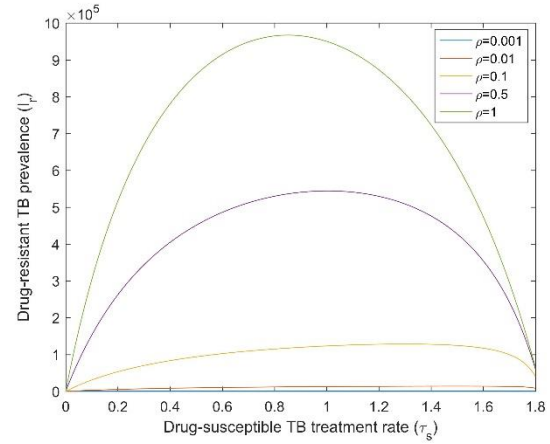


Figure 5. 13 Effect of DS-TB treatment rate ( $\tau_s$ ) on equilibrium level of DR-TB prevalence when both infectious rates ( $\beta_s, \beta_r$ ) are fixed. All remaining parameter values assume their baseline values given in Table 5.1.

## 5.7 Discussion and conclusion

In this paper, we formulated and analysed a novel two-strain TB model with amplification: one strain for DS-TB; and another for DR-TB. Here, we considered amplification as the process by which an individual infected with DS-TB develops infection with a resistant strain of TB, reflecting treatment failure for individuals on first line drug therapy.

We found three equilibrium points of our proposed model; the disease-free equilibrium; the mono-existent equilibrium, when DR-TB dominated in this system; and the co-existent equilibrium, when DS-TB dominated in this system. The next generation matrix method was used to calculate the basic reproduction number of the different TB strains, denoted by  $R_{0s}$  for DS-TB and  $R_{0r}$  for DR-TB. The value of the basic reproduction numbers, namely  $R_{0s}$  and  $R_{0r}$ , and biological parameters of the model, were estimated on the basis of available data and are tabulated in Table 5.1. Furthermore, the Routh-Hurwitz conditions were also used to investigate the local stability of the disease-free equilibrium and mono-existent equilibrium. This analysis showed that stability depends on the threshold quantities, i.e. the basic reproduction numbers  $R_{0s}$  and  $R_{0r}$ . If  $\max[R_{0s}, R_{0r}] < 1$ , the disease-free equilibrium is globally asymptotically stable, which means that the disease naturally dies out. If  $R_{0r} > \max[R_{0s}, 1]$ , DS-TB dies out but DR-TB persists in the population. If  $R_{0s} > \max[R_{0r}, 1]$ , then DS-TB and DR-TB both persist in the population.

Our model determined that from the explicit formulae for  $R_{0s}$  and  $R_{0r}$ , it is clear that these basic reproduction numbers depend on transmission rates  $\beta_s$  ( $\beta_r$ ), progression rates  $\alpha_s$  ( $\alpha_r$ ), recovery rates

$\omega_s$  ( $\omega_r$ ), disease related death rates  $\phi_s$  ( $\phi_r$ ), and treatment rates  $\tau_s$  ( $\tau_r$ ). From the sensitivity analysis it is also clear that the most important parameters are transmission rates  $\beta_s$  ( $\beta_r$ ) followed by treatment rates  $\tau_s$  ( $\tau_r$ ). Therefore, to control and eradicate DS-TB and DR-TB infection, it is important to consider the following strategies: the first and most important strategy is to minimize the contact rates  $\beta_s$  ( $\beta_r$ ) with infected individuals by decreasing the values of  $\beta_s$  ( $\beta_r$ ); the second-most important strategy is to increase the treatment rates  $\tau_s$  ( $\tau_r$ ) of infective individuals. However, in developing countries (e.g. Bangladesh) it is very difficult to isolate infectious individuals due to the high cost of long term treatment. Therefore, we propose the most feasible and optimal strategy to eliminate DS-TB and DR-TB in Bangladesh is to increase the treatment rates by decreasing the treatment cost so that poor people can obtain treatment.

## Funding

This research did not receive any specific grant from funding agencies in the public, commercial, or not-for-profit sectors.

## Declaration of Interest

None

## References

1. WHO, *Global tuberculosis report 2017*. WHO/HTM/TB/2017.23, Geneva, 2017.
2. Fogel, N., *Tuberculosis: a disease without boundaries*. Tuberculosis, 2015. **95**(5): p. 527-531.
3. Dutta, N. K., and Karakousis, P. C., *Latent tuberculosis infection: myths, models, and molecular mechanisms*. Microbiology and Molecular Biology Reviews 2014. **78**(3): p. 343-371.
4. Ai, J. W., et al., *Updates on the risk factors for latent tuberculosis reactivation and their managements*. Emerging Microbes & Infections, 2016. **5**(2): p. e10.
5. Davies, P. D. O., *Drug-resistant tuberculosis*. Journal of the Royal Society of Medicine, 2001. **94**(6): p. 261-263.
6. Seung, K. J., Keshavjee, S., and Rich, L. M., *Multidrug-resistant tuberculosis and extensively drug-resistant tuberculosis*. Cold Spring Harbor Perspectives in Medicine, 2015. **5**(9): p. a017863.
7. Kendall, E. A., Fofana, O. M., and Dowdy, W. D., *Burden of transmitted multidrug resistance in epidemics of tuberculosis: a transmission modelling analysis*. The Lancet Respiratory Medicine, 2015. **3**(12): p. 963-972.
8. Harris, R. C., et al., *Systematic review of mathematical models exploring the epidemiological impact of future TB vaccines*. Human Vaccines & Immunotherapeutics, 2016. **12**(11): p. 2813-2832.
9. Zwerling, A., Shrestha, S., and Dowdy, W. D., *Mathematical modelling and tuberculosis: advances in diagnostics and novel therapies*. Advances in Medicine, 2015. **2015**.
10. Nkamba, L. N., et al., *Mathematical model to assess vaccination and effective contact rate impact in the spread of tuberculosis*. Journal of Biological Dynamics, 2019. **13**(1): p. 26-42.
11. Murphy, B. M., et al., *Comparing epidemic tuberculosis in demographically distinct heterogeneous populations*. Mathematical Biosciences, 2002. **180**: p. 161-85.

12. Kim, S., et al., *What Does a Mathematical Model Tell About the Impact of Reinfection in Korean Tuberculosis Infection?* *Osong Public Health and Research Perspectives*, 2014. **5**(1): p. 40-45.
13. Liu, L., Zhao, X.Q., and Zhou, Y., *A tuberculosis model with seasonality*. *Bulletin of Mathematical Biology*, 2010. **72**(4): p. 931-952.
14. Trauer, J. M., Denholm, T. J., and McBryde, E. S., *Construction of a mathematical model for tuberculosis transmission in highly endemic regions of the Asia-Pacific*. *Journal of Theoretical Biology*, 2014. **358**: p. 74-84.
15. Heffernan, J. M., Smith, J. R., and Wahl, M. L., *Perspectives on the basic reproductive ratio*. *Journal of the Royal Society Interface*, 2005. **2**(4): p. 281-293.
16. Diekmann, O., Heesterbeek, J., and Roberts, G. M., *The construction of next-generation matrices for compartmental epidemic models*. *Journal of the Royal Society Interface*, 2009. **7**(47): p. 873-885.
17. Meehan, M. T., et al., *Coupled, multi-strain epidemic models of mutating pathogens*. *Mathematical Biosciences*, 2018. **296**: p. 82-92.
18. NTP, *Tuberculosis control in Bangladesh*. Annual report 2015.
19. Yali, Y., et al., *Global stability of two models with incomplete treatment for tuberculosis*. *Chaos, Solutions & Fractals*, 2010. **43**: p. 79-85.
20. Trauer, J. M., Denholm, J. T., and McBryde, E. S., *Construction of a mathematical model for tuberculosis transmission in highly endemic regions of the Asia-Pacific*. *Journal of Theoretical Biology*, 2014. **358**: p. 74-84.
21. Ullah, S., et al., *Modeling and analysis of Tuberculosis (TB) in Khyber Pakhtunkhwa, Pakistan*. *Mathematics and Computers in Simulation*, 2019.
22. Bhunu, C., et al., *Modelling the effects of pre-exposure and post-exposure vaccines in tuberculosis control*. *Journal of Theoretical Biology*, 2008. **254**(3): p. 633-649.
23. Kim, S., Aurelio, A., and Jung, E., *Mathematical model and intervention strategies for mitigating tuberculosis in the Philippines*. *Journal of Theoretical Biology*, 2018. **443**: p. 100-112.
24. Chitnis, N., Cushing, J. M., and Hyman, J., *Bifurcation analysis of a mathematical model for malaria transmission*. *Journal on Applied Mathematics*, 2006. **67**(1): p. 24-45.

# CHAPTER 6

---

## Modelling drug-resistant tuberculosis amplification rates and intervention strategies in Bangladesh

---

### Statement of joint authorship

**Md Abdul Kuddus** initiated the concept of the study, wrote the manuscript, developed the model, analysed the data, and wrote code for model.

**Michael T. Meehan** assisted with the development of the model, proof read and critically reviewed the manuscript.

**Lisa J. White** critically reviewed the manuscript.

**Emma S. McBryde** assisted with the development of the model, proof read and critically reviewed the manuscript.

**Adeshina I. Adekunle** assisted with the development of the model and code, proof read and critically reviewed the manuscript.

**Kuddus, M. A., Meehan, M. T., White, L. J., McBryde, E. S., & Adekunle, A. I. (2020).** Modelling drug-resistant tuberculosis amplification rates and intervention strategies in Bangladesh. *PLOS ONE*, *15*(7), e0236112.

## **Abstract**

Tuberculosis (TB) is the seventh leading cause of morbidity and mortality in Bangladesh. Although the National TB Control Program (NTP) of Bangladesh is implementing its nationwide TB control strategies, more specific and effective single or combination interventions are needed to control DS and MDR-TB. In this study, we developed a two-strain TB mathematical model with amplification and fit it to Bangladesh TB surveillance data to understand the transmission dynamics of DS and MDR-TB. Sensitivity analysis was used to identify important parameters. We evaluated the cost-effectiveness of varying combinations of four basic control strategies including distancing, latent case finding, case holding and active case finding, all within the optimal control framework. From our fitting, the model with different transmission rates between DS and MDR-TB best captured the Bangladesh TB reported case counts. The estimated basic reproduction number for DS-TB was 1.14 and for MDR-TB was 0.54, with an amplification rate of 0.011 per year. The sensitivity analysis also indicated that the transmission rates for both DS and MDR-TB had the largest influence on prevalence. To reduce the burden of TB (both DS and MDR), our finding suggested that a quadruple control strategy that combines distancing control, latent case finding, case holding and active case finding is the most cost-effective. Alternative strategies can be adopted to curb TB depending on availability of resources and policy makers' decisions.

**Keywords:** MDR-TB, mathematical model, sensitivity analysis, optimal control theory and cost-effective analysis.

## 6.1 Introduction

TB is an airborne bacterial infection that causes millions of deaths worldwide each year [1]. The TB bacteria (*Mtb*) generally enter the body through the lungs, spreading to other parts of the body through the bloodstream, the lymphatic system, or through direct extension to additional organs (extra-pulmonary TB) [2, 3]. Following an infectious person coughing, sneezing, speaking or singing thousands or tens of thousands of droplet nuclei are created [4]. These minute droplet nuclei can remain suspended in the air for several minutes to an hour, allowing spread to other persons through inhalation [4, 5].

Once infected, the individual will first undergo a period without visible clinical symptoms, called latent TB infection (LTBI). The latent period is the timespan from the point of infection to the beginning of the state of infectiousness, and may last for weeks, months or the entire life of the infected individual. In fact, the lifetime risk of progression to active TB for a person with LTBI is around 5-15%, depending on the age at infection. For those who do progress from LTBI to active TB, the majority will do so within the first two years of initial infection [6].

In Bangladesh, TB is one of the most important public health problems. Globally, Bangladesh has the 7<sup>th</sup> largest TB incidence in the world and it is estimated that 70,000 people die of TB and 300,000 new cases are generated each year [7]. Moreover, Bangladesh is ranked 10<sup>th</sup> among the 27 high MDR-TB burden countries. Thus, there is a great need to reduce TB incidence, prevalence, and mortality in Bangladesh [8].

In Bangladesh, under the Ministry of Health and Family Welfare, the NTP of the Directorate General of Health Services (DGHS) provides nationwide TB control services. These services include screening, case detection through diagnosis, treatment following appropriate regimen, follow up and evaluation in all areas [9]. The goals of this program are to reduce illness, death and transmission of TB, and to achieve universal high quality service for all people with active and latent TB [10]. More than 44 partner organizations (NGOs) also support the NTP in all areas, including advocacy, communication, and social mobilization (ACSM) activities. The NTP adopted the recent WHO recommended strategies -namely the DOTS Strategy-1993, the Stop TB Strategy-2006, and the End TB Strategy-2015 for its TB control [9, 11].

Mathematical modelling is one of the most important tools for understanding TB transmission dynamics and for predicting the epidemic trajectories [12-18]. In the last few decades, mathematicians and public

health professionals have developed different types of mathematical models to investigate TB disease dynamics in different endemic regions. For example, Kim *et al.* (2014) constructed a mathematical model for TB with exogenous reinfection and examined the current situation of active TB incidence in Korea, and found that case detection was the most important intervention for decreasing active TB cases [13]. Yang *et al.* (2016) developed another TB model with seasonality and determined that seasonality has a high impact on TB related incidence, prevalence and mortality, especially in the winter season [14]. Brooks *et al.* (2010) developed a TB mathematical model with survivorship to discover the impact of age structure on the prevalence of TB, the basic reproduction number, and the effect of control interventions [15]. Mishra and Srivastava (2014) constructed a transmission dynamic mathematical model to simulate the spread of TB disease in the human population of Jharkhand, India, for DS and MDR-TB cases with vaccination [16]. A 10-compartmental TB model constructed by Trauer *et al.* (2014) modelled limited vaccine effectiveness, reinfection, MDR-TB, and de novo resistance through treatment [17].

In this study, we develop a two-strain TB model to describe the transmission dynamics of DS and MDR-TB in Bangladesh. We perform a sensitivity analysis to explore the impact of model parameters. The model is calibrated to the TB Bangladesh data to estimate amplification rate and other key transmission parameters such as infection and treatment rates. Based on the calibration, four different control strategies or policies are considered. Several scenarios are examined to explore the optimal control policy for reducing the spread of DS and MDR-TB. The purpose of optimal control is to decrease the prevalence of DS and MDR-TB as well as to minimize the cost incurred in the implementation of control procedures. To the author's best knowledge, this study is the first TB model to characterise the TB amplification rate in Bangladesh and use the result to identify optimal control strategies.

## **6.2 Material and methods**

### **6.2.1 Bangladesh TB epidemiological data**

Bangladesh is a TB disease endemic country in South-East Asia [1]. Control of TB in such a resource-scare country should be informed by an in-depth mathematical and epidemiological understanding of the disease. This study is based on the yearly reported Bangladesh DS and MDR-TB incidence data that was obtained from the WHO report from 2000 to 2018 [19-21]. For this data, TB incidence is separated into patients who had DS or MDR-TB and does not include prevalence rates for the years 2000, 2001 and 2002. We estimated prevalence rates for these years by fitting a linear model to our prevalence data in GraphPad Prism [22].

The Bangladesh TB data that were made available has a single distinction between DS-TB and MDR-TB. The DS-TB are all patients with TB strains that are fully-susceptible to all the first-line anti-TB drugs or have resistance to first line anti-mycobacterial agents other than rifampicin, while MDR-TB is regarded as at least rifampicin-resistant (on GeneXpert) and in the case of cultured isolates, is rifampicin and isoniazid resistant. The MDR-TB tests were conducted using GeneXpert as first line testing for rifampicin followed by culturing and sensitivity testing for other drugs. Extensive drug resistant (XDR) is a subset of MDR-TB and is not reported separately in Bangladesh.

### 6.2.2 Model description

We developed a deterministic transmission dynamics mathematical model of DS and MDR-TB strains between the following mutually exclusive compartments: susceptible individuals,  $S(t)$ ; those exposed to TB or latently infected,  $L(t)$ , representing those that are infected and have not yet developed active TB; the infectious  $I(t)$ , containing individuals with active TB that are infectious; the recovered  $R(t)$  who were previously infected and successfully recovered either naturally or through treatment. The subscripts  $s$  and  $m$  denote variables associated with the DS strain and MDR strain respectively. We assume that MDR strains were initially generated through inadequate treatment of DS-TB, i.e. amplification, and that these strains could subsequently be transmitted to other individuals.

The total population size  $N(t)$  is assumed to be constant and well mixed:

$$N(t) = S(t) + L_s(t) + L_m(t) + I_s(t) + I_m(t) + R(t). \quad (6.1)$$

To ensure the population size remains constant, we replace all deaths as newborns in the susceptible compartment. This includes death through natural causes, which occurs in all states at the constant per-capita rate  $\mu$ , and TB-related deaths, which occur at the constant per-capita rate  $\phi_i$  ( $i = s, m$ ). Individuals may also return to the susceptible compartment following recovery at the constant per-capita rate  $\gamma$ .

Susceptible individuals may be infected with a circulating strain of TB at the rate  $\lambda_i = \beta_i I_i(t)$  and move to the corresponding latently infected compartment  $L_i(t)$ . Here,  $\beta_i$  is the probability a susceptible individual contracts infection after contact with an infectious individuals with TB strain  $i$  ( $i = s, m$ ). Those with latent infection progress to active TB as a result of endogenous reactivation of the latent bacilli at the rate  $\alpha_i$ ; however, some latent individuals do not progress to the infectious class  $I_i(t)$  but instead undergo endogenous recovery and move directly to the recovery class  $R(t)$  at a per capital rate  $\delta_i$  ( $i = s, m$ ). Individuals with DS and MDR active TB,  $I_i(t)$  may eventually be detected and treated at rates  $\tau_s$  and  $\tau_m$  respectively. A proportion  $(1 - \rho)\tau_s$  of the treated DS active TB individuals

fully recover to move into the recovered compartment  $R(t)$ ; whilst the complementary  $\rho\tau_s$  (amplification rate) develop MDR-TB due to incomplete treatment or lack of strict compliance in the use of first-line drugs (drugs used to treat the DS forms of TB) – and move into the compartment  $I_m(t)$ . Furthermore, individuals in the compartment  $I_i(t)$  recover naturally and move into the recovered class  $R(t)$  at the rate  $\omega_i$ . Active TB cases in  $I_i$  ( $i = s, m$ ) experience disease related death at a rate  $\phi_i$  ( $i = s, m$ ). The model flow diagram is presented in Figure 6.1.

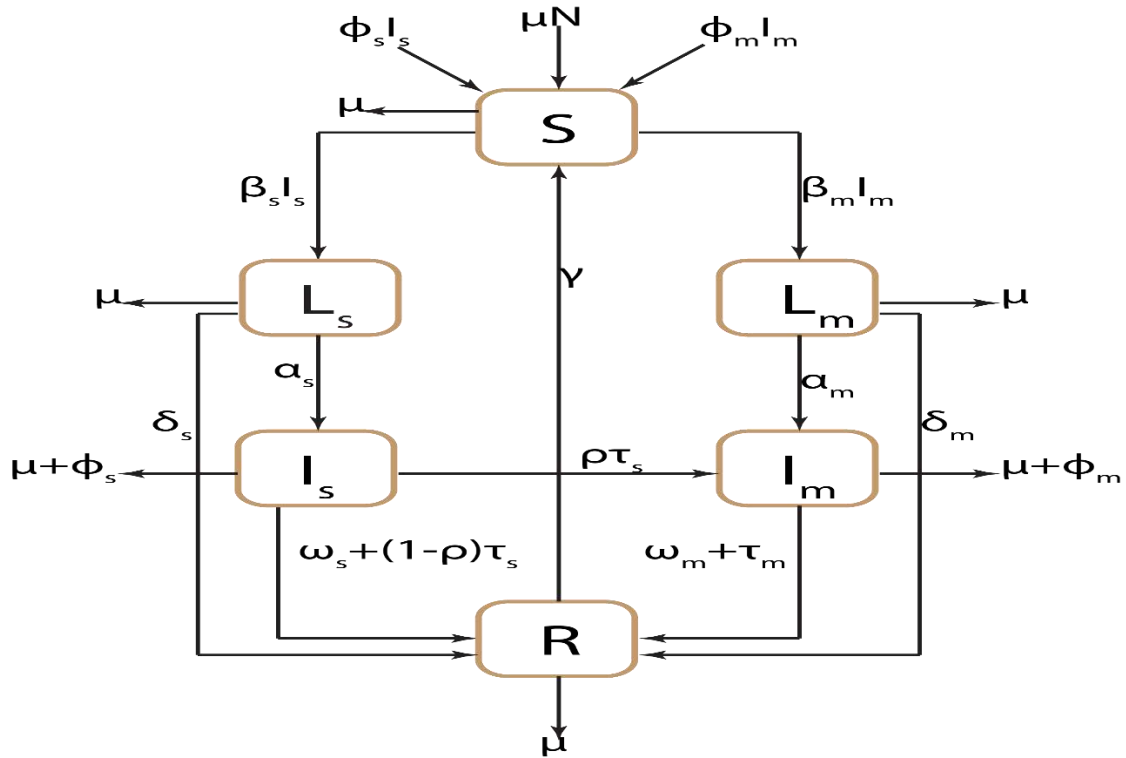


Figure 6. 1 Schematic diagram of two-strain TB transmission model for Bangladesh TB setting.

From the aforementioned, the DS and MDR-TB model is given by the following deterministic system of nonlinear ordinary differential equations:

$$\begin{aligned}
 \frac{dS}{dt} &= \mu N - \beta_s I_s S - \beta_m I_m S - \mu S + \gamma R + \phi_s I_s + \phi_m I_m, \\
 \frac{dL_s}{dt} &= \beta_s I_s S - \alpha_s L_s - \delta_s L_s - \mu L_s, \\
 \frac{dI_s}{dt} &= \alpha_s L_s - (1 - \rho)\tau_s I_s - \rho\tau_s I_s - \phi_s I_s - \omega_s I_s - \mu I_s, \\
 \frac{dL_m}{dt} &= \beta_m I_m S - \alpha_m L_m - \delta_m L_m - \mu L_m, \\
 \frac{dI_m}{dt} &= \alpha_m L_m + \rho\tau_s I_s - \omega_m I_m - \phi_m I_m - \tau_m I_m - \mu I_m, \\
 \frac{dR}{dt} &= (1 - \rho)\tau_s I_s + \tau_m I_m + \omega_s I_s + \omega_m I_m + \delta_s L_s + \delta_m L_m - \gamma R - \mu R.
 \end{aligned} \tag{6.2}$$

### 6.2.3 Model calibration and control strategies

We estimated the TB model parameters from fitting different combinations of parameters in equation (6.2) to the actual DS and MDR-TB incidence data from Bangladesh [1, 10]. In order to parameterize the TB model (6.2), we obtained some of the parameter values from the literature (see Table 6.1), whilst others were estimated from fitting to the data. The aim is to determine the rate of amplification of MDR-TB and its dynamics. Note that in quantifying the amplification rate, both drug-susceptible and drug-resistant treatment rates are also determined.

Hence, the models we consider are:

- Model 1 (Drug-failure only):  $\beta_s, \beta_m = 0, \tau_s, \tau_m = 0$  and  $\rho$  (3 parameter model). Here, we assumed the dynamics of MDR-TB are purely driven by drug-failure from DS-TB.
- Model 2 (Drug-failure and equal transmission and treatment rates between DS and MDR-TB):  $\beta_s = \beta_m, \tau_s = \tau_m$  and  $\rho$  (3 parameter model). Here, we assumed the fitness cost of MDR-TB is negligible and the treatment outcome is the same for both DS and MDR-TB.
- Model 3 (Drug-failure and unequal transmission rates between DS and MDR-TB):  $\beta_s \neq \beta_m, \tau_s = \tau_m$  and  $\rho$  (4 parameter model). Here, we assumed the fitness cost to MDR-TB is significant and the treatment outcome is the same for both DS and MDR-TB.
- Model 4 (Drug-failure and unequal treatment rates between DS and MDR-TB):  $\beta_s = \beta_m, \tau_s \neq \tau_m$  and  $\rho$  (4 parameter model). Here, we assumed the fitness cost to MDR-TB is negligible and the treatment outcome differs between DS and MDR-TB.
- Model 5 (Drug failure and unequal transmission and treatment rates between DS and MDR-TB):  $\beta_s \neq \beta_m, \tau_s \neq \tau_m$  and  $\rho$  (5 parameter model). Here, we assumed the fitness cost to MDR-TB is significant and the treatment outcome differs between both DS and MDR-TB.

With other parameters derived from the literature (see Table 6.1), the models were fitted in MATLAB using the multi-start algorithm with 1000 starting points [23]. The convergent results are kept and the confidence intervals are constructed assuming that the estimates are approximately normally distributed. The best model selection is done by using the associated Akaike Information Criterion (AIC) of the model fit [24]. Further we performed both local and global sensitivity analyses of the model parameters to determine the parameters that have the most influence on the equilibrium prevalence and basic reproduction number of TB.

We further use the parameters from the best model fit from above to mitigate the spread of TB in Bangladesh by developing four combination strategies using these four control strategies:

- (a)  $u_1(t)$  (the distancing control strategy) – that is the effort of preventing susceptible individuals from getting exposed to TB bacilli. This includes personal respiratory protection, environmental controls, diagnosis campaigns, and educational programs for public health.
- (b)  $u_2(t)$  (latent case finding) – which includes chemoprophylaxis treatment, high-risk exposure screening and other forms of latent TB treatment. WHO estimated that treatment for LTBI can decrease the risk of developing active TB by at least 60% [1].
- (c)  $u_3(t)$  (case holding) – this refers to activities that ensure treatment completion to reduce relapse following treatment. Patients receiving treatment for either DS or MDR-TB should be monitored to ensure the completion of the whole course of treatment. Otherwise, TB infection may become resistant to existing antibiotics.
- (d)  $u_4(t)$  (active case finding) – this represents the prevention of disease development with effective treatment for exposed persons or identification of active TB cases.

The resulting optimal control problems are solved using the forward-backward sweep method [25] and implemented in MATLAB [23]. The outputs from this simulation are subjected to cost-effective analysis using the incremental cost-effectiveness ratio (ICER) to determine the intervention strategy that is the best value for money.

Table 6. 1 Parameter description and estimates for Bangladesh TB model (6.2).

Parameters	Description	Estimated value (range)	References
$N$	Population at year 2000	137,439,261	[26]
$\mu$	Birth/Death rate	$\frac{1}{70} \text{ yr}^{-1}$	[27]
$\beta_s$	Transmission rate for DS-TB	$1.56 \times 10^{-8} \text{ yr}^{-1}$	data fitted
$\beta_m$	Transmission rate for MDR-TB	$5.9 \times 10^{-9} \text{ yr}^{-1}$	data fitted
$\alpha_s$	Activation rate from $L_s$ to $I_s$	$0.116 \text{ yr}^{-1}$	[17, 28]
$\alpha_m$	Activation rate from $L_m$ to $I_m$	$0.116 \text{ yr}^{-1}$	[17, 28]
$\omega_s$	Recovery rate for DS-TB	$0.2873 \text{ yr}^{-1}$	[29]
$\omega_m$	Recovery rate for MDR-TB	$0.12 \text{ yr}^{-1}$	assumed
$\delta_s$	Recovery rate from $L_s$ to R	$0.108 \text{ yr}^{-1}$	estimated
$\delta_m$	Recovery rate from $L_m$ to R	$0.108 \text{ yr}^{-1}$	estimated

$\rho$	Proportion of amplification	[0 – 0.34]	data fitted
$\varphi_s$	Disease-related death rate for DS-TB	0.37 over 3 years	[17]
$\varphi_m$	Disease-related death rate for MDR-TB	0.37 over 3 years	[17]
$\tau_s$	Treatment rate for DS-TB	0.470 yr <sup>-1</sup>	data fitted
$\tau_m$	Treatment rate for MDR-TB	0.470 yr <sup>-1</sup>	data fitted
$\gamma$	Rate of waning immunity	0.10 yr <sup>-1</sup>	[30]
$\tau_1$	Treatment rate for latent DS-TB	0.2 yr <sup>-1</sup>	[31]
$\tau_2$	Treatment rate for latent MDR-TB	0.2 yr <sup>-1</sup>	[31]

## 6.3 Results

### 6.3.1 Bangladesh TB prevalence rates

There were four TB surveillance studies conducted in Bangladesh between 1964 and 2015 [32]. Hence the TB prevalence rates are not available for years 2000, 2001 and 2002. To determine the TB prevalence rates for the missing years, we first fitted a linear model to the available TB prevalence rates (Figure 6.2). The slope of the linear fit was -8.51 (95 % CI: -10.40, -6.67) and the y-intercept is 481 at the year 1999. Using this model to predict the TB prevalence for the missing years 2000, 2001 and 2002, we found the estimated prevalence rates per 100,000 people were 473, 464, 456. The decline in prevalence rate is justifiable considering that DOTS was introduced in 1993 and 100% DOTS coverage was reached in 2003. By 2000, the treatment success rate of the DOTS program had reached the targeted 85% and has been maintained above 90% since 2005. In 2006, the program successfully treated 94% of notified new smear-positive cases and the case detection rate was about 70%.

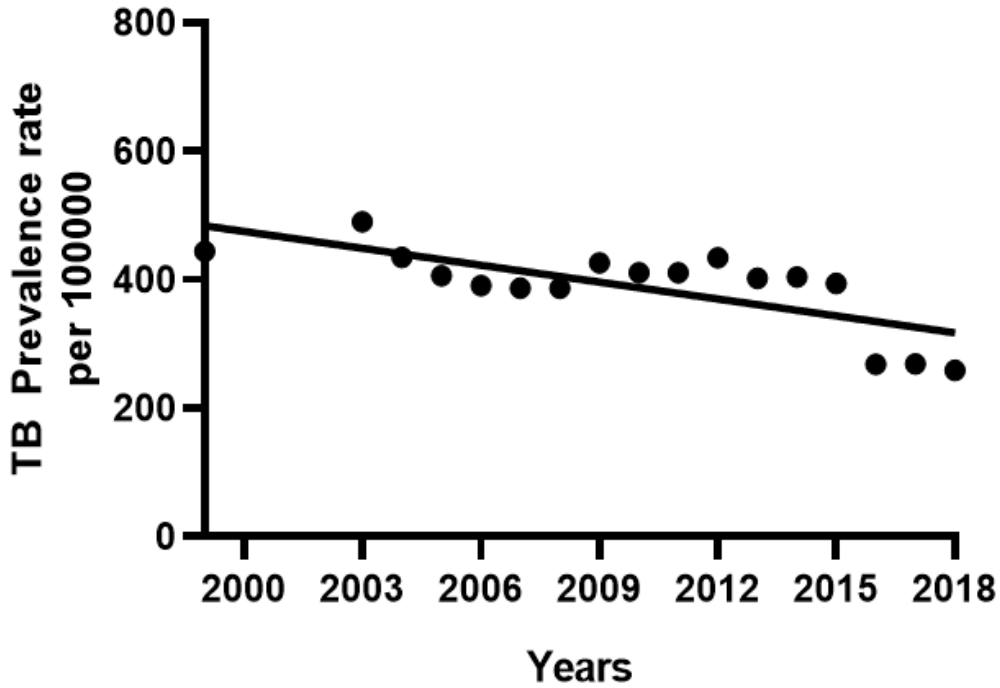


Figure 6. 2 Linear fit to Bangladesh TB prevalence data.

### 6.3.2 TB dynamical process in Bangladesh

For the two-strain TB model (6.2), the basic reproduction number is

$$R_0 = \max(R_{0s}, R_{0m}), \quad (6.3)$$

where  $R_{0s} = \frac{N\alpha_s\beta_s}{(\alpha_s+\delta_s+\mu)(\omega_s+\phi_s+\tau_s+\mu)}$  and  $R_{0m} = \frac{N\alpha_m\beta_m}{(\alpha_m+\delta_m+\mu)(\omega_m+\phi_m+\tau_m+\mu)}$ . The strain-specific reproduction numbers  $R_{0s}$  and  $R_{0m}$  determine whether a specific strain will persist or die out in relation to the other strain. Both strains die out when both  $R_{0m} < 1$  and  $R_{0s} < 1$ . However, the MDR strain will persist in the community even if  $R_{0m} < 1$  and  $R_{0s} > 1$  as the resistant strain is fuelled in two ways: transmission and amplification of the DS strain (Figure 6.3A). If  $R_{0m} > 1$  and  $R_{0s} < 1$ , the DS strain dies out remaining the MDR strain in the community (Figure 6.3B). Similarly, the DS strain dies out if both strain specific basic reproduction number are greater than one and the  $R_{0m} > R_{0s}$  (Figure 6.3C). Otherwise, both are sustained (Figure 6.3D).

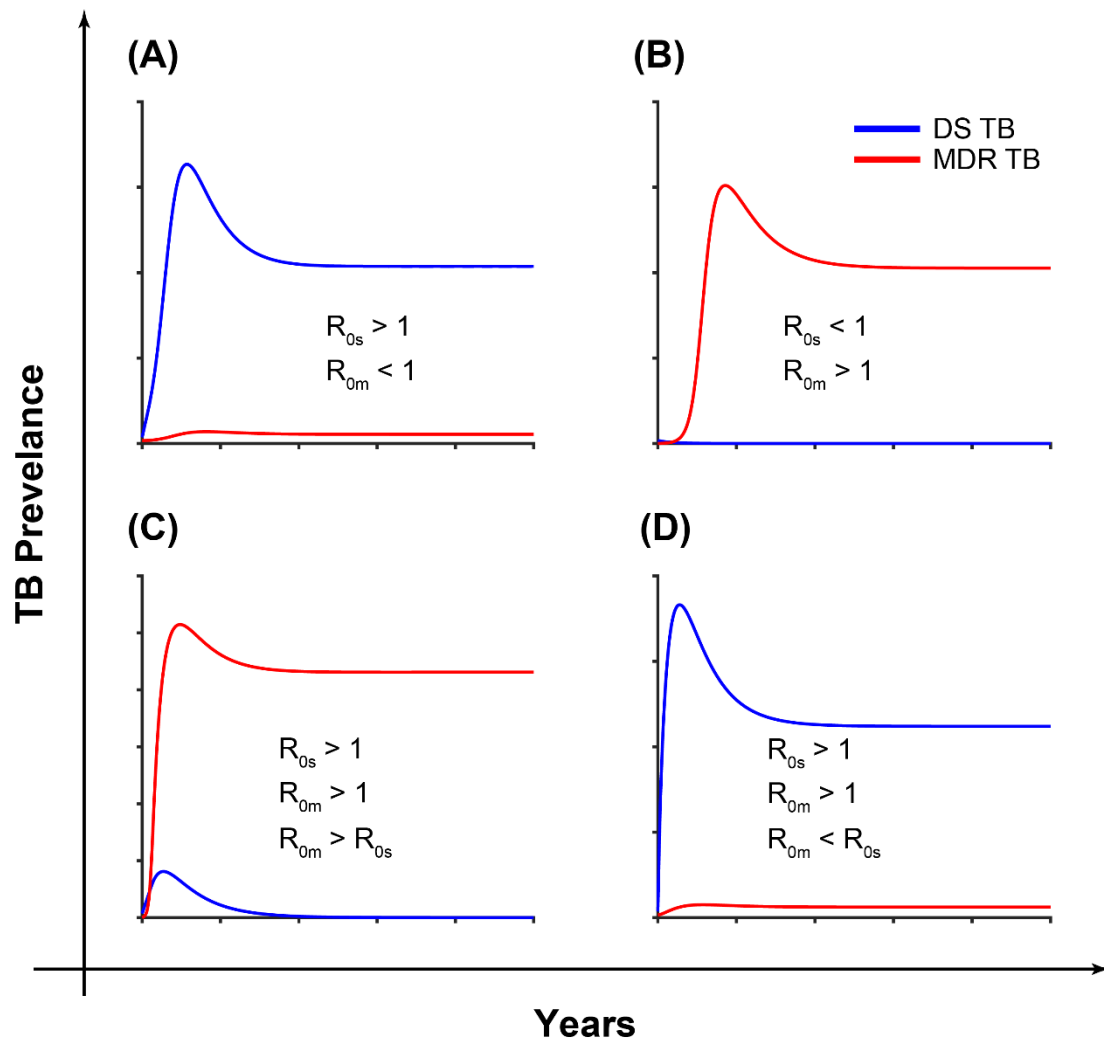


Figure 6. 3 The impacts of the strain specific basic reproduction number on the long-time dynamics of the TB model (6.2).

With clear understanding of the dynamics of model (6.2), we fitted all the five models described in the model calibration section to the cumulative DS and MDR-TB incidence data in Bangladesh to estimate the rate of amplification and the strain specific basic reproduction numbers. According to the AIC metric, we found that Model 2 captures the drug-sensitive TB data better and Model 3 captures the drug-resistant TB data better. See Table 6.2 for the fitting results of Model 2 and 3. While Model 1 is a good fit for the DS-TB incidence data, it was worse for the MDR-TB incidence. Model 4 did well for drug-sensitive TB but failed to capture the drug-resistant TB model well, while Model 5 gave the same fitting results as Model 3. See the supporting information section S6.1 for the fitting results of Model 1 and 4.

Table 6. 2 Fitting results

Parameter	Est.	95% CI
<b>Model 2</b>		
$\beta_s = \beta_m$	$1.53 \times 10^{-8}$	$(1.44 \times 10^{-8}, 1.64 \times 10^{-8})$
$\tau_s = \tau_m$	0.513	(0.491, 0.535)
$\rho$	0.00005	(0, 0.008)
$\rho\tau_s$	0.0003	(0, 0.00434)
	<b>DS</b>	<b>MDR</b>
AIC	369.11	361.10
<b>Model 3 and Model 5</b>		
$\beta_s$	$1.54 \times 10^{-8}$	$(1.5 \times 10^{-8}, 1.67 \times 10^{-8})$
$\beta_m$	$5.9 \times 10^{-9}$	$(4.2 \times 10^{-9}, 7.6 \times 10^{-9})$
$\tau_s = \tau_m$	0.470	(0.229, 0.711)
$\rho$	0.024	(0.017, 0.03)
	<b>DS</b>	<b>MDR</b>
AIC	421.74	353.38

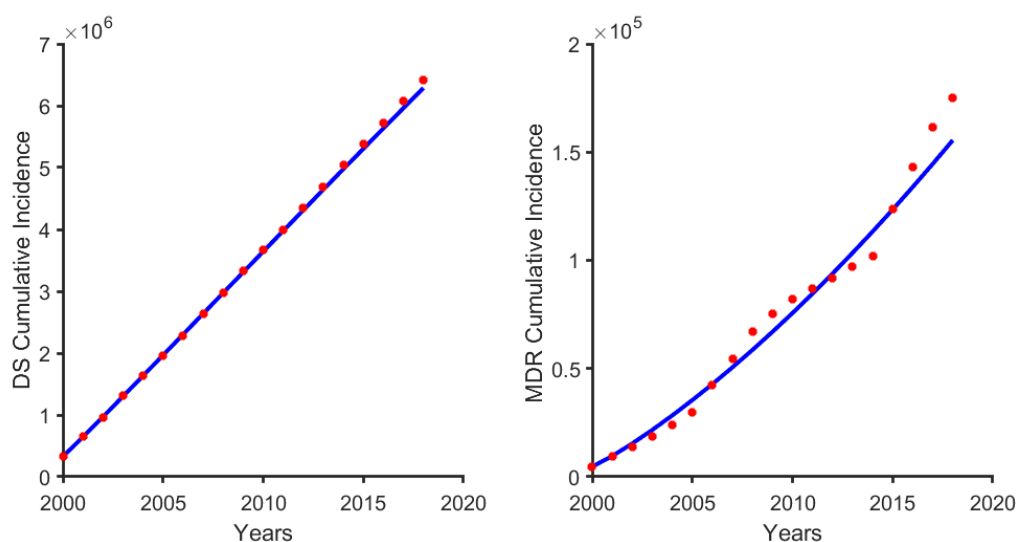


Figure 6. 4 A fit of model 3 to the Bangladesh TB cumulative incidence: (A) DS-TB and (B) MDR-TB.

Both Models 2 and 3 can explain the dynamics of DS and MDR-TB in Bangladesh. For instance, we expect the same treatment rate for DS and MDR-TB and, assuming the same average number of contacts between DS and MDR-TB, then we also expect  $\beta_s > \beta_m$  due to the fitness cost associated with drug-resistance (as postulated by Model 3) [33-35]. Similar conclusions can be reached from the estimates from Model 2. Model 2 (Drug-failure and equal transmission rates between DS and MDR-TB) captures the DS-TB better than Model 3 (Drug-failure and unequal transmission rates between DS and MDR-TB) but since our focus is on MDR-TB, we chose model 3 which captures MDR-TB better and did not do worse for DS-TB (see Figure 6.4) for our further analysis. For Model 2, the estimated strain specific basic reproduction numbers are  $R_{0s} = 1.1$  and  $R_{0m} = 1.34$  suggesting MDR-TB will take over in the

long run (Figure 6.3B), and for Model 3,  $R_{0s} = 1.14$  and  $R_{0m} = 0.54$ , which means that DS-TB will dominate and MDR-TB will persist (Figure 6.3A). For Model 3, the amplification rate was 0.011, which is an average of 90 days between conversions from DS-TB to MDR-TB.

### 6.3.3 Sensitivity analysis of model parameters

We found  $\beta_i$  (the transmission rate),  $\tau_i$  (the treatment rate) and  $\rho$  (the amplification rate) are important for the epidemiology of TB in Bangladesh. However, there are other key parameters that influence the transmission of DS and MDR-TB. The understanding of these key parameters may also provide alternative intervention paradigms for TB control. As demonstrated in the previous sections, the scale and severity of TB transmission are directly associated with the basic reproduction numbers  $R_{0s}$  and  $R_{0m}$ . Here, we estimated the sensitivity indices of the reproduction numbers  $R_{0s}$  and  $R_{0m}$  to the model parameters.

The indices express how vital each parameter is to  $R_{0s}$  and  $R_{0m}$ , and in turn, to TB transmission dynamics, and allow us to identify which areas should be targeted by intervention policies. Here, we further computed partial rank correlation coefficients (PRCCs) which is a global sensitivity analysis technique using Latin Hypercube Sampling (LHS) to study the effects of other parameters that are not present in the basic reproduction number on the TB dynamics. Specifically, each parameter is assumed to be uniformly distributed and we performed 1,000,000 simulations of the TB model. Here, the model outputs are the both basic reproduction numbers namely  $R_{0s}$  and  $R_{0m}$  as well as the equilibrium DS-TB prevalence ( $I_s$ ), MDR-TB prevalence ( $I_m$ ) and total TB prevalence ( $I_s + I_m$ ). Positive (negative) PRCC values refer to a positive (negative) correlation of the model parameter and model outcome. A positive (negative) correlation suggest that a positive (negative) variation in the parameter will increase (decrease) the model outcome. The bigger (smaller) the absolute value of the PRCC, the greater (lesser) the correlation of the parameter with the model outcome.

Figure 6.5 shows the correlation between  $R_{0s}$  and  $R_{0m}$ , and the corresponding model parameters. Parameters  $\beta_s$  and  $\beta_m$  have positive PRCC values, implying that a positive change of these parameters will increase the basic reproduction numbers  $R_{0s}$  and  $R_{0m}$  respectively. In contrast, parameters  $\omega_s$ ,  $\phi_s$ , and  $\tau_s$  as well as  $\omega_m$ ,  $\phi_m$ , and  $\tau_m$  have negative PRCC values, which implies that raising these parameters will consequently decrease  $R_{0s}$  and  $R_{0m}$ .

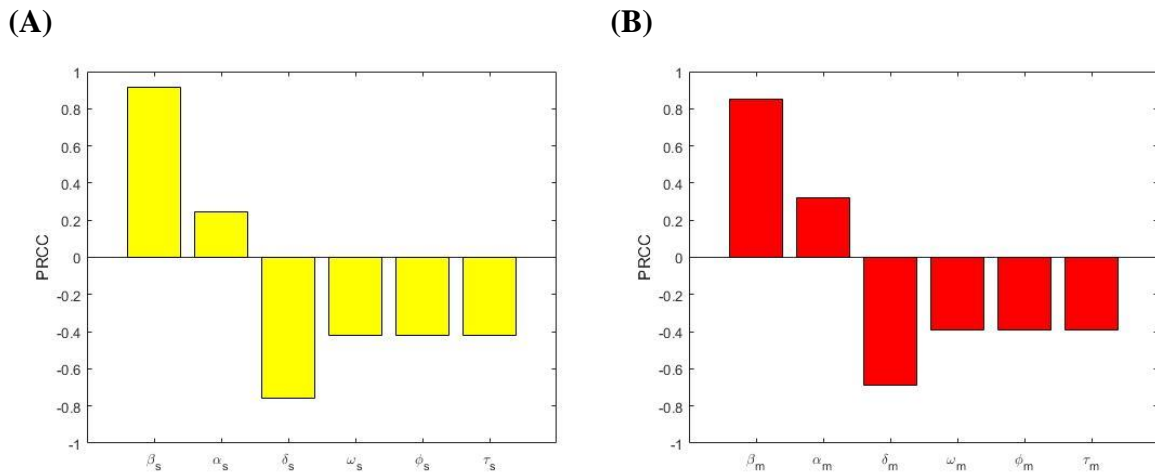


Figure 6.5 PRCC values depicting the sensitivities of the model output: (A)  $R_{0s}$  with respect to the estimated parameters  $\beta_s$ ,  $\alpha_s$ ,  $\delta_s$ ,  $\omega_s$ ,  $\phi_s$ , and  $\tau_s$ , and (B)  $R_{0m}$  with respect to the estimated parameters  $\beta_m$ ,  $\alpha_m$ ,  $\delta_m$ ,  $\omega_m$ ,  $\phi_m$ , and  $\tau_m$ .

Figure 6.6 (A) shows a positive correlation between DS active TB prevalence ( $I_s$ ) and the model parameters  $\beta_s, \alpha_s, \beta_m, \alpha_m$  and  $\gamma$ , for  $R_{0s} > \max[R_{0m}, 1]$ . This implies that a positive change of these parameters will increase the number of people with DS active TB. In contrast, parameters  $\delta_s, \omega_s, \phi_s, \tau_s, \delta_m, \omega_m, \phi_m, \tau_m$  and  $\rho$  have a negative correlation with  $I_s$ . Figure 6.6 (B) represents the correlation between the MDR-TB prevalence ( $I_m$ ) and corresponding model parameters  $\beta_s, \alpha_s, \beta_m, \alpha_m, \omega_s, \phi_s, \tau_s, \beta_m, \alpha_m, \omega_m, \phi_m, \tau_m, \rho$  and  $\gamma$  for  $R_{0s} > \max[R_{0m}, 1]$ . The parameters  $\beta_s, \alpha_s, \beta_m, \alpha_m, \rho$  and  $\gamma$  have the positive PRCC values, while the following parameters  $\delta_s, \omega_s, \phi_s, \tau_s, \delta_m, \omega_m, \phi_m$  and  $\tau_m$  have negative PRCC values. Figure 6.6 (C) represents the correlation between total TB prevalence ( $I_s + I_m$ ) and the corresponding model parameters when  $R_{0s} > \max[R_{0m}, 1]$ . We observed positive correlation with  $\beta_s, \alpha_s, \beta_m, \alpha_m, \rho$  and  $\gamma$ , implying an increase in the total TB prevalence with an increase in these parameter values. However, the parameters  $\delta_s, \omega_s, \phi_s, \tau_s, \delta_m, \omega_m, \phi_m$  and  $\tau_m$  have a negative correlation with total TB prevalence, which means increasing these parameters values will consequently decrease the total TB prevalence. Figure 6.6 (D) represents the correlation between the MDR-TB prevalence and corresponding model parameters  $\beta_s, \alpha_s, \omega_s, \phi_s, \tau_s, \beta_m, \alpha_m, \omega_m, \phi_m, \tau_m, \rho$  and  $\gamma$  when  $R_{0m} > R_{0s}$  and  $R_{0m} > 1$ . Parameters  $\beta_s, \alpha_s, \beta_m, \alpha_m, \rho$  (small values not shown) and  $\gamma$  have positive PRCC values and parameters  $\delta_s, \omega_s, \phi_s, \tau_s, \delta_m, \omega_m, \phi_m$  and  $\tau_m$  have negative PRCC values.

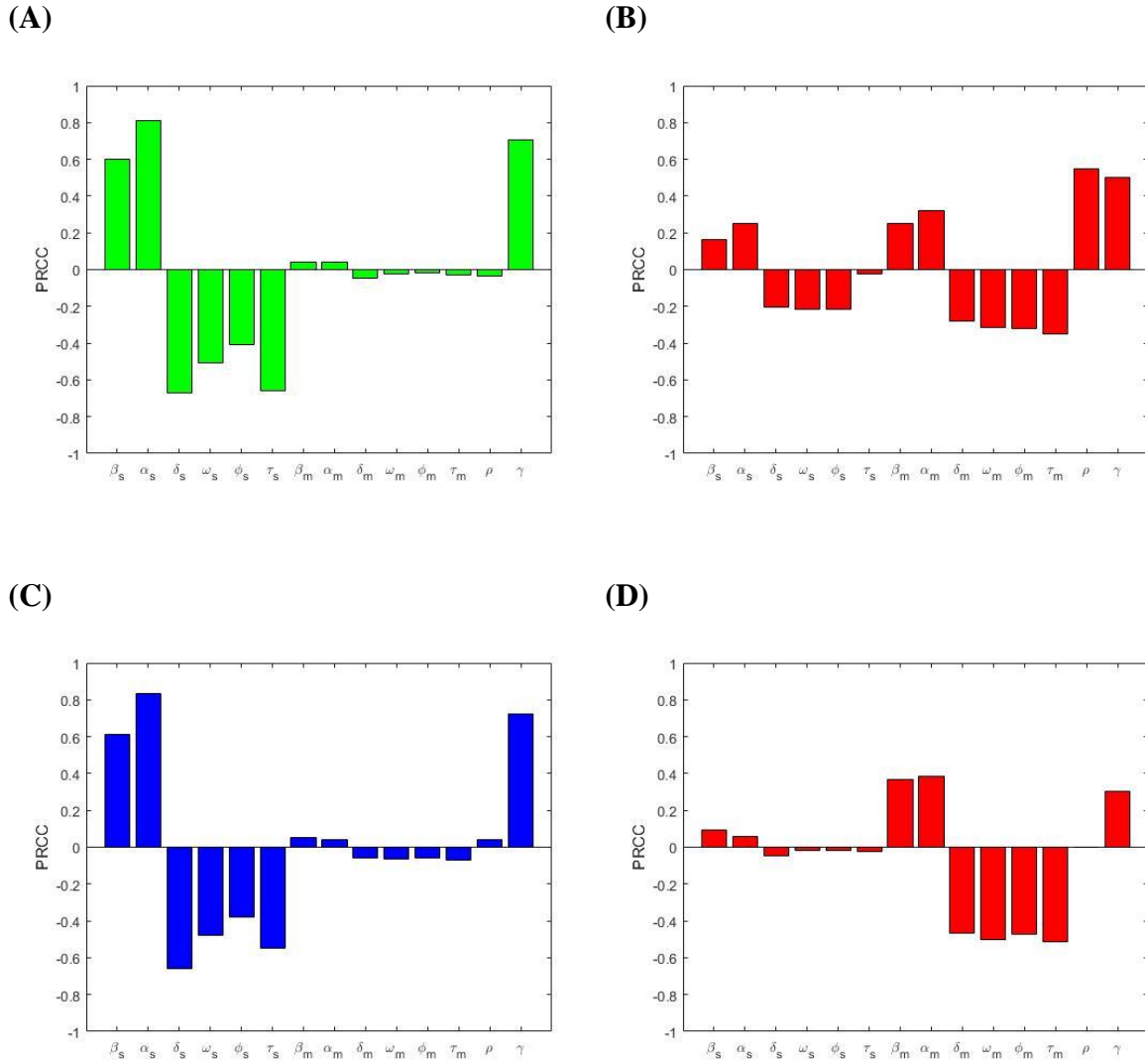


Figure 6. 6 PRCC values depicting the sensitivities of the model DS, MDR and total TB prevalences.

(A)  $I_s$  with respect to the estimated parameters  $\beta_s, \alpha_s, \omega_s, \delta_s, \phi_s, \tau_s, \beta_m, \alpha_m, \omega_m, \delta_m, \phi_m, \tau_m$  and  $\rho$ , (B)  $I_m$  with respect to the estimated parameters  $\beta_s, \alpha_s, \omega_s, \delta_s, \phi_s, \tau_s, \beta_m, \alpha_m, \omega_m, \delta_m, \phi_m, \tau_m$  and  $\rho$ , (C)  $(I_s + I_m)$  with respect to the estimated parameters  $\beta_s, \alpha_s, \omega_s, \delta_s, \phi_s, \tau_s, \beta_m, \alpha_m, \omega_m, \delta_m, \phi_m, \tau_m$  and  $\rho$ , when  $R_{0s} > \max[R_{0m}, 1]$ , and (D)  $I_m$  with respect to the estimated parameters  $\beta_s, \alpha_s, \omega_s, \delta_s, \phi_s, \tau_s, \beta_m, \alpha_m, \omega_m, \delta_m, \phi_m, \tau_m$  and  $\rho$ , when  $R_{0m} > R_{0s}$  and  $R_{0m} > 1$ .

From the explicit formula for  $R_{0s}$  and  $R_{0m}$ , the analytical expression for the sensitivity indices can be derived applying the method in [36] to each of the parameters, e.g.

$$Y_{\beta_s}^{R_{0s}} = \frac{\partial R_{0s}}{\partial \beta_s} \times \frac{\beta_s}{R_{0s}}. \quad (6.4)$$

Now using the parameter values in Table 6.1 and Table 6.2, we have the following results (Table 6.3).

Table 6. 3 Sensitivity indices to parameters for the model (6.2)

Parameter	Sensitivity index ( $R_{0s}$ )	Parameter	Sensitivity index ( $R_{0m}$ )
$\beta_s$	+ 1.000	$\beta_m$	+1.000
$\alpha_s$	+0. 513	$\alpha_m$	+0.513
$\delta_s$	-0.453	$\delta_m$	-0.453
$\omega_s$	- 0.251	$\omega_m$	- 0.123
$\phi_s$	- 0.324	$\phi_m$	- 0.379
$\tau_s$	-0.413	$\tau_m$	- 0.484

In the sensitivity indices of  $R_{0s}$  and  $R_{0m}$ , the most sensitive parameter is the effective contact rate of DS-TB,  $\beta_s$  and MDR-TB,  $\beta_m$ . Other significant parameters are activation rates ( $\alpha_s$  and  $\alpha_m$ ). The least sensitive parameters are the recovery rates  $\omega_s$  and  $\omega_m$ . Hence, increasing (or decreasing) the effective contact rates,  $\beta_s$  and  $\beta_m$  of DS-TB and MDR-TB by 100%, increases (or decreases) the reproduction numbers  $R_{0s}$  and  $R_{0m}$  by 100%. Similarly, increasing (or decreasing) the recovery rates  $\omega_s$  and  $\omega_m$  by 100% decreases (or increases)  $R_{0s}$  and  $R_{0m}$ , by 25.1% and 12.3% respectively.

### 6.3.4 Optimal control strategies and cost-effectiveness analysis

We incorporated the earlier defined control strategies in the Bangladesh TB model (see equation (6.5) below) and from it derived alternative measures to reduce the burden of TB. Our goal is to maximize the total number of active TB cases averted (TATBA)

$$\frac{dS}{dt} = \mu N - (1 - u_1(t))\beta_s I_s S - (1 - u_1(t))\beta_m I_m S - \mu S + \gamma R + \varphi_s I_s + \varphi_m I_m,$$

$$\frac{dL_s}{dt} = (1 - u_1(t))\beta_s I_s S - (\alpha_s + (\delta_s + u_2(t)\tau_1) + \mu)L_s,$$

$$\frac{dI_s}{dt} = \alpha_s L_s - (\omega_s + (1 + u_4(t))\tau_s + \phi_s + \mu)I_s,$$

$$\frac{dL_m}{dt} = (1 - u_1(t))\beta_m I_m S - (\alpha_m + (\delta_m + u_2(t)\tau_2) + \mu)L_m,$$

$$\frac{dI_m}{dt} = \alpha_m L_m + (\rho (1 - u_3(t))) (1 + u_4(t))\tau_s I_s - (\omega_m + \tau_m(1 + u_4(t)) + \phi_m + \mu)I_m,$$

$$\frac{dR}{dt} = (1 - \rho(1 - u_3(t))) (1 + u_4(t))\tau_s I_s + \tau_m(1 + u_4(t))I_m + \omega_s I_s + \omega_m I_m +$$

$$(\delta_s + u_2(t)\tau_1)L_s + (\delta_m + u_2(t)\tau_2)L_m - \gamma R - \mu R. \quad (6.5)$$

From equation (6.5),  $\tau_1$  and  $\tau_2$  are the treatment rates of the DS and MDR latent TB. The “do-nothing-more” control is the baseline control with zero additional cost and is used as the reference to calculate the total number of active TB infections averted. The objective of the optimal control strategy is to

minimize the cost of reducing the number of latent DS and MDR-TB ( $L_s$  and  $L_m$ ), and infectious individuals ( $I_s$  and  $I_m$ ). The controls range between 0 and 1, and when  $u_1(t), u_2(t), u_3(t), u_4(t) = 0$ , that is the “do-nothing-more” control, while  $u_1(t), u_2(t), u_3(t), u_4(t) \equiv 1$  refers to maximum effort of the control policy being implemented. We formulated four different control strategies with different alternatives and determined the cost-effective of these strategies.

### 6.3.4.1 Single control strategy

For this control strategy, we have four alternatives:

- a.  $u_1(t)$ , only distancing control
- b.  $u_2(t)$ , only latent case finding
- c.  $u_3(t)$ , only case holding
- d.  $u_4(t)$ , only active case finding.

For each of these alternatives, the objective function is of the form:

$$\text{minimize: } J(u_i) = \int_{t_0}^{t_f} \left( A_1 L_s + A_2 I_s + A_3 L_m + A_4 I_m + \frac{B_i}{2} u_i^2 \right) dt, \quad (6.6)$$

Here, the total cost on a finite time horizon  $[t_0, t_f]$  (where initial time  $t_0 = 0$ , final time  $t_f = 20$  year period) consists of the cost induced by the DS and MDR-TB cases themselves and the cost induced by the efforts of the four different types of control [37, 38] strategies including distancing, latent case finding, case holding, and active case finding. We split the cost induced by latent DS and MDR-TB,  $\int_{t_0}^{t_f} A_1 L_s(t) dt$  and  $\int_{t_0}^{t_f} A_3 L_m(t) dt$ , proportional to the number of latently infected individuals of DS and MDR-TB respectively. Further, the cost induced by active DS and MDR-TB cases,  $\int_{t_0}^{t_f} A_2 I_s(t) dt$  and  $\int_{t_0}^{t_f} A_4 I_m(t) dt$ , proportional to the number of actively infected individuals of DS and MDR-TB respectively. Here, we consider the biquadratic form in the four control strategies to represent high expensiveness of these strategies. The cost involved in the distancing, latent case finding, case holding, and active case finding strategies is taken as  $\int_{t_0}^{t_f} \frac{B_1}{2} u_1^2(t) dt$ ,  $\int_{t_0}^{t_f} \frac{B_2}{2} u_2^2(t) dt$ ,  $\int_{t_0}^{t_f} \frac{B_3}{2} u_3^2(t) dt$ , and  $\int_{t_0}^{t_f} \frac{B_4}{2} u_4^2(t) dt$ , respectively. It is assumed that the cost of each control strategy is nonlinear and takes a quadratic form, which is found to be consistent with previous works [37].

The coefficients  $A_i$  are the cost of diagnosing and treating latently infected and infectious individuals. Here, we consider  $A_1 = \text{US\$}18.40$  per latent DS-TB case and  $A_2 = \text{US\$}119.58$  per active DS-TB

case. Conversely, since MDR-TB treatment is far more expensive, we take  $A_3 = \text{US\$}4055$  per latent MDR-TB case and  $A_4 = \text{US\$}3955$  per active MDR-TB case [39].

The coefficients  $B_i$  ( $i = 1,2,3,4$ ) represent the weight constants associated to the relative costs of implementing the respective control strategies. The distancing programme involves education, media coverage, and encouraging reduction of contacts with infectious TB patients. In Bangladesh, the cost of telecast for 90 minutes is  $\text{US\$}2916$  and the cost per hospital bed per day is around  $\text{US\$}19.29$  [40-42]. There are approximately 97,800 hospital beds in Bangladesh [43] and we assume that around 432 beds are involved for TB transmission control protecting susceptible individuals from infected individuals. Thus for a year run of the distancing control programme the total cost is around  $B_1 = \text{US\$}4,103,583$ . The unit cost per diagnosis of TB is  $\text{US\$}3804$  [40] and there is an average of 1744 health workers in Bangladesh [44]. Hence, we have  $B_2 = B_4 = \text{US\$}6,634,176$ . For the case holding, we assume 1000 health workers are recruited for this purpose. The unit cost per health worker is  $\text{US\$}3607$  [40] and hence  $B_3 = \$3,607,000$ .

The supplementary materials section S6.2 shows the optimal characterization of the control problems. Figure 6.7 and supplementary materials section S6.2 and Figure S6.4 show the optimal solutions of the single control strategy. For each of these alternatives, the application of each control leads to a reduction in TB prevalence. However, we used cost-effectiveness analysis to determine the most cost-effective strategy to use in the control of TB in Bangladesh. This is performed by associating the differences among the costs and outcomes of each intervention; obtained by estimating the incremental cost-effective ratio (ICER) which is defined as the extra cost per additional intervention outcome. Incrementally, when analyzing two or more competing intervention policies, one intervention is associated with the next less effective option. The ICER numerator is given by the difference in intervention costs, active TB cases averted costs and averted productivity losses if applicable, between each scenario and baseline. The ICER denominator is the total number of active TB cases averted. The ICER is obtained by the following formula:

$$\text{ICER}_i = \frac{\text{TC}_i}{\text{TATBA}_i} \tag{6.7}$$

where,  $i =$  list of control strategies

Table 6. 4 Incremental cost-effective ratio of single control strategy

Single Control	Total Cost (TC)	TATBA	ICER
Distancing	US\$ $1.40 \times 10^9$	$3.09 \times 10^6$	$4.52 \times 10^2$
Latent case finding	US\$ $1.92 \times 10^9$	$2.25 \times 10^6$	$8.56 \times 10^2$
Case holding	US\$ $3.22 \times 10^9$	$1.47 \times 10^1$	$2.19 \times 10^8$
Active case finding	US\$ $2.86 \times 10^9$	$6.77 \times 10^5$	$4.22 \times 10^3$

From Table 6.4, the distancing strategy is less expensive and more effective than other alternatives. Hence, it is the preferable single control strategy. Alternatively, latent case finding is another good choice.

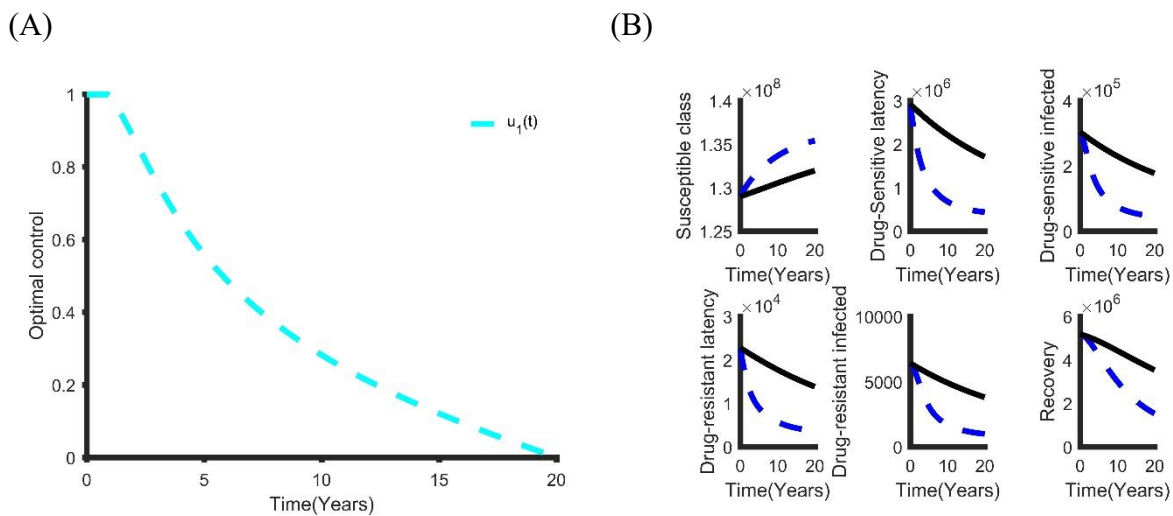


Figure 6. 7 The single optimal control strategy: (A) The optimal distancing control strategy. (B) The benefits of using only distancing control strategy.

### 6.3.4.2 Dual control strategy

In the dual implementation scenario we have six alternative strategies:

- $u_1(t)$  and  $u_2(t)$ : distancing and latent case finding
- $u_1(t)$  and  $u_3(t)$ : distancing and case holding
- $u_1(t)$  and  $u_4(t)$ : distancing and active case finding
- $u_2(t)$  and  $u_3(t)$ , latent case finding and case holding
- $u_2(t)$  and  $u_4(t)$ , latent case finding and active case finding
- $u_3(t)$  and  $u_4(t)$ , case holding and active case finding

The objective functional in this case is:

$$\text{minimize: } J(u_i, u_j) = \int_{t_0}^{t_f} \left( A_1 L_s + A_2 I_s + A_3 L_m + A_4 I_m + \frac{B_1}{2} u_i^2 + \frac{B_j}{2} u_j^2 \right) dt, \quad (6.8)$$

where the parameters in equation (6.8) are as defined above. Each of the strategies resulted in decreasing the number of infected people at different levels of control (Figure 6.8 and supplementary materials section S6.2, Figure S6.5). The cost-effective analysis shows that a combination of the distancing and latent case finding is the best dual strategy (see Table 6.5).

Table 6. 5 Incremental cost-effective ratio of coupled control strategy

Dual Control	Total Cost (TC)	TATBA	ICER
Distancing and latent case finding	US\$1.22 × 10 <sup>9</sup>	3.40 × 10 <sup>6</sup>	3.59 × 10 <sup>2</sup>
Distancing and case holding	US\$1.40 × 10 <sup>9</sup>	3.09 × 10 <sup>6</sup>	4.52 × 10 <sup>2</sup>
Distancing and active case finding	US\$1.40 × 10 <sup>9</sup>	3.08 × 10 <sup>6</sup>	4.53 × 10 <sup>2</sup>
Latent case finding and case holding	US\$1.92 × 10 <sup>9</sup>	2.25 × 10 <sup>6</sup>	8.55 × 10 <sup>2</sup>
Latent and active case finding	US\$1.82 × 10 <sup>9</sup>	2.42 × 10 <sup>6</sup>	7.54 × 10 <sup>2</sup>
Case holding and active case finding	US\$2.85 × 10 <sup>9</sup>	6.77 × 10 <sup>5</sup>	4.21 × 10 <sup>3</sup>

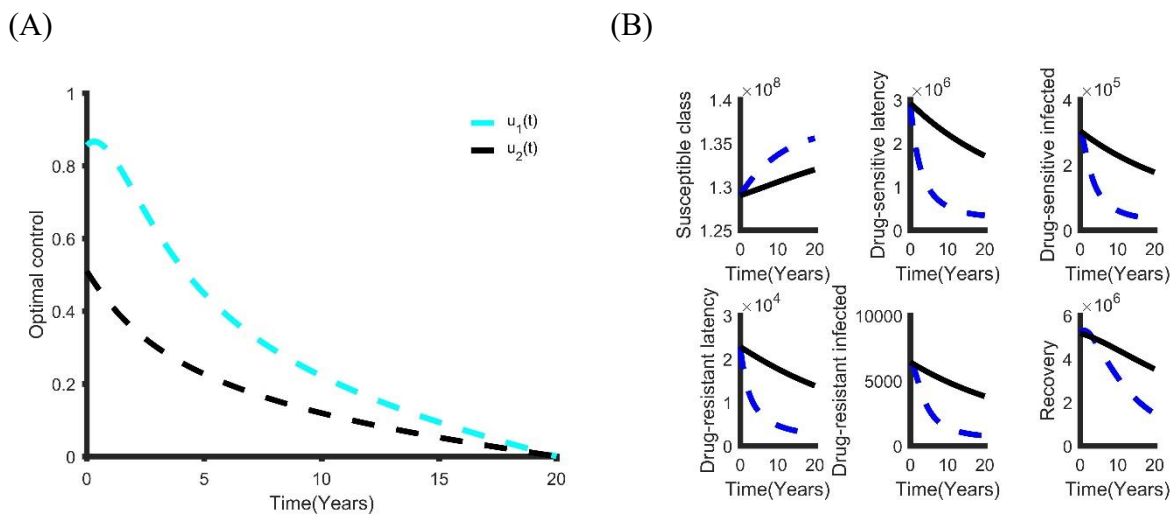


Figure 6. 8 The double optimal control strategy: (A) The Distancing and latent case finding control strategy. (B) The benefits of using distancing and latent case finding control strategy.

### 6.3.4.3 Triple control strategy

For the combination of three different control practices, we have four alternative strategies:

- a.  $u_1(t), u_2(t)$  and  $u_4(t)$ : distancing, latent case finding and active case finding
- b.  $u_1(t), u_2(t)$  and  $u_3(t)$ : distancing, latent case finding and case holding
- c.  $u_1(t), u_3(t)$  and  $u_4(t)$ : distancing, case holding and active case finding
- d.  $u_2(t), u_3(t)$  and  $u_4(t)$ : latent case finding, case holding and active case finding

Hence, the objective functional is

$$\text{minimize: } J(u_i, u_j, u_k) = \int_{t_0}^{t_f} \left( A_1 L_s + A_2 I_s + A_3 L_m + A_4 I_m + \frac{B_i}{2} u_i^2 + \frac{B_j}{2} u_j^2 + \frac{B_k}{2} u_k^2 \right) dt, \quad (6.9)$$

As expected, each of the strategies resulted in decreasing the number of infected people at different levels of cost (Figure 6.9 and supplementary materials section S6.2, Figure S6.6), and we used cost-effectiveness analysis to determine which of these strategies is the most cost-effective (Table 6.6). The combination of distancing, latent case finding and case holding is the best triple control strategy. Alternatively, distancing, latent case finding and active case finding also provides cost-effective results.

Table 6. 6 Incremental cost-effectiveness ratio of each triple control strategy

Triple Control	Total Cost (TC)	TATBA	ICER
$u_1(t), u_2(t)$ and $u_3(t)$	US\$1.22 × 10 <sup>9</sup>	3.40 × 10 <sup>6</sup>	3.58 × 10 <sup>2</sup>
$u_1(t), u_2(t)$ and $u_4(t)$	US\$1.22 × 10 <sup>9</sup>	3.39 × 10 <sup>6</sup>	3.58 × 10 <sup>2</sup>
$u_1(t), u_3(t)$ and $u_4(t)$	US\$1.40 × 10 <sup>9</sup>	3.08 × 10 <sup>6</sup>	4.53 × 10 <sup>2</sup>
$u_2(t), u_3(t)$ and $u_4(t)$	US\$1.82 × 10 <sup>9</sup>	2.42 × 10 <sup>6</sup>	7.53 × 10 <sup>2</sup>

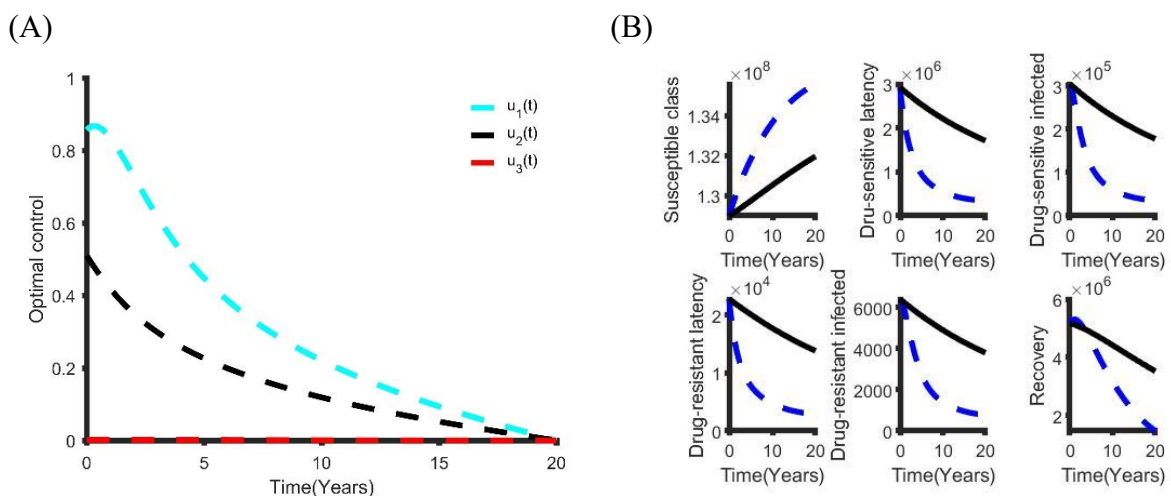


Figure 6. 9 The triple optimal control strategy: (A) The Distancing, latent case finding and case holding control strategy. (B) The benefits of using distancing, latent case finding and case holding control strategy.

### 6.3.4.4. Quadruple control strategy

In this case, all the four controls are used. The objective function is:

$$\text{minimize: } J(u_1, u_2, u_3, u_4) = \int_{t_0}^{t_f} \left( A_1 L_s + A_2 I_s + A_3 L_m + A_4 I_m + \frac{B_1}{2} u_1^2 + \frac{B_2}{2} u_2^2 + \frac{B_3}{2} u_3^2 + \frac{B_4}{2} u_4^2 \right) dt. \quad (6.10)$$

Figure 6.10 shows the optimal controls and the benefits of this intervention method. The number of individuals with DS and MDR-TB reduces to zero in less than 12 years of rolling out this policy. This outcome is similar to the triple control strategy but comes at a cost of  $\text{US}\$5.87 \times 10^8$  with a total of  $4.46 \times 10^6$  infections averted within 20 years. We compared all the control strategies with each other to determine which is the most cost-effective (Table 6.7). The quadruple control strategy (distancing, latent case finding, case holding and active case finding) is the best strategy. However, depending on availability of funding, other strategies in Table 6.7 can be considered.

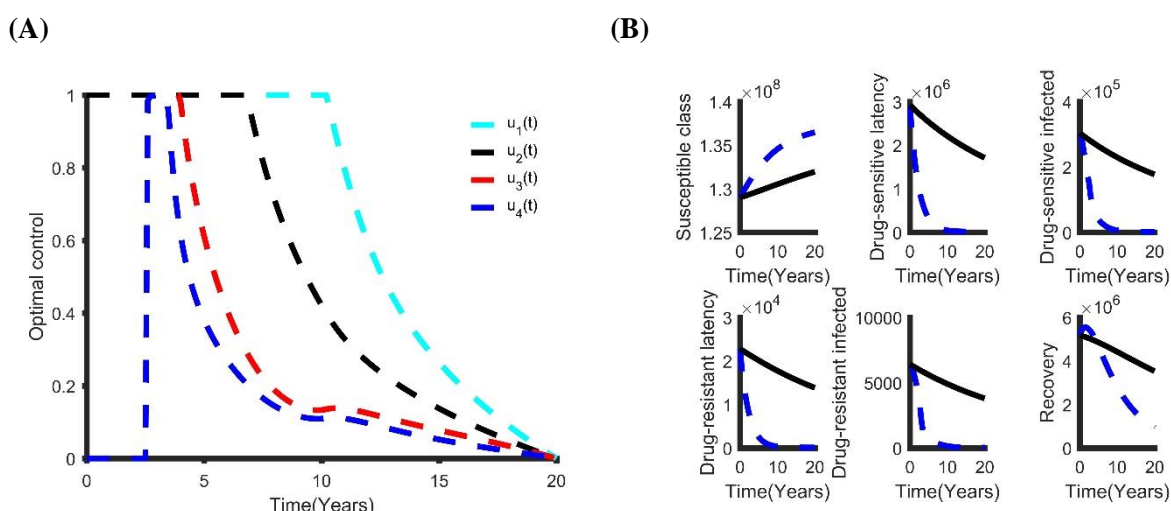


Figure 6. 10 (A) The optimal quadruple control strategy; and (B) its effect on TB prevalence in Bangladesh.

Table 6. 7 Selecting best control strategy

Best control strategy	Total Cost (TC)	TATBA	ICER
$u_1(t), u_2(t), u_3(t)$ and $u_4(t)$	$\text{US}\$5.87 \times 10^8$	$4.46 \times 10^6$	$1.32 \times 10^2$
$u_1(t), u_2(t)$ and $u_4(t)$	$\text{US}\$1.22 \times 10^9$	$3.39 \times 10^6$	$3.58 \times 10^2$
$u_1$ and $u_2(t)$	$\text{US}\$1.22 \times 10^9$	$3.40 \times 10^6$	$3.59 \times 10^2$
$u_1(t)$	$\text{US}\$1.40 \times 10^9$	$3.09 \times 10^6$	$4.52 \times 10^2$

### 6.3.4.5 Sensitivity analysis of our best optimal control strategies

We performed a sensitivity analysis on the weighted costs associated with each control from our selected best strategies to determine how variability in the weighted costs affects our objective functional and the optimal control adopted. For the single control strategies, the distancing control  $u_1(t)$  is the best strategy for this class. Hence, we vary  $B_1$  from 1 to  $10^7$  with an equidistant step resulting into 1000 variates of  $B_1$ . In general, if the weighted cost is smaller, the relative unit cost of using control is cheaper and the control is fully utilized for all the intervention period (Figure 6.11). Otherwise, the increase weighted cost penalizes the control and it's proportionally applied to adjust for high cost. The corresponding state variables are shown in Figure 6.12.

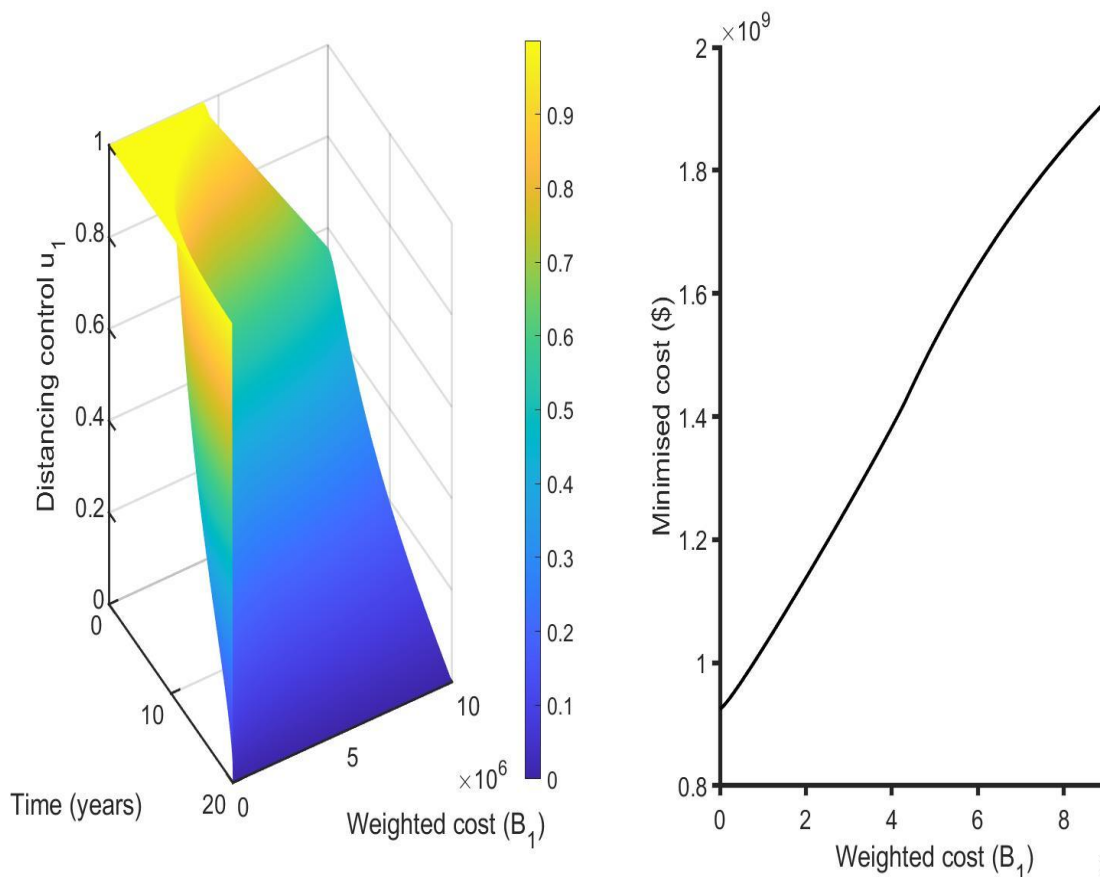


Figure 6. 11 Effects of varying the weighted cost ( $B_1$ ) on the distancing control ( $u_1$ ) (left Figure) and the objective functional (right Figure).

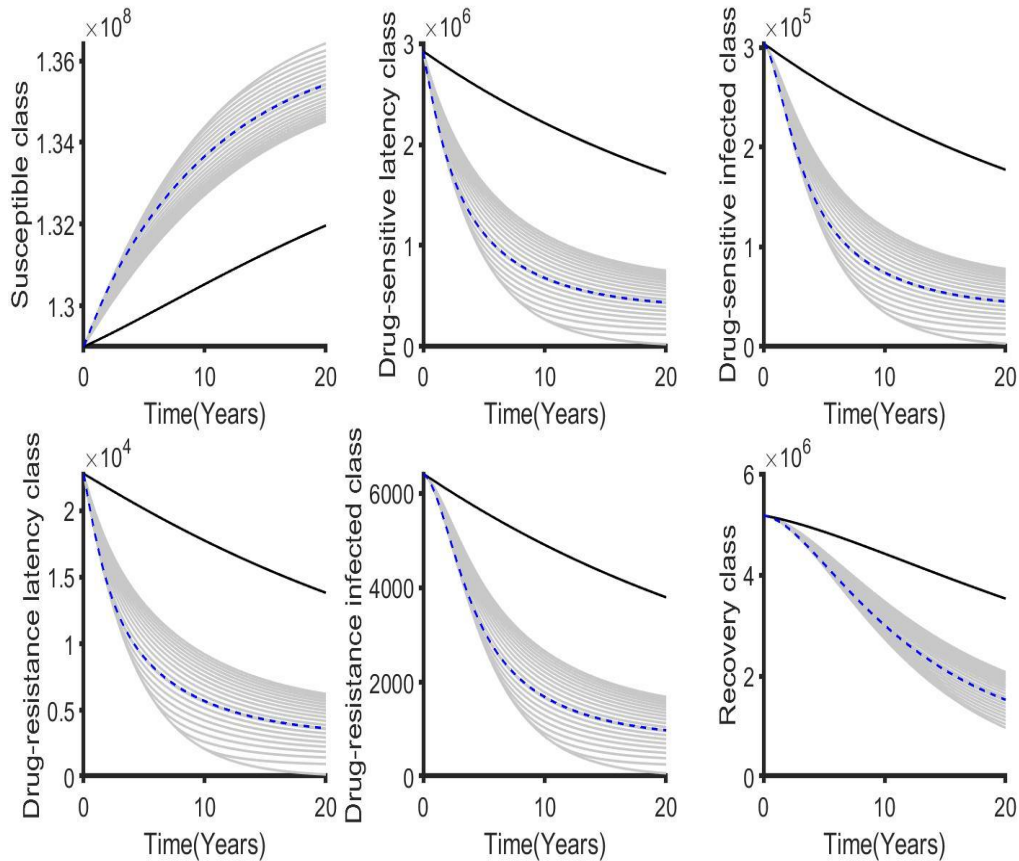


Figure 6. 12 The corresponding state variables associated with varying the weighted cost ( $B_1$ ) while applying the distancing control ( $u_1$ ). The state variables with and without controls are plotted by gray/blue dotted and black lines respectively.

For the double control strategies, the combination of distancing  $u_1(t)$  and latent case finding  $u_2(t)$  is the best strategy for this class. Figures 6.13, 6.14, 6.15, 6.16, 6.17 and 6.18 show the combination of optimal control strategies including distancing and latent case finding and their effects on the state variables. In Figure 6.13, we considered three threshold values for  $B_2$ :  $B_2 = 10^5, 10^6$  and  $10^7$ , and varied the weighted cost  $B_1$ . This increase in  $B_2$  shows little effect on the distancing control  $u_1(t)$  (Figure 6.13) but strong effect on the latent case finding control  $u_2(t)$  (Figure 6.14). In a similar way, when we fixed the weighted cost  $B_1$ , both controls change, with reductions in the amount of control required at higher cost (see Figure 6.16 and 6.17). As expected higher weighted cost increases the cost of implementation of the controls (see the right lower quadrant of Figure 6.13 and 6.16), and the effects on the state variables are shown in Figure 6.15 and 6.18.

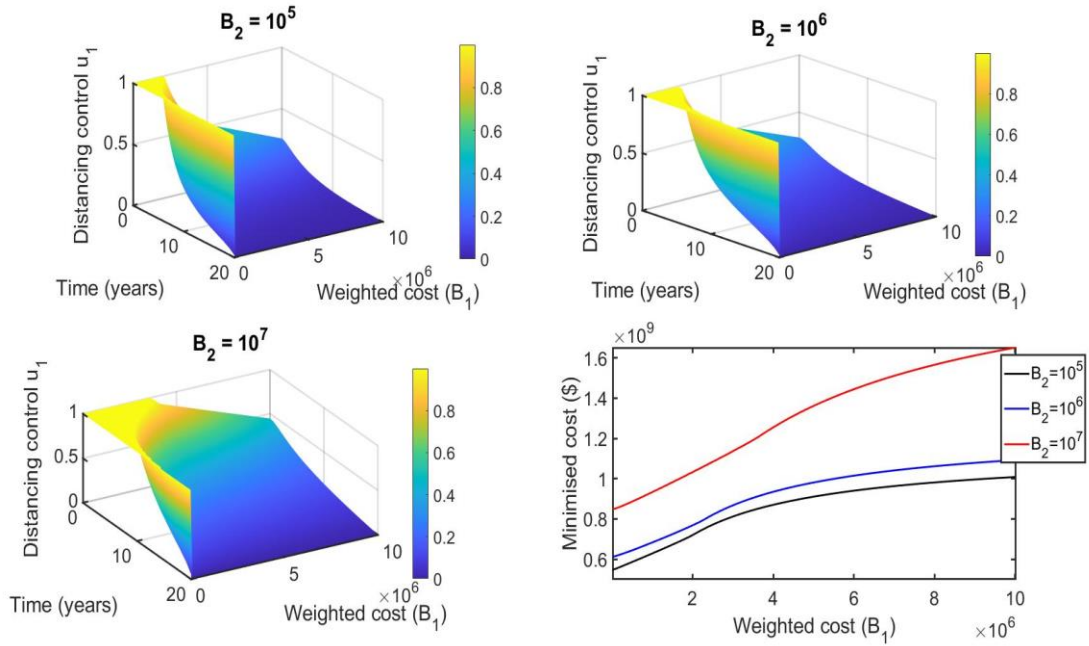


Figure 6. 13 Combination of distancing control ( $u_1$ ) and latent case finding control ( $u_2$ ) strategy, and considering distancing control ( $u_1$ ) strategy as a function of time and weighted cost ( $B_1$ ). The weighted cost ( $B_2$ ) is set to the threshold values  $B_2=10^5=10^6=10^7$ .

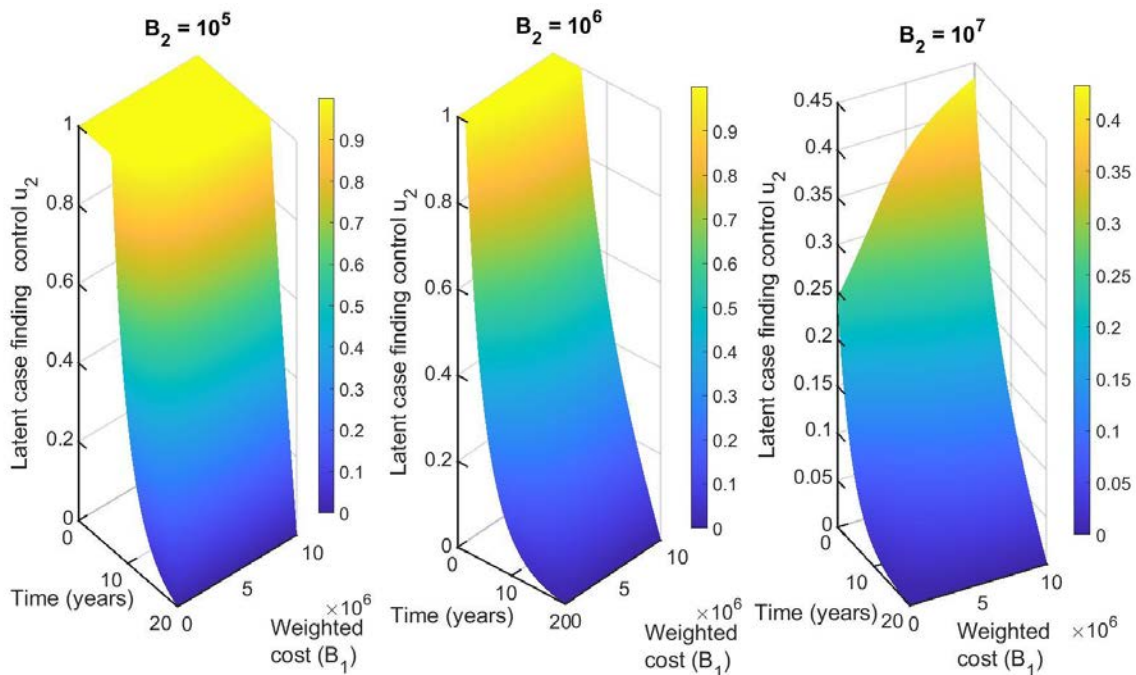


Figure 6. 14 Combination of distancing control ( $u_1$ ) and latent case finding control ( $u_2$ ) strategy, and considering latent case finding control ( $u_2$ ) strategy as a function of time and weighted cost ( $B_1$ ). The weighted cost ( $B_2$ ) determined by three threshold values  $B_2=10^5=10^6=10^7$ .

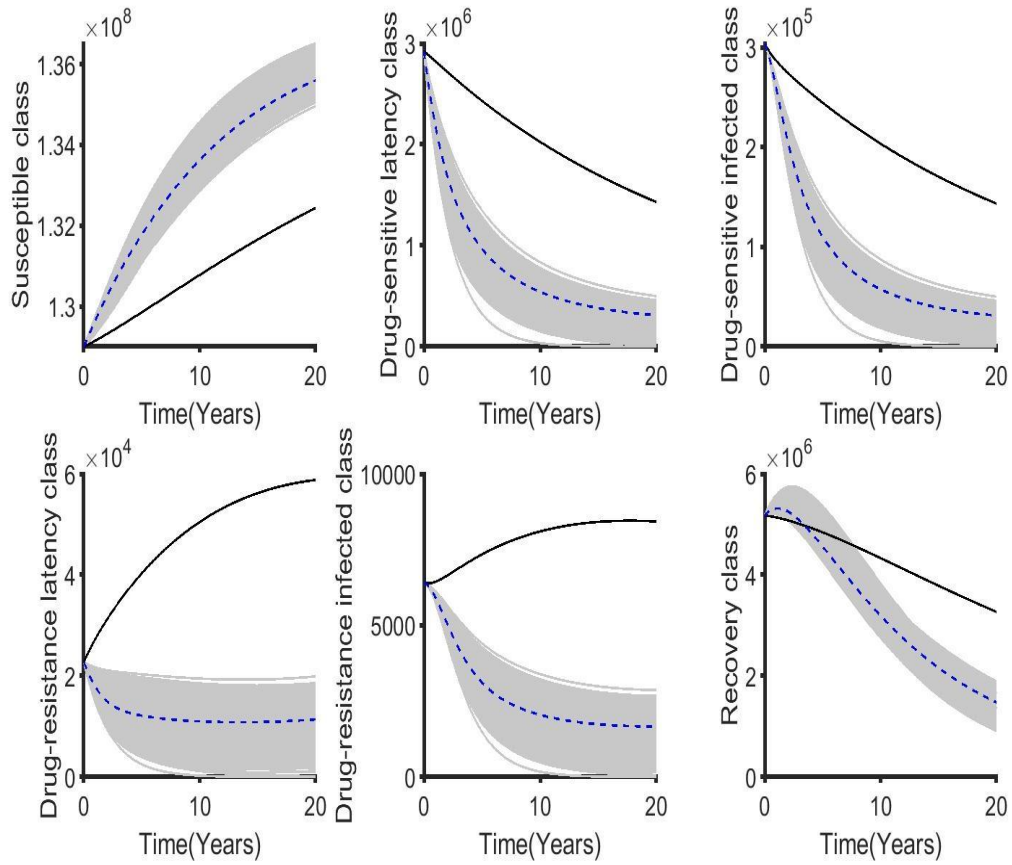


Figure 6. 15 The corresponding state variables of the combination of distancing control ( $u_1$ ) and latent case finding control ( $u_2$ ) strategy and considering the weighted cost  $B_1$  is varied and  $B_2=10^5=10^6=10^7$ . The state variables with and without controls are plotted by grays/blue dotted and black lines respectively.

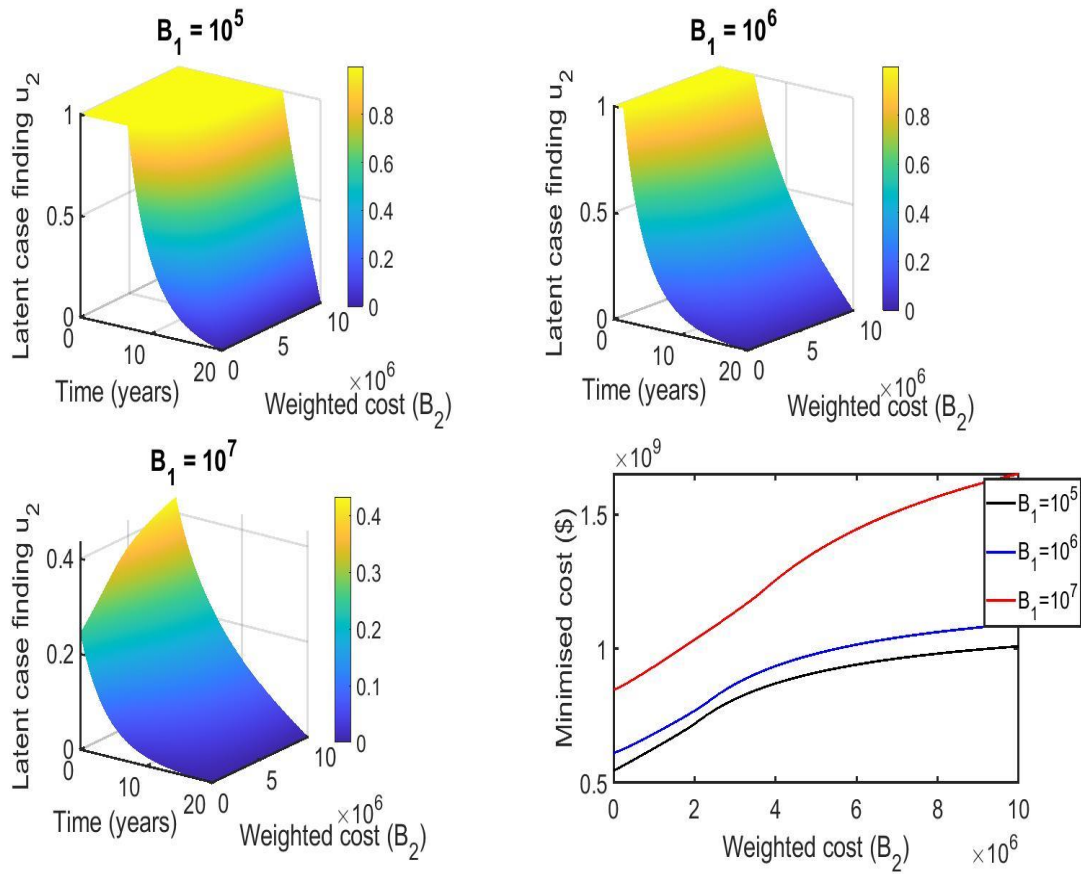


Figure 6. 16 Combination of distancing control ( $u_1$ ) and latent case finding control ( $u_2$ ) strategy, and considering latent case finding ( $u_2$ ) strategy as a function of time and weighted cost ( $B_2$ ). The weighted cost ( $B_1$ ) determined by three threshold values  $B_1=10^5=10^6=10^7$ .

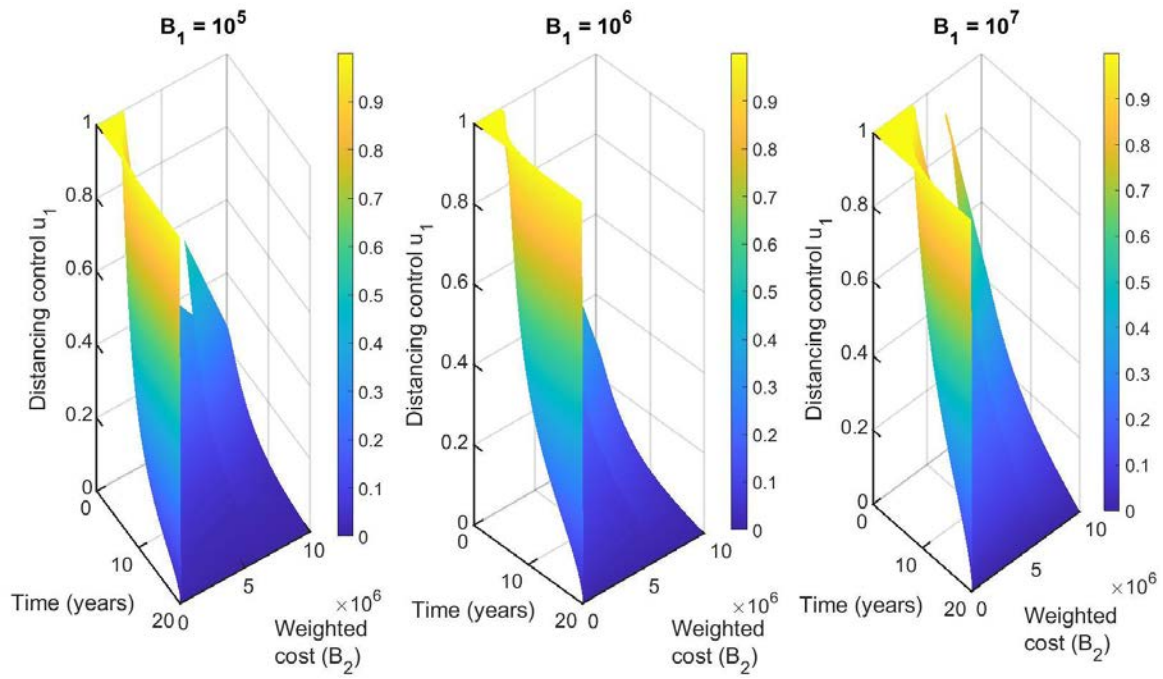


Figure 6. 17 Combination of distancing control ( $u_1$ ) and latent case finding ( $u_2$ ) control strategy, and considering distancing control ( $u_1$ ) strategy as a function of time and weighted cost ( $B_2$ ). The weighted cost ( $B_1$ ) determined by three threshold values  $B_1=10^5=10^6=10^7$ .

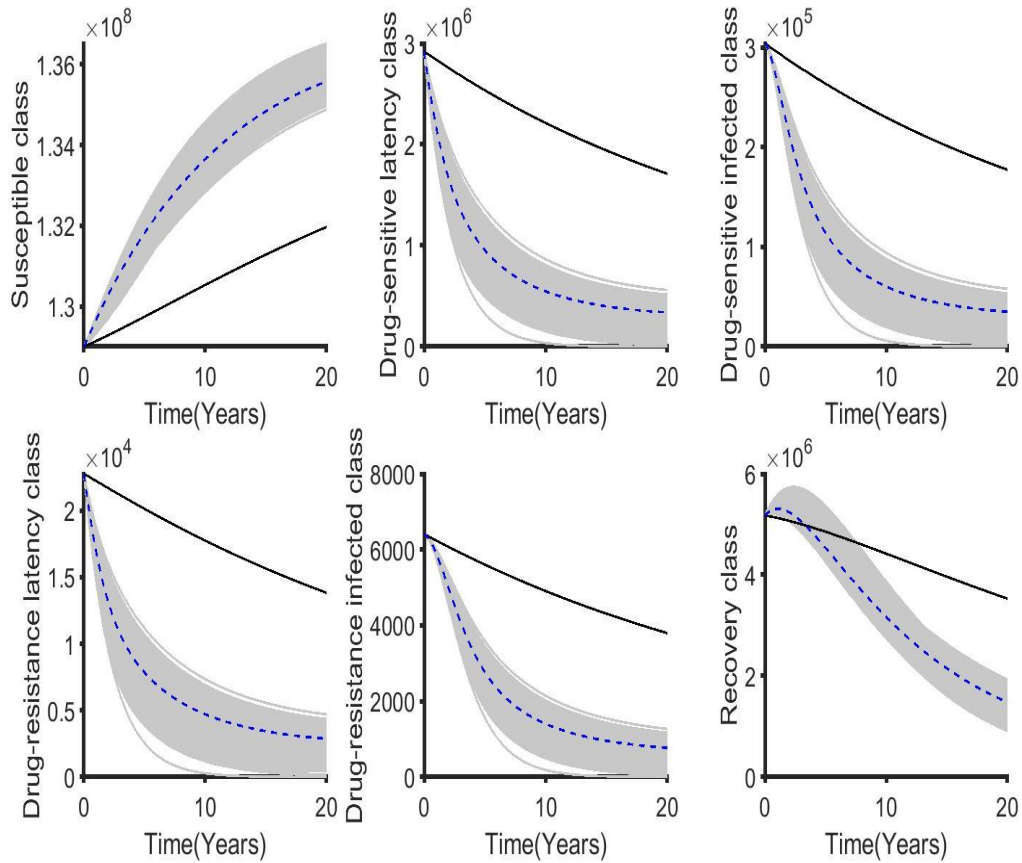


Figure 6. 18 The corresponding state variables of the combination of distancing control ( $u_1$ ) and latent case finding control ( $u_2$ ) strategy and considering the weighted cost  $B_2$  is varied and  $B_1=10^5=10^6=10^7$ . The state variables with and without controls are plotted by grays/blue dotted and black lines respectively.

We further performed similar sensitivity of the weighted costs on both triple and quadruple control strategies (see section S 6.3 of the supplementary materials).

## 6.4 Discussion and conclusion

TB (DS and MDR) is one of the most pressing public health problems in Bangladesh [1]. Overall, the transmission dynamics and epidemiology of TB (DS and MDR) in Bangladesh are poorly understood. Bangladesh's government initiated various intervention programs to eliminate DS and MDR-TB in the last decades. Although DS and MDR-TB control in Bangladesh has significantly progressed – improved case finding, availability of free diagnostic and treatment services, the involvement of multiple partners, newer diagnostic facilities, sufficient human resources, adequate capacity, and guidelines – more effort is required. To reduce DS and MDR-TB incidence, prevalence and prevent deaths from DS and MDR-TB in Bangladesh, we need to identify the critical factors for developing TB (DS and MDR) disease, improve treatment effectiveness, and reduce failure of treatment in infectious individuals.

In this paper, we presented a two-strain TB compartmental model with amplification to understand the transmission dynamics of DS and MDR-TB in Bangladesh. We derived the basic reproduction number of each TB strain, and evaluated the role of the strain-specific reproduction number on the dynamics of DS and MDR-TB. We proposed five different TB models and applied them to DS and MDR-TB incidence data in Bangladesh. The model with unequal transmission DS and MDR-TB transmission rates and same treatment rate captured the MDR-TB dynamics the best. With these parameters estimated, we calculated the basic reproduction number of TB in Bangladesh and found it to be greater than one. However, the uncertainty around the parameter estimates could bring the basic reproduction number to below one. This is reflective of the effective reproduction number indicating whether control measures are effective or not. Nonetheless, the estimate helps to identify interventions that may be effective via sensitivity analysis of the associate parameters and suggests further intervention that can be achieved via optimal control strategies. Both were carried out in the study with transmission rates influencing the TB dynamics more than any other variable.

We adopted optimal control analysis via Pontryagin's Maximal principle [45] and formulated the optimal strategies for controlling the DS and MDR-TB epidemic in Bangladesh. Four different control strategies were considered (single, dual, triple and quadruple) from combinations of distancing, latent case finding, case holding and active case finding controls and were examined to measure their cost-effectiveness.

Among the four single-controls, the distancing control strategy is the most cost-effective. Latent case finding control appears to be more effective than active case finding. The least effective is the case holding control. Therefore, when only one control strategy is used, our results suggest that the

Bangladesh government should improve distancing control interventions, reducing contact between infectious and susceptible people.

Within the six-dual-control strategies, combinations with distancing control performed best, and adding latent case finding control is the most cost-effective and more rapidly reduces DS and MDR-TB compared to other dual control strategies. The active case finding control is more feasible than the case holding control in light of not only reducing the number of DS and MDR-TB cases but also reducing control implementation duration. In view of the difficulty of implementing distancing measures which involves a high social cost, pharmaceutical control which includes latent case finding, active case finding and case holding should also be considered. We found that latent case finding and active case finding control as a dual control strategy is more cost-effective than the other dual pharmaceutical control strategies and rapidly reduces DS and MDR-TB. Therefore, if two control strategies are considered, we recommended that distancing control should be included. If distancing control is implemented successfully, the Bangladesh government can achieve the WHO TB elimination goal with fewer pharmaceutical control processes. However, if distancing is infeasible, combined latent and active therapy is also worthwhile.

Considering the triple control strategy structure, distancing with latent case finding and case holding control is the most cost-effective. If distancing control is difficult to implement, it is suggested that pharmaceutical controls including latent case finding, case holding and active case finding can be used. From the analysis of all the control strategies, we found that the most cost-effective control is the quadruple control strategy, followed by the double control strategy, triple control and single control.

Optimal control strategies has been applied in other endemic settings to minimize the number of TB cases and the intervention implementation costs. Previous studies show that for the single control strategy, distancing control is the best strategy and for the double control strategy, distancing and latent case finding control is the best strategy to decrease the number of TB cases and intervention costs [37, 46], which is similar to our results. However, our study shows that for the four triple-control strategies, distancing, latent case finding and case holding is the best option, which is similar to [46] but dissimilar to [37]. We can speculate as to why active case finding becomes less important in the triple control strategy compared with the double control strategy. It may be because case numbers decline, making the strategy more costly for every active case found.

Our principal finding in this study is that the quadruple control strategy, which includes distancing, latent case finding, case holding and active case finding control together is the most impactful and cost-effective approach for decreasing the spread of DS and MDR-TB in Bangladesh. Our findings also

suggests that to focus on a single control strategy will not dramatically affect the decline in DS and MDR-TB in Bangladesh, whereas to combine two or more control strategies simultaneously will decrease the burden of DS and MDR-TB in Bangladesh, which is found to be consistent with previous works [13, 37, 38, 47].

In Bangladesh, infectious disease surveillance does not detect all cases of tuberculosis, hence our estimates may be biased by underreporting. Therefore, more accurate data should be put in place to address concerns related to DS and MDR-TB. Accurate data leads to better estimation and conclusions based on these data become more robust. Hence, policy-makers need to consider the possibility of under-reporting bias when analyzing our findings.

### **Ethical Approval**

This study is based on aggregated TB surveillance data in Bangladesh provided by NTP and the World Health Organization (WHO). No confidential information was included because mathematical analyses were performed at the aggregate level. All of the methods were conducted under the approved research protocol. The research protocol was approved by the James Cook University human ethics approval board, H7300.

### **Acknowledgements**

This work was conducted as a part of a PhD programme of the first authors and funded by the College of Medicine and Dentistry at the James Cook University, Australia (JCU-QLD-835481). The authors would like to thank the National TB Control Program of Bangladesh for providing TB data.

### **Author Contributions**

M.A.K., A.I.A., E.S.M. and M.T.M conceived of the project concept; M.A.K. cleaned the data. M.A.K., A.I.A., E.S.M. and M.T.M. development model. M.A.K. performed the data analysis and interpretation. M.A.K. drafted the manuscript. All of the authors have read and approved the final manuscript.

## References

1. WHO, *Global tuberculosis report 2017*. WHO/HTM/TB/2017.23, Geneva, 2017.
2. Koch, R., I., *Die Aetiologie der Tuberculose: Nach einem in der physiologischen Gesellschaft zu Berlin am 24. März cr. gehaltenen Vortrage*. Zentralblatt für Bakteriologie, Mikrobiologie und Hygiene. 1. Abt. Originale. A, Medizinische Mikrobiologie, Infektionskrankheiten und Parasitologie, 1982. **251**(3): p. 287-296.
3. Golden, M. P., and Vikram, R. H., *Extrapulmonary tuberculosis: an overview*. American Family Physician, 2005. **72**(9).
4. Frieden, T. R., et al., *Tuberculosis*. Lancet, 2003. **362**(9387): p. 887-99.
5. Ahmed, N., and Hasnain, E. S., *Molecular epidemiology of tuberculosis in India: Moving forward with a systems biology approach*. Tuberculosis, 2011. **91**(5): p. 407-413.
6. Ai, J-W., et al., *Updates on the risk factors for latent tuberculosis reactivation and their managements*. Emerging Microbes & Infections, 2016. **5**(1): p. 1-8.
7. Zaman, K., et al., *Tuberculosis in Bangladesh: A 40-Year Review*. 11 ASCON. ICDDR,B. Scientific session, abstract book, 2007. **86**: p. 4-6.
8. Banu, S., et al., *Multidrug-resistant tuberculosis in Bangladesh: results from a sentinel surveillance system*. The International Journal of Tuberculosis and Lung Disease, 2017. **21**(1): p. 12-17.
9. NTP, *National Guidelines and Operational Manual for Programmatic Management of Drug Resistant Tuberculosis, 2nd edition*. 2016.
10. NTP, *Tuberculosis control in Bangladesh. Annual report, 2017*.
11. WHO, *The End TB Strategy*. 2015.
12. Maude, R. J., et al., *The role of mathematical modelling in guiding the science and economics of malaria elimination*. International Health, 2010. **2**(4-6): p. 239-246.
13. Kim, S., et al., *What Does a Mathematical Model Tell About the Impact of Reinfection in Korean Tuberculosis Infection?* Osong Public Health and Research Perspectives, 2014. **5**(1): p. 40-45.
14. Yang, Y., et al., *Seasonality impact on the transmission dynamics of tuberculosis*. Computational and Mathematical Methods in Medicine, 2016. **2016**.
15. Brooks-Pollock, E., Cohen, T., and Murray, M., *The impact of realistic age structure in simple models of tuberculosis transmission*. PLoS One, 2010. **5**(1): p. e8479.
16. Mishra, B. K., and Srivastava, J., *Mathematical model on pulmonary and multidrug-resistant tuberculosis patients with vaccination*. Journal of the Egyptian Mathematical Society, 2014. **22**(2): p. 311-316.
17. Trauer, J. M., Denholm, T. J., and McBryde, E. S., *Construction of a mathematical model for tuberculosis transmission in highly endemic regions of the Asia-Pacific*. Journal of Theoretical Biology, 2014. **358**: p. 74-84.
18. Agosto, F. B., and Adekunle, I. A., *Optimal control of a two-strain tuberculosis-HIV/AIDS co-infection model*. Biosystems, 2014. **119**: p. 20-44.
19. WHO, *Global tuberculosis report 2013*. . WHO/HTM/TB/2013.11, Switzerland, 2013.
20. WHO, *Global tuberculosis report*. WHO/HTM/TB/2010.7, Switzerland, 2010.
21. WHO, *Global tuberculosis report 2011*. WHO/HTM/TB/2011.16, Switzerland, 2011.
22. Prism, G., *Graphpad software*. San Diego, CA, USA, 1994.
23. MATLAB, V., *9.2. 0 (R2017a)*. The MathWorks Inc.: Natick, MA, USA, 2017.
24. Banks, H.T., and Joyner, L. M., *AIC under the framework of least squares estimation*. Applied Mathematics Letters, 2017. **74**: p. 33-45.
25. Lenhart, S., and Workman, T. J., *Optimal control applied to biological models*. 2007: Chapman and Hall/CRC.
26. NTP, *Tuberculosis control in Bangladesh. Annual report, 2002*.
27. Yang, Y., et al., *Global stability of two models with incomplete treatment for tuberculosis*. Chaos, Solitons & Fractals, 2010. **43**(1-12): p. 79-85.

28. Diel, R., et al., *Negative and positive predictive value of a whole-blood interferon- $\gamma$  release assay for developing active tuberculosis: an update*. American Journal of Respiratory and Critical Care Medicine, 2011. **183**(1): p. 88-95.
29. Ullah, S., et al., *Modeling and analysis of Tuberculosis (TB) in Khyber Pakhtunkhwa, Pakistan*. Mathematics and Computers in Simulation, 2019.
30. Bhunu, C., et al., *Modelling the effects of pre-exposure and post-exposure vaccines in tuberculosis control*. Journal of Theoretical Biology, 2008. **254**(3): p. 633-649.
31. Lobato, M. N., Leary, S. L., and Simone, M. P., *Treatment for latent TB in correctional facilities: a challenge for TB elimination*. American Journal of Preventive Medicine, 2003. **24**(3): p. 249-253.
32. Onozaki, I., et al., *National tuberculosis prevalence surveys in Asia, 1990-2012: an overview of results and lessons learned*. Tropical Medicine & International Health, 2015. **20**(9): p. 1128-1145.
33. Grandjean, L., et al., *Transmission of multidrug-resistant and drug-susceptible tuberculosis within households: a prospective cohort study*. PLoS Medicine, 2015. **12**(6): p. e1001843.
34. Billington, O., McHugh, D. T., and Gillespie, H. S., *Physiological cost of rifampin resistance induced in vitro in Mycobacterium tuberculosis*. Antimicrobial Agents and Chemotherapy, 1999. **43**(8): p. 1866-1869.
35. Borrell, S., and Gagneux, S., *Infectiousness, reproductive fitness and evolution of drug-resistant Mycobacterium tuberculosis [State of the art]*. The International Journal of Tuberculosis and Lung Disease, 2009. **13**(12): p. 1456-1466.
36. Chitnis, N., Cushing, M. J., and Hyman, J., *Bifurcation analysis of a mathematical model for malaria transmission*. SIAM Journal on Applied Mathematics, 2006. **67**(1): p. 24-45.
37. Kim, S., Aurelio, A., and Jung, E., *Mathematical model and intervention strategies for mitigating tuberculosis in the Philippines*. Journal of Theoretical Biology, 2018. **443**: p. 100-112.
38. Gao, D-P., and Huang, N-J., *Optimal control analysis of a tuberculosis model*. Applied Mathematical Modelling, 2018. **58**: p. 47-64.
39. Shayla, I., and Anna, V., *Post-2015 development agenda, Bangladesh perspectives tuberculosis*. 2015.
40. Islam, M., et al., *Cost-effectiveness of community health workers in tuberculosis control in Bangladesh*. Bulletin of the World Health Organization, 2002. **80**: p. 445-450.
41. ATN Bangla, *Telecast Fee for Package Program/ Tele Film & Short Films with Sponsorship*. 2018.
42. WHO, *Estimates of Unit Costs for Patient Services for Bangladesh*. 2005.
43. The World Bank, *Bangladesh Hospital Beds Per 1 000 People*. 2011.
44. Ministry of health and family welfare, *Human resources development, Bangladesh*. 2011.
45. Pontryagin, L. S., *Mathematical theory of optimal processes*. 2018: Routledge.
46. Whang, S., Choi, S., and Jung, E., *A dynamic model for tuberculosis transmission and optimal treatment strategies in South Korea*. Journal of Theoretical Biology, 2011. **279**(1): p. 120-131.
47. Okuonghae, D., and Ikhimwin, O. B., *Dynamics of a mathematical model for tuberculosis with variability in susceptibility and disease progressions due to difference in awareness level*. Frontiers in Microbiology, 2016. **6**: p. 1530.

## Supplementary materials

### Section S6.1: Model Fit

The fitting results of other parameter variation are shown in the table and Figures below.

**Table S6.1** Model 1 (drug-failure only):  $\beta_s, \beta_m = 0, \tau_s, \tau_m = 0$  and  $\rho$  (3 parameter model).

Parameter	Est.	CI
$\beta_s$	$1.545 \times 10^{-8}$	$(1.481 \times 10^{-8}, 2.431 \times 10^{-8})$
$\tau_s$	0.520	(0.272, 0.400)
$\rho$	0.28	(0.239, 0.4)
$\rho\tau_s$	0.146	(0.079, 1.46)
	<b>DS</b>	<b>MDR</b>
AIC	382.54	439.61

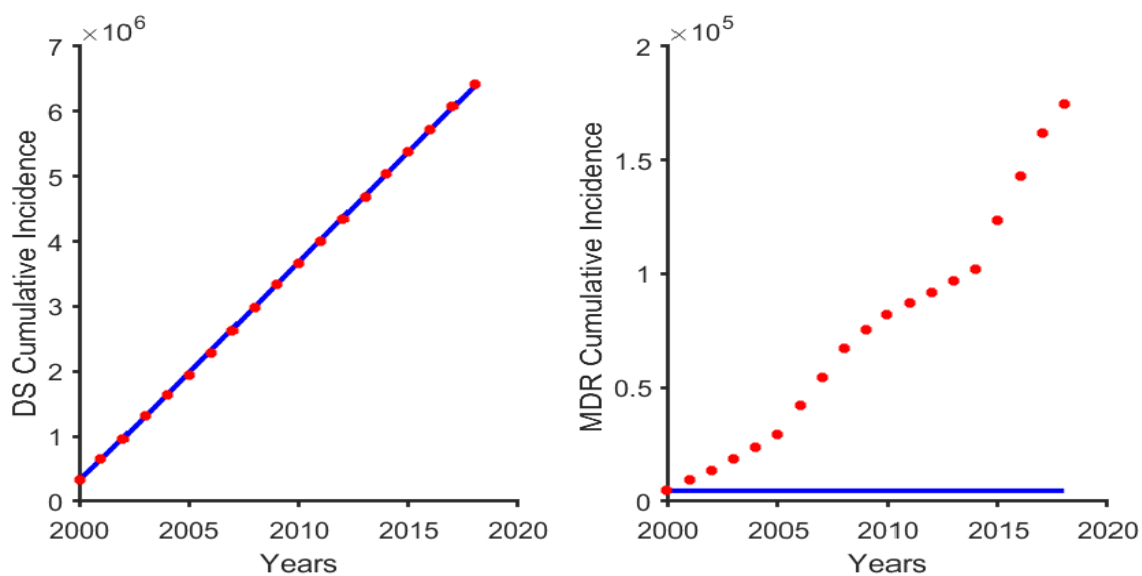


Figure S6.1. A fit of model 1 to the Bangladesh TB cumulative incidence: (A) drug- susceptible (DS) TB and (B) multidrug-resistant (MDR) TB.

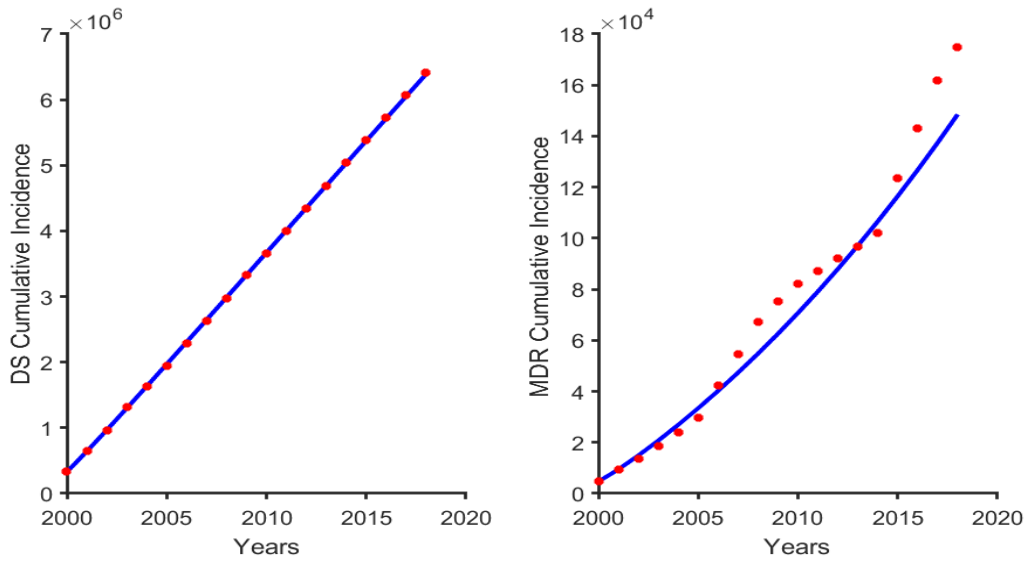


Figure S6.2. A fit of model 2 to the Bangladesh TB cumulative incidence: (A) drug- susceptible (DS) TB and (B) multidrug-resistant (MDR) TB.

**Table S6.2.** Model 4 (drug failure and different treatment outcome between DS and MDR):  $\beta_s = \beta_m$ ,  $\tau_s \neq \tau_m$  and  $\rho$  (4 parameter model).

Parameter	Est.	CI
$\beta_s = \beta_m$	$1.55 \times 10^{-8}$	$(1.50 \times 10^{-8}, 1.60 \times 10^{-8})$
$\tau_s$	0.494	(0.266, 0.724)
$\tau_m$	0.025	(0, 0.301)
$\rho$	0.075	(0.067, 0.082)
$\rho\tau_s$	0.0019	(0, 0.0013)
	<b>DS</b>	<b>MDR</b>
AIC	378.79	425.66

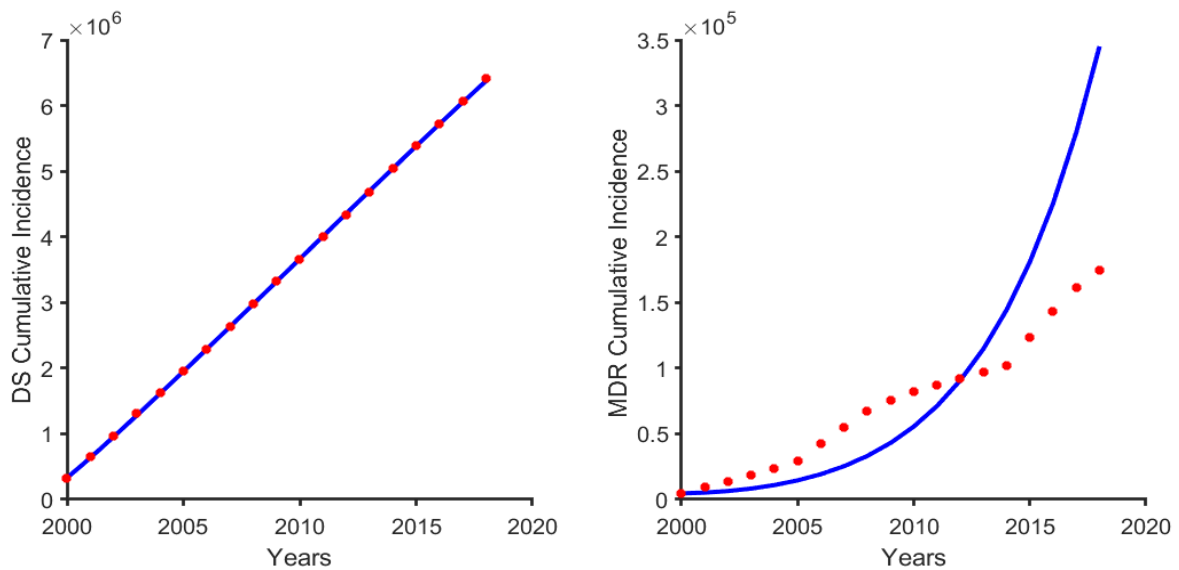


Figure S6.3. A fit of model 4 to the Bangladesh TB cumulative incidence: (A) drug- susceptible (DS) TB and (B) multidrug-resistant (MDR) TB.

## Section S 6.2: Optimal control analysis

We use Pontryagin's Maximum Principle on our model (6.5). The aim is to reduce the number of DS and MDR-TB cases and corresponding costs. Pontryagin's Maximum Principle changes into problem that minimize pointwise a Hamiltonian  $H$ , with respect to the control. The Hamiltonian is given as

$$\begin{aligned}
 H = & L_s + I_s + L_m + I_m + \frac{B_1}{2} u_1^2(t) + \frac{B_2}{2} u_2^2(t) + \frac{B_3}{2} u_3^2(t) + \frac{B_4}{2} u_4^2(t) \\
 & + \lambda_1(\mu N - (1 - u_1(t))\beta_s I_s S - (1 - u_1(t))\beta_m I_m S - \mu S + \gamma R + \varphi_s I_s + \varphi_m I_m) \\
 & + \lambda_2((1 - u_1(t))\beta_s I_s S - (\alpha_s + (\delta_s + u_2(t)\tau_1) + \mu)L_s) \\
 & + \lambda_3(\alpha_s L_s - (\omega_s + (1 + u_4(t))\tau_s + \phi_s + \mu)I_s) \\
 & + \lambda_4((1 - u_1(t))\beta_m I_m S - (\alpha_m + (\delta_m + u_2(t)\tau_2) + \mu)L_m) \\
 & + \lambda_5(\alpha_m L_m + (\rho(1 - u_3(t)))(1 + u_4(t))\tau_s I_s - (\omega_m + \tau_m(1 + u_4(t)) + \phi_m + \mu)I_m) \\
 & + \lambda_6\left(\left(1 - \rho(1 - u_3(t))\right)(1 + u_4(t))\tau_s I_s + \tau_m(1 + u_4(t))I_m + \omega_s I_s + \omega_m I_m + (\delta_s + \right. \\
 & \left. u_2(t)\tau_1)L_s + (\delta_m + u_2(t)\tau_2)L_m - \gamma R - \mu R\right).
 \end{aligned}$$

Now using Pontryagin's maximum principle, we obtain the following theorem.

Theorem: There exist optimal controls  $u_1^*(t)$ ,  $u_2^*(t)$ ,  $u_3^*(t)$ , and  $u_4^*(t)$  minimizing the objective function  $\Omega = \{(u_1, u_2, u_3, u_4) \mid a \leq u_i(t) \leq b, u_i \in \mathcal{L}^2(0, 20), i = 1, 2, 3, 4\}$ .

Given these optimal solutions, there exist adjoint variables,  $\lambda_1, \lambda_2, \lambda_3, \lambda_4, \lambda_5$ , and  $\lambda_6$  which satisfy,

$$\begin{aligned}
 \frac{d\lambda_1}{dt} &= \lambda_1((1 - u_1)\beta_s I_s + (1 - u_1)\beta_m I_m + \mu) - \lambda_2(1 - u_1)\beta_s I_s - \lambda_4(1 - u_1)\beta_m I_m, \\
 \frac{d\lambda_2}{dt} &= -1 + \lambda_2\{\alpha_s + (\delta_s + u_2\tau_1) + \mu\} - \lambda_3\alpha_s - \lambda_6(\delta_s + u_2\tau_1), \\
 \frac{d\lambda_3}{dt} &= -1 + \lambda_1((1 - u_1)\beta_s S - \phi_s) - \lambda_2(1 - u_1)\beta_s S + \lambda_3(\omega_s + \phi_s + \tau_s(1 + u_4) + \mu) \\
 &\quad - \lambda_5\rho(1 - u_3)(1 + u_4)\tau_s - \lambda_6\left(\left(1 - \rho(1 - u_3)\right)(1 + u_4)\tau_s + \omega_s\right), \\
 \frac{d\lambda_4}{dt} &= -1 + \lambda_4\{\alpha_m + (\delta_m + u_2\tau_2) + \mu\} - \lambda_5\alpha_m - \lambda_6(\delta_m + u_2\tau_2), \\
 \frac{d\lambda_5}{dt} &= -1 + \lambda_1\{(1 - u_1)\beta_m S - \phi_m\} - \lambda_4(1 - u_1)\beta_m S + \lambda_5(\omega_m + \phi_m + \tau_m(1 + u_4) + \mu) \\
 &\quad - \lambda_6(\omega_m + \tau_m(1 + u_4)), \\
 \frac{d\lambda_6}{dt} &= \lambda_6(\gamma + \mu) - \lambda_1\gamma.
 \end{aligned}$$

with transversality conditions  $\lambda_i = 0$ , for  $i = 1, 2, 3, 4, 5, 6$ .

Furthermore,

$$u_1^*(t) = \min \left( b, \max \left( a, \frac{1}{B_1} ((\lambda_2 - \lambda_1)\beta_s I_s S + (\lambda_4 - \lambda_1)\beta_m I_m S) \right) \right),$$

$$u_2^*(t) = \min \left( b, \max \left( a, \frac{1}{B_2} ((\lambda_2 - \lambda_6)\tau_1 L_s + (\lambda_4 - \lambda_6)\tau_2 L_m) \right) \right),$$

$$u_3^*(t) = \min \left( b, \max \left( a, m_1 + \frac{m_1}{m_2} (m_3 + (\lambda_5 - \lambda_6)\tau_m I_m + (\lambda_5 - \lambda_6)m_1 \rho \tau_s I_s) \right) \right),$$

$$u_4^*(t) = \min \left( b, \max \left( a, \frac{1}{m_2} (m_3 + (\lambda_5 - \lambda_6)\tau_m I_m + (\lambda_5 - \lambda_6)m_1 \rho \tau_s I_s) \right) \right),$$

Where,

$$m_1 = \frac{(\lambda_5 - \lambda_6)\rho \tau_s I_s}{B_3}, m_2 = B_4 - (\lambda_5 - \lambda_6)\rho \tau_s I_s m_1, \text{ and } m_3 = (\lambda_3 - \rho \lambda_5 - \lambda_6 + \rho \lambda_6)\tau_s I_s.$$

Proof: The existence of optimal controls  $u_1^*(t)$ ,  $u_2^*(t)$ ,  $u_3^*(t)$  and  $u_4^*(t)$  such that

$J(u_1^*(t), u_2^*(t), u_3^*(t), u_4^*(t)) = \min_{\Omega} J(u_1, u_2, u_3, u_4)$  with state system (4) is given by the convexity of the objective functional integrand. By Pontryagin's Maximum Principle, the adjoint equations and transversality conditions are obtained. Differentiation of Hamiltonian H with respect to the state variables gives the following system,

$$\frac{d\lambda_1}{dt} = -\frac{\partial H}{\partial S},$$

$$\frac{d\lambda_2}{dt} = -\frac{\partial H}{\partial L_s},$$

$$\frac{d\lambda_3}{dt} = -\frac{\partial H}{\partial I_s},$$

$$\frac{d\lambda_4}{dt} = -\frac{\partial H}{\partial L_m},$$

$$\frac{d\lambda_5}{dt} = -\frac{\partial H}{\partial I_m},$$

$$\frac{d\lambda_6}{dt} = -\frac{\partial H}{\partial R},$$

with  $\lambda_i = 0$ , for  $i = 1, 2, 3, 4, 5, 6$ .

Optimal controls  $u_1^*(t)$ ,  $u_2^*(t)$ ,  $u_3^*(t)$  and  $u_4^*(t)$  are derived by the following optimality conditions

$$\frac{\partial H}{\partial u_1} = B_1 u_1 + \lambda_1 \beta_s I_s S + \lambda_1 \beta_m I_m S - \lambda_2 \beta_s I_s S - \lambda_4 \beta_m I_m S = 0,$$

$$\frac{\partial H}{\partial u_2} = B_2 u_2 - \lambda_2 \tau_1 L_s - \lambda_4 \tau_2 L_m + \lambda_6 \tau_1 L_s + \lambda_6 \tau_2 L_m = 0,$$

$$\frac{\partial H}{\partial u_3} = B_3 u_3 - \lambda_5 \rho (1 + u_4) \tau_s I_s + \lambda_6 \rho (1 + u_4) \tau_s I_s = 0,$$

$$\frac{\partial H}{\partial u_4} = B_4 u_4 - \lambda_3 \tau_s I_s + \lambda_5 \rho (1 - u_3) \tau_s I_s - \lambda_5 \tau_m I_m + \lambda_6 (1 - \rho(1 - u_3))(1 + u_4) \tau_s I_s + \lambda_6 \tau_m I_m =$$

0,

at  $u_1^*(t)$ ,  $u_2^*(t)$ ,  $u_3^*(t)$  and  $u_4^*(t)$  on the set  $\Omega$ . On this set

$$u_1^*(t) = \frac{(\lambda_2 - \lambda_1)\beta_S I_S S + (\lambda_4 - \lambda_1)\beta_M I_M S}{B_1},$$

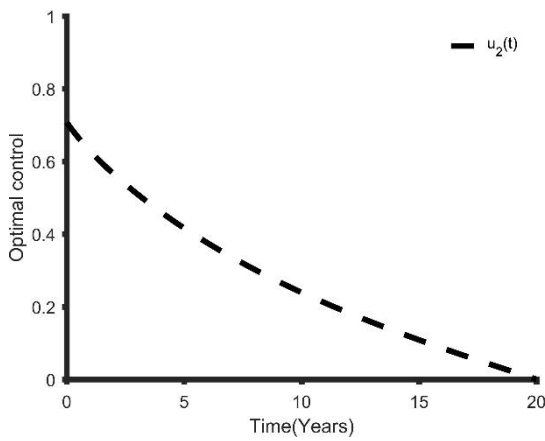
$$u_2^*(t) = \frac{(\lambda_2 - \lambda_6)\tau_1 L_S + (\lambda_4 - \lambda_6)\tau_2 L_M}{B_2},$$

$$u_3^*(t) = \frac{(\lambda_5 - \lambda_6)\rho(1 + u_4)\tau_S I_S}{B_3},$$

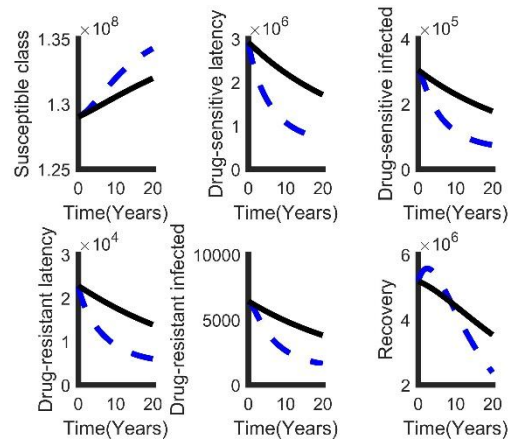
$$u_4^*(t) = \frac{(\lambda_3 - \rho(1 - u_3)\lambda_5 - (1 - \rho(1 - u_3))\lambda_6)\tau_S I_S + (\lambda_5 - \lambda_6)\tau_M I_M}{B_4}.$$

The Figures below shows the optimal solutions of our control strategies.

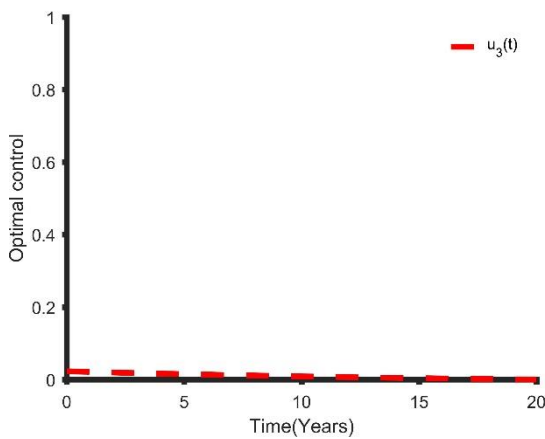
(A)



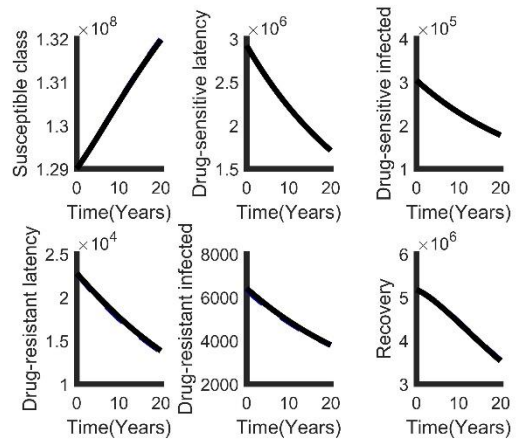
(B)



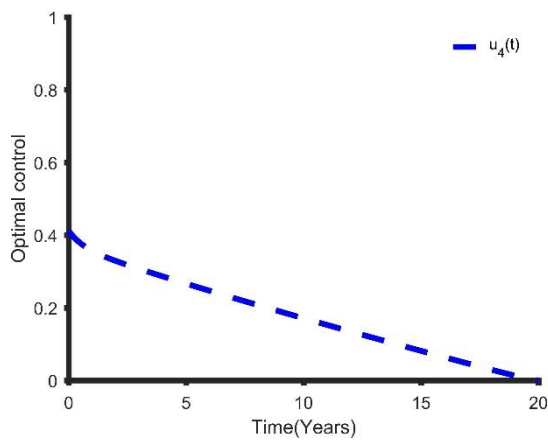
(C)



(D)



(E)



(F)

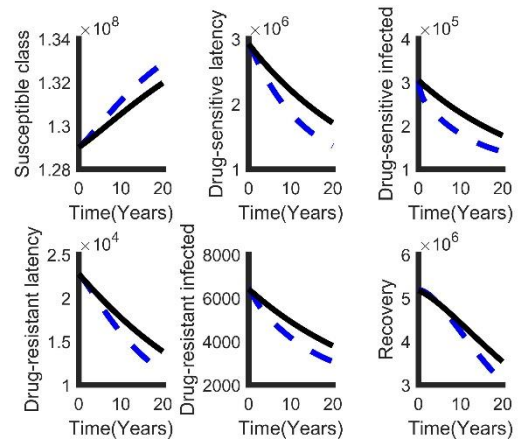
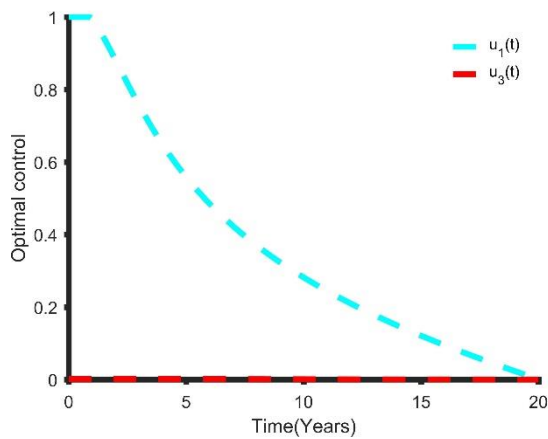
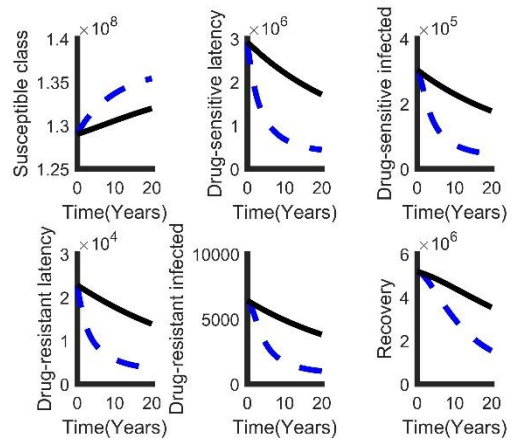


Figure S6.4. The single optimal control strategy: (A) The optimal latent case finding control. (B) The corresponding benefits of the latent case finding. (C) The optimal case holding strategy. (D) The corresponding effects of using the case holding strategy. (E) The optimal active case finding strategy. (F) The benefits of optimal active case finding.

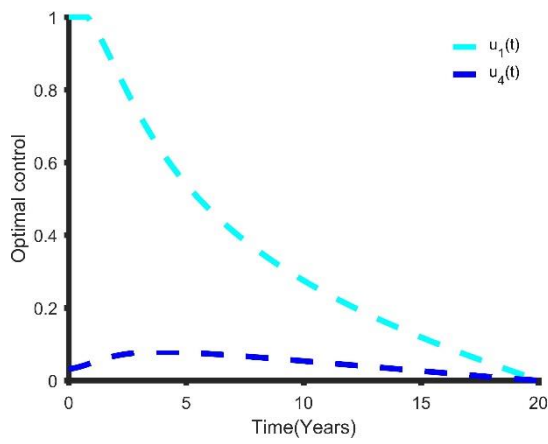
(A)



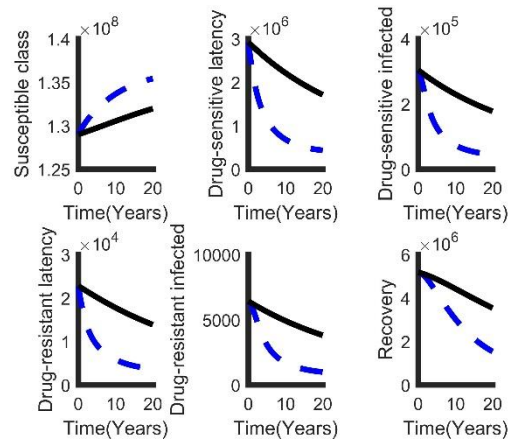
(B)



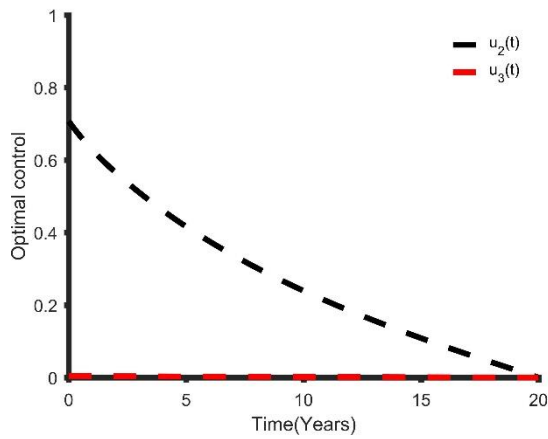
(C)



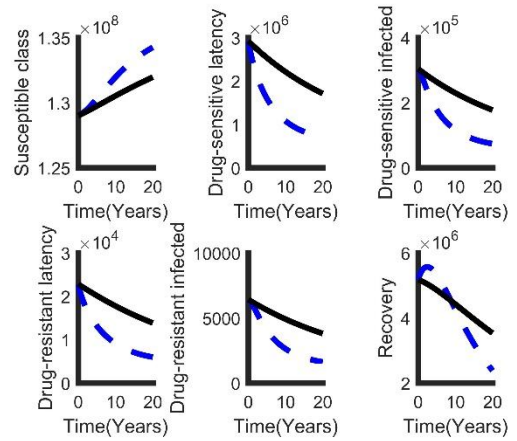
(D)



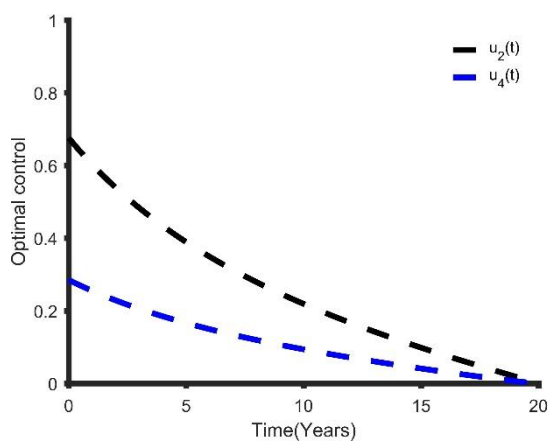
(E)



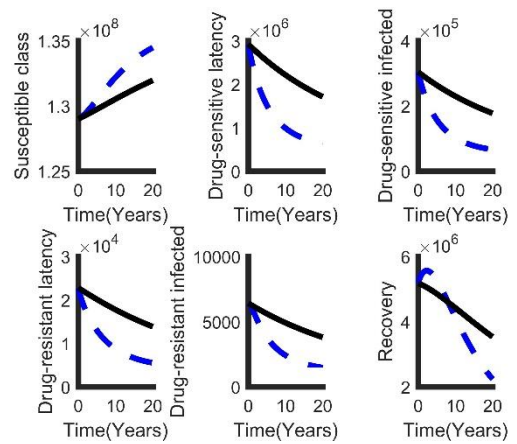
(F)



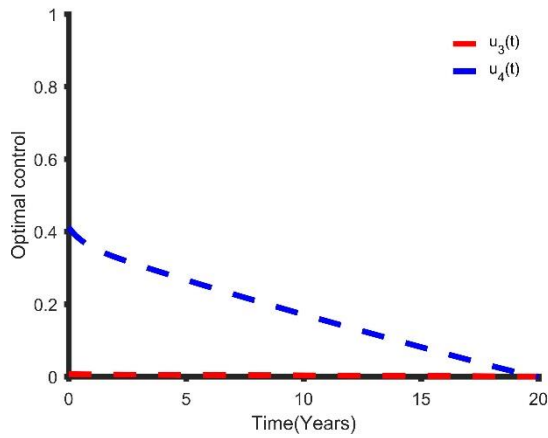
(G)



(H)



(I)



(J)

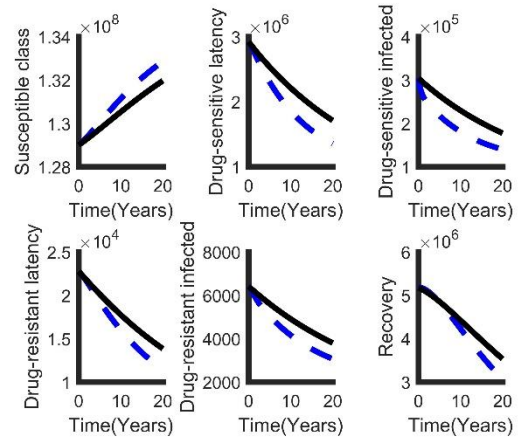


Figure S6.5. The double optimal control strategy: (A) The optimal distancing and case holding strategies. (B) The corresponding benefits of the distancing and case holding. (C) The optimal distancing and active case finding strategies. (D) The corresponding effects of using the distancing and active case finding. (E) The optimal latent case finding and case holding strategies. (F) The benefits of optimal latent case finding and case holding. (G) The optimal latent and active case finding strategies. (H) The benefits of optimal latent and active case finding. (I) The optimal case holding and active case finding strategies. (J) The benefits of optimal case holding and active case finding.

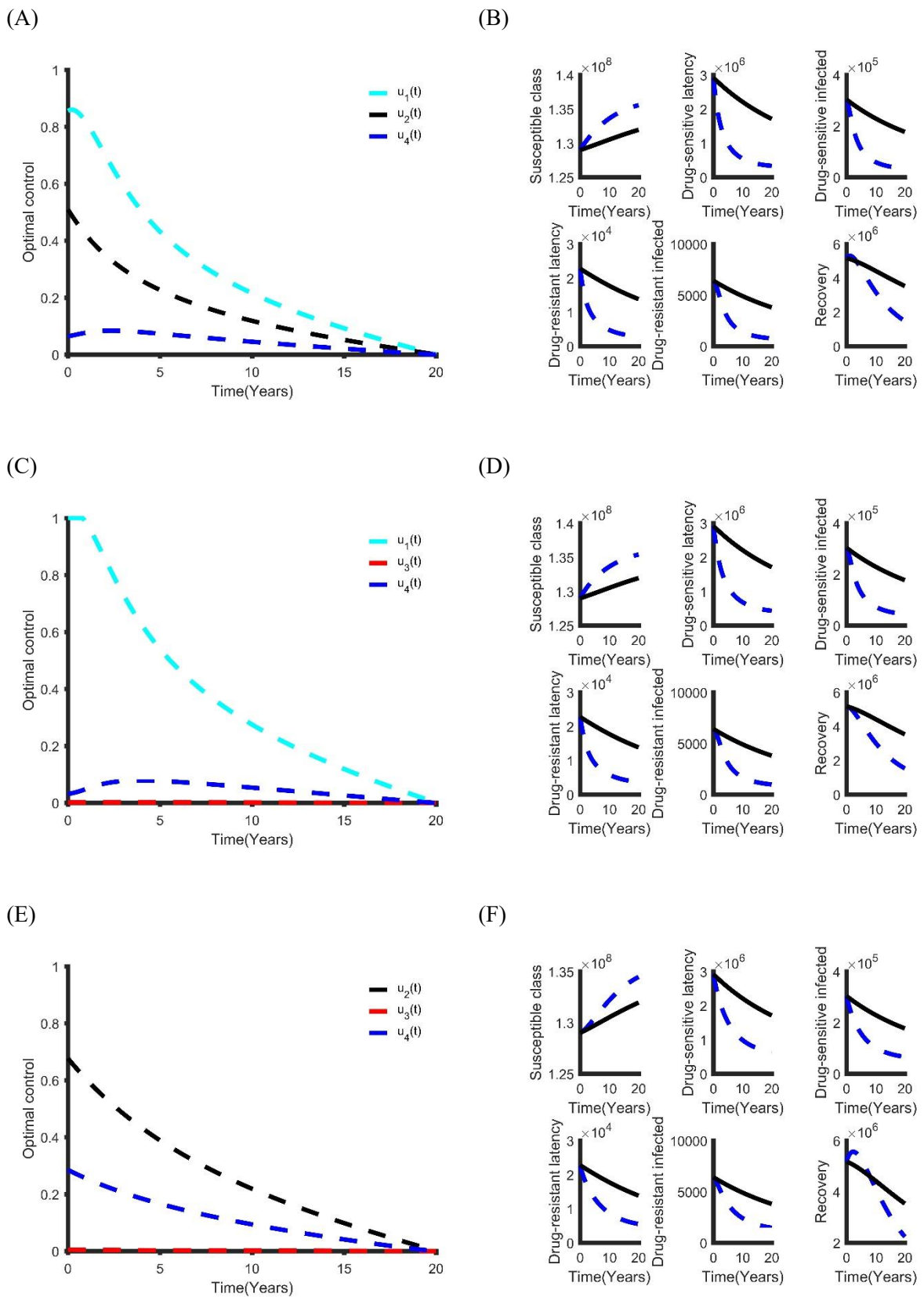


Figure S6.6. The tripled optimal control strategy: (A) The optimal distancing, latent and active case finding control strategy. (B) The corresponding benefits of the distancing, latent case finding and case

holding. (C) The optimal distancing, case holding and active case finding strategy. (D) The corresponding effects of using the distancing, case holding and active case finding. (E) The optimal latent case finding, case holding and active case finding strategy. (F) The benefits of optimal latent case finding, case holding and active case finding.

### Section S6.3

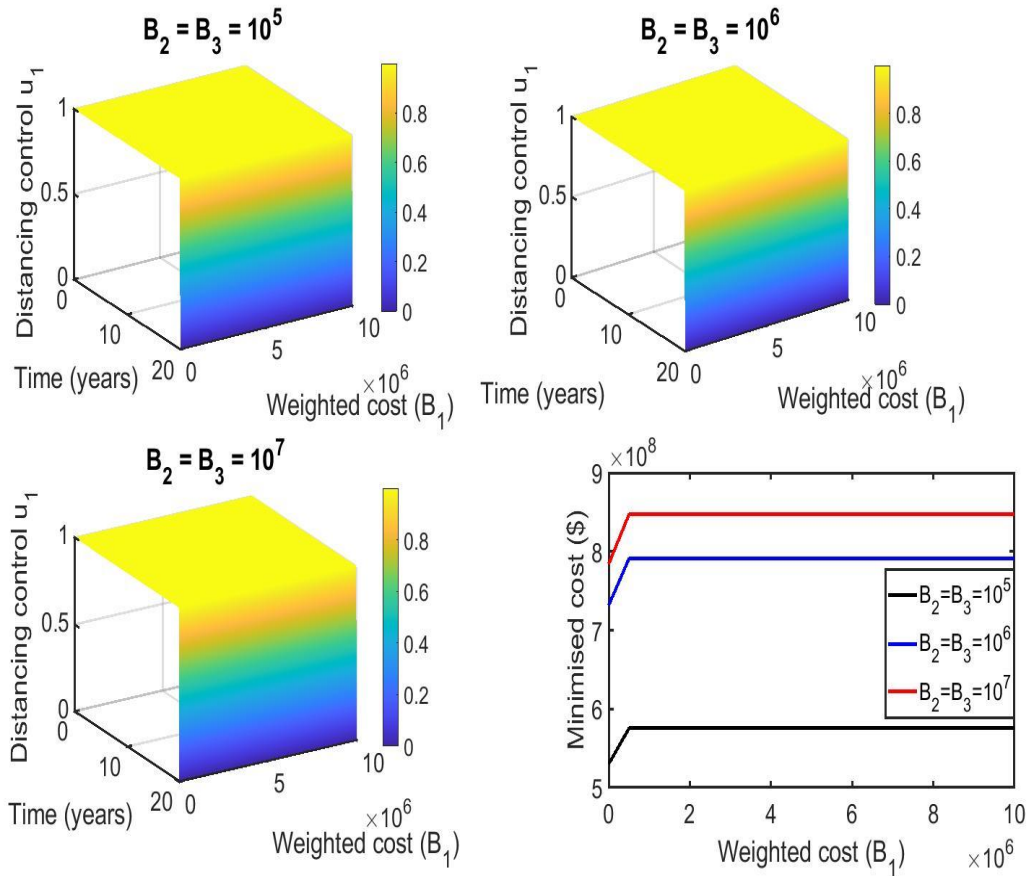


Figure S6.7 (A). Combination of distancing ( $u_1$ ), latent case finding ( $u_2$ ) and case holding ( $u_3$ ) strategy, and considering distancing control ( $u_1$ ) strategy as a function of time and weighted cost ( $B_1$ ). The weighted cost ( $B_2$  and  $B_3$ ) determined by three threshold values  $B_2 = B_3 = 10^5 = 10^6 = 10^7$ .

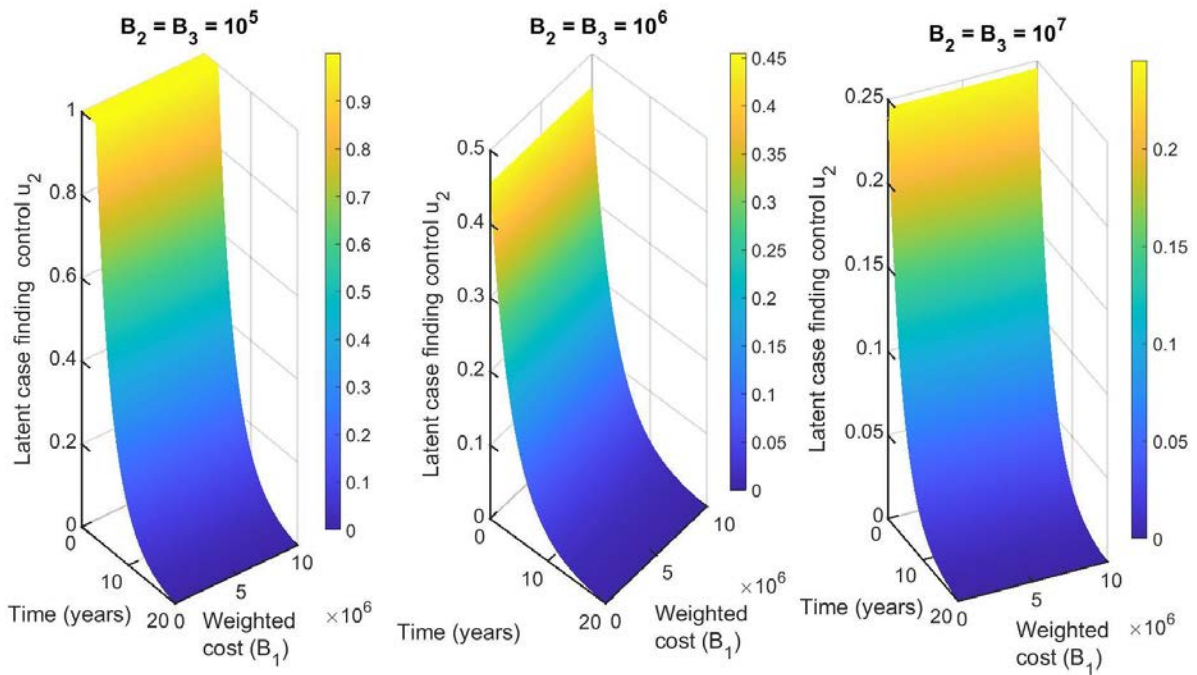


Figure S6.7 (B). Combination of distancing ( $u_1$ ), latent case finding ( $u_2$ ) and case holding ( $u_3$ ) strategy, and considering latent case finding control ( $u_2$ ) strategy as a function of time and weighted cost ( $B_1$ ). The weighted cost ( $B_2$  and  $B_3$ ) determined by three threshold values  $B_2 = B_3 = 10^5 = 10^6 = 10^7$ .

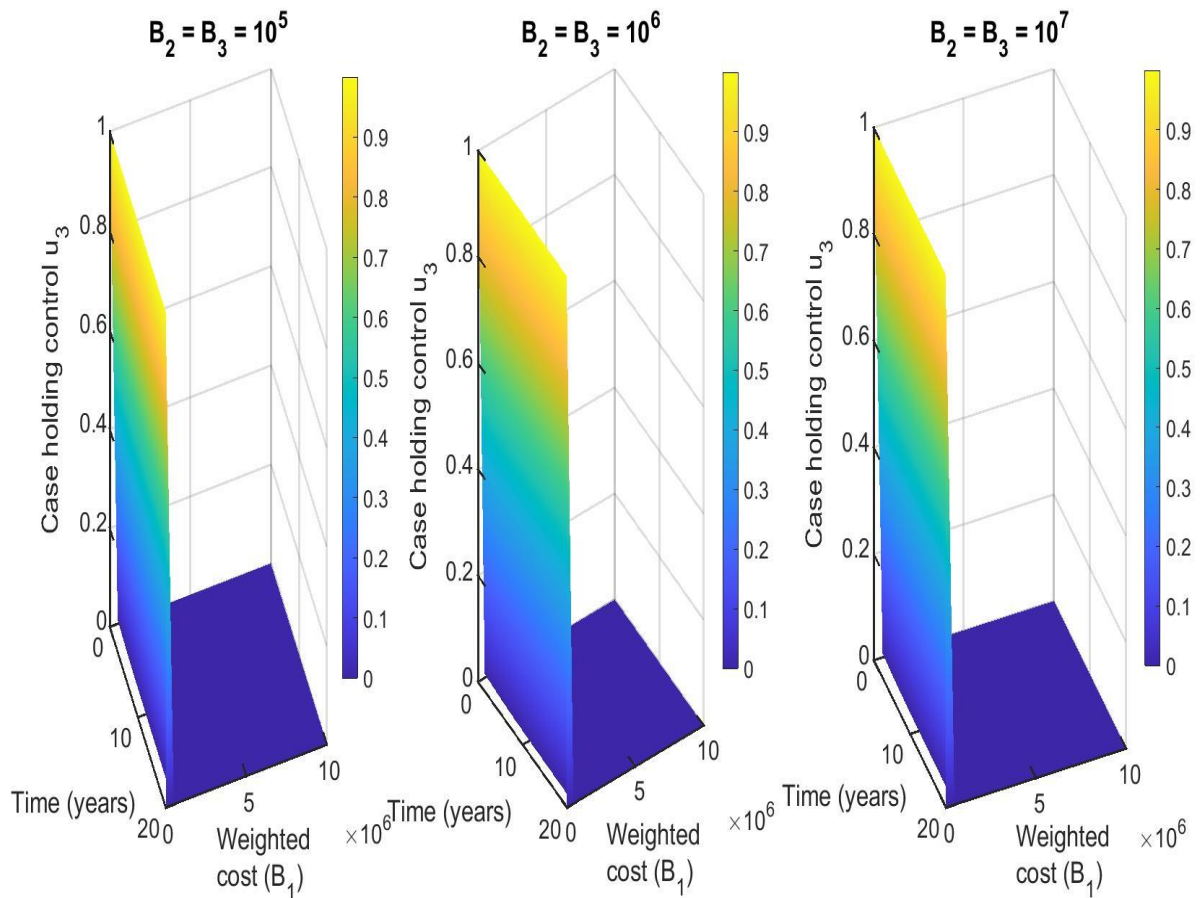


Figure S6.7 (C). Combination of distancing ( $u_1$ ), latent case finding ( $u_2$ ) and case holding ( $u_3$ ) strategy, and considering case holding control ( $u_2$ ) strategy as a function of time and weighted cost ( $B_1$ ). The weighted cost ( $B_2$  and  $B_3$ ) determined by three threshold values  $B_2 = B_3 = 10^5 = 10^6 = 10^7$ .

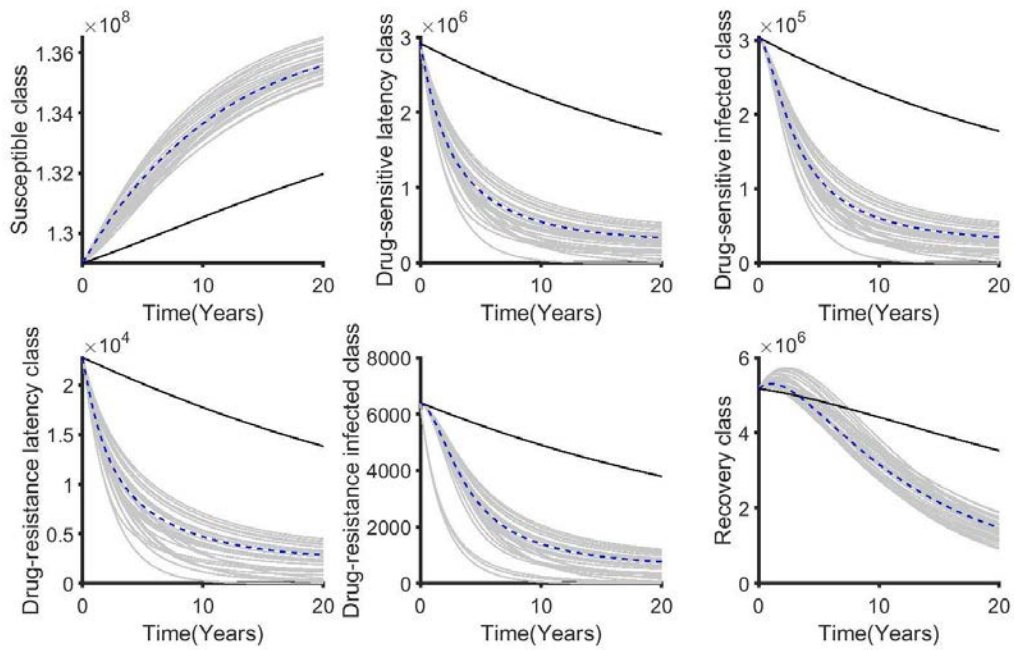


Figure S6.7 (D). The corresponding state variables of the combination of distancing control ( $u_1$ ), latent case finding ( $u_2$ ) and case holding ( $u_3$ ) control strategy and considering the weighted cost  $B_1$  is varied and  $B_2 = B_3 = 10^5 = 10^6 = 10^7$ . The state variables with and without controls are plotted by grays and black lines respectively.

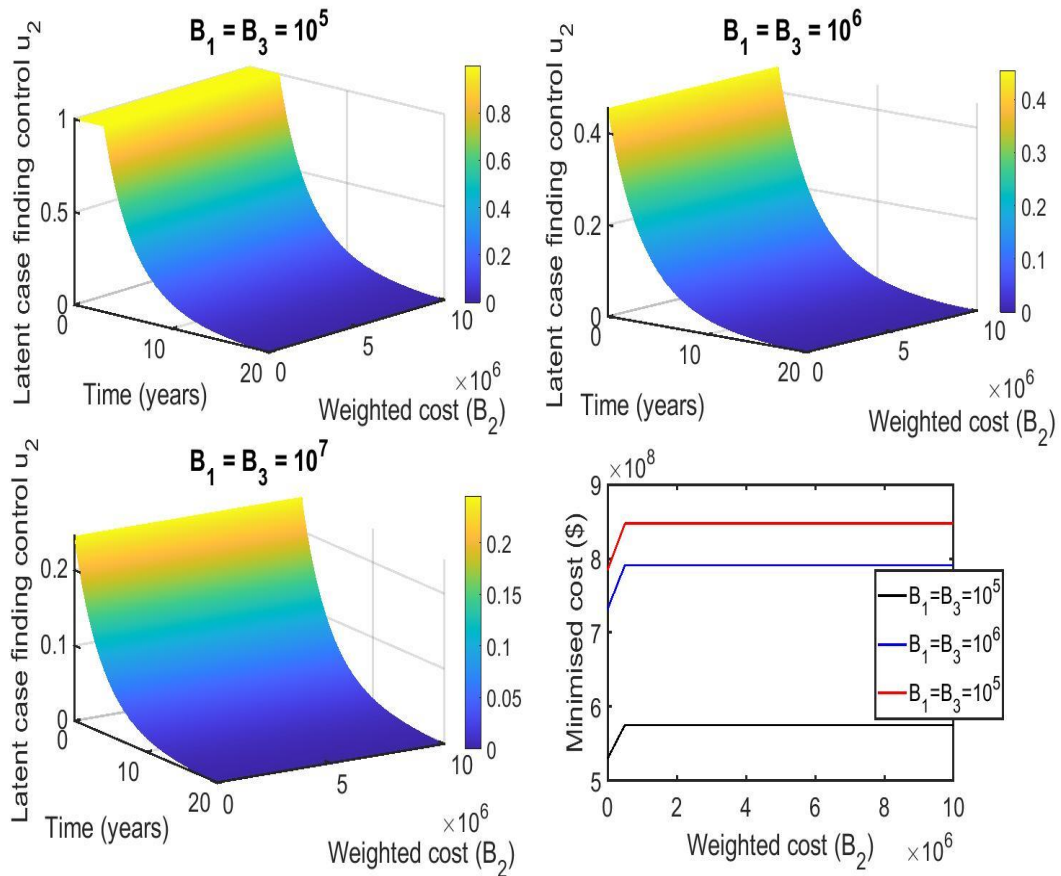


Figure S6.8 (A). Combination of distancing ( $u_1$ ), latent case finding ( $u_2$ ) and case holding ( $u_3$ ) strategy, and considering latent case finding control ( $u_2$ ) strategy as a function of time and weighted cost ( $B_2$ ). The weighted cost ( $B_1$  and  $B_3$ ) determined by three threshold values  $B_1 = B_3 = 10^5 = 10^6 = 10^7$ .

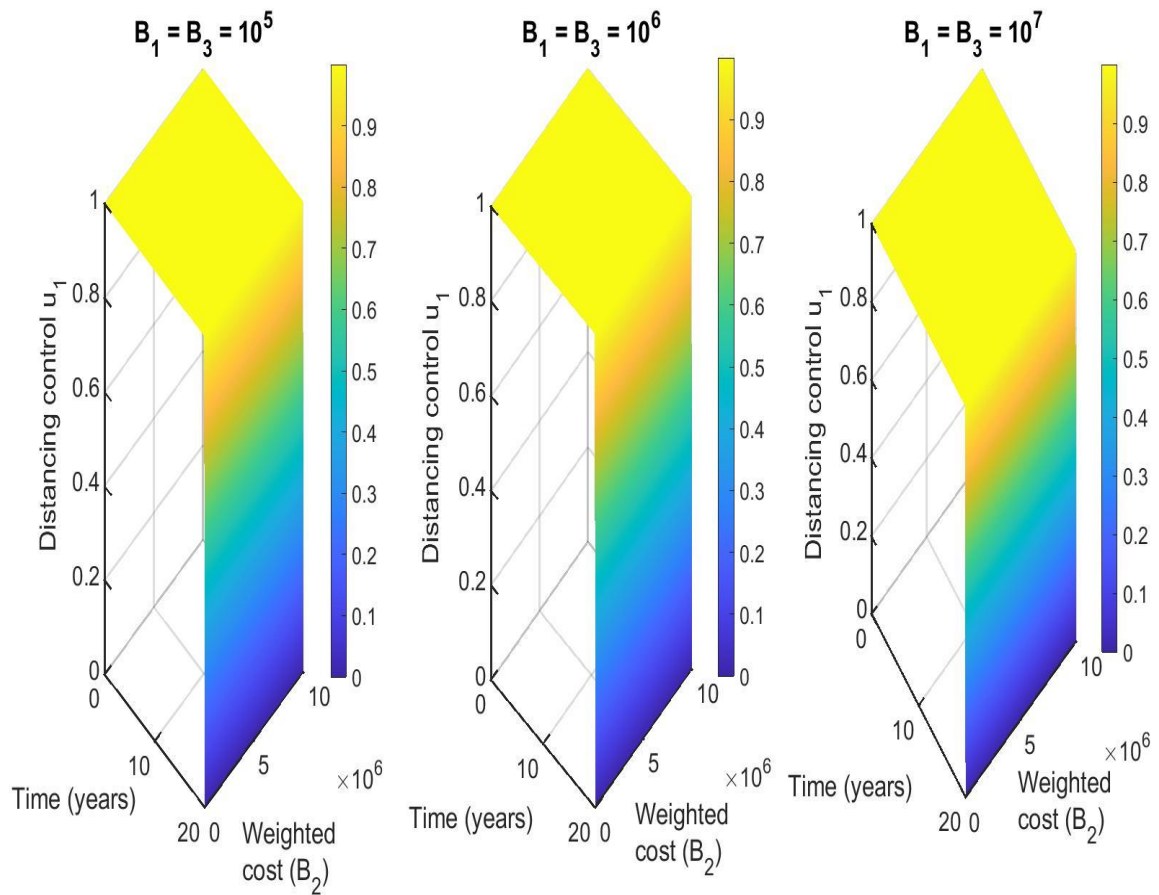


Figure S6.8 (B). Effects of combining of distancing ( $u_1$ ), latent case finding ( $u_2$ ) and case holding ( $u_3$ ) strategy, and considering distancing control ( $u_1$ ) strategy as a function of time and weighted cost ( $B_2$ ). The weighted cost ( $B_1$  and  $B_3$ ) determined by three threshold values  $B_1 = B_3 = 10^5 = 10^6 = 10^7$ .

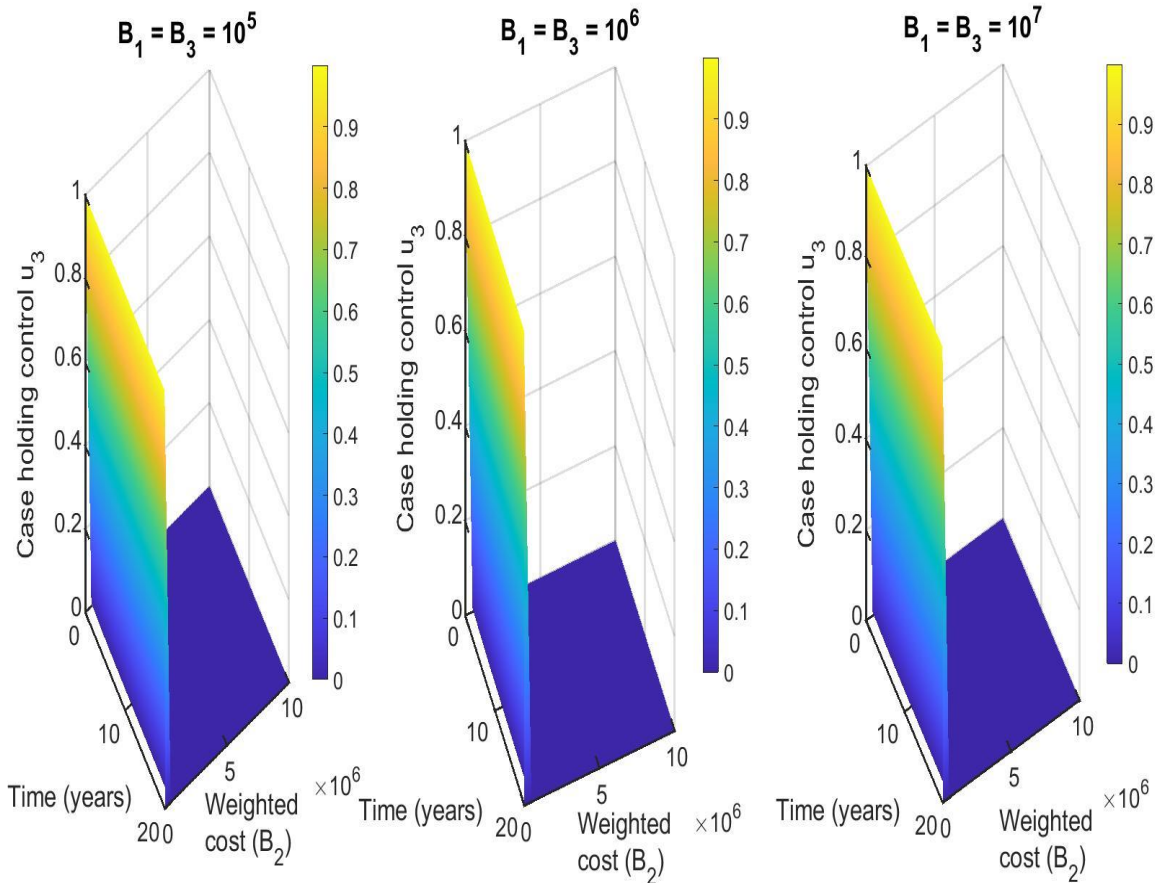


Figure S6.8 (C). Combination of distancing ( $u_1$ ), latent case finding ( $u_2$ ) and case holding ( $u_3$ ) strategy, and considering case holding control ( $u_3$ ) strategy as a function of time and weighted cost ( $B_2$ ). The weighted cost ( $B_1$  and  $B_3$ ) determined by three threshold values  $B_1 = B_3 = 10^5 = 10^6 = 10^7$ .

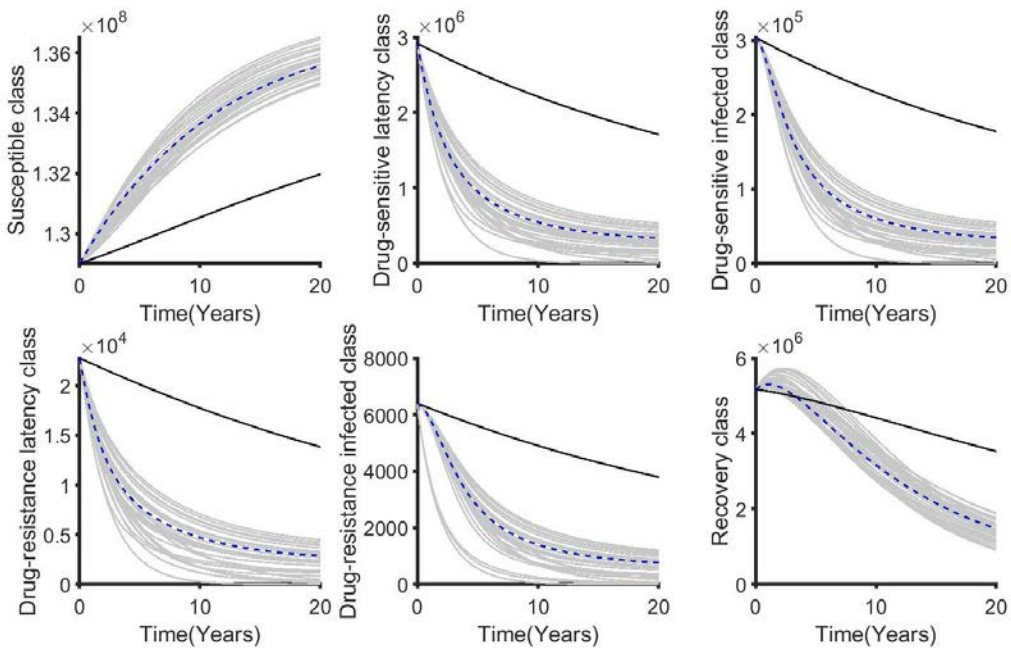


Figure S6.8 (D). The corresponding state variables of the combination of distancing control ( $u_1$ ), latent case finding ( $u_2$ ) and case holding ( $u_3$ ) control strategy and considering the weighted cost  $B_2$

is varied and  $B_1 = B_3 = 10^5 = 10^6 = 10^7$ . The state variables with and without controls are plotted by grays and black lines respectively.

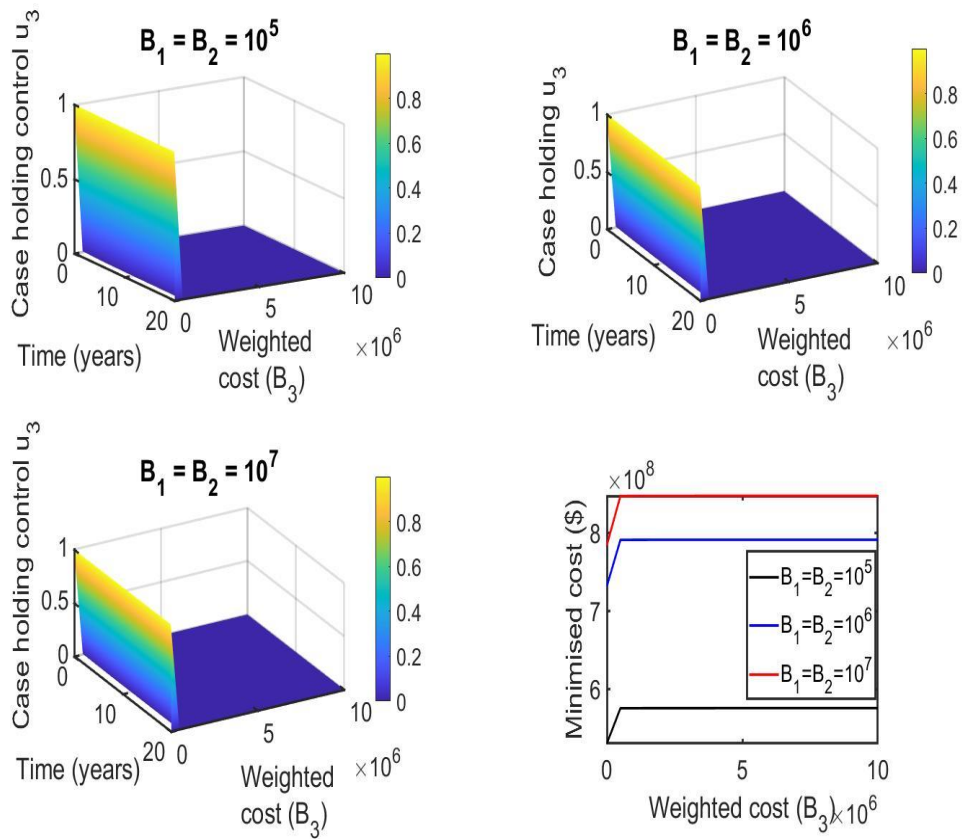


Figure S6.9 (A). Combination of distancing ( $u_1$ ), latent case finding ( $u_2$ ) and case holding ( $u_3$ ) strategy, and considering case holding control ( $u_3$ ) strategy as a function of time and weighted cost ( $B_3$ ). The weighted cost ( $B_1$  and  $B_2$ ) determined by three threshold values  $B_1 = B_2 = 10^5 = 10^6 = 10^7$ .

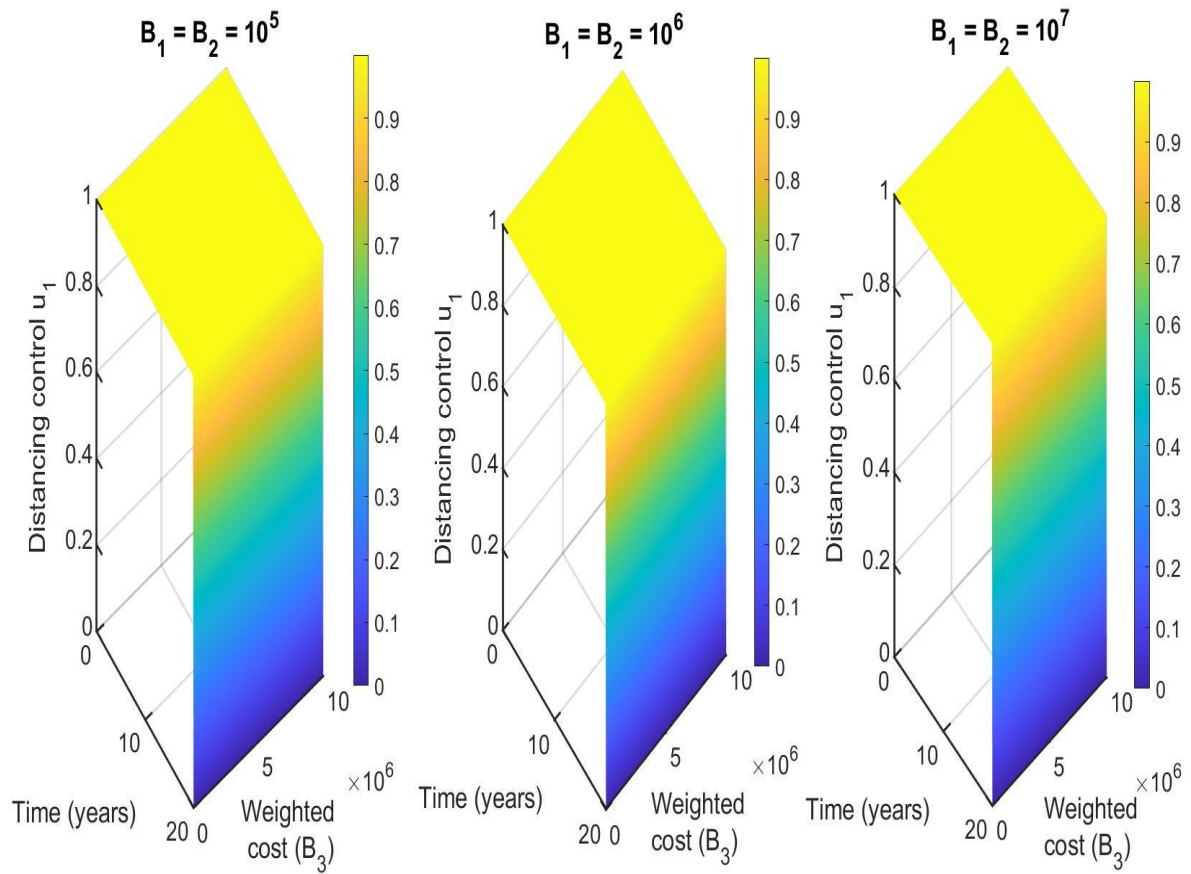


Figure S6.9 (B). Combination of distancing ( $u_1$ ), latent case finding ( $u_2$ ) and case holding ( $u_3$ ) strategy, and considering distancing control ( $u_1$ ) strategy as a function of time and weighted cost ( $B_3$ ). The weighted cost ( $B_1$  and  $B_2$ ) determined by three threshold values  $B_1 = B_2 = 10^5 = 10^6 = 10^7$ .

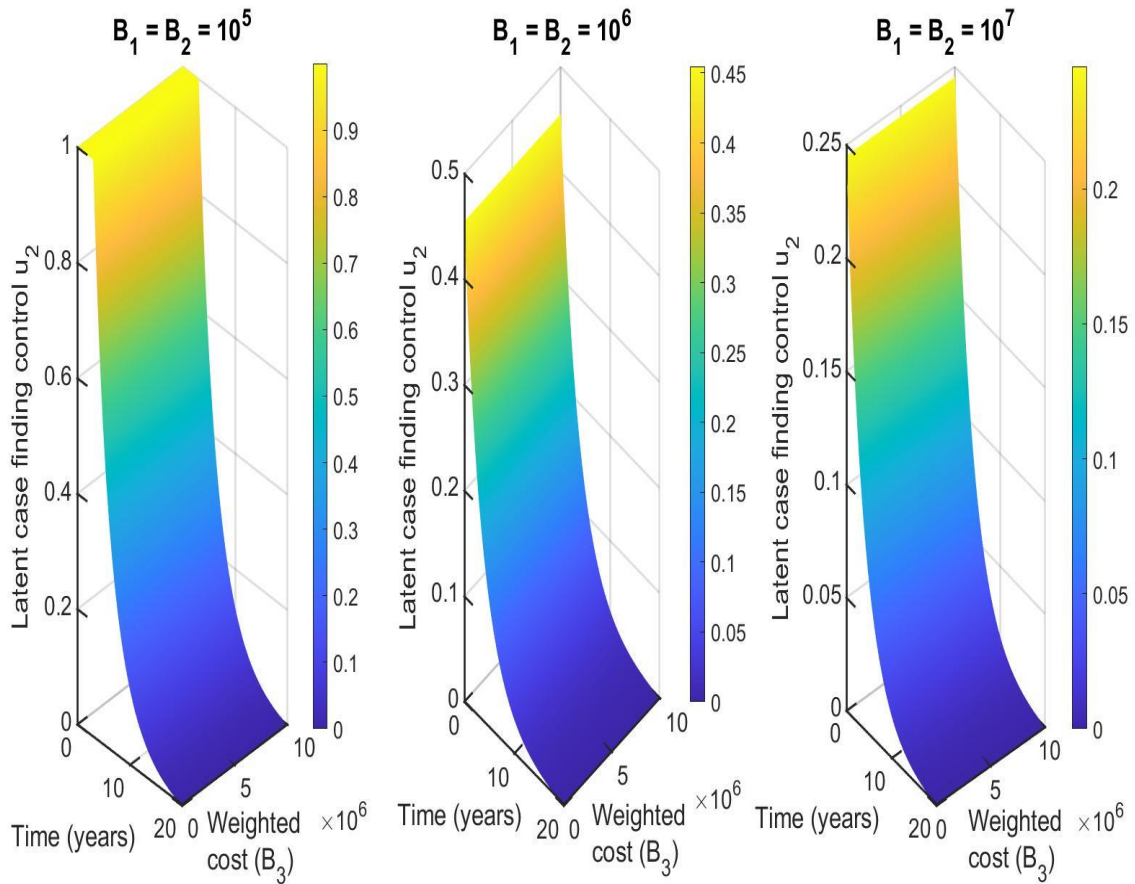


Figure S6.9 (C). Combination of distancing ( $u_1$ ), latent case finding ( $u_2$ ) and case holding ( $u_3$ ) strategy, and considering latent case finding control ( $u_2$ ) strategy as a function of time and weighted cost ( $B_3$ ). The weighted cost ( $B_1$  and  $B_2$ ) determined by three threshold values  $B_1 = B_2 = 10^5 = 10^6 = 10^7$ .

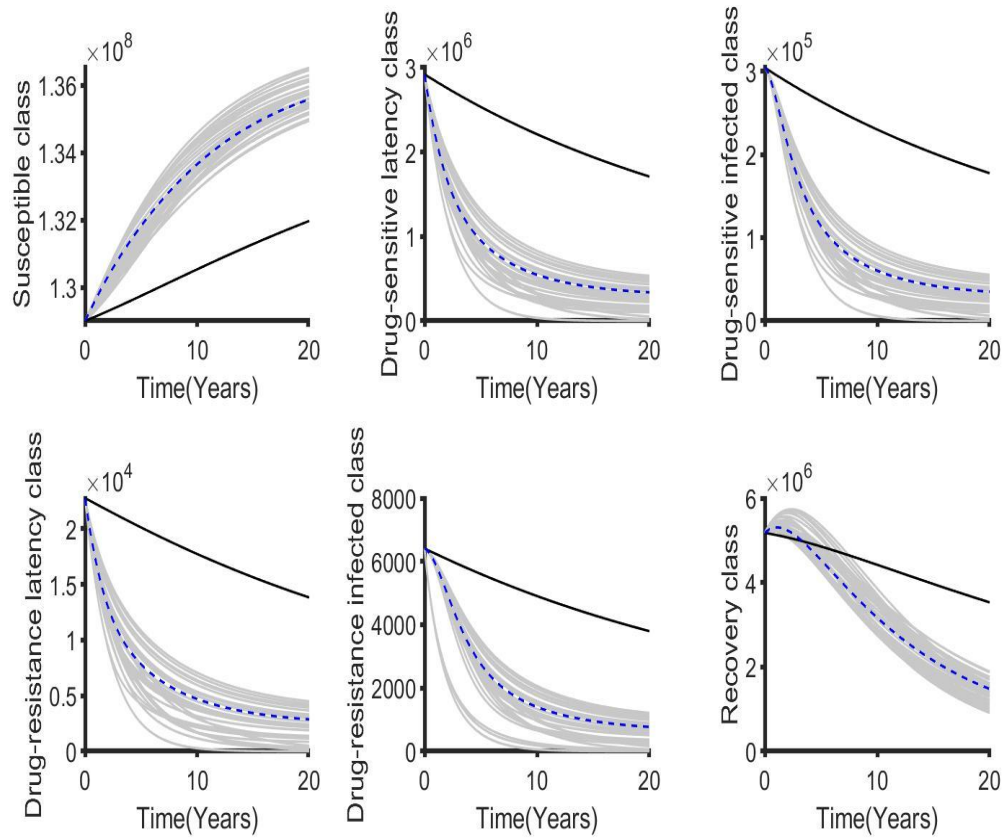


Figure S6.9 (D). The corresponding state variables of the combination of distancing control ( $u_1$ ), latent case finding ( $u_2$ ) and case holding ( $u_3$ ) control strategy when the weighted cost  $B_3$  is varied and  $B_1 = B_2 = 10^5 = 10^6 = 10^7$ . The state variables with and without controls are plotted by grays and black lines respectively.

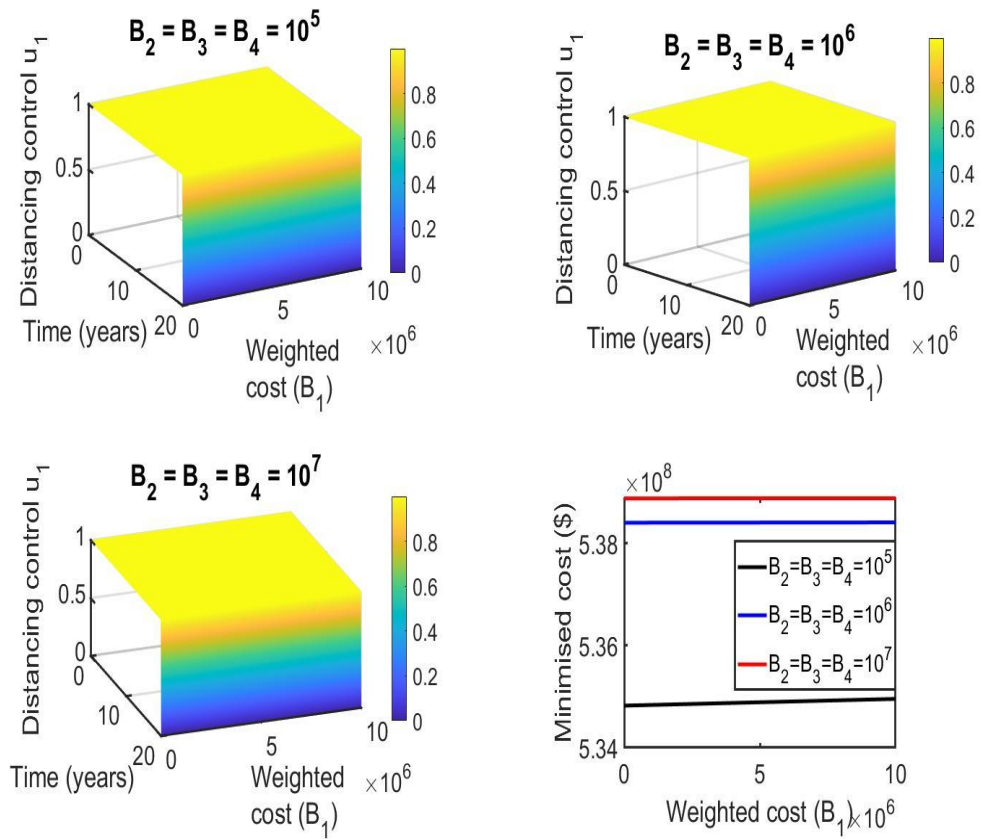


Figure S6.10 (A). Combination of distancing ( $u_1$ ), latent case finding ( $u_2$ ), case holding ( $u_3$ ) and active case finding control strategy, and considering distancing control ( $u_1$ ) strategy as a function of time and weighted cost ( $B_1$ ). The weighted costs ( $B_2, B_3$  and  $B_4$ ) determined by three threshold values  $B_2 = B_3 = B_4 = 10^5 = 10^6 = 10^7$ .

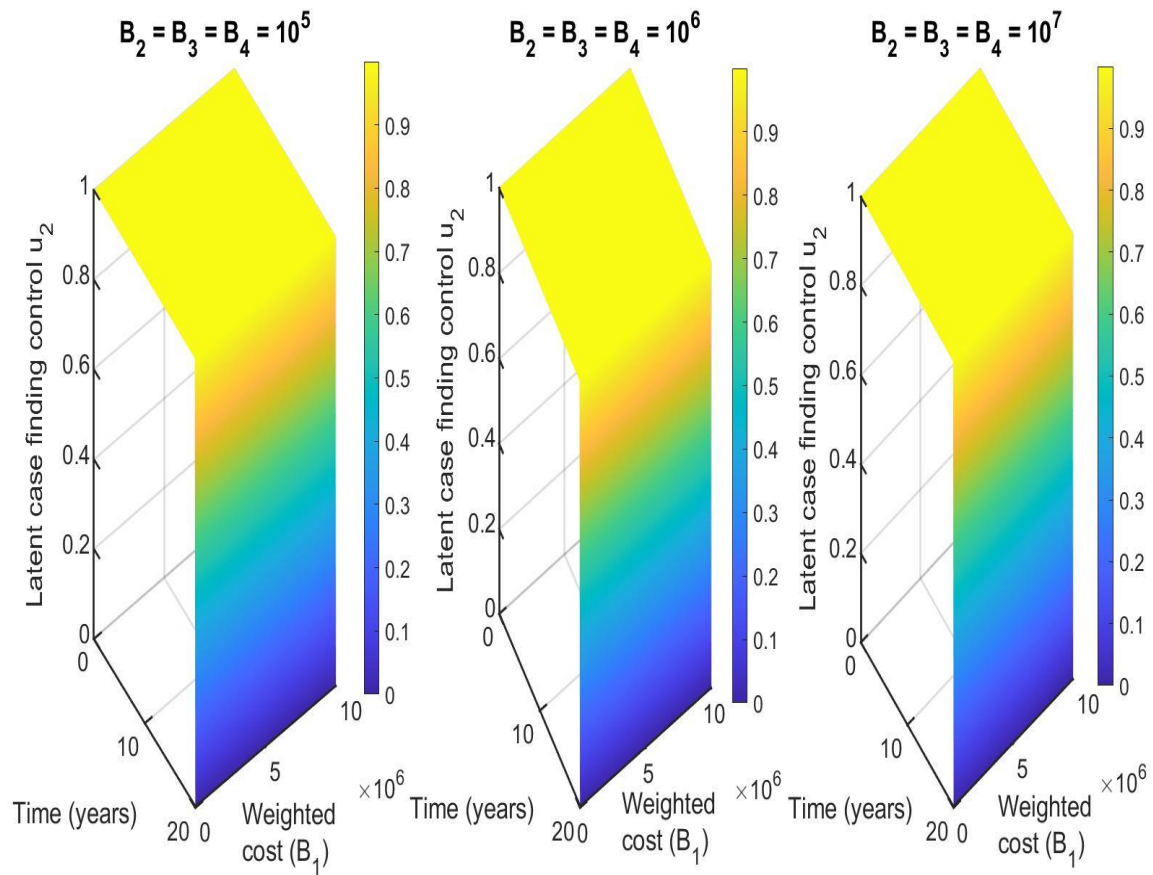


Figure S6.10 (B). Combination of distancing ( $u_1$ ), latent case finding ( $u_2$ ), case holding ( $u_3$ ) and active case finding control strategy, and considering latent case finding control ( $u_2$ ) strategy as a function of time and weighted cost ( $B_1$ ). The weighted costs ( $B_2, B_3$  and  $B_4$ ) determined by three threshold values  $B_2 = B_3 = B_4 = 10^5 = 10^6 = 10^7$ .

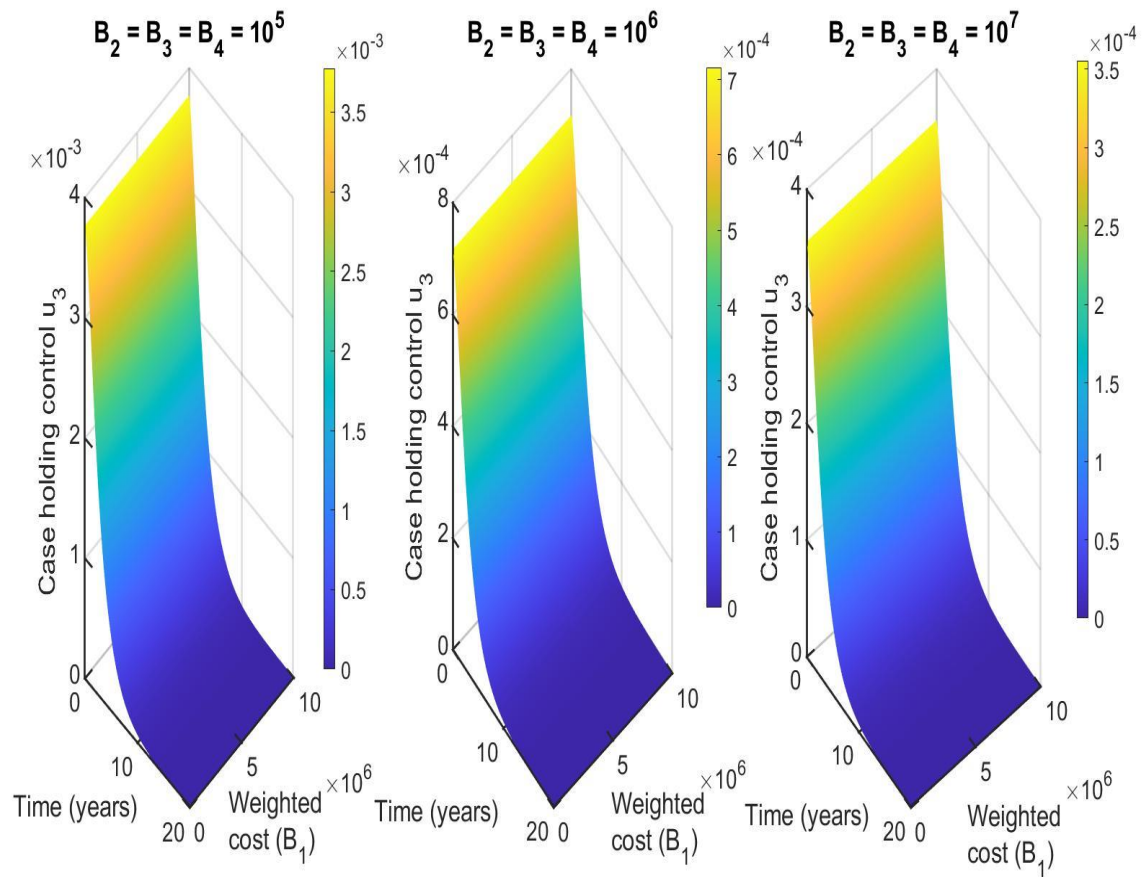


Figure S6.10 (C). Combination of distancing ( $u_1$ ), latent case finding ( $u_2$ ), case holding ( $u_3$ ) and active case finding control strategy, and considering case holding control ( $u_3$ ) strategy as a function of time and weighted cost ( $B_1$ ). The weighted costs ( $B_2, B_3$  and  $B_4$ ) determined by three threshold values  $B_2 = B_3 = B_4 = 10^5 = 10^6 = 10^7$ .

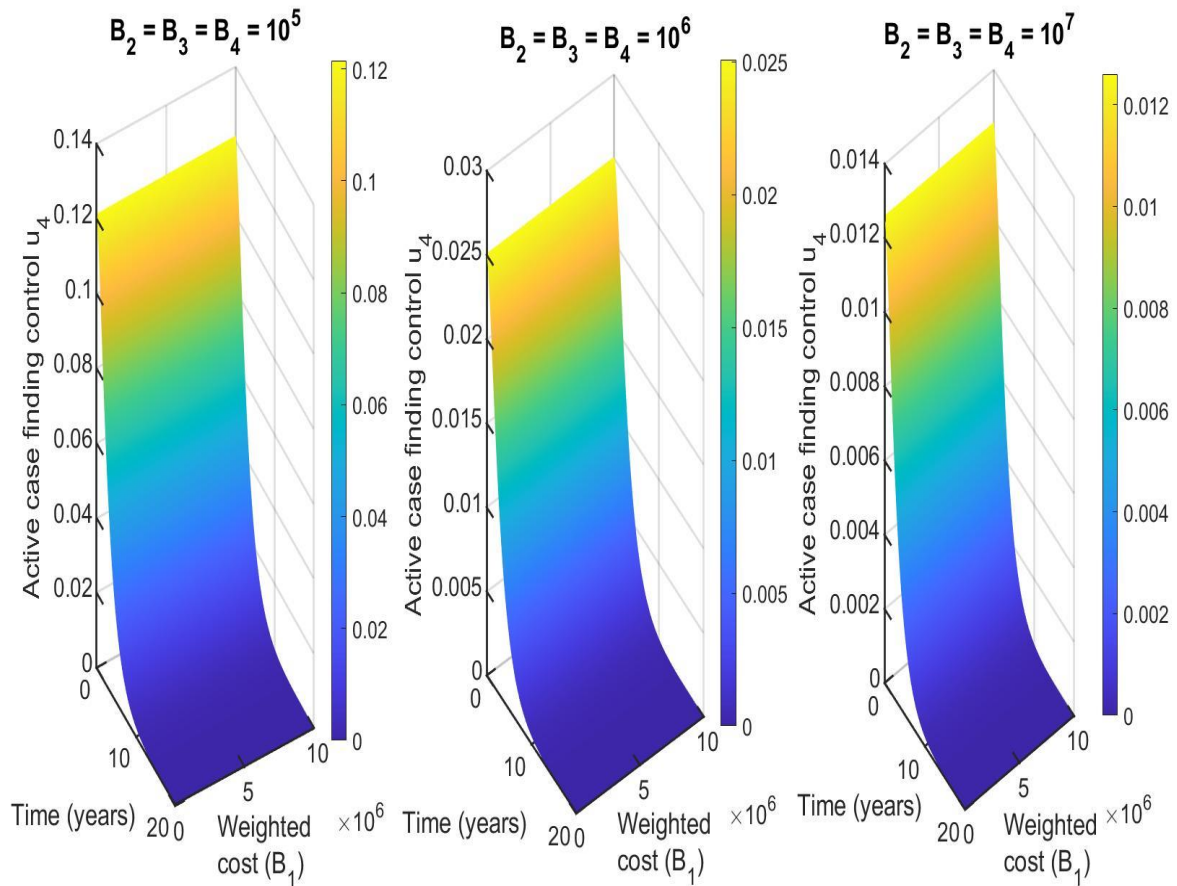


Figure S6.10 (D). Combination of distancing ( $u_1$ ), latent case finding ( $u_2$ ), case holding ( $u_3$ ) and active case finding control strategy, and considering active case finding control ( $u_4$ ) strategy as a function of time and weighted cost ( $B_1$ ). The weighted costs ( $B_2, B_3$  and  $B_4$ ) determined by three threshold values  $B_2 = B_3 = B_4 = 10^5 = 10^6 = 10^7$ .

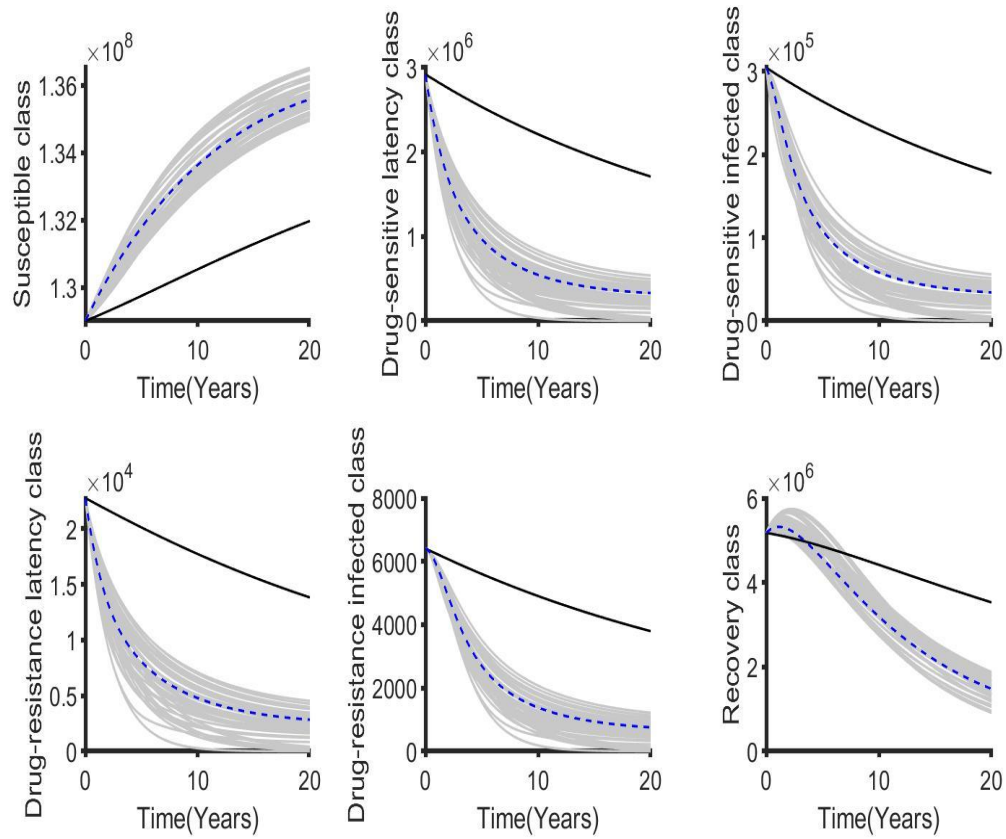


Figure S6.10 (E). The corresponding state variables of the combination of distancing control ( $u_1$ ), latent case finding ( $u_2$ ), case holding ( $u_3$ ) and active case finding ( $u_4$ ) control strategy when the weighted cost  $B_1$  is varied and  $B_2 = B_3 = B_4 = 10^5 = 10^6 = 10^7$ . The state variables with and without controls are plotted by grays and black lines respectively.

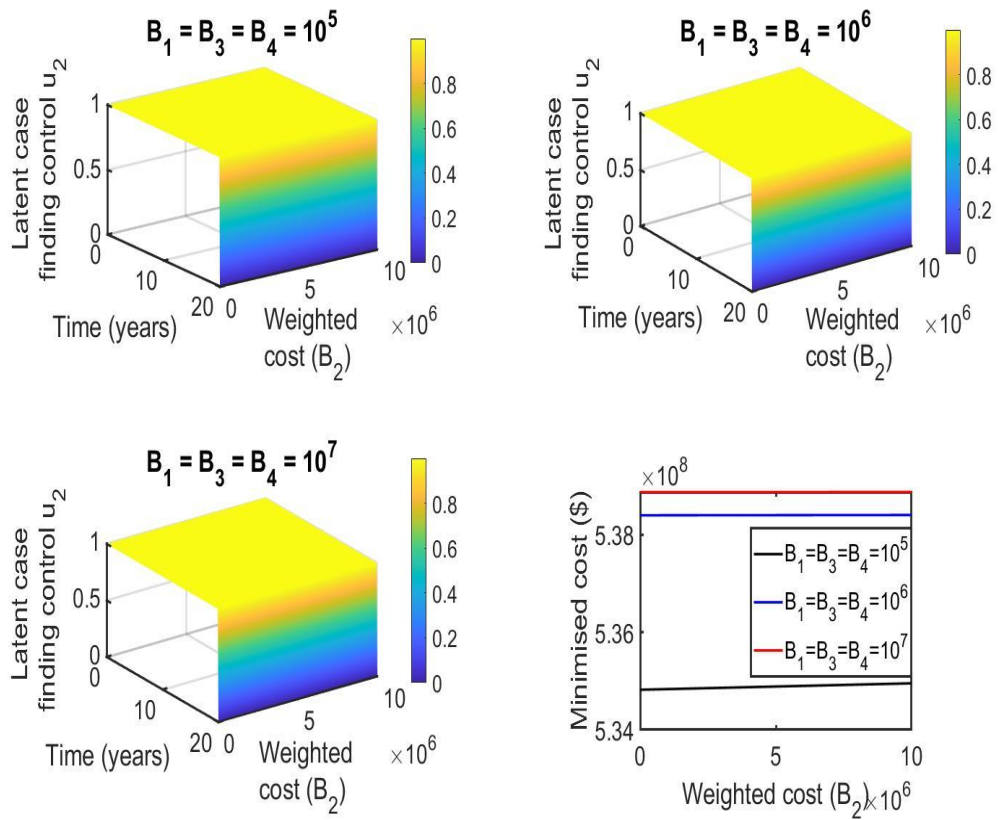


Figure S6.11 (A). Combination of distancing ( $u_1$ ), latent case finding ( $u_2$ ), case holding ( $u_3$ ) and active case finding control strategy, and considering latent case finding control ( $u_2$ ) strategy as a function of time and weighted cost ( $B_2$ ). The weighted costs ( $B_1, B_3$  and  $B_4$ ) determined by three threshold values  $B_1 = B_3 = B_4 = 10^5 = 10^6 = 10^7$ .

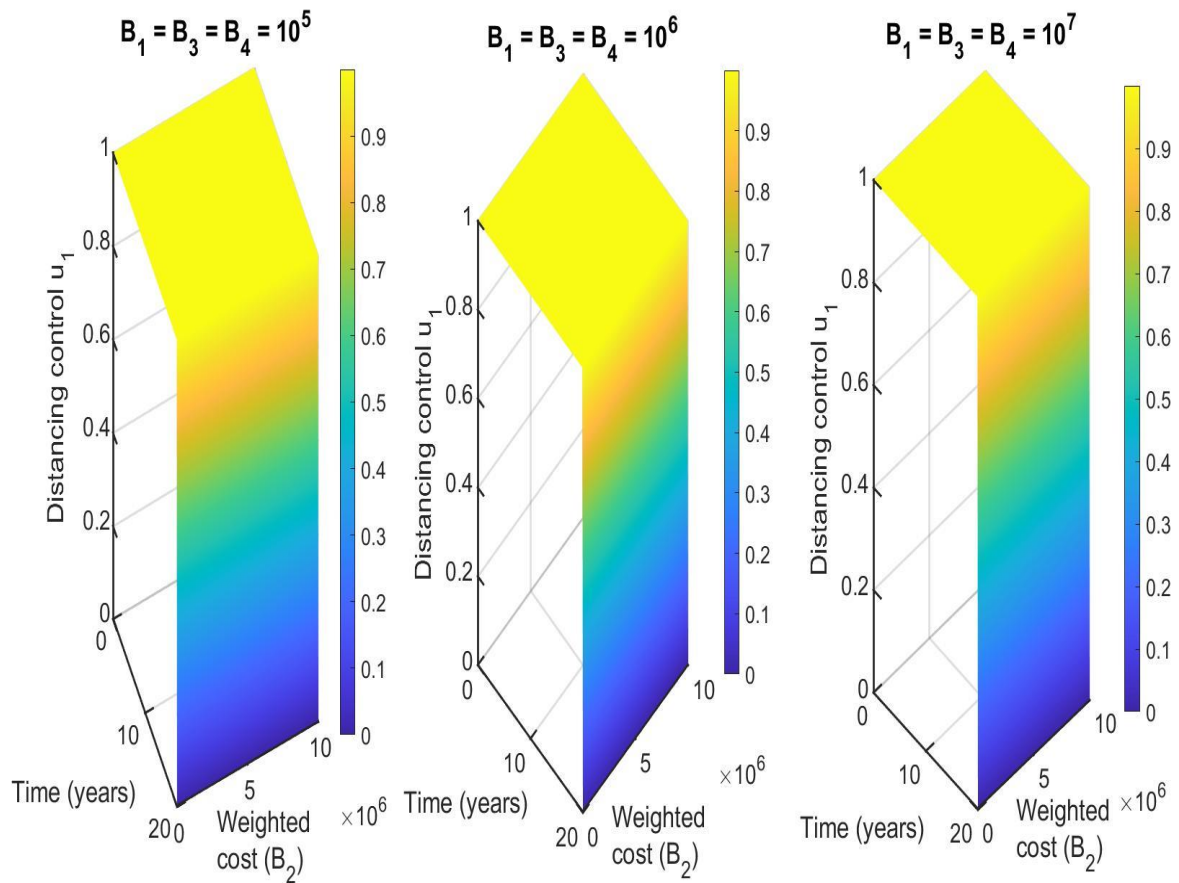


Figure S6.11 (B). Combination of distancing ( $u_1$ ), latent case finding ( $u_2$ ), case holding ( $u_3$ ) and active case finding control strategy, and considering distancing control ( $u_1$ ) strategy as a function of time and weighted cost ( $B_2$ ). The weighted costs ( $B_1, B_3$  and  $B_4$ ) determined by three threshold values  $B_1 = B_3 = B_4 = 10^5 = 10^6 = 10^7$ .

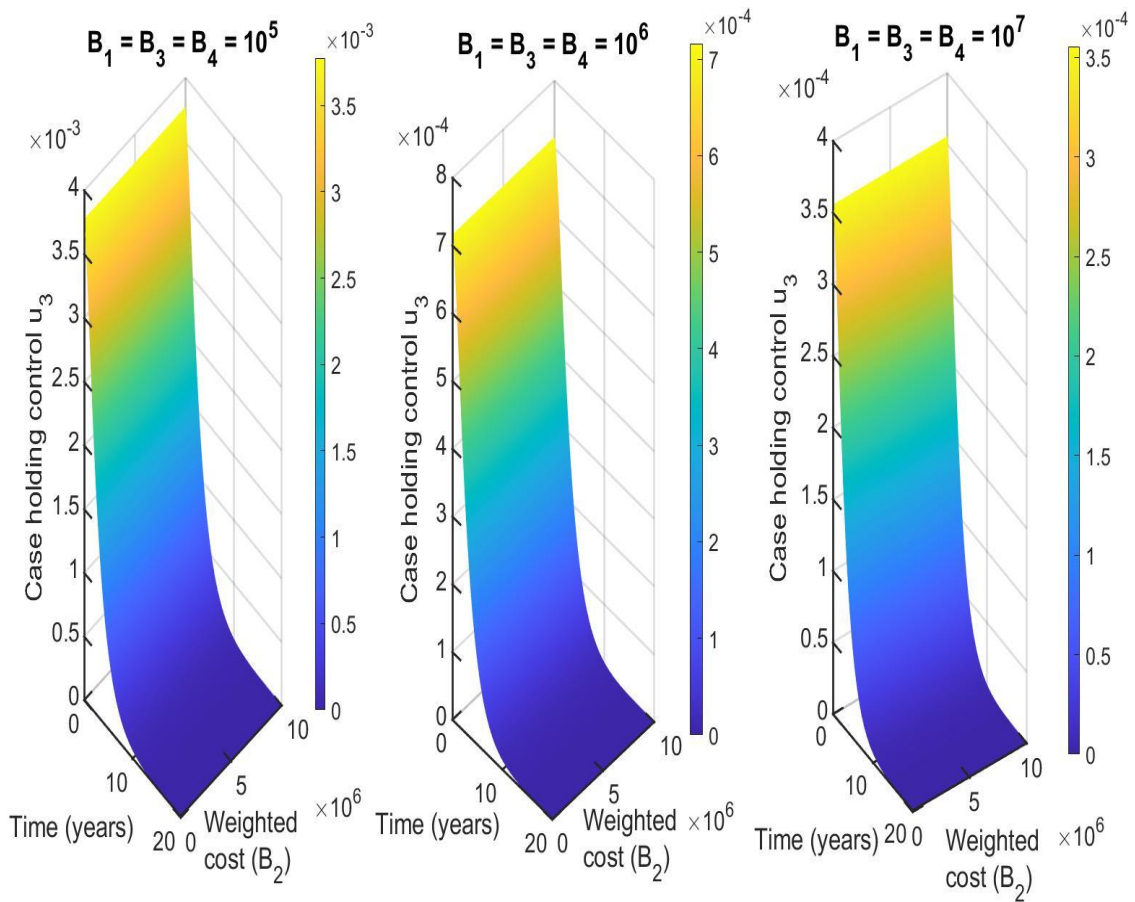


Figure S6.11 (C). Combination of distancing ( $u_1$ ), latent case finding ( $u_2$ ), case holding ( $u_3$ ) and active case finding control strategy, and considering case holding control ( $u_3$ ) strategy as a function of time and weighted cost ( $B_2$ ). The weighted costs ( $B_1, B_3$  and  $B_4$ ) determined by three threshold values  $B_1 = B_3 = B_4 = 10^5 = 10^6 = 10^7$ .

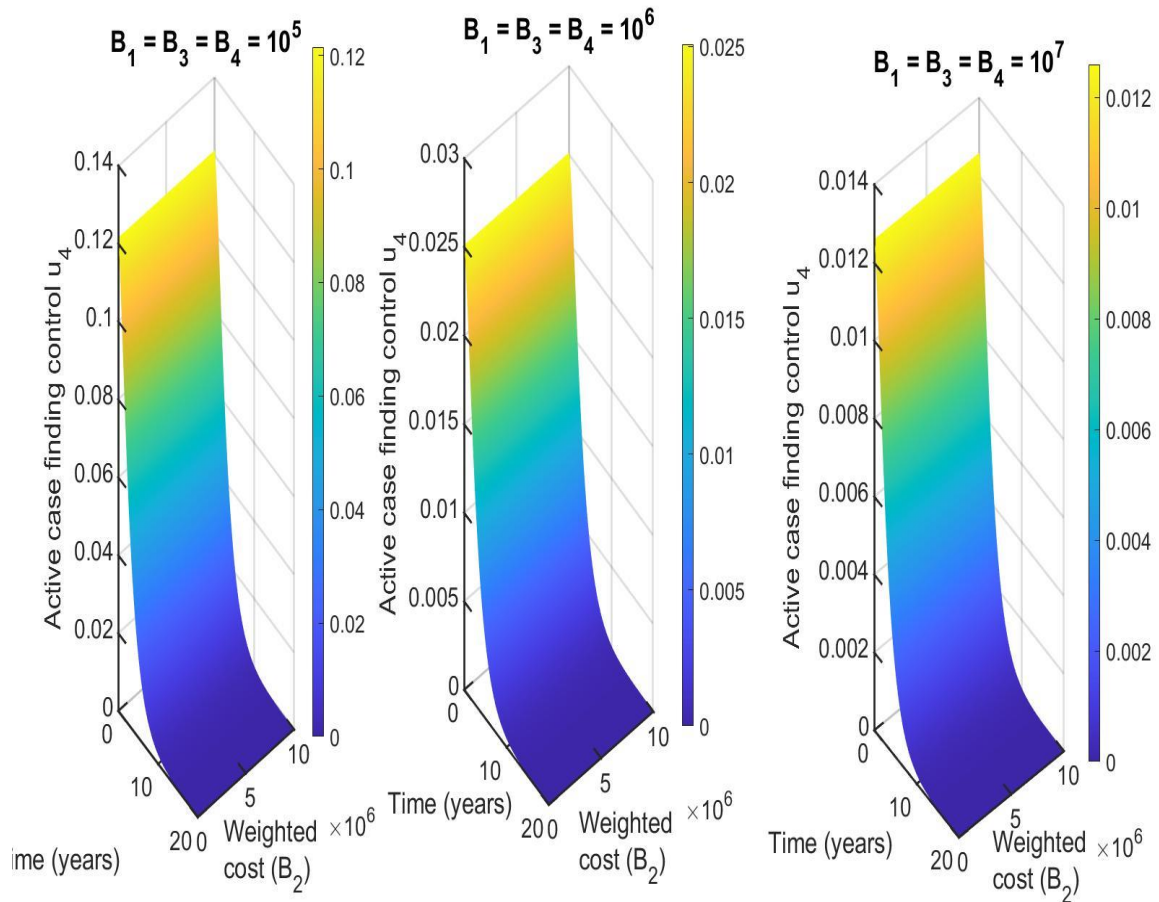


Figure S6.11 (D). Combination of distancing ( $u_1$ ), latent case finding ( $u_2$ ), case holding ( $u_3$ ) and active case finding control strategy, and considering active case finding control ( $u_4$ ) strategy as a function of time and weighted cost ( $B_2$ ). The weighted costs ( $B_1, B_3$  and  $B_4$ ) determined by three threshold values  $B_1 = B_3 = B_4 = 10^5 = 10^6 = 10^7$ .

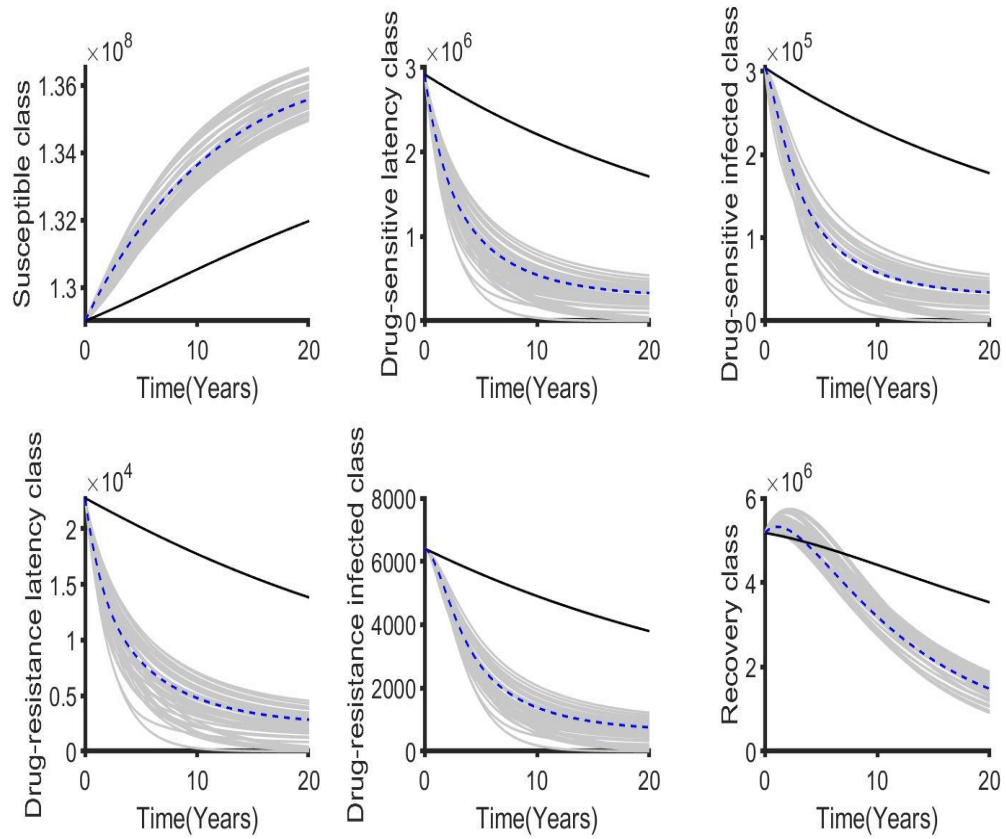


Figure S6.11 (E). The corresponding state variables of the combination of distancing control ( $u_1$ ), latent case finding ( $u_2$ ), case holding ( $u_3$ ) and active case finding ( $u_4$ ) control strategy when the weighted cost  $B_2$  is varied and  $B_1 = B_3 = B_4 = 10^5 = 10^6 = 10^7$ . The state variables with and without controls are plotted by grays and black lines respectively.

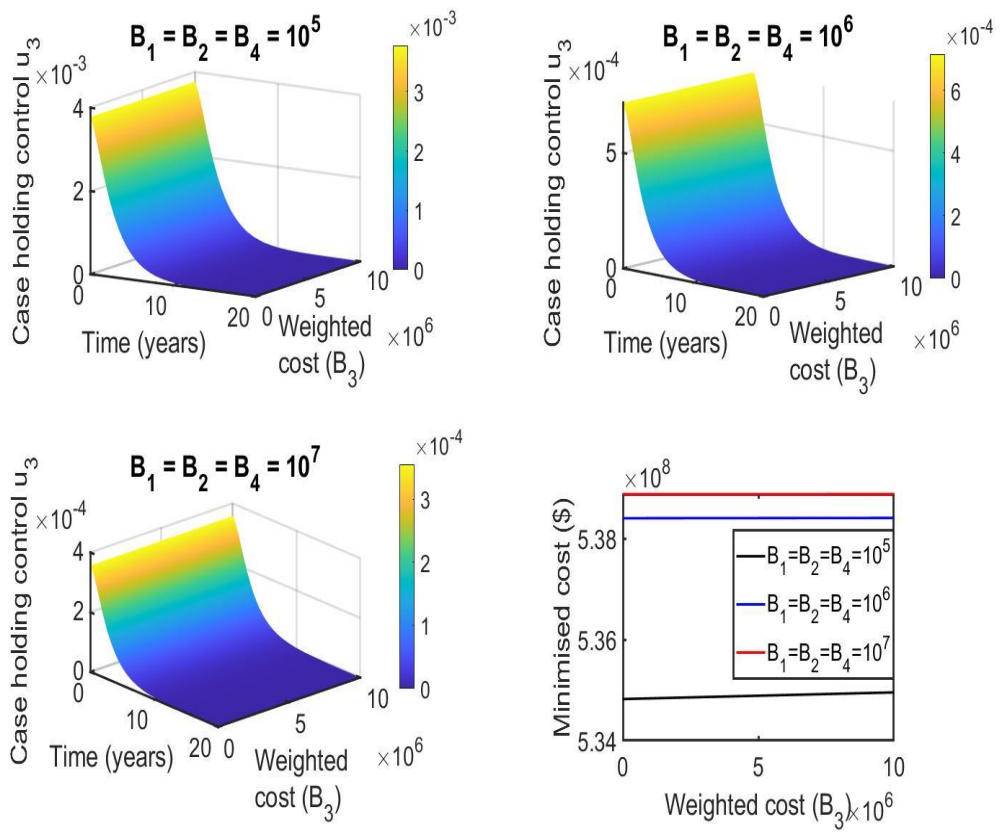


Figure S6.12 (A). Combination of distancing ( $u_1$ ), latent case finding ( $u_2$ ), case holding ( $u_3$ ) and active case finding control strategy, and considering case holding control ( $u_3$ ) strategy as a function of time and weighted cost ( $B_3$ ). The weighted costs ( $B_1, B_2$  and  $B_4$ ) determined by three threshold values  $B_1 = B_2 = B_4 = 10^5 = 10^6 = 10^7$ .

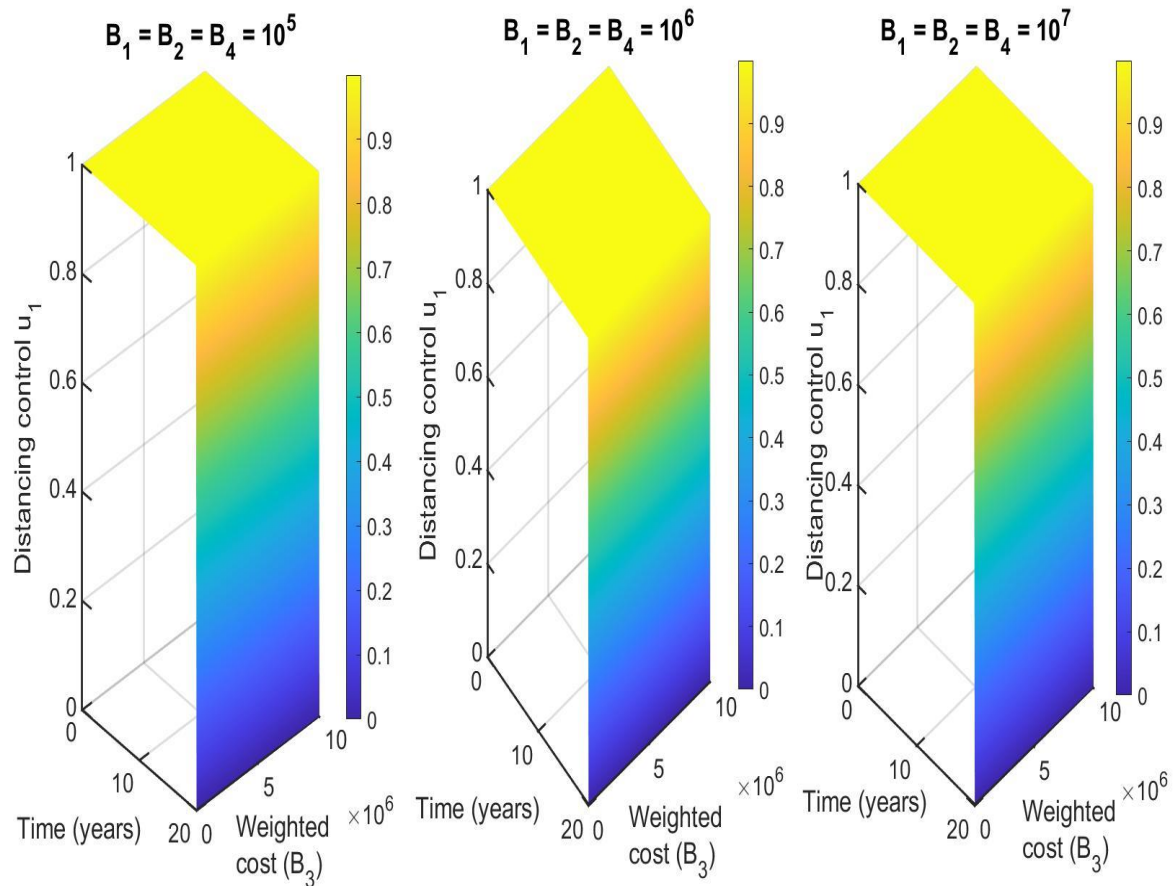


Figure S6.12 (B). Combination of distancing ( $u_1$ ), latent case finding ( $u_2$ ), case holding ( $u_3$ ) and active case finding control strategy, and considering distancing control ( $u_1$ ) strategy as a function of time and weighted cost ( $B_3$ ). The weighted costs ( $B_1, B_2$  and  $B_4$ ) determined by three threshold values  $B_1 = B_2 = B_4 = 10^5 = 10^6 = 10^7$ .

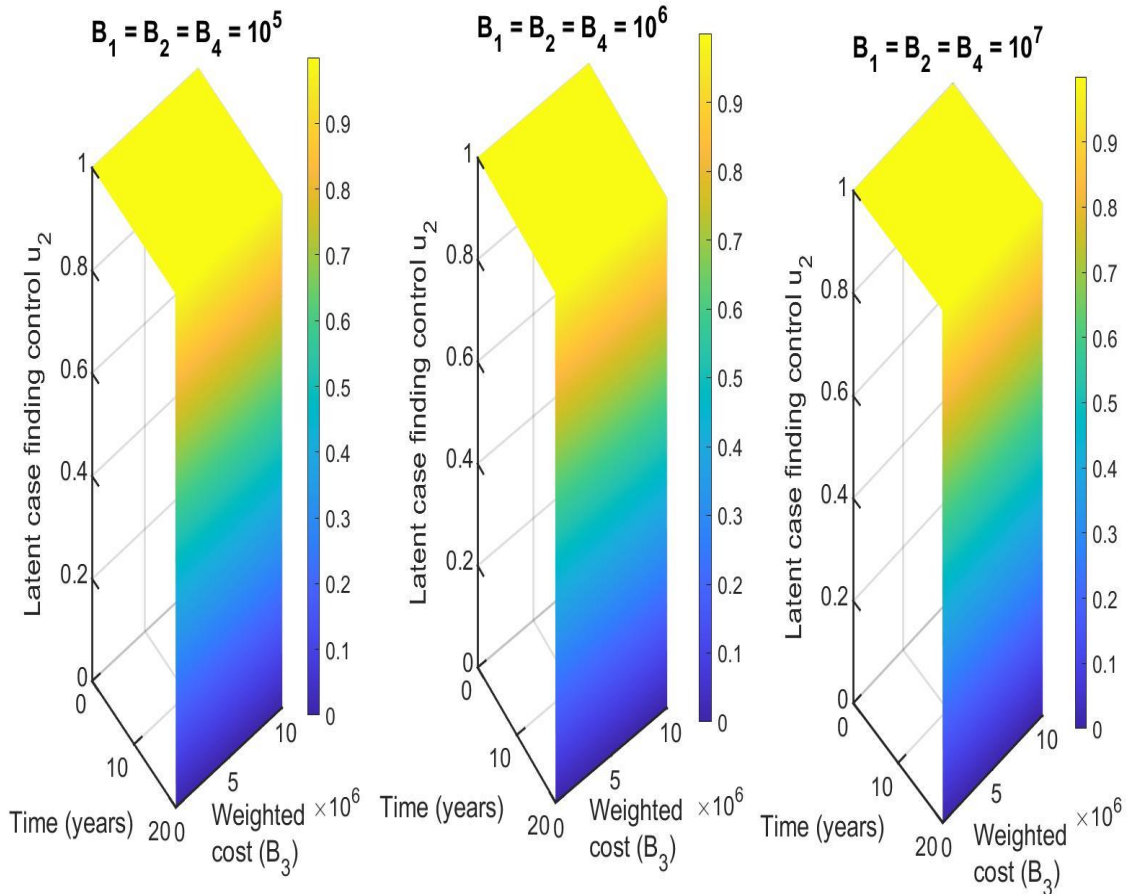


Figure S6.12 (C). Combination of distancing ( $u_1$ ), latent case finding ( $u_2$ ), case holding ( $u_3$ ) and active case finding control strategy, and considering latent case finding control ( $u_2$ ) strategy as a function of time and weighted cost ( $B_3$ ). The weighted costs ( $B_1, B_2$  and  $B_4$ ) determined by three threshold values  $B_1 = B_2 = B_4 = 10^5 = 10^6 = 10^7$ .

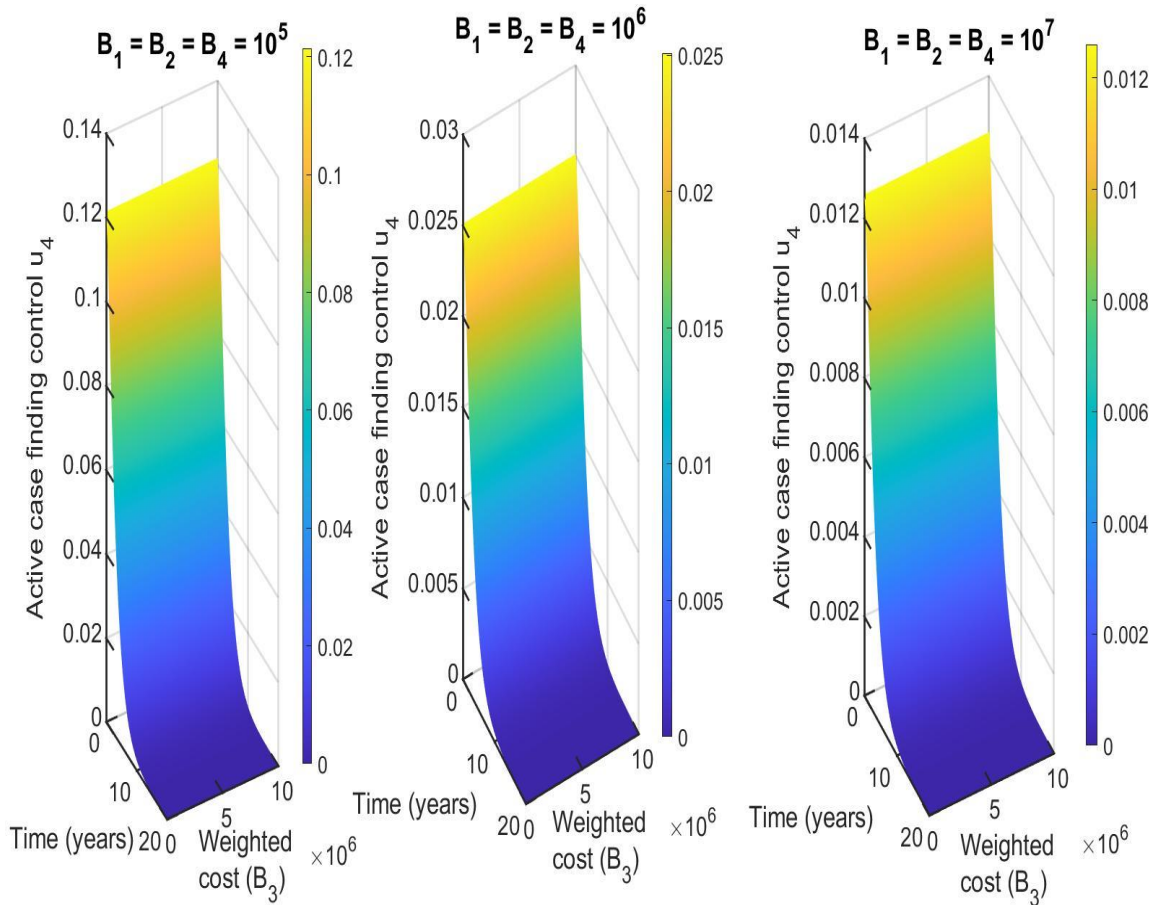


Figure S6.12 (D). Combination of distancing ( $u_1$ ), latent case finding ( $u_2$ ), case holding ( $u_3$ ) and active case finding control strategy, and considering active case finding control ( $u_4$ ) strategy as a function of time and weighted cost ( $B_3$ ). The weighted costs ( $B_1, B_2$  and  $B_4$ ) determined by three threshold values  $B_1 = B_2 = B_4 = 10^5 = 10^6 = 10^7$ .

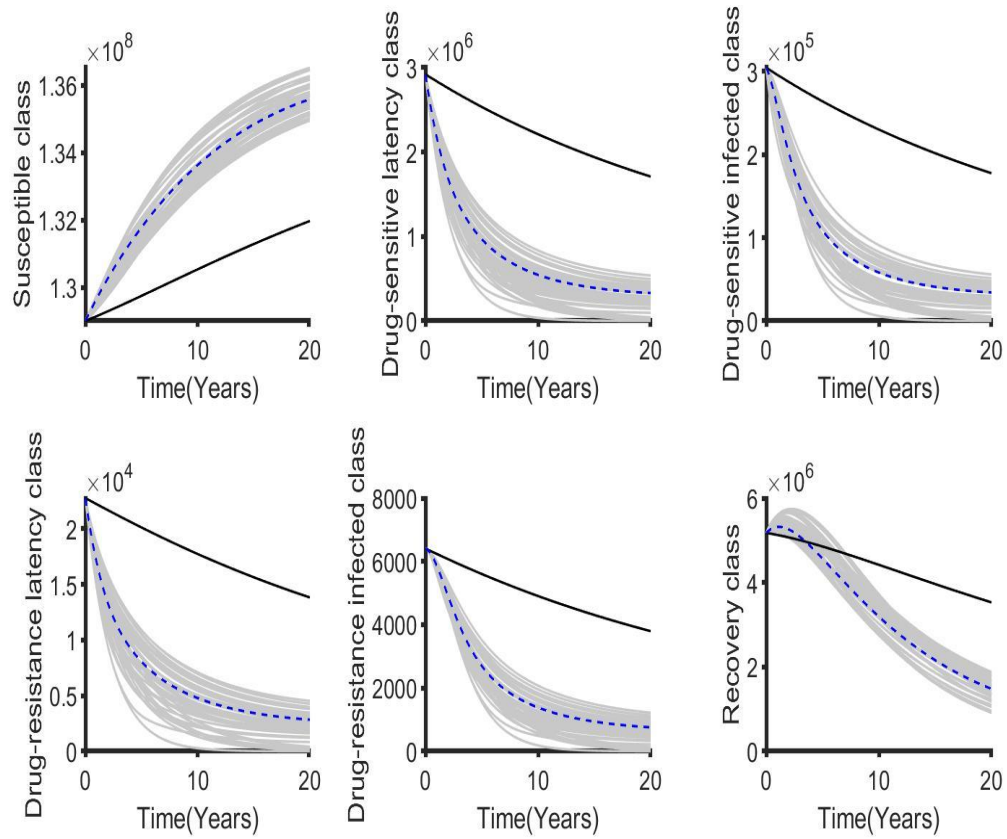


Figure S6.12 (E). The corresponding state variables of the combination of distancing control ( $u_1$ ), latent case finding ( $u_2$ ), case holding ( $u_3$ ) and active case finding ( $u_4$ ) control strategy when the weighted cost  $B_3$  is varied and  $B_1 = B_2 = B_4 = 10^5 = 10^6 = 10^7$ . The state variables with and without controls are plotted by grays and black lines respectively.

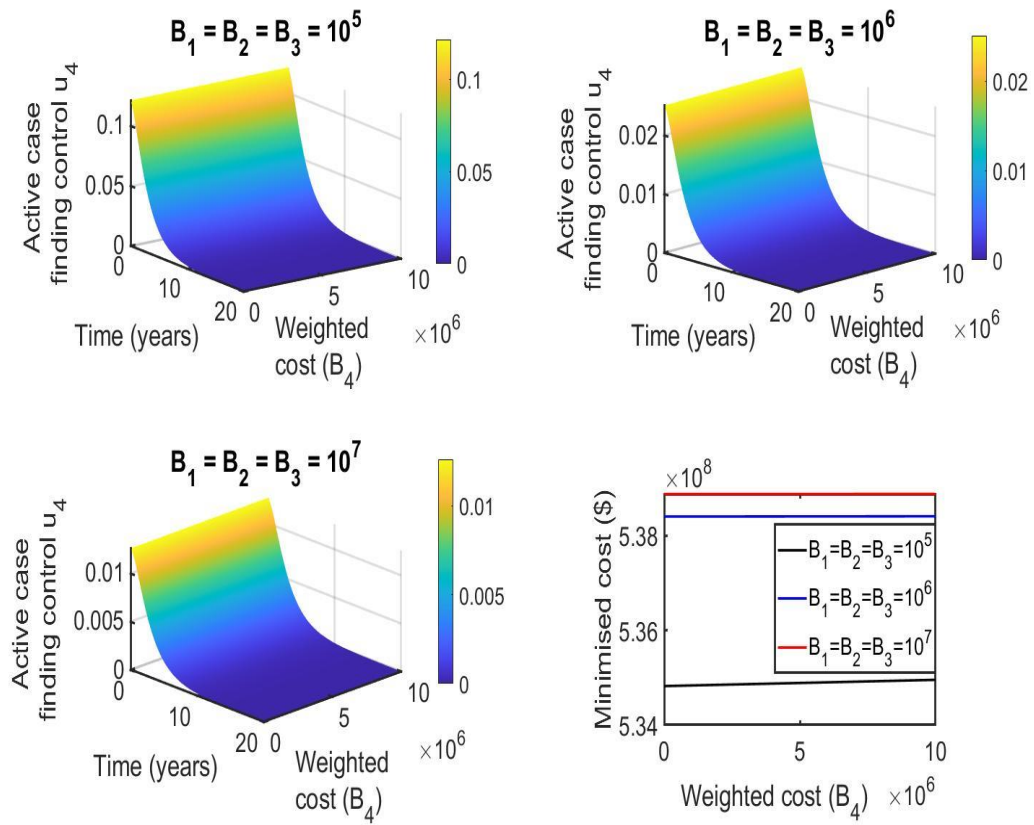


Figure S6.13 (A). Combination of distancing ( $u_1$ ), latent case finding ( $u_2$ ), case holding ( $u_3$ ) and active case finding control strategy, and considering active case finding control ( $u_1$ ) strategy as a function of time and weighted cost ( $B_4$ ). The weighted costs ( $B_1, B_2$  and  $B_3$ ) determined by three threshold values  $B_1 = B_2 = B_3 = 10^5 = 10^6 = 10^7$ .

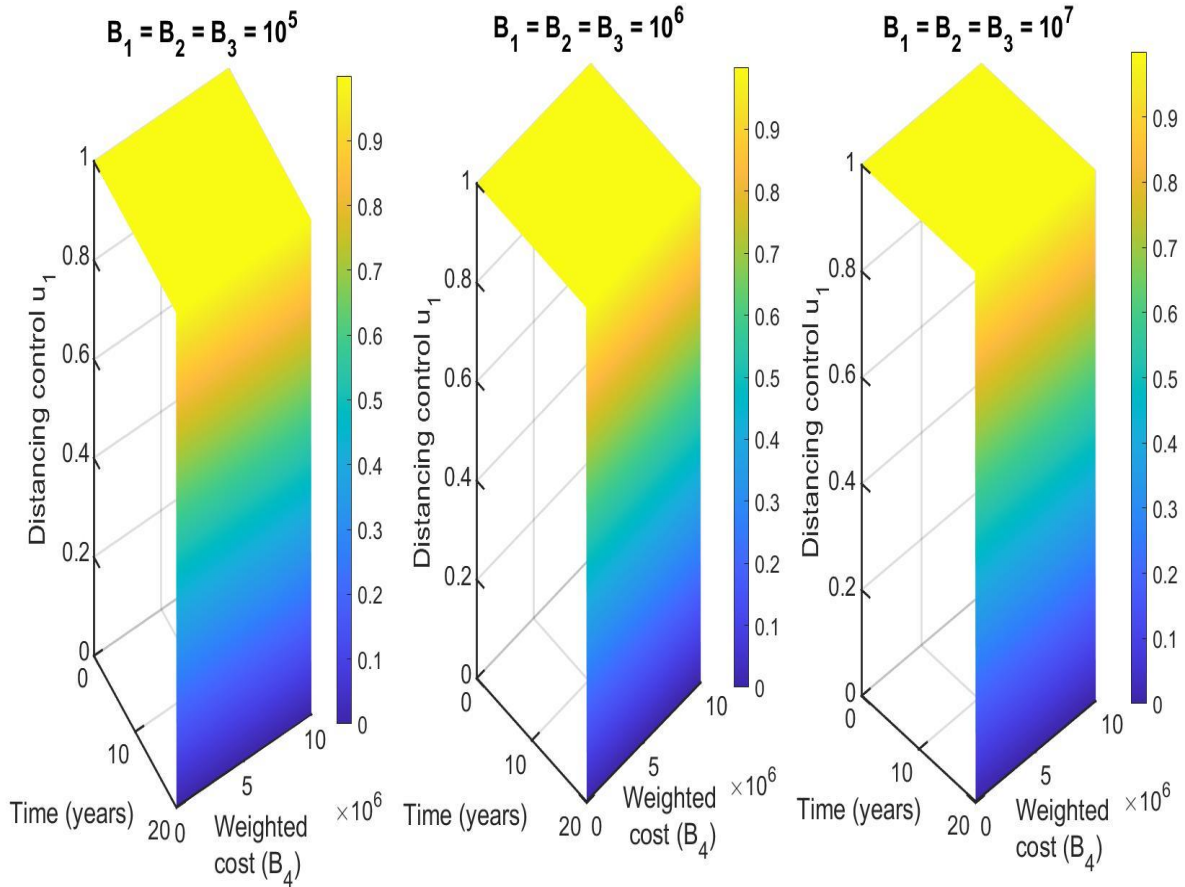


Figure S6.13 (B). Combination of distancing ( $u_1$ ), latent case finding ( $u_2$ ), case holding ( $u_3$ ) and active case finding control strategy, and considering distancing control ( $u_1$ ) strategy as a function of time and weighted cost ( $B_4$ ). The weighted costs ( $B_1, B_2$  and  $B_3$ ) determined by three threshold values  $B_1 = B_2 = B_3 = 10^5 = 10^6 = 10^7$ .

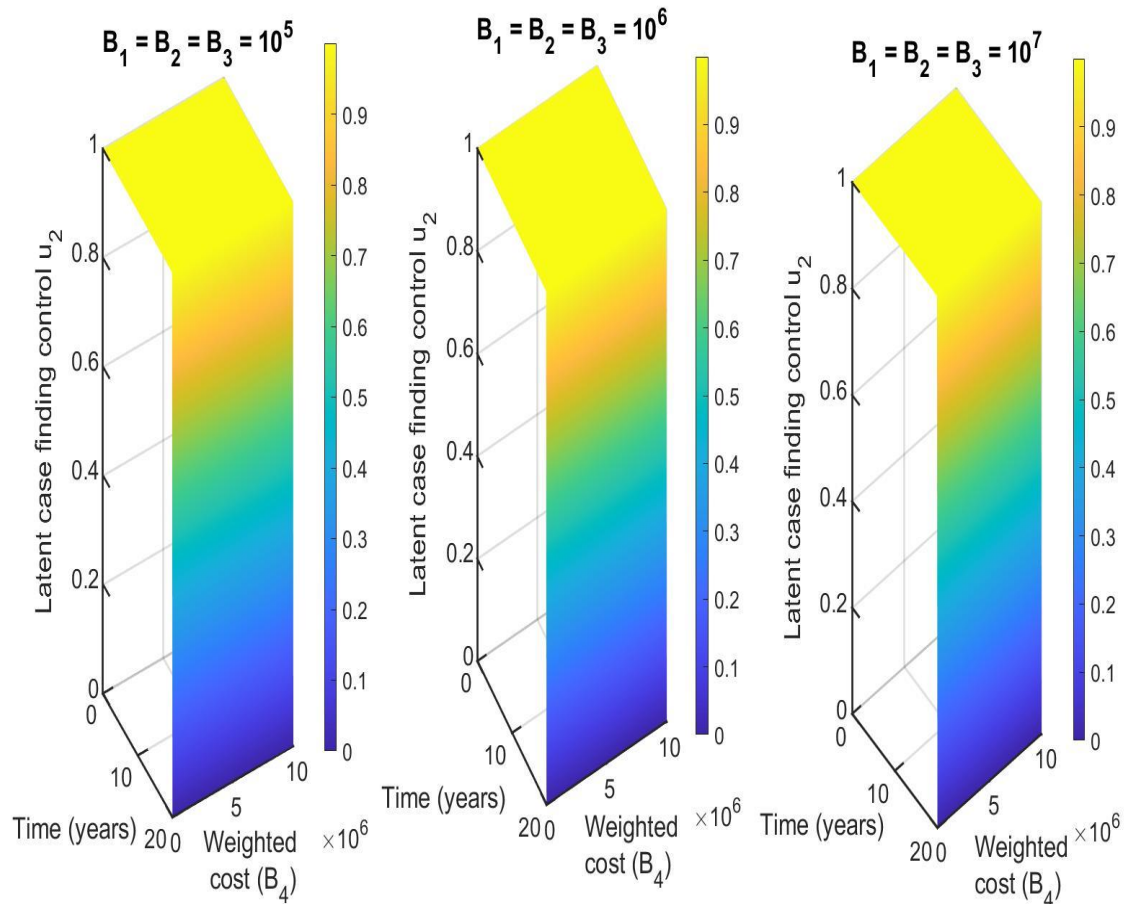


Figure S6.13 (C). Combination of distancing ( $u_1$ ), latent case finding ( $u_2$ ), case holding ( $u_3$ ) and active case finding control strategy, and considering latent case finding control ( $u_2$ ) strategy as a function of time and weighted cost ( $B_4$ ). The weighted costs ( $B_1, B_2$  and  $B_3$ ) determined by three threshold values  $B_1 = B_2 = B_3 = 10^5 = 10^6 = 10^7$ .

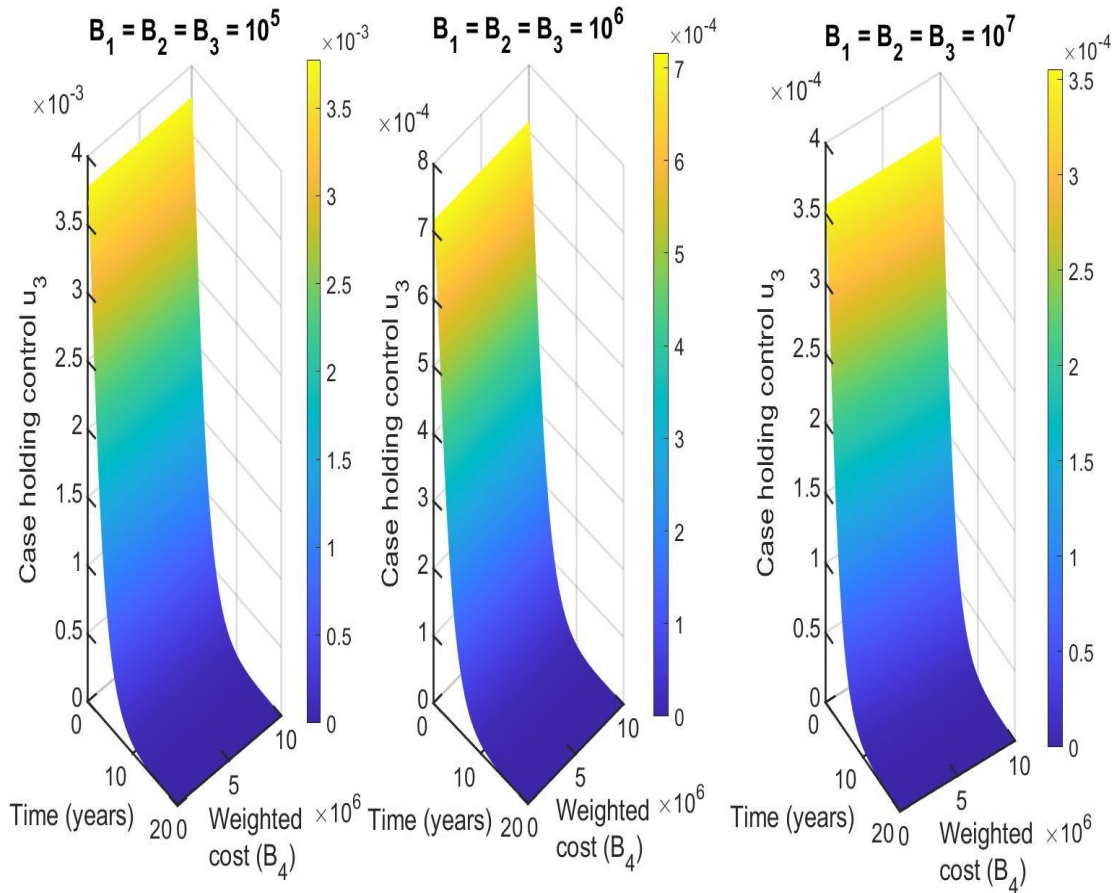


Figure S6.13 (D). Combination of distancing ( $u_1$ ), latent case finding ( $u_2$ ), case holding ( $u_3$ ) and active case finding control strategy, and considering case holding control ( $u_3$ ) strategy as a function of time and weighted cost ( $B_4$ ). The weighted costs ( $B_1, B_2$  and  $B_3$ ) determined by three threshold values  $B_1 = B_2 = B_3 = 10^5 = 10^6 = 10^7$ .

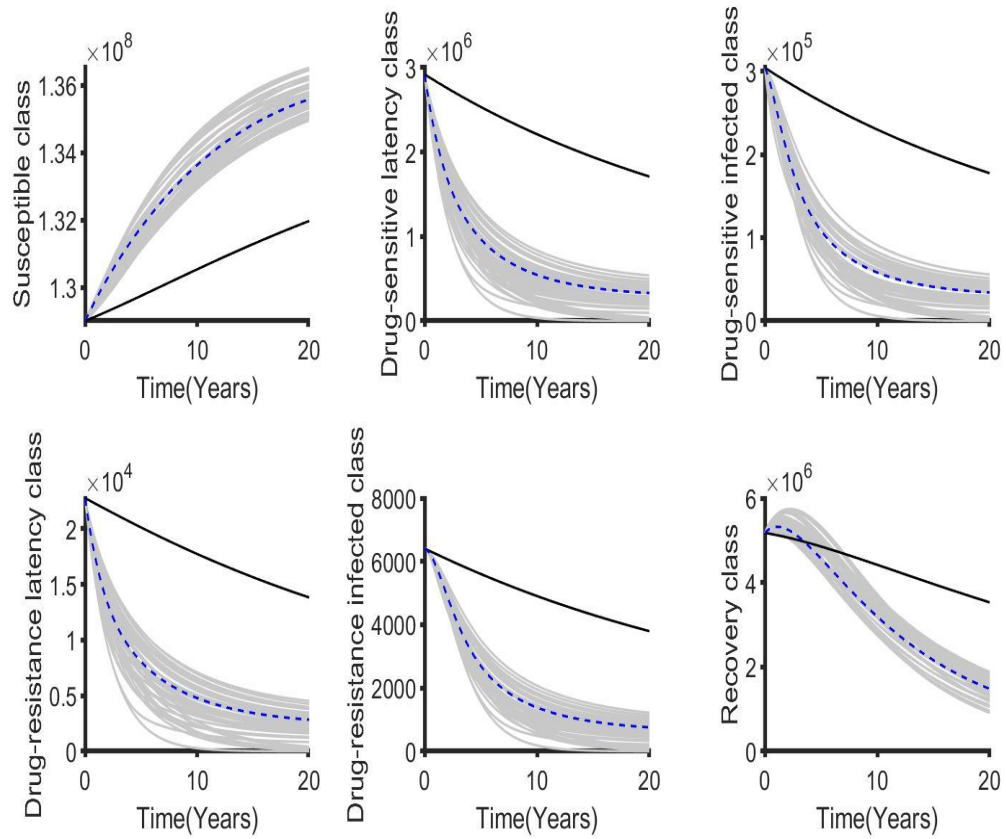


Figure S6.13 (E). The corresponding state variables of the combination of distancing control ( $u_1$ ), latent case finding ( $u_2$ ), case holding ( $u_3$ ) and active case finding ( $u_4$ ) control strategy when the weighted cost  $B_4$  is varied and  $B_1 = B_2 = B_3 = 10^5 = 10^6 = 10^7$ . The state variables with and without controls are plotted by grays and black lines respectively.

# CHAPTER 7

---

## Scenario analysis for programmatic tuberculosis control in Bangladesh: A mathematical modelling study

---

### Statement of joint authorship

**Md Abdul Kuddus** initiated the concept of the study, wrote the manuscript, developed the model, analysed the data, wrote code for the model, and acted as corresponding author.

**Michael T. Meehan** assisted with the development of the model, proof read and critically reviewed the manuscript.

**Md. Abu Sayem** critically reviewed the manuscript.

**Emma S. McBryde** assisted with the development of the model and code, proof read and critically reviewed the manuscript.

**Kuddus, M. A., Meehan, T. M., Sayem, A., McBryde, E. S. (2021).** Scenario analysis for programmatic tuberculosis control in Bangladesh: A mathematical modelling study. *Scientific Reports*, 11(1), 4354.

## Abstract

Tuberculosis (TB) is a major public health problem in Bangladesh. Although the National TB control program (NTP) of Bangladesh is implementing a comprehensive expansion of TB control strategies, logistical challenges exist, and there is significant uncertainty concerning the disease burden. Mathematical modelling of TB is considered one of the most effective ways to understand the dynamics of infection transmission and allows quantification of parameters in different settings, including Bangladesh. In this study, we present a two-strain mathematical modelling framework to explore the dynamics of drug-susceptible (DS) and multidrug-resistant (MDR) TB in Bangladesh. We calibrated the model using DS and MDR-TB annual incidence data from Bangladesh from years 2001 to 2015. Further, we performed a sensitivity analysis of the model parameters and found that the contact rate of both strains had the largest influence on the basic reproduction numbers  $R_{0s}$  and  $R_{0m}$  of DS and MDR-TB, respectively. Increasingly powerful intervention strategies were developed, with realistic impact and coverage determined with the help of local staff. We simulated for the period from 2020 to 2035. Here, we projected the DS and MDR-TB burden (as measured by the number of incident cases and mortality) under a range of intervention scenarios to determine which of these scenario is the most effective at reducing burden. Of the single-intervention strategies, enhanced case detection is the most effective and prompt in reducing DS and MDR-TB incidence and mortality in Bangladesh and that with GeneXpert testing was also highly effective in decreasing the burden of MDR-TB. Our findings also suggest combining additional interventions simultaneously leads to greater effectiveness, particularly for MDR-TB, which we estimate requires a modest investment to substantially reduce, whereas DS-TB requires a strong sustained investment.

**Keywords:** Tuberculosis, mathematical model, sensitivity and scenario analysis

## 7.1 Introduction

Tuberculosis (TB) kills more people each year than any other infectious disease, including HIV and malaria, making it one of the primary global health problems [1]. In 2019, the WHO estimated there were approximately 10.0 million new cases of TB, and 1.2 million died from TB disease. Most of the estimated cases in 2019 occurred in Asia (44%) and Africa (24%) and 87% of tuberculosis deaths occurred in low and middle-income countries [1]. A significant proportion of cases occurred in the Western Pacific region (18%), with the Eastern Mediterranean region (8%), the European region (3%) and the Americas region (3%) also contributing small proportions [1]. Worldwide there is an imbalance in case notification between males (5.6 million new cases in 2010) and females (3.2 million new cases in 2010), which may have many causes, including missed cases. Childhood TB is often missed, as classical diagnosis with sputum smear is insensitive [2].

In recent years, antibiotic resistance to the most effective treatments (first-line combination therapies) has emerged and spread. This has led to a decline in the efficacy of antibiotics used to treat TB, with drug-resistant (DR) TB patients experiencing much higher failure rates. The treatment regime for DR patients is more expensive than it is for DS patients and the diagnosis for DR patients is difficult – especially in low- and middle-income countries. As a result, the DR- TB mortality rate is much higher than that of DS-TB [3].

There are two ways DR-TB can develop: one is called amplification; and the other is primary transmission. Amplification develops mainly through naturally-occurring mutations and inappropriate treatment [4]. Once preliminary resistance has been established, acquisition of further resistance to supplementary drugs becomes more likely as treatment with standard regimens may be suboptimal.

Primary transmission is when an individual with DR-TB directly infects a susceptible individual. Primary transmission was initially not expected to contribute significantly to the overall DR-TB burden due to the reduced fitness/transmissibility of DR organisms [5]. However, subsequent evolution and compensatory mutations can restore fitness in the absence or presence of antimicrobials [6]. The WHO recommends that timely identification of DR-TB and adequate treatment regimens with second-line drugs administered early in the course of the disease are essential to stop primary transmission [1].

Currently, multidrug-resistant (MDR) TB is emerging as the greatest threat to TB control globally [1]. MDR-TB is defined as TB that is resistant to both isoniazid and rifampicin (the two most effective and commonly used first-line drugs) with or without resistance to additional first-line drugs. Cohort studies within programs of TB treatment estimate that approximately 1% of a treated population who begin with a susceptible organism will develop MDR-TB [7]. Once these new MDR-TB cases have emerged in the community, they are capable of spreading the infection through primary transmission, further contributing to the growing pool of MDR cases. Therefore, control of MDR-TB requires the prevention of both acquired drug resistance and subsequent transmission as well as effective diagnosis and treatment for those cases that do emerge [8].

The highest burden of TB is not surprisingly in regions where health systems are weak. In 2015, the WHO recognised 22 high burden countries according to their actual number of TB cases [9]. Among these is Bangladesh, a country where poverty, high population densities, and malnutrition are commonplace, creating a favorable environment for TB outbreaks. Furthermore, TB treatment compliance is poor in Bangladesh – presumably as a result of the extensive period of therapy – leading to a rise in the number of TB cases [10]. Each year it is estimated that 70,000 people die of TB and 300,000 new cases appear in Bangladesh [2]. Prior to 2014, the case notification rates per 100,000 population were 68 and 122 for new smear-positive cases (i.e. cases that are usually more infectious and have a higher mortality) and all forms of TB cases respectively, but by the end of 2014 the number of all types of TB cases had increased, with a substantial increase in the number of extra-pulmonary cases due to better case detection [10].

In Bangladesh, the NTP aims to sustain the global targets of achieving at least 70% case detection and 85% treatment success among new smear-positive TB cases for the whole country. The overall progress in case finding was slow and steady until 2016 reaching a case notification rate 138 per 100,000 population. The NTP achieved its objectives in effective treatment, case detection and overall management through partnership with other public and private health care providers, engaging all care providers (GO-NGOs) and making available free diagnostic and treatment support, particularly for DS-TB [11]. By 2003, the treatment success rate of this program reached the targeted 85% and has been maintained at 90% since 2005. In 2013, the program successfully treated 94% of notified new smear-positive cases and the case detection rate was about 58% [12].

Mathematical models can improve our understanding of the epidemiology of TB as well as those components that are significant to TB diagnosis, treatment, and control [13-18]. Mathematical models are also useful for simulating different interventions and “what if” scenarios that would otherwise be infeasible in clinical trials due to ethical/logistical/practical concerns. These tools inspire researchers to

eliminate trial and error methods and direct them towards rational, evidence-based decisions [19-24]. For example, Okuonghae and Ikhimwin (2015) developed a realistic compartmental transmission dynamic TB model [25]. According to the awareness level of the population, Okuonghae and Ikhimwin model divided susceptible persons into two groups; the high risk group (low level of awareness), and low risk group (high level of awareness), and incorporated an active case finding parameter. This study showed that TB treatment alone may not significantly reduce TB burden at the community level but if we take two or more interventions together, such as treatment, awareness and active case finding, then it may be possible to reduce TB burden. Kim *et al.* (2014) developed a mathematical model for TB with exogenous reinfection and examined the current situation of active TB incidence in Korea [22]. The results showed that case detection was the most important intervention for decreasing active TB cases and demonstrated that treatment or case discovery alone will not dramatically affect the decline in active TB incidence. Okuonghae and Omosigho (2011) developed a qualitative and quantitative approach to a transmission dynamic TB mathematical model in Benin City, Nigeria [26]. This study showed that developing a TB awareness program and also increasing the active cough identification rate decreased the TB burden in the population, ultimately bringing down the basic reproduction number under unity. Furthermore, mutually raising the TB consciousness program and the raising or lowering of the cost of treatment in recognized cases can also decrease the basic reproduction number below unity [26].

In a previous TB modelling study [27] we investigated the cost-effectiveness of time-varying combinations of different intervention strategies including distancing (which contains individual respiratory protection, environmental protection, diagnosis campaigns, and public awareness through education curricula), latent case finding (this contains chemoprophylaxis treatment, screening for high-risk exposure and additional procedures of latent TB treatment), case holding (this includes to actions that guarantee treatment completion to decrease relapse following treatment), and active case finding (this refers the prevention of disease progress with effective treatment for exposed individuals or identification of active TB cases) using an optimal control framework. This study found that for the single intervention strategy, the distancing control strategy is the most cost-effective for reducing the number of DS and MDR-TB cases in Bangladesh. However, the main finding of this study was that the combination of all intervention strategies is the most cost-effective.

In this paper we examine less-idealized strategies developed in partnership with the Bangladeshi National TB program. Specifically, we project the future outcomes of four specific intervention strategies: increased case detection proportion, improved drug-susceptibility testing and increased DS and MDR-TB treatment success, to assess the effect of these responses on our proposed TB model during the period from 2020 to 2035. Here, we additionally considered important parameters including

the drug-susceptibility testing rate and reproductive fitness cost of MDR-TB that are not considered in the previous study [27].

Finally, in this study we considered a two-strain TB model to describe the transmission dynamics of DS and MDR-TB in Bangladesh. The model is calibrated to the Bangladesh demographic and DS and MDR-TB annual incidence data from years 2001 to 2015 to estimate the key transmission and fitness cost parameters. Multiple intervention strategies were considered to explore the impact of each on its own and when combined on DS and MDR-TB incidence and mortality. This study depicts Bangladesh-specific elimination policies and describes the results of different levels of investment in future on TB control: business as usual, modest investment (low and higher), strong investment for five years and sustained investment.

This paper is structured as follows: Section 7.2 describes the model. Model calibration and sensitivity analysis are performed in Sections 7.3 and 7.4, respectively. In Section 7.5, we investigate four different types of intervention scenarios. A brief discussion and concluding remarks finalize the paper.

## 7.2 Model description

We developed a deterministic mathematical model of the transmission of DS and MDR-TB strains between the following mutually exclusive compartments: susceptibles  $S(t)$ , uninfected individuals who are susceptible to TB infection; those exposed to TB and latently infected  $L(t)$ , representing those who are infected and have not yet developed active TB; infectives  $I(t)$ , comprising individuals with active TB who are infectious; the recovered  $R(t)$ , who were previously infected and successfully cleared the infection through treatment or natural recovery. We use the subscripts  $s$  and  $m$  to denote DS-TB and MDR-TB quantities respectively.

The total population size,  $N(t)$ , is given by

$$N(t) = S(t) + L_s(t) + I_s(t) + L_m(t) + I_m(t) + R(t) = N. \quad (7.1)$$

$N$  is assumed to be constant and individuals mix randomly.

To assure the population size remains constant, we replace all deaths as newborns in the susceptible compartment. This involves death through natural causes, which occurs in all states at the constant per-capita rate  $\mu$ , and TB-related deaths, which happen at the same constant per-capita rate  $\phi$  for individuals in the  $I_s$  and  $I_m$  compartments. Individuals may also return to the susceptible compartment following

recovery at the constant per-capita rate  $\omega$ . Individuals enter the susceptible compartment at a constant rate  $\mu$  through birth, where they may be infected with a circulating MTB strain at a time-dependent rate  $\lambda_i(t) = \beta I_i(t)$  [27]. Here,  $\beta$  is the probability of a susceptible individual being infected with MTB strain  $i$  ( $i = s, m$ ) by an untreated infectious individual per day [27]. A proportion  $\beta I_s(t)S(t)$  and  $(1 - c)\beta I_m(t)S(t)$  of the MTB susceptible individuals move to the latently infected compartment  $L_s(t)$  and  $L_m(t)$  respectively. Here,  $c$  represents the MDR-TB fitness cost. We assumed that MDR-TB is initially generated through the inadequate treatment of DS-TB and could subsequently be transmitted to other individuals.

A proportion of latently infected individual's progress to active TB as a result of endogenous reactivation of the latent bacilli at rates  $\alpha$ . Moreover, since latently infected individuals have acquired partial immunity which reduces the risk of subsequent infection, a proportion also move to the susceptible compartment  $S(t)$  at the constant per-capita rates  $\eta_i$  ( $i = s, m$ ). This rate can be accelerated by treatment of latent TB. Some infectious TB cases will undergo spontaneous recovery at a rate  $\gamma$ , while others will die from TB-related causes at a rate,  $\varphi$ . The remaining individuals with drug-sensitive and MDR active TB  $I_i(t)$  will eventually be detected and treated at rates  $\delta$  and  $\tau_i$  ( $i = s, m$ ) respectively. A proportion  $\delta\tau_s$  of the treated DS active TB recover to move into the recovered compartment  $R(t)$ , and a proportion of amplification ( $\rho$ ) develops multi-drug resistance due to incomplete treatment or lack of strict compliance in the use of first-line drugs (drugs used to treat the DS forms of TB) to move into compartment  $I_m(t)$ .

To confirm MDR-TB drug-susceptibility testing ( $\kappa$ ) is required, therefore a proportion  $\delta\kappa\tau_m$  of MDR active TB cases recover to move to the recovered compartment  $R(t)$ . Furthermore, a proportion  $\gamma_s$  and  $\gamma_m$  of individuals in compartments  $I_s(t)$  and  $I_m(t)$  naturally recover into  $R(t)$ . A per-capita rate  $\omega$  from the recovered compartment  $R(t)$  move into the completely susceptible compartment  $S(t)$  due to the loss of immunity. The model flow diagram is presented in Figure 7.1.

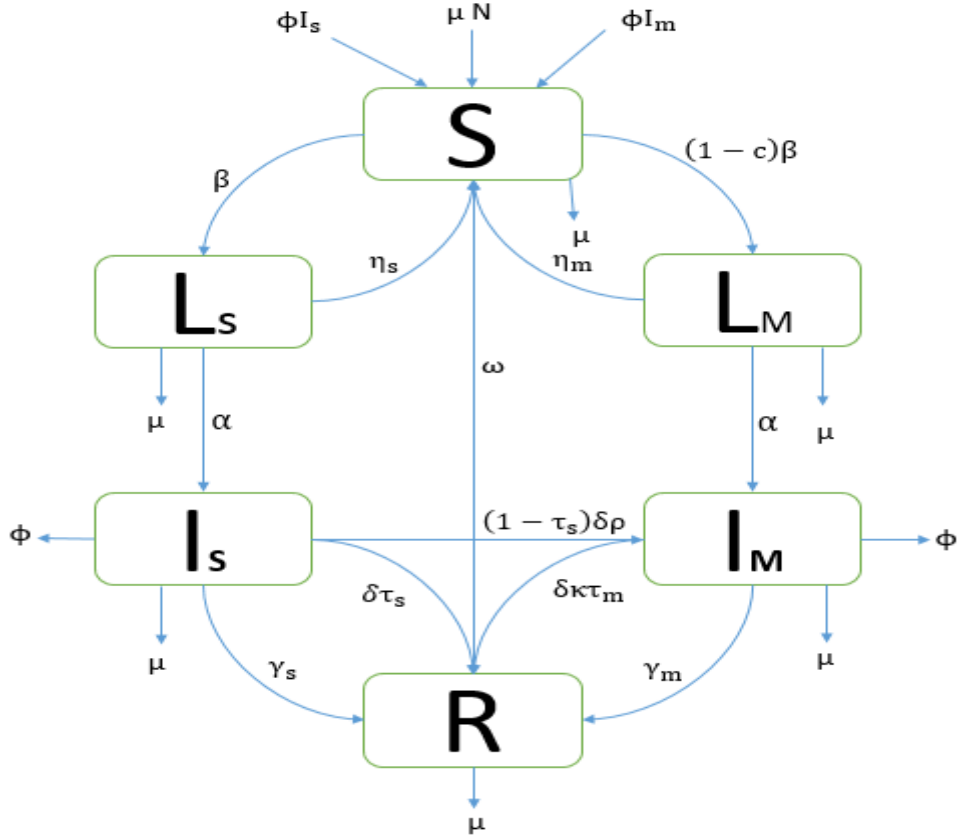


Figure 7. 1 Schematic diagram of TB model for Bangladesh TB setting.

From the aforementioned, the system dynamics are governed by the following deterministic set of nonlinear ordinary differential equations:

$$\begin{aligned}
 \frac{dS}{dt} &= \mu N - \beta I_S S - (1 - c)\beta I_M S - \mu S + \omega R + \phi I_S + \phi I_M + \eta_S L_S + \eta_M L_M, \\
 \frac{dL_S}{dt} &= \beta I_S S - \alpha L_S - \mu L_S - \eta_S L_S, \\
 \frac{dI_S}{dt} &= \alpha L_S - \gamma_S I_S - \mu I_S - \delta \tau_S I_S - \phi I_S - (1 - \tau_S)\delta \rho I_S, \\
 \frac{dL_M}{dt} &= (1 - c)\beta I_M S - \alpha L_M - \mu L_M - \eta_M L_M, \\
 \frac{dI_M}{dt} &= \alpha L_M - \gamma_M I_M - \mu I_M + (1 - \tau_S)\delta \rho I_S - \phi I_M - \delta \kappa \tau_M I_M, \\
 \frac{dR}{dt} &= \gamma_S I_S + \gamma_M I_M + \delta \tau_S I_S + \delta \kappa \tau_M I_M - \omega R - \mu R.
 \end{aligned} \tag{7.2}$$

### 7.2.1 Basic reproduction numbers

The basic reproduction number is well defined as the expected number of secondary cases created by a single infectious case introduced into a totally susceptible population. A disease can spread in a population only if the basic reproduction number is greater than one. An epidemic occurs when an

infection spreads through and infects a significant proportion of a population. A disease-free population is possible when the basic reproduction number is less than one, which means that the disease naturally fades-out [28, 29]. Here, we used the next-generation matrix method [30] to estimate the basic reproduction numbers in our proposed model. The model has four infected states:  $L_s, I_s, L_m, I_m$ , and two uninfected states:  $S$  and  $R$ . At the infection-free steady state  $L_s^0 = I_s^0 = L_m^0 = I_m^0 = R^0 = 0$ , hence  $S^0 = N$ . Since the total population size is constant, the only occurrence of the variable  $S$  in equations ( $L_s, I_s, L_m, I_m$ ), are either directly or implicitly via  $N$ . To calculate the basic reproduction numbers of the DS and MDR-TB strains we follow [31] and focus on the linearized infection subsystem derived from equations (7.2):

$$\begin{aligned}\frac{dL_s}{dt} &= \beta I_s S - \psi_s L_s, \\ \frac{dI_s}{dt} &= \alpha L_s - \chi_s I_s, \\ \frac{dL_m}{dt} &= (1 - c)\beta I_m S - \psi_m I_m, \\ \frac{dI_m}{dt} &= \alpha L_m - \chi_m I_m + (1 - \tau_s)\delta\rho I_s\end{aligned}\tag{7.3}$$

where  $\psi_s = \alpha + \mu + \eta_s$ ,  $\psi_m = \alpha + \mu + \eta_m$ ,  $\chi_s = \gamma_s + \mu + \delta\tau_s + \phi + (1 - \tau_s)\delta\rho$  and

$$\chi_m = \gamma_m + \mu + \delta\kappa\tau_m + \phi.$$

We refer to the ODEs (7.3) as the infection subsystem, as it only describes the production of new infected individuals and changes in the states of existing infected individuals. If we set  $\mathbf{X} = (L_s, I_s, L_m, I_m)^T$ , where  $T$  denotes transpose, we now want to write the infection subsystem in the form

$$\dot{\mathbf{X}} = (T + \Sigma)\mathbf{X}.\tag{7.4}$$

The matrix  $T$  corresponds to transmissions and the matrix  $\Sigma$  to transitions. They are obtained from system (7.3) by separating the transmission events from other events: if we refer to the infected states with indices  $i$  and  $j$ , with  $i, j \in 1, 2, 3, 4$ , then entry  $T_{ij}$  is the rate at which individuals in infected state  $j$  give rise to individuals in infected state  $i$  in the system. For the subsystem (7.3) we obtain

$$T = \begin{pmatrix} 0 & \beta N & 0 & 0 \\ 0 & 0 & 0 & 0 \\ 0 & 0 & 0 & (1 - c)\beta N \\ 0 & 0 & 0 & 0 \end{pmatrix} \text{ and } \Sigma = \begin{pmatrix} -\psi_s & 0 & 0 & 0 \\ \alpha & -\chi_s & 0 & 0 \\ 0 & 0 & -\psi_m & 0 \\ 0 & (1 - \tau_s)\delta\rho & \alpha & -\chi_m \end{pmatrix}.$$

Hence, the Next-Generation Matrix  $K$  is four-dimensional, and given by (note the essential minus sign)

$$K = -T\Sigma^{-1} = T(-\Sigma^{-1}),$$

$$= \begin{pmatrix} \frac{N\alpha\beta}{\Psi_s\chi_s} & \frac{N\beta}{\chi_s} & 0 & 0 \\ 0 & 0 & 0 & 0 \\ \frac{N\delta\rho(c-1)(\tau_s-1)}{\Psi_s\chi_s\chi_m} & \frac{N\beta\delta\rho(c-1)(\tau_s-1)}{\chi_s\chi_m} & \frac{-N\alpha\beta(c-1)}{\Psi_m\chi_m} & \frac{-N\beta(c-1)}{\chi_m} \\ 0 & 0 & 0 & 0 \end{pmatrix}$$

$$= \begin{pmatrix} A & B \\ C & D \end{pmatrix}$$

where  $A = \begin{pmatrix} \frac{N\alpha\beta}{\Psi_s\chi_s} & \frac{N\beta}{\chi_s} \\ 0 & 0 \end{pmatrix}$ ,  $B = \begin{pmatrix} 0 & 0 \\ 0 & 0 \end{pmatrix}$ ,  $C = \begin{pmatrix} \frac{N\delta\rho(c-1)(\tau_s-1)}{\Psi_s\chi_s\chi_m} & \frac{N\beta\delta\rho(c-1)(\tau_s-1)}{\chi_s\chi_m} \\ 0 & 0 \end{pmatrix}$  and

$$D = \begin{pmatrix} \frac{-N\alpha\beta(c-1)}{\Psi_m\chi_m} & \frac{-N\beta(c-1)}{\chi_m} \\ 0 & 0 \end{pmatrix}.$$

Now

$$\det(K) = \det(A)\det(D - CA^{-1}B),$$

$$= \det(A)\det(D).$$

The dominant eigenvalue of this matrix is equal to the basic reproduction number. In this system we have two dominant eigenvalues, one is for DS-TB and another is for MDR-TB, where

$$R_{0s} = \frac{N\alpha\beta}{\Psi_s\chi_s} = \frac{N\alpha\beta}{(\alpha+\mu+\eta_s)(\gamma_s+\mu+\delta\tau_s+\phi+(1-\tau_s)\delta\rho)} \quad (7.a)$$

and

$$R_{0m} = \frac{N\alpha\beta(1-c)}{\Psi_m\chi_m} = \frac{N\alpha\beta(1-c)}{(\alpha+\mu+\eta_m)(\gamma_m+\mu+\delta\kappa\tau_m+\phi)}. \quad (7.b)$$

The strain-specific reproduction numbers  $R_{0s}$  and  $R_{0m}$  regulate whether a particular strain will persist or fade out from the population in relation to the other strain. Figure 7.2 (A) shows that TB disease will eventually die out from the population when the condition  $\max[R_{0s}, R_{0m}] < 1$  holds. The condition  $R_{0m} > \max[R_{0s}, 1]$  implies that DS-TB dies out but MDR-TB persists in the population (see Figure 7.2 (B)). Finally, the condition  $R_{0s} > \max[R_{0m}, 1]$  implies that both DS-TB and MDR-TB persist in the population (see Figure 7.2 (C)).

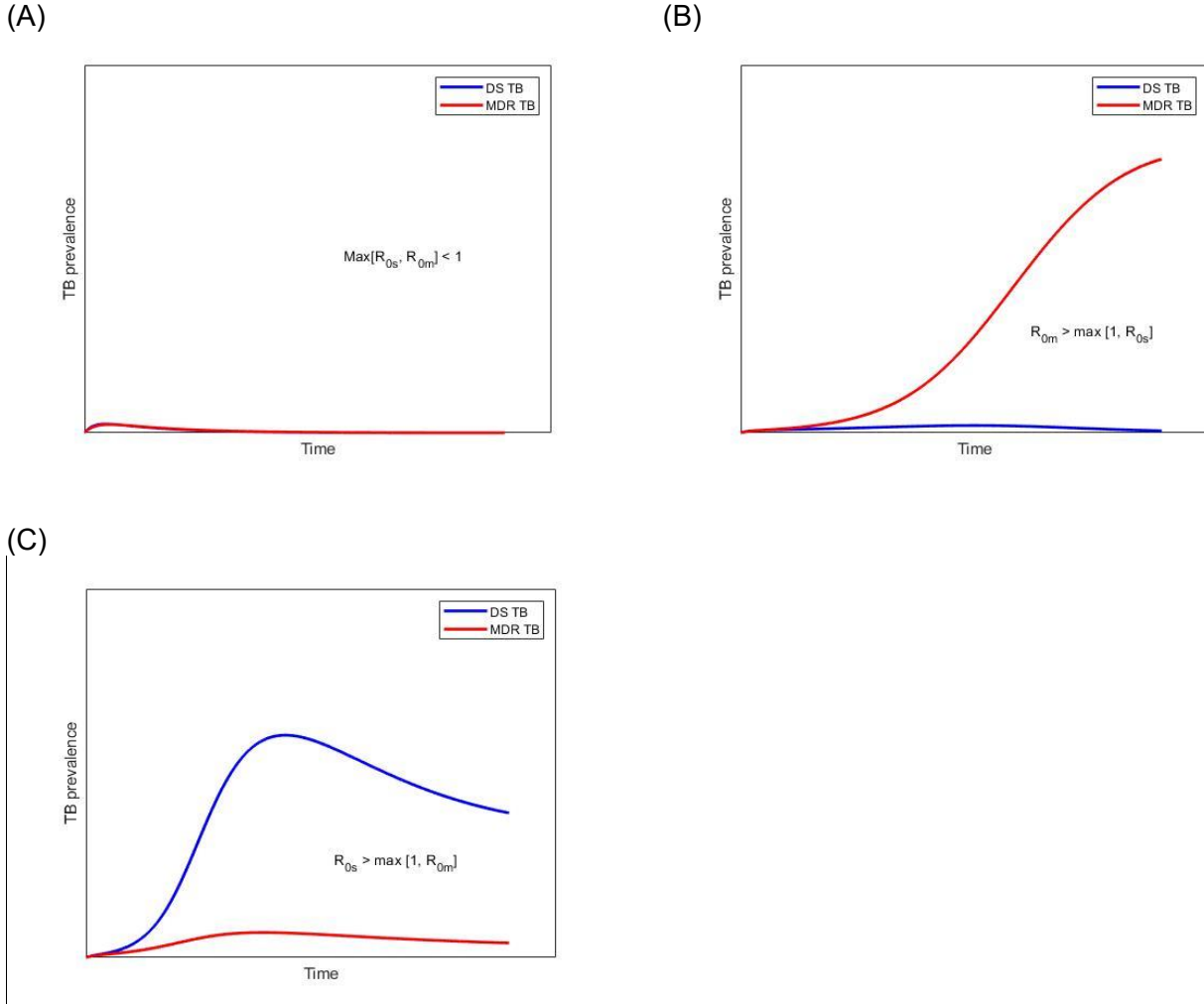


Figure 7. 2 The effects of the strain-specific basic reproduction number on the dynamics of model (7.2).

### 7.3 Estimation of model parameters

In this section, we estimated the model parameters based on DS and MDR-TB annual incidence data taken from the World Health Organization (WHO) report from 2001 to 2015. In order to fully parameterise the TB model (7.2), we obtained some of the parameter values from the literature (Table 7.1), and the rest of the model parameters were estimated using the least-squares fitting method which provides a better fit of the model solution to the annual DS and MDR-TB incidence data (Figure 7.3). The objective function used in the parameter estimation is as follows

$$\hat{\theta} = \operatorname{argmin} \sum_{i=1}^n \left( \int_{t_i}^{t_i+1} (\alpha L_s(t')) dt' - \text{data}_{t_{ip}} \right)^2, \text{ and}$$

$$\hat{\theta}_1 = \operatorname{argmin} \sum_{i=1}^n \left( \int_{t_i}^{t_i+1} ((1 - \tau_s) \delta \rho I_s(t') + \alpha L_m(t')) dt' - \text{data}_{t_{iq}} \right)^2,$$

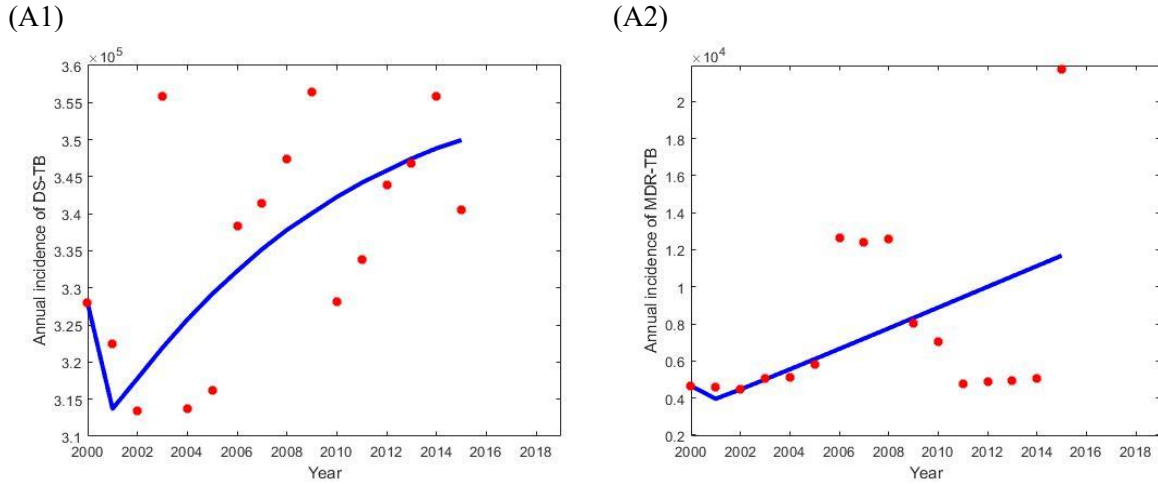


Figure 7. 3 Reported Bangladesh TB annual incidence data as estimated The WHO (red dots) and the corresponding best fit (blue solid curve): (left) drug-susceptible (DS) TB and (right) multidrug-resistant (MDR) TB.

where  $data_{t_{ip}}$  and  $data_{t_{iq}}$  denote the DS and MDR-TB annual incidence data respectively and  $\int_{t_i}^{t_i+1} (\alpha L_s(t')) dt'$  and  $\int_{t_i}^{t_i+1} ((1 - \tau_s) \delta \rho I_s(t') + \alpha L_m(t')) dt'$  are the corresponding model solution at time  $t_i$  respectively, while  $n$  is the number of available actual data points. The associated parameters of the model (7.2) are tabulated in Table 7.1. We assume the initial condition for the state variables are,  $N(0) = 159,000,000$ ,  $I_s(0) = 205,899$ ,  $L_s(0) = \frac{\beta I_s(0) N(0)}{(\alpha + \eta_s + \mu)} = 759,908$ ,  $I_m(0) = L_m(0) = 1,100$ ,  $\frac{(1-c)\beta I_m(0) N(0)}{(\alpha + \eta_m + \mu)} = 2,273$ ,  $R(0) = 0$  and  $S(0) = N(0) - L_s(0) - I_s(0) - L_m(0) - I_m(0) - R(0)$ .

Table 7. 1 List of parameters, symbols, plausible values, units and references.

Parameters Name	Symbol	Value	Units	References
Bangladesh population in 2015	$N$	159,000,000		[12]
Bangladesh birth / death rate	$\mu$	$\frac{1}{70}$	year <sup>-1</sup>	[32]
Transmission rate	$\beta$	$9.424 \times 10^{-8}$	year <sup>-1</sup>	fitted
MDR-TB fitness cost	$c$	0.45		fitted
Progression rate from L to I	$\alpha$	0.40	year <sup>-1</sup>	[33]
Natural recovery rate for DS-TB	$\gamma_s$	0.233	year <sup>-1</sup>	[34]
Natural recovery rate for MDR-TB	$\gamma_m$	0.233	year <sup>-1</sup>	[34]
TB related death rate	$\phi$	0.39	year <sup>-1</sup>	[34]
Treatment rate for DS-TB	$\tau_s$	0.94	year <sup>-1</sup>	[35]

Treatment rate for MDR-TB	$\tau_m$	0.78	year <sup>-1</sup>	[35]
Proportion of amplification	$\rho$	0.07		[36]
Rate of losing immunity	$\omega$	0.10	year <sup>-1</sup>	[18]
Progression rate from L <sub>s</sub> to S	$\eta_s$	3.65	year <sup>-1</sup>	[33]
Progression rate from L <sub>m</sub> to S	$\eta_m$	3.65	year <sup>-1</sup>	[33]
Detection rate	$\delta$	0.87	year <sup>-1</sup>	Default fitted to ensure proportion detected fits with WHO reported rates
Drug-susceptibility testing rate	$\kappa$	0.18	year <sup>-1</sup>	[35]

### Calculation of the detection rate ( $\delta$ ):

We use the case detection proportion reported by [37] to inform  $\delta$ . This measure is often referred to as the “case detection rate” (CDR) by WHO although it is actually a proportion. For the model presented in Figure 7.2, the CDR is given by

$$\text{CDR} = \frac{\delta}{\gamma_s + \phi + \mu + \delta}$$

which we can rearrange to obtain

$$\delta = \frac{\text{CDR}}{(1-\text{CDR})} (\gamma_s + \phi + \mu) = \frac{0.578558011}{(1-0.578558011)} \left(0.233 + 0.39 + \frac{1}{70}\right) = 0.87,$$

$$\text{where CDR} = \frac{\text{Number of detected I}}{\text{Number of I}} = \frac{209438}{362000} = 0.578558011[37].$$

## 7.4 Sensitivity analysis

Sensitivity analysis is used to measure the degree of adequacy of our proposed model and determine which parameters impact on the model outputs [38, 39]. Here, we considered the partial rank correlation coefficient (PRCC), a global sensitivity analysis metric to explore the influence of model parameters on the model outcomes [39, 40]. To calculate the PRCC values, we employed the *Latin Hypercube Sampling* (LHS) technique (a stratified sampling without replacement technique which allows for an efficient analysis of parameter variation). Specifically, a uniform distribution is allocated from 0 to 3 times the baseline value for each model parameter and sampling is performed individually. A total of 1,000,000 simulations are implemented with sampled parameter values. In this analysis, the model outcomes we considered are the basic reproduction numbers  $R_{0s}$  and  $R_{0m}$ .

Figure 7.4 and Figure 7.5 depict the correlation between the basic reproduction numbers, namely  $R_{0s}$  and  $R_{0m}$ , and the corresponding model parameters. Parameters  $\beta$  and  $\alpha$  have positive PRCC values, implying that a positive change in these parameters (i.e. increasing transmission and progression rates)

will increase the basic reproduction numbers  $R_{0s}$  and  $R_{0m}$ . In contrast, parameters  $\phi, \delta, \gamma_s, \tau_s, \rho$  and  $\eta_s$  have negative PRCC values with  $R_{0s}$ , which implies that raising these parameters will consequently decrease  $R_{0s}$ . Further, parameters  $\phi, \delta, \gamma_m, \kappa, \tau_m, \eta_m$  and  $c$  have negative PRCC values with  $R_{0m}$ , which implies that increasing these parameters will consequently decrease  $R_{0m}$ . We observed that the effect of the transmission rate  $\beta$  has the largest influence on both  $R_{0s}$  and  $R_{0m}$ . Therefore, to control and eradicate DS and MDR-TB infection, it is important to minimize the transmission rate  $\beta$ .

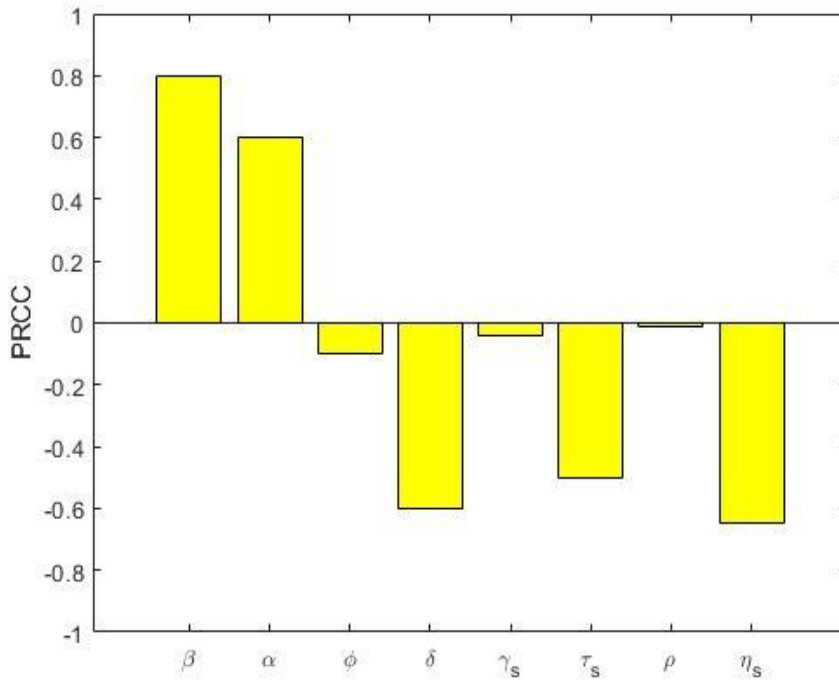


Figure 7. 4 PRCC values depicting the sensitivity of the drug-susceptible basic reproduction number  $R_{0s}$  with respect to the parameters  $\beta, \alpha, \phi, \delta, \gamma_s, \tau_s, \rho$  and  $\eta_s$ .

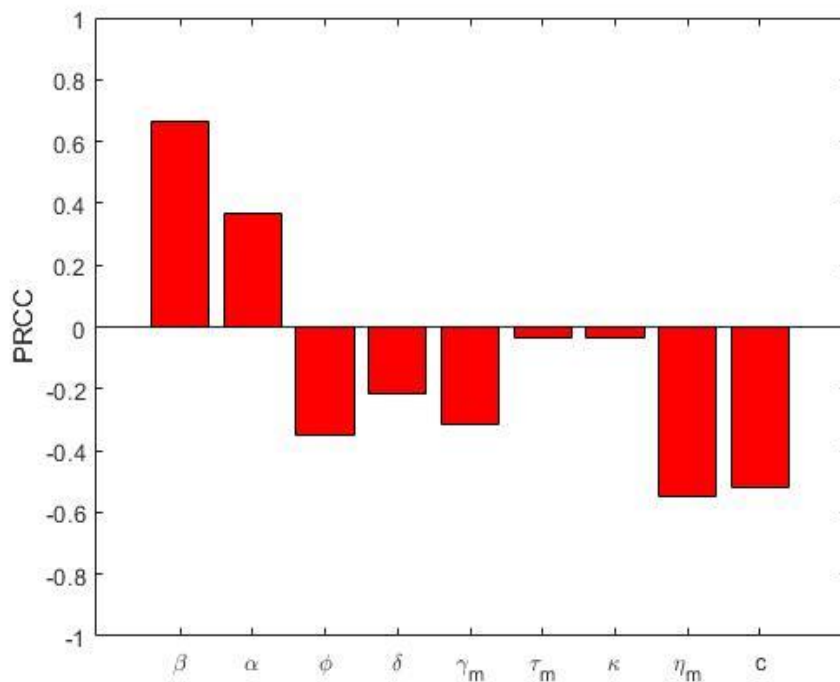


Figure 7. 5 PRCC values depicting the sensitivity of the drug-resistant basic reproduction number  $R_{0m}$  with respect to the parameters  $\beta$ ,  $\alpha$ ,  $\phi$ ,  $\delta$ ,  $\gamma_m$ ,  $\tau_m$ ,  $\kappa$ ,  $\eta_m$  and  $c$ .

From the explicit formulae for  $R_{0s}$  and  $R_{0m}$  given in equations (7.a)-(7.b), analytical expressions for the sensitivity indices to each of the parameters can be derived following the method in [41]. For example, for the parameter  $\beta$  we have:

$$\Upsilon_{\beta}^{R_{0s}} = \frac{\partial R_{0s}}{\partial \beta} \times \frac{\beta}{R_{0s}}$$

Now using the parameter values in Table 7.1, we have the following results (Table 7.2).

Table 7. 2 Sensitivity indices to parameters for the model (7.2).

Parameter	Sensitivity index ( $R_{0s}$ )	Parameter	Sensitivity index ( $R_{0m}$ )
$\beta$	+1.000	$\beta$	+1.000
$\alpha$	+0.902	$\alpha$	+0.902
$\phi$	-0.267	$\phi$	-0.514
$\delta$	-0.647	$\delta$	-0.161
$\gamma_s$	-0.160	$\gamma_m$	-0.307
$\tau_s$	-0.521	$\tau_m$	-0.161
$\rho$	-0.003	$\kappa$	-0.161
$\eta_s$	-0.898	$\eta_m$	-0.898
		$c$	-0.818

In the sensitivity indices of  $R_{0s}$  and  $R_{0m}$ , the most sensitive parameter is the effective contact rate ( $\beta$ ). Other significant parameters are the activation rate ( $\alpha$ ), and progression rates ( $\eta_s$  and  $\eta_m$ ), followed by fitness cost ( $c$ ). The least sensitive parameter is the amplification rate ( $\rho$ ). Increasing (or decreasing) the effective contact rate,  $\beta$  of DS-TB and MDR-TB by 100%, increases (or decreases) the reproduction numbers  $R_{0s}$  and  $R_{0m}$  by 100%. Similarly, increasing (or decreasing) the amplification rate ( $\rho$ ) of DS-TB by 100% decreases (or increases)  $R_{0s}$ , by 0.3%.

## 7.5 Scenario development and analysis

In this section, we developed multiple potential intervention scenarios in consultation with staff at the National TB Control Program (NTP) in Bangladesh. The input parameters in this study, over a 15-year time frame, included: detection proportion, DS and MDR-TB treatment rates, drug-susceptibility testing rate. Here, the detection proportion is improved through a combination of case finding strategies and improved knowledge of standard operating procedures for TB diagnosis and treatment commencement. Case finding is considered as identification of symptomatic patients attending a health facility, either of their own initiative or referred by another health facility, health worker, and community volunteer. These activities are assumed to progressively increase the detection proportion from baseline (58%) to 90%.

Further, DS and MDR-TB treatment rates are improved through infectious TB patients immediately seeking medical care and going to the health care facilities to undergo treatment. Programmatic management of drug-resistant TB (PMDT) is one of the most effective strategies for the control and prevention of DR-TB [42]. PMDT activities include proper management of contacts by ensuring that optimal treatment, a reliable drug supply and adequate health facilities are available [43]. Directly observed treatment, short-course (DOTS) is an important component in the internationally recommended policy package for TB control. During DOTS, a qualified practitioner observes the patient ingest their medication, which results in a demonstrable improvement in treatment rates and patient outcomes [35]. Accordingly, we assumed the DS and MDR-TB treatment rates progressively increased from (94% and 78%) to 100% and 95% successfully treated, respectively.

The efficient control of DS-TB and MDR-TB depends on rapid diagnosis, adequate and early initiation of treatment with the proper regimen, appropriate contact tracing, addressing adverse drug reaction and infection control measures in both facilities and communities. For diagnosis of MDR-TB, drug susceptibility testing plays a vital role which is also recommended by global policy makers through the

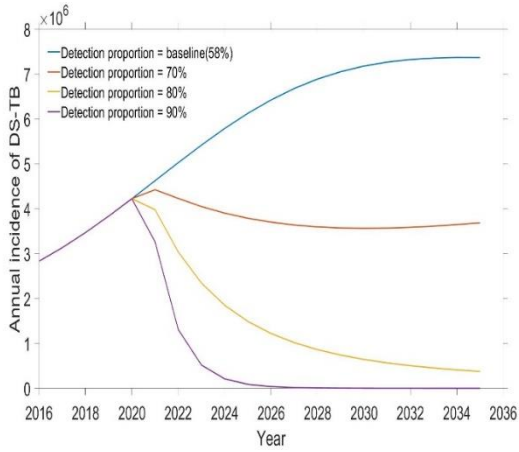
WHO's End TB Strategy. In Bangladesh, around 18% of facilities are covered with drug-susceptibility testing by Gene Xpert [35]. Therefore, we assumed the drug-susceptibility testing rate, which includes the criteria for resistance, progressively increasing from baseline (18%) to 100% successfully tested. Each category of intervention could involve several potential specific activities. For example, DS and MDR-TB treatments could include training of doctors, nurse and pharmacists on TB guidelines, monitoring and managing of supplies of high quality drugs. For each of these alternatives, the application of each separate intervention leads to a reduction in DS and MDR-TB incidence and mortality.

Here, we analyzed multiple potential intervention scenarios including four-single, and their combination (baseline, modest investment 1, modest investment 2, strong investment 5 years then revert to baseline, and strong sustained investment) to assess the effect of these responses on DS and MDR-TB incidence and mortality during the time period from 2020 to 2035. These scenarios are detailed in Table 7.3 and 7.4. We parameterized these proposed responses to our model structure to assess the effect of these responses during the time period 2020 – 2035.

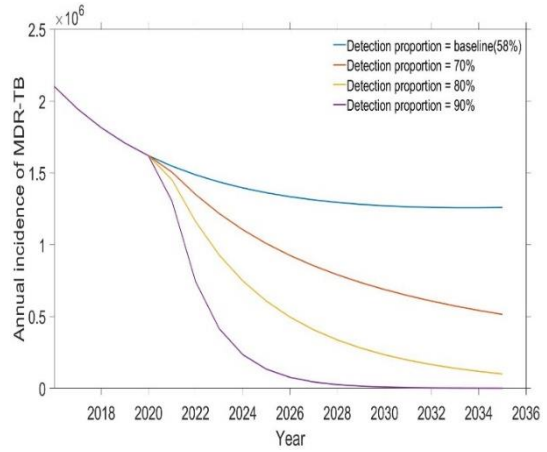
Single intervention strategy simulates a continuation from the baseline values of each intervention to the high expected quantity of the programmatic situation during the time period 2020-2035. During this time, we simulated four separate intervention strategies: increasing the detection proportion (from baseline of 58% incrementally up to 90%); increasing both the DS and MDR-TB treatment rates (from baselines of 94% to 100% and from baseline of 78% to 95% respectively); and improving the drug-susceptibility testing rate (from 18% to 100%). We implement these as single interventions and compare them with baseline (see Table 7.3 and Figures 7.6 and 7.7) to explore the impact of each intervention on DS and MDR-TB incidence and mortality.

Results from the first tier of single intervention strategies are presented in Table 7.3, Figure 7.6 and Figure 7.7. From this tier, we observed that amongst the four single interventions considered increasing the detection proportion is more effective than any other single intervention at reducing DS and MDR-TB incidence and mortality (see Table 7.3 and Figures 7.6 (A1 and A2) and Figure 7.7 (A1 and A2)) in Bangladesh. Alternatively, the DS-TB treatment rate is another option for reducing DS-TB but has adverse impact on MDR-TB. Similarly, increasing the drug-susceptibility testing rate is additional choice for reducing MDR-TB.

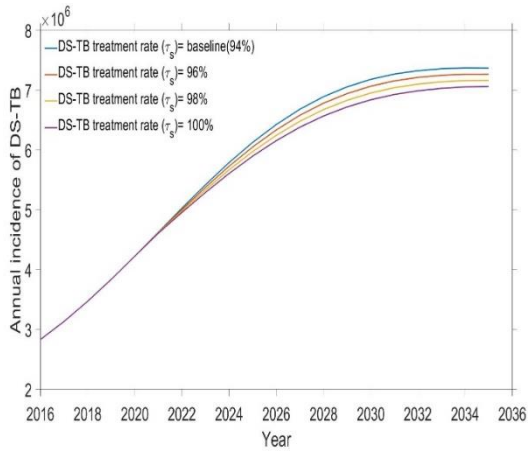
(A1)



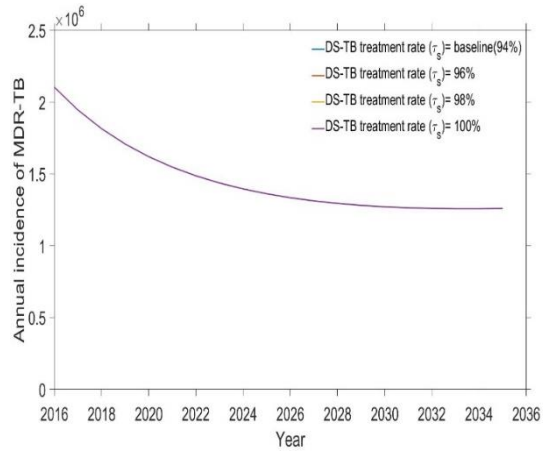
(A2)



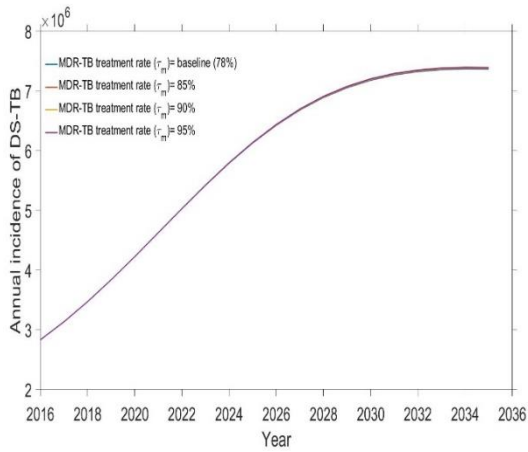
(B1)



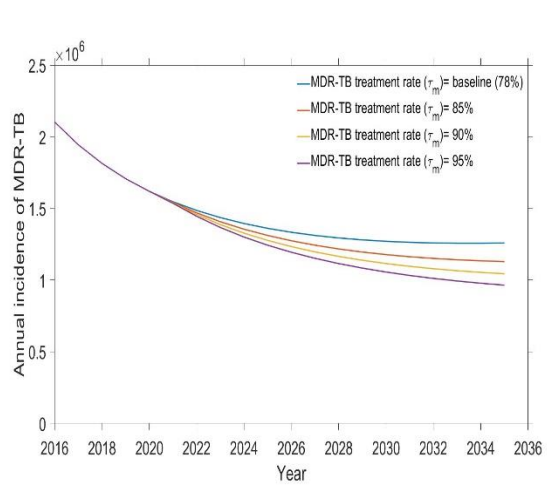
(B2)



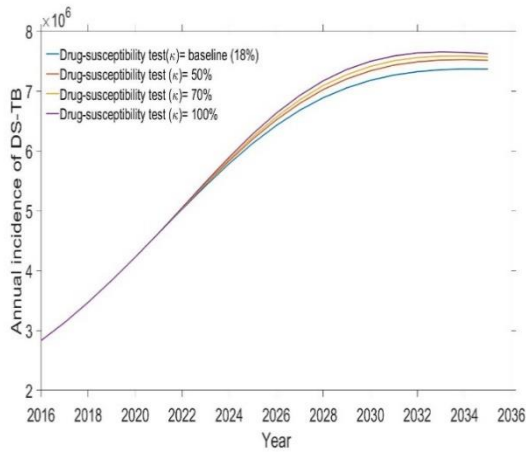
(C1)



(C2)



(D1)



(D2)

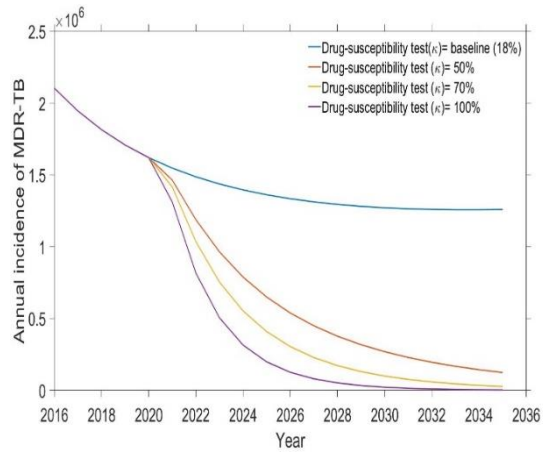
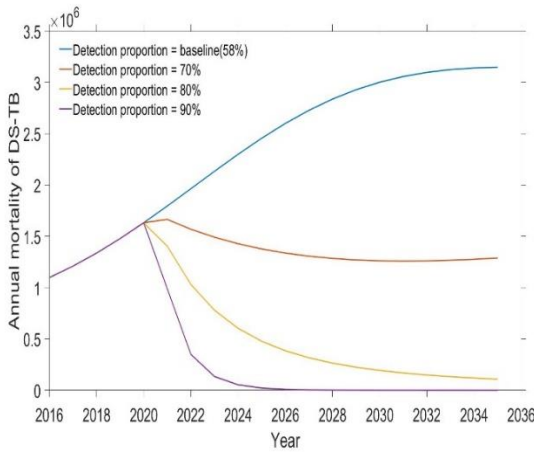


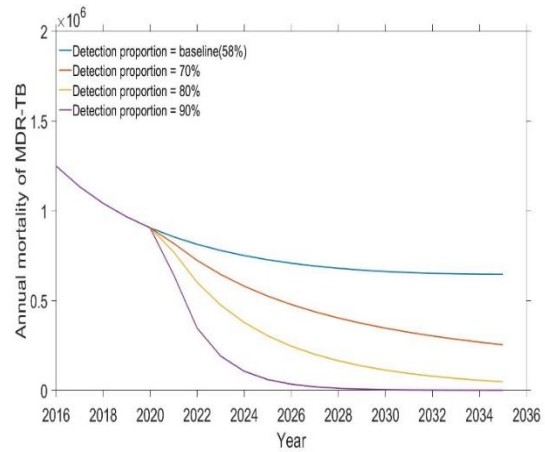
Figure 7. 6 Impact of the four single intervention strategies on TB burden.

Left-hand side DS-TB annual incidence and right-hand side MDR-TB annual incidence: (A1 & A2) varying detection rate, (B1 & B2) varying DS-TB treatment rate, (C1 & C2) varying MDR-TB treatment rate, and (D1 & D2) varying Drug-susceptibility testing rate.

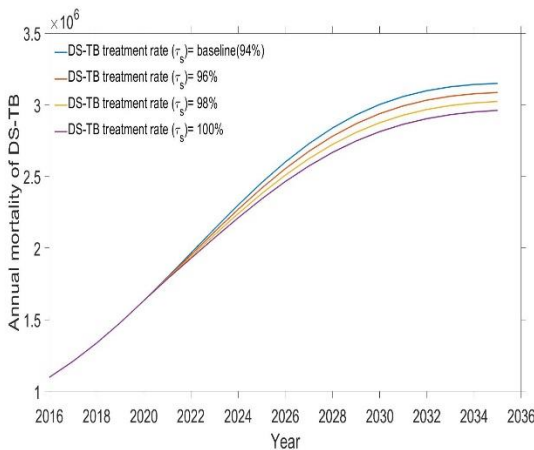
(A1)



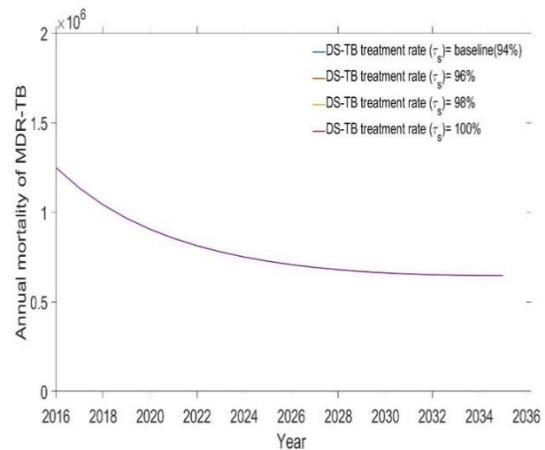
(A2)



(B1)



(B2)



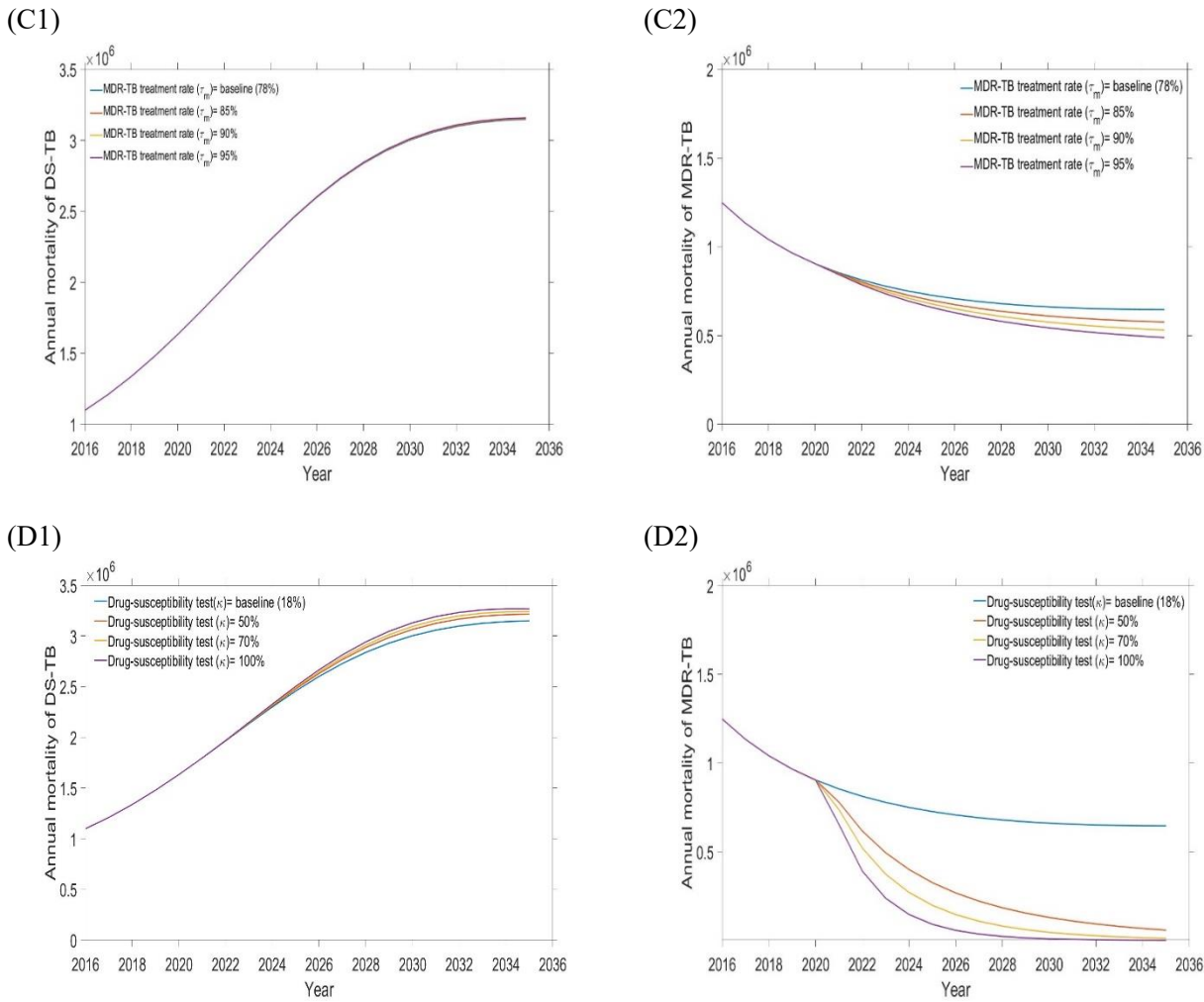


Figure 7. 7 Impact of the four single intervention strategies on TB mortality. Left-hand side DS-TB annual mortality and right-hand side MDR-TB annual mortality: (A1 & A2) varying detection rate, (B1 & B2) varying DS-TB treatment rate, (C1 & C2) varying MDR-TB treatment rate, and (D1 & D2) varying Drug-susceptibility testing rate.

Table 7. 3 Hypothetical single intervention strategy implemented in our proposed model of DS and MDR-TB control in Bangladesh, for the period 2020 – 2035.

Parameters	Parameter values	Estimated DS-TB annual incident cases	Reduction from baseline	Estimated MDR-TB annual incident cases	Reduction from baseline	Estimated DS- TB annual mortality	Reduction from baseline	Estimated MDR-TB annual mortality	Reduction from baseline
Proportion detected per year (CDR)	Baseline (58%)	$7.35 \times 10^6$	$0.00 \times 10^6$	$1.26 \times 10^6$	$0.00 \times 10^6$	$3.15 \times 10^6$	$0.00 \times 10^6$	$0.65 \times 10^6$	$0.00 \times 10^6$
	70%	$3.73 \times 10^6$	$3.62 \times 10^6$	$0.49 \times 10^6$	$0.77 \times 10^6$	$1.30 \times 10^6$	$1.85 \times 10^6$	$0.24 \times 10^6$	$0.41 \times 10^6$
	80%	$0.34 \times 10^6$	$7.01 \times 10^6$	$0.08 \times 10^6$	$1.18 \times 10^6$	$0.92 \times 10^4$	$3.14 \times 10^6$	$0.04 \times 10^6$	$0.61 \times 10^6$
	90%	$0.15 \times 10^2$	$7.35 \times 10^6$	$0.37 \times 10^3$	$1.26 \times 10^6$	$0.30 \times 10^1$	$3.15 \times 10^6$	$0.16 \times 10^3$	$0.65 \times 10^6$

DS-TB treatment success proportion	Baseline (94%)	$7.35 \times 10^6$	$0.00 \times 10^6$	$1.261608 \times 10^6$	$0.00 \times 10^6$	$3.15 \times 10^6$	$0.00 \times 10^6$	$0.656690 \times 10^6$	$0.00 \times 10^6$
	96%	$7.25 \times 10^6$	$0.10 \times 10^6$	$1.261610 \times 10^6$	$-0.02 \times 10^2$	$3.09 \times 10^6$	$0.06 \times 10^6$	$0.646691 \times 10^6$	$-0.1 \times 10^1$
	98%	$7.16 \times 10^6$	$0.19 \times 10^6$	$1.261612 \times 10^6$	$-0.04 \times 10^2$	$3.03 \times 10^6$	$0.12 \times 10^6$	$0.646692 \times 10^6$	$-0.2 \times 10^1$
	100%	$7.06 \times 10^6$	$0.29 \times 10^6$	$1.261614 \times 10^6$	$-0.06 \times 10^2$	$2.96 \times 10^6$	$0.19 \times 10^6$	$0.646693 \times 10^6$	$-0.3 \times 10^1$
MDR-TB treatment success proportion	Baseline (78%)	$7.35 \times 10^6$	$0.00 \times 10^6$	$1.26 \times 10^6$	$0.00 \times 10^6$	$3.15 \times 10^6$	$0.00 \times 10^6$	$0.65 \times 10^6$	$0.00 \times 10^6$
	85%	$7.36 \times 10^6$	$-0.01 \times 10^6$	$1.13 \times 10^6$	$0.13 \times 10^6$	$3.16 \times 10^6$	$-0.01 \times 10^6$	$0.57 \times 10^6$	$0.08 \times 10^6$
	90%	$7.37 \times 10^6$	$-0.02 \times 10^6$	$1.04 \times 10^6$	$0.22 \times 10^6$	$3.17 \times 10^6$	$-0.02 \times 10^6$	$0.53 \times 10^6$	$0.12 \times 10^6$
	95%	$7.38 \times 10^6$	$-0.03 \times 10^6$	$0.95 \times 10^6$	$0.31 \times 10^6$	$3.17 \times 10^6$	$-0.02 \times 10^6$	$0.48 \times 10^6$	$0.17 \times 10^6$
Proportion of frontline tests that have Drug-susceptibility testing	Baseline (18%)	$7.35 \times 10^6$	$0.00 \times 10^6$	$1.26 \times 10^6$	$0.00 \times 10^6$	$3.15 \times 10^6$	$0.00 \times 10^6$	$0.65 \times 10^6$	$0.00 \times 10^6$
	50%	$7.49 \times 10^6$	$-0.14 \times 10^6$	$0.11 \times 10^6$	$1.15 \times 10^6$	$3.21 \times 10^6$	$-0.06 \times 10^6$	$0.05 \times 10^6$	$0.60 \times 10^6$
	70%	$7.54 \times 10^6$	$-0.19 \times 10^6$	$0.02 \times 10^6$	$1.24 \times 10^6$	$3.24 \times 10^6$	$-0.09 \times 10^6$	$0.94 \times 10^4$	$0.64 \times 10^6$
	100%	$7.58 \times 10^6$	$-0.23 \times 10^6$	$0.17 \times 10^4$	$1.25 \times 10^6$	$3.26 \times 10^6$	$-0.11 \times 10^6$	$0.73 \times 10^3$	$0.65 \times 10^6$

We next considered the combination of all four single-intervention strategies implemented simultaneously. Table 7.4, Figure 7.8 and Figure 7.9 present the outcomes for 5 combination strategies of incremental strength:

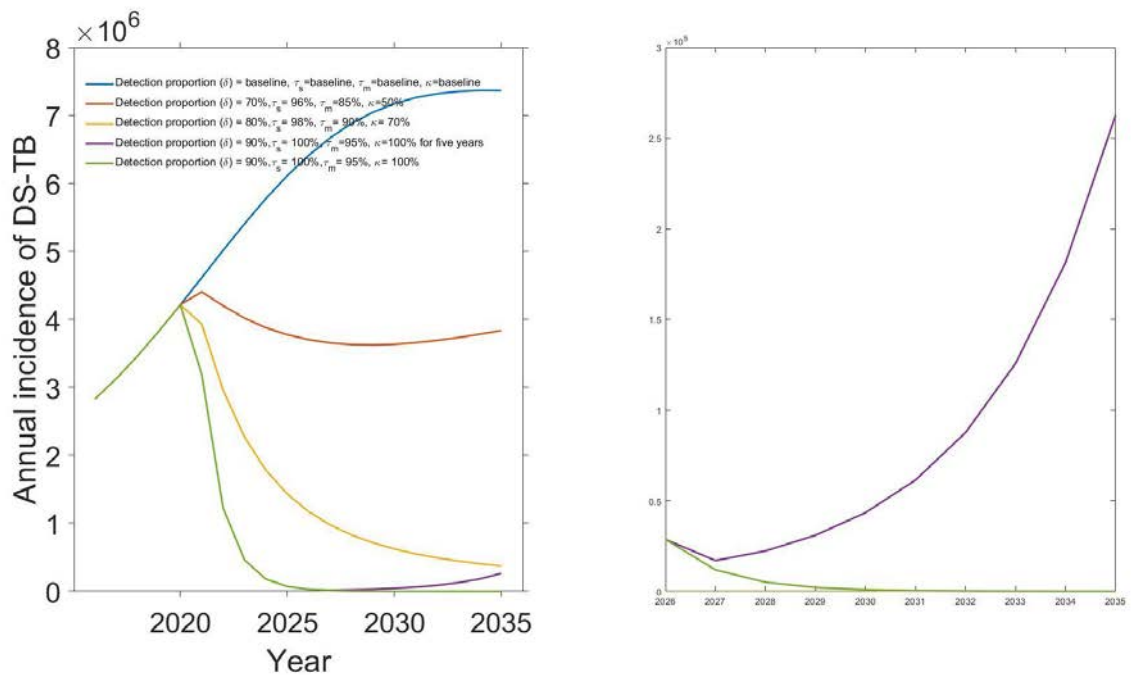
Baseline control strategy consists of a combination of baseline values of the four potential interventions including detection proportion (58%), DS and MBD-TB treatment rates (94% and 78%), and drug-susceptible testing rate (18%). The analysis shows that DS and MDR-TB are likely to increase with the current baseline control strategy.

Modest investment 1 intervention strategy which includes combination of detection proportion, DS and MBD-TB treatment rates, drug-susceptible testing rate from 58%, 94%, 78%, and 18% (baseline) to 70%, 96%, 85% and 50% respectively. As expected, the strategy resulted in decreasing the number of DS and MDR-TB incidence and mortality in Bangladesh. Here, we observed that modest investment 1 strategy is most effective than the baseline strategy which reduce massive number of DS and MDR-TB incidence and mortality in Bangladesh (see Table 7.4, Figure 7.8, and Figure 7.9). Modest investment 2 strategy represents combination of four potential interventions from baseline to 80%, 98%, 90% and 70% respectively. Result from this strategy shows that it is most successful than the modest investment 1 in light of not only reducing the number of DS and MDR-TB cases but also reducing the mortality.

The strategy strong investment 5 years and then revert to baseline strategy includes extensive expansion of detection proportion, DS and MBD-TB treatment rates, drug-susceptible testing rate from baseline to 90%, 100%, 95% and 100% respectively for 5 years and then revert to baseline. The analysis shows that strong investment for 5 years then revert to baseline strategy is highly effective for MDR with minimal rebound after reverting to baseline, as shown in Figures 7.8 and 7.9. For DS-TB however, there is substantial rebound, but the strategy continues to out-perform the next best strategy (modest investment 2) up until 2035, as shown in Figures 7.8 and 7.9.

Finally, strong sustained investment strategy incorporates extensive expansion of detection proportion, DS and MBD-TB treatment rates, drug-susceptible testing rate from baseline to 90%, 100%, 95% and 100% respectively over 15 years period. The analysis shows that the strong sustained investment strategy is the most impactful intervention strategy, which reach the End TB targets reduces DS and MDR-TB cases by 90% and TB related death by 95% in Bangladesh. However, depending on funding availability, other scenarios in Table 7.4 can be considered.

(A)



(B)

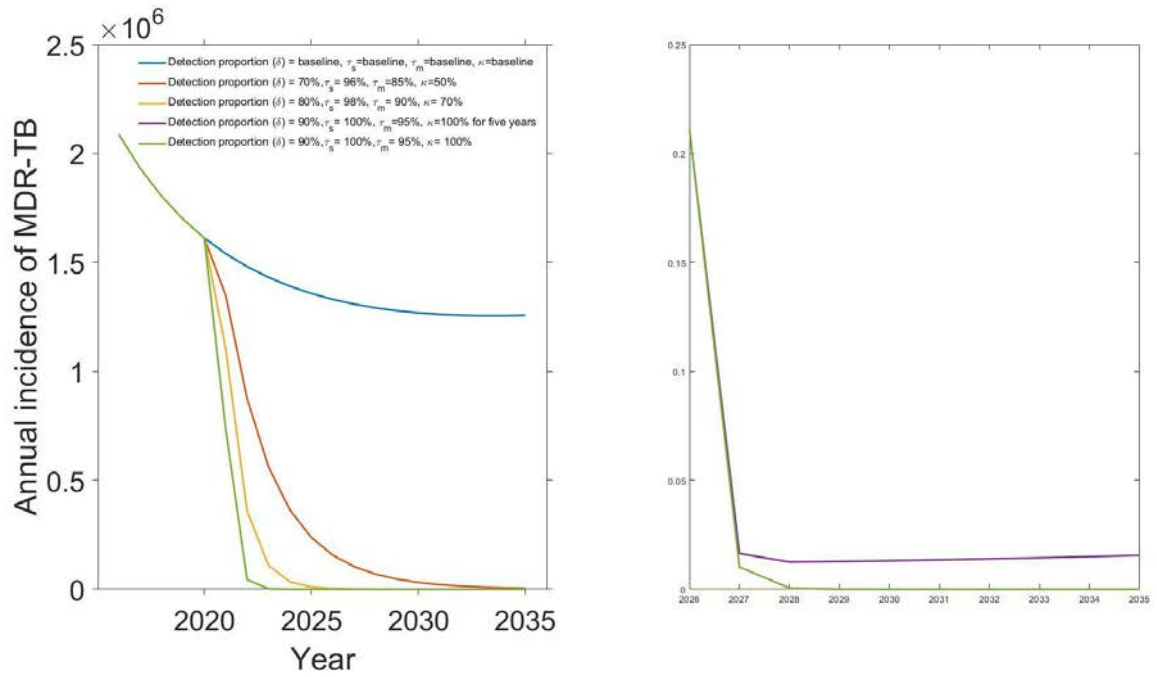
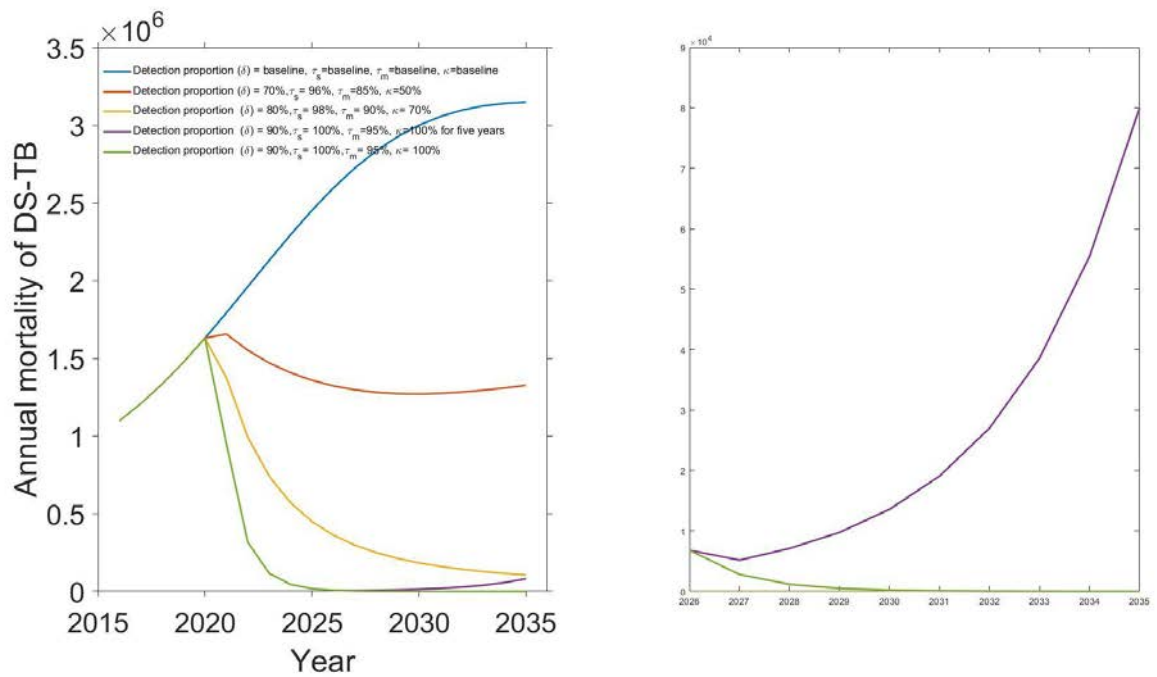


Figure 7. 8 Combination intervention strategy and its effect on (A) DS-TB and (B) MDR-TB annual incidence cases in Bangladesh.

(A)



(B)

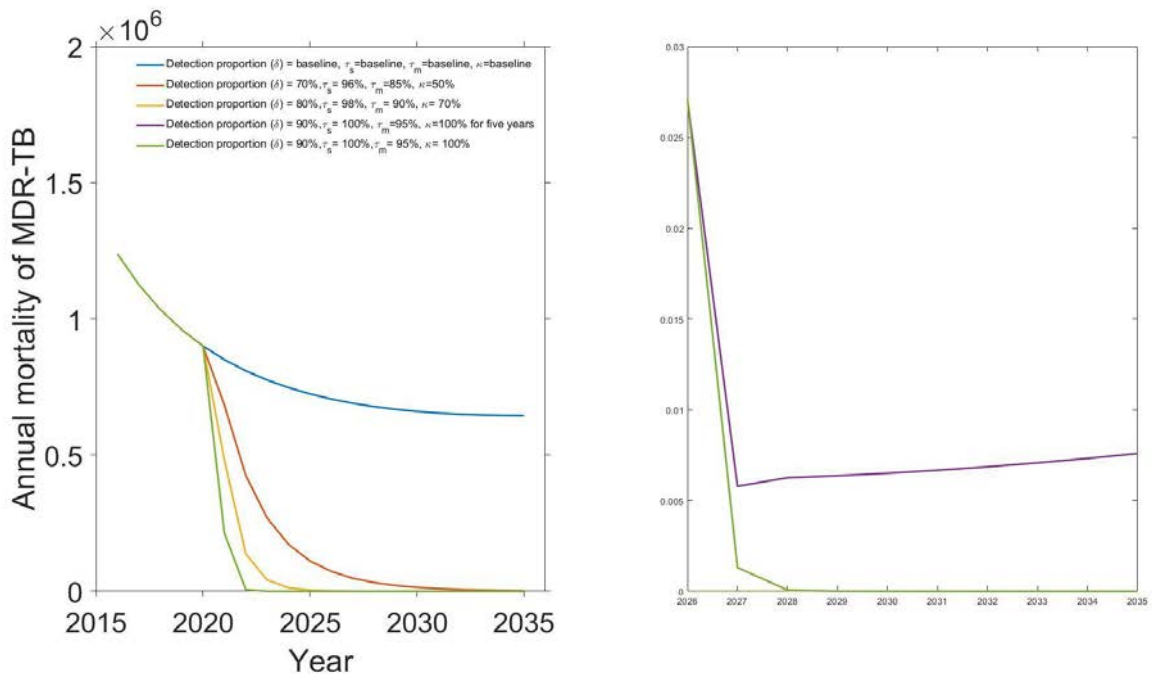


Figure 7. 9 Combination intervention strategy and its effect on (A) DS-TB and (B) MDR-TB annual mortality in Bangladesh.

Table 7. 4 Hypothetical combination intervention strategy implemented in our proposed model of DS and MDR-TB control in Bangladesh, for the period 2020 – 2035.

Scenarios	Parameters changed	Parameter values	Estimated DSTB annual incident cases	Reduction from baseline	Estimated MDR-TB annual incident cases	Reduction from baseline	Estimated DSTB annual mortality	Reduction from baseline	Estimated MDR-TB annual mortality	Reduction from baseline
Baseline	Proportion detected	58%	$7.35 \times 10^6$	$0.00 \times 10^6$	$1.26 \times 10^6$	$0.00 \times 10^6$	$3.15 \times 10^6$	$0.00 \times 10^6$	$0.65 \times 10^6$	$0.00 \times 10^6$
	DS-TB success	94%								
	MDR-TB success	78%								
	Genexpert use	18%								
Modest investment 1	Proportion detected	70%	$3.89 \times 10^6$	$3.46 \times 10^6$	$0.03 \times 10^5$	$1.25 \times 10^6$	$1.34 \times 10^6$	$1.81 \times 10^6$	$0.01 \times 10^5$	$0.64 \times 10^6$
	DS-TB success	96%								
	MDR-TB success	85%								
	Genexpert use	50%								
Modest investment 2	Proportion detected	80%	$0.34 \times 10^6$	$7.01 \times 10^6$	$0.003 \times 10^1$	$1.26 \times 10^6$	$0.09 \times 10^6$	$3.06 \times 10^6$	$0.001 \times 10^1$	$0.65 \times 10^6$
	DS-TB success	98%								
	MDR-TB success	90%								
	Genexpert use	70%								
Strong investment 5 years then revert to baseline	Proportion detected	90%	$0.26 \times 10^6$	$7.09 \times 10^6$	$0.002 \times 10^1$	$1.26 \times 10^6$	$0.08 \times 10^6$	$3.07 \times 10^6$	$0.000 \times 10^1$	$0.65 \times 10^6$
	DS-TB success	100%								
	MDR-TB success	95%								
	Genexpert use	100%								

Strong sustained investment	Proportion detected	90%	$0.69 \times 10^1$	$7.35 \times 10^6$	$0.000 \times 10^1$	$1.26 \times 10^6$	$0.15 \times 10^1$	$3.15 \times 10^6$	$0.000 \times 10^1$	$0.65 \times 10^6$
	DS-TB success	100%								
	MDR-TB success	95%								
	Genexpert use	100%								

## 7.6 Discussion and conclusion

Bangladesh is a resource poor, high burden TB country, and the transmission dynamics and epidemiology of TB are poorly understood. Recently, Bangladesh introduced programmatic management of MDR-TB at the community level to reduce the high utilization of inpatient beds that resulted from MDR-TB treatment under standard regimens [44]. As the effectiveness of the community-based short-course MDR-TB management Bangladesh regimen was found to be significantly higher than hospital-based management, it is important to identify the factors responsible for effective MDR-TB management, public awareness through education, and financial support from the treatment program, and programmatic strengths [12]. Although TB control in Bangladesh has significantly progressed – improved case finding, availability of free diagnostic and treatment services, involvement of multiple partners, newer diagnostic facilities, sufficient human resources, adequate capacity and guidelines – more effort is required.

In this paper, we presented a two-strain TB model with amplification: one strain for DS-TB; and another for MDR-TB. Here, we considered amplification as the process by which an individual infected with a DS-TB develops MDR-TB. We derived the basic reproduction number of each TB strain, and found that both basic reproduction numbers play an important role in the dynamics of DS and MDR-TB outbreaks. We fitted our model using DS and MDR-TB annual incidence data from the WHO Bangladesh reports. Sensitivity analyses were performed to determine the relative importance of several parameters used in our model. Our analysis led to the observations that, of the modifiable parameters, the *treatment of latent TB* parameter had the negative correlation with the basic reproduction numbers of DS and MDR-TB dynamics. This correlates with case detection (allowing increased treatment) having the greatest impact of the interventions and strongly suggests that investments in public health responses that focus on case detection should be the foundation of improved TB control.

As a single-intervention, increasing the detection proportion was found to be the most effective strategy for reducing the incidence and mortality of DS and MDR-TB in Bangladesh compared to other single-intervention strategies, which is consistent with previous studies [25, 26]. For DS-TB the second most effective intervention was improve treatment success rate, which reduces both mortality of the treated

individual and transmission.[1]. For MDR-TB, drug-susceptibility testing is the second most important intervention as it has a multiplicative effect with case detection in leading to proper implementation of effective second-line treatment [45].

Traditional wisdom is that more treatment of drug-susceptible TB will translate to better outcomes for DS and MDR-TB. However, one condition in our study is that *increased* treatment does not mean *improved* treatment, so our model predicts that the risk of MDR acquisition for a given treatment course remains the same. If the MDR strain has reasonable fitness, such that the basic reproduction number is greater than one ( $R_0 > 1$ ), reducing the DS strain will increase the ecological niche for the resistant strain. Further, even if the MDR strain is not as fit as the DS strain, if treatment does not achieve and  $R_{\text{effective}}$  less than one for the DS strain, the MDR strain will increase through treatment with amplification. On the other hand, if  $R_0$  is less than one for the MDR strain, then if treatment of DS-TB achieves and  $R_{\text{effective}}$  less than one, treatment (DOTS) for DS-TB will also eliminate MDR-TB.

We acknowledged the importance of comprehensive countrywide programmatic improvements to TB control in Bangladesh. Without such extensive approaches, further rises in the overall disease burden are expected, and the problem of drug resistance may possibly expand. Five scenarios all incorporating improved case notification, treatment success rates and drug susceptibility testing were examined to measure the effectiveness of these strategies.

From the analysis of implementing combination intervention strategies simultaneously, we found that a modest investment (detection proportion 70%, DS-TB treatment success 96%, MDR-TB treatment success 85%, drug-susceptibility testing 50%) is sufficient to substantially reduce MDR TB, whereas a strong sustained investment strategy (detection proportion 90%, DS-TB treatment 100%, MDR-TB treatment 95%, drug-susceptibility testing 100%) is required to substantially reduce DS-TB. For MDR-TB, implementing multiple interventions simultaneously is the more effective than single intervention strategies, whereas for DS-TB which already has a very high treatment success rate in Bangladesh, case detection remains the key intervention.

Our strategies describe a variety of potential responses, extending from inaction to extremely ambitious multifactorial strategies. Despite the challenges faced in delivering effective programmatic TB control in Bangladesh, we believe it is essential to consider such responses because previous programs have demonstrated substantial public health gains in resource-limited settings such as Bangladesh [1]. Although the extensive approaches are not presently recommended by the World Health Organization or Bangladesh National TB Control Program, our modelling suggests that the high burden of DS and MDR-TB in Bangladesh is likely to increase with the existing, DOTS-based programmatic response.

## **Ethical approval**

This study is based on aggregated TB surveillance data in Bangladesh provided by the National TB Control Program and the World Health Organization. No confidential information was included because mathematical analyses were performed at the aggregate level. All of the methods were conducted under the approved research protocol. The research protocol was approved by the James Cook University human ethics approval board, H7300.

## **Data availability**

The datasets produced during the study are available from the corresponding author on reasonable request.

## **Acknowledgements**

The authors would like to thank the National TB Control Program in Bangladesh and Dr. Md. Abu Sayem for his contribution and data sharing.

## **Author contributions**

M.A.K, E.S.M and M.T.M conceived of the project concept; M.A.K cleaned the data. M.A.K wrote the initial code, E.S.M added additional lines of code. M.A.K performed the data analysis, model development and interpretation, E.S.M, M.T.M and M.A.S refined this further. M.A.K wrote the initial draft of this manuscript, and all authors provided input into revisions and approved the final manuscript and submission for publication.

## **Conflict of interest**

The authors declare that they have no potential conflict of interest.

## **References**

1. WHO, *Global tuberculosis report. WHO/CDS/TB/2019.15, Geneva.* 2019.
2. WHO, *Global tuberculosis report. WHO/HTM/TB/2010.7, Switzerland,* 2010.
3. Chung-Delgado, K., et al., *Mortality among MDR-TB cases: comparison with drug-susceptible tuberculosis and associated factors.* PloS One, 2015. **10**(3).
4. Aslam, B., et al., *Antibiotic resistance: a rundown of a global crisis.* Infection and Drug Resistance, 2018. **11**: p. 1645.
5. Song, W-M., et al., *Primary drug resistance of mycobacterium tuberculosis in Shandong, China, 2004–2018.* Respiratory Research, 2019. **20**(1): p. 223.

6. Zur Wiesch, P. S., Engelstädter, J., and Bonhoeffer, S., *Compensation of fitness costs and reversibility of antibiotic resistance mutations*. Antimicrobial Agents and Chemotherapy, 2010. **54**(5): p. 2085-2095.
7. Pai, M., et al., *Tuberculosis*. Nature Reviews Disease Primers, 2016. **2**,16076.
8. Davies, P. D., *Drug-resistant tuberculosis*. Royal Society of Medicine, 2001. **94**(6).
9. WHO, *Global tuberculosis report*. WHO/HTM/TB/2015.22, Switzerland, 2015.
10. Jabbari, A., et al., *A two-strain TB model with multiple latent stages*. Mathematical Biosciences and Engineering, 2016. **13**(4): p. 741-785.
11. DGHS, *National Tuberculosis Control Program (NTP). National guidelines and operational manual for tuberculosis control, 4th and 5th edition*. 2013.
12. NTP, *Tuberculosis control in Bangladesh*. Annual report 2015.
13. Carvalho, A. C., et al., *Transmission of Mycobacterium tuberculosis to contacts of HIV-infected tuberculosis patients*. American Journal of Respiratory and Critical Care Medicine, 2001. **164**(12): p. 2166-2171.
14. Diez, M., et al., *Determinants of health system delay among confirmed tuberculosis cases in Spain*. The European Journal of Public Health, 2005. **15**(4): p. 343-349.
15. Prinja, S., et al., *Availability of medicines in public sector health facilities of two North Indian States*. BMC Pharmacology and Toxicology, 2015. **16**(1): p. 43.
16. Amo-Adjei, J., *Views of health service providers on obstacles to tuberculosis control in Ghana*. Infectious Diseases of Poverty, 2013. **2**(1): p. 9.
17. Allos, B. M., et al., *Management of an outbreak of tuberculosis in a small community*. Annals of Internal Medicine, 1996. **125**(2): p. 114-117.
18. Bhunu, C., et al., *Modelling the effects of pre-exposure and post-exposure vaccines in tuberculosis control*. Journal of Theoretical Biology, 2008. **254**(3): p. 633-649.
19. Trauer, J. M., Denholm, T. J., and McBryde, E. S., *Construction of a mathematical model for tuberculosis transmission in highly endemic regions of the Asia-Pacific*. Journal of Theoretical Biology, 2014. **358**: p. 74-84.
20. Trauer, J. M., et al., *Modular programming for tuberculosis control, the "AuTuMN" platform*. BMC Infectious Diseases, 2017. **17**(1): p. 546.
21. Maude, R. J., et al., *The role of mathematical modelling in guiding the science and economics of malaria elimination*. International Health, 2010. **2**(4): p. 239-246.
22. Kim, S., et al., *What Does a Mathematical Model Tell About the Impact of Reinfection in Korean Tuberculosis Infection?* Osong Public Health and Research Perspectives, 2014. **5**(1): p. 40-45.
23. Brooks-Pollock, E., Cohen, T., and Murray, M., *The impact of realistic age structure in simple models of tuberculosis transmission*. PLoS One, 2010. **5**(1): p. e8479.
24. Mishra, B. K., and Srivastava, J., *Mathematical model on pulmonary and multidrug-resistant tuberculosis patients with vaccination*. Journal of the Egyptian Mathematical Society, 2014. **22**(2): p. 311-316.
25. Okuonghae, D., and Ikhimwin, O. B., *Dynamics of a mathematical model for tuberculosis with variability in susceptibility and disease progressions due to difference in awareness level*. Frontiers in Microbiology, 2016. **6**: p. 1530.
26. Okuonghae, D., and Omosigho, S., *Analysis of a mathematical model for tuberculosis: What could be done to increase case detection*. Journal of Theoretical Biology, 2011. **269**(1): p. 31-45.
27. Kuddus, M. A., et al., *Modeling drug-resistant tuberculosis amplification rates and intervention strategies in Bangladesh*. PloS One, 2020. **15**(7): p. e0236112.
28. Diekmann, O., Heesterbeek, J. A. P., and Roberts, G. M., *The construction of next-generation matrices for compartmental epidemic models*. Journal of the Royal Society, Interface, 2010. **7**(47): p. 873-885.
29. Van, D. P., *Reproduction numbers of infectious disease models*. Infectious Disease Modelling, 2017. **2**(3): p. 288-303.
30. Diekmann, O., Heesterbeek, J., and Roberts, G. M., *The construction of next-generation matrices for compartmental epidemic models*. Journal of the Royal Society Interface, 2009. **7**(47): p. 873-885.

31. Heffernan, J. M., Smith, J. R., and Wahl, M. L., *Perspectives on the basic reproductive ratio*. Journal of the Royal Society Interface, 2005. **2**(4): p. 281-293.
32. Yang, Y., et al., *Global stability of two models with incomplete treatment for tuberculosis*. Chaos, Solitons & Fractals, 2010. **43**(1-12): p. 79-85.
33. Ragonnet, R., et al., *Optimally capturing latency dynamics in models of tuberculosis transmission*. Epidemics, 2017. **21**: p. 39-47.
34. Ragonnet, R., et al., *Revisiting the Natural History of Pulmonary Tuberculosis: a Bayesian Estimation of Natural Recovery and Mortality rates*. BioRxiv, 2019: p. 729426.
35. WHO, *Global tuberculosis report*. WHO/HTM/TB/2017.23, Geneva, 2017.
36. Cox, H. S., et al., *Risk of acquired drug resistance during short-course directly observed treatment of tuberculosis in an area with high levels of drug resistance*. Clinical Infectious Diseases, 2007. **44**(11): p. 1421-1427.
37. WHO, *Global tuberculosis report*. WHO/HTM/TB/2016.13, Geneva, 2016.
38. Rahman, A., and Kuddus, A., *Cost-effective modeling of the transmission dynamics of malaria: A case study in Bangladesh*. Communications in Statistics: Case Studies, Data Analysis and Applications, 2020: p. 1-17.
39. Kim, S., Aurelio, A., and Jung, E., *Mathematical model and intervention strategies for mitigating tuberculosis in the Philippines*. Journal of Theoretical Biology, 2018. **443**: p. 100-112.
40. Njagarah, J. B., and Nyabadza, F., *Modelling optimal control of cholera in communities linked by migration*. Computational and Mathematical Methods in Medicine, 2015. **2015**.
41. Chitnis, N., Cushing, J. M., and Hyman, J., *Bifurcation analysis of a mathematical model for malaria transmission*. Journal on Applied Mathematics, 2006. **67**(1): p. 24-45.
42. Mitnick, C. D., et al., *Programmatic management of drug-resistant tuberculosis: An updated research agenda*. PLoS One, 2016. **11**(5): p. e0155968.
43. Daley, C. L., *Global scale-up of the programmatic management of multidrug-resistant tuberculosis*. The Indian Journal of Tuberculosis, 2014. **61**(2): p. 108-15.
44. NTP, *National Guidelines and Operational Manual for Programmatic Management of Drug Resistant Tuberculosis, 2nd edition*. 2016.
45. Kalokhe, A. S., et al., *Multidrug-resistant tuberculosis drug susceptibility and molecular diagnostic testing*. The American Journal of the Medical Sciences, 2013. **345**(2): p. 143-148.

# CHAPTER 8

**Discussion and future directions**

## 8.1 Discussion of main findings

The research presented in this thesis encompasses our knowledge of TB epidemiology as well as those components that are significant for TB outbreaks in Bangladesh. This enables us to gain a better understanding of TB transmission and risk factors, and fill the gap of knowledge from prior studies.

Although TB has been endemic in Bangladesh since the first recorded epidemic in 1965, little has been published on its transmission dynamics and epidemiology; also, no mathematical model structure exists that has been specifically tailored to Bangladesh. The narrative review in Chapter 2 discussed TB's emergence and establishment as endemic, and the risk factors for transmission, including health system factors, environmental factors, host factors, and sociological factors. An extensive literature search was performed to understand the relative influence of weather variables on the incidence of TB, indicating that projected changes in weather variables increase or decrease the potential for TB epidemics and therefore, must be considered in predicting the impact of future changes in weather variables on TB transmission. The literature review also demonstrated the extent of uncertainty about the optimal method for structuring TB models, and highlighted the wide variation in approaches to assembling and parameterizing compartments to simulate some of the most fundamental aspects of TB epidemiology, thereby clearly reflecting the lack of understanding of these processes at the mathematical, biological, clinical and epidemiological levels.

In addressing structural uncertainty, the original approach to model construction relied primarily on a review of published literature, both previously published models and epidemiological data. Although the first iteration of the model was constructed within the timeframe and with programmatic applications in mind, the fundamental structure was retained throughout this research. The model has increased markedly in complexity, with elaborations undertaken primarily in order to permit simulation of interventions acting on sub-populations of compartments included within the original two-strain six compartment model. However, both simple and complex structure models have advantages and disadvantages. Complex models may have the potential to more accurately simulate reality and so have greater predictive power. Complex models also require more parameters to be estimated and greater programming coding skill to minimize the risk of errors. Simple models conversely have the advantage of being understood by a broader readership. A simple model with definite conclusions has the potential to make a strong and clear point to readers, and allow for analytical expressions to visualize the impact of parameters on model outputs. Thus, chapter 2 offered a comprehensive understanding of the simple and complex TB models as well as history and epidemiology of TB in developed and developing countries, particularly in Bangladesh, laying down the foundations for the modelling which follows.

In chapter 3, a generalized linear Poisson regression model was used to investigate the association between weather factors and the number of TB cases reported to the Bangladesh NTP between 2007 and 2012 in three known endemic districts of Rajshahi, Bangladesh. The model was implemented using a frequentist approach with the aim of identifying weather variables, including temperature, humidity and rainfall, which significantly influence TB transmission in Rajshahi. A wide range of diagnostic tests were performed to confirm the goodness of fit of the model. The model revealed that the number of TB cases is strongly associated with temperature, humidity and rainfall in Rajshahi province, Bangladesh. Low temperature, low humidity and low rainfall are all associated with higher TB incidence. Temperature and rainfall effects were delayed and increased over the lag period while humidity was immediate and the risk decreased with longer exposure. This suggests that temperature may govern transmission, and humidity may govern reactivation (incubation period). The significant positive influence of temperature, humidity and rainfall on TB incidence in Rajshahi province found in our data analysis in this thesis is consistent with the findings of other studies [1-3].

In chapter 4, I developed a two-strain disease model with amplification to simulate the prevalence of Drug-susceptible (DS) and Drug-resistant (DR) disease strains. Here, I performed a dynamic analysis of the resulting system and found that the model contained three equilibrium points: a disease-free equilibrium; a mono-existent equilibrium with respect to the DR strain; and a co-existent equilibrium, where both the DS and DR strains persisted. I found two basic reproduction numbers: one associated with the DS strain and the other, the DR strain, and found that they both played an important role in the outbreak of disease. Global sensitivity analysis was performed, finding that the contact rate of both strains had the largest influence on disease prevalence. I also investigated the impact of the amplification and treatment rates of both strains and found that poor quality treatment (drug) makes coexistence more likely and increases the relative abundance of resistant infections.

The two-strain TB model developed in Chapter 5, and extended in Chapters 6 and 7 combined prevalence, notification, DS, MDR and total TB incidence data to create models accounting for TB transmission dynamics over time.

In chapter 5, I developed a parsimonious mathematical model of TB epidemiology dynamics, particularly the prolonged latency period and possibility of fast and slow progression to active TB. The model was then extended to incorporate two-circulating TB strains: a DS-TB strain and a DR-TB strain. I then incorporated the amplification pathway from DS-TB to DR-TB, and investigated the role of amplification in the Bangladesh TB model. Amplification develops mainly through the choice of naturally occurring mutations selected by inappropriate treatment. When preliminary resistance has established, acquisition of resistance to supplementary drugs is more likely, making treatment with usual regimens suboptimal [4]. Therefore, in this mathematical model, I considered the emergence of

DR-TB in response to inappropriate and poorly administered treatment, and then assessed the relationship between the rate of amplification and the rate of treatment of DS-TB.

Following this analysis, I also performed a rigorous analytical analysis of the system properties and solutions to predict both the early- and late-time behaviour of the model. After deriving the basic reproduction numbers for DS-TB ( $R_{0s}$ ) and DR-TB ( $R_{0r}$ ) using the next generation matrix technique, I investigated the impact of their relative magnitudes on the infected populations of both DS-TB and DR-TB. DS-TB and DR-TB can spread in a population only if  $\max[R_{0s}, R_{0r}] > 1$  (epidemic), but are maintained in a population without the need for external inputs when  $\max[R_{0s}, R_{0r}] = 1$  (endemic). A disease-free population will result when both basic reproduction numbers are  $\max[R_{0s}, R_{0r}] < 1$ , which means that the disease naturally dies out. Furthermore, if  $R_{0r} > \max[R_{0s}, 1]$ , then DS-TB dies out but DR-TB persists in the population, and if  $R_{0s} > \max[R_{0r}, 1]$ , then both DS-TB and DR-TB persist in the population. Therefore, in order to control transmission, the period of infectiousness needs to be reduced until  $\max[R_{0s}, R_{0r}] < 1$ . I also performed a sensitivity analysis of the model outcomes and parameters, and found that the contact rate of both strains had the largest influence on DS and DR-TB prevalence. The information that I generated from this Chapter can be used to advise the Bangladesh NTP of the programmatic effect of treatment regimens.

In Chapter 6, I extended the previous two-strain TB model structure and allowed latently infected people to move directly to the recovered classes due to prophylactic treatment. In this model, I integrated four different types of control strategies: distancing, latent case finding, case holding and active case finding, and their economical cost into the mathematical framework of my transmission dynamic TB model. The economical compartment assessed the financial consequences of different interventions and explored their impact on the spatial spread of DS and MDR-TB in Bangladesh. Furthermore, I established a relationship between different intervention packages combining currently recommended and other available interventions to predict how the spread of DS and MDR-TB can be avoided or delayed.

The economical compartment also evaluated the economic effect on both patients and the health system considering factors such as schedule shortening for first line TB treatment and examining the unit cost for interventions. The evaluation found that shorter treatment duration would result in financial gains from a patient perspective, and the possible financial gains for health facilities may also be significant but would be framework-specific, and dependent on the proper pricing of any new schedule. The finding suggests that among the four-single intervention strategies, the distancing control strategy is the most cost-effective. Within the six-dual control strategies with distancing control, the latent case finding control strategy is the most cost-effective, and more rapidly reduces DS and MDR-TB compared to

other dual control strategies. I observed that why active case finding becomes less important with distancing compared with latent case finding because case numbers decline, making the strategy more costly for every active case found. Considering the triple control strategy structure, distancing with latent case finding and case holding control is the most cost-effective. From the analysis of all the control strategies, I found that the most cost-effective control is the quadruple control strategy which includes distancing, latent case finding, case holding and active case finding, triple control strategy is similar to dual control strategy and followed by single control. Results also suggest that focusing on a single control strategy does not dramatically affect the decline in DS and MDR-TB in Bangladesh instead, combining two or more control strategies simultaneously is the most effective way to decrease the burden of DS and MDR-TB in Bangladesh, which is consistent with previous works [5-8].

In Chapter 7, I extended the two-strain TB model from the previous model structure. I allowed the flow from the latently infected people to move to the susceptible compartment due to the loss of immunity. I calibrated the model with DS and MDR-TB annual incidence data to estimate the model parameters' value. I considered four specific intervention scenarios: enhancing the detection proportion, drug-susceptibility testing rate, and the DS and MDR-TB treatment rates and their combination, to assess the effect of these responses on my TB model during the period from 2020 to 2035. To explore the impact of each intervention of TB incidence and mortality in Bangladesh, four-single intervention strategies, increasing an individual's intervention from baseline to comprehensive expansion of high expected value. The finding suggests that the detection proportion is the most important intervention for decreasing DS and MDR-TB incidence and mortality in Bangladesh. However, focussing on DS and MDR-TB treatment rates alone will not dramatically affect the decline in DS and MDR-TB incidence and mortality in Bangladesh. Taking more key parameters simultaneously is the most effective way to reduce the burden of DS and MDR-TB incidence and mortality in Bangladesh.

However, scenarios illustrated a family of possible outcomes, increasing from inaction to remarkably ambitious multifactorial approaches. Although there are difficulties in delivering practical programmatic TB control in Bangladesh, we consider it imperative to recognize such approaches. This is because extreme impacts from mere public health interventions have earlier been shown in resource-limited contexts in Bangladesh when performed at a community level, and because it will help in future ambitious programs. Although the widespread strategies are not immediately recommended by the WHO or Bangladesh NTP, and improvements in achievement and cure rates have not been perceived, this modelling implies that the high burden of DS and MDR-TB incidence and mortality in Bangladesh likely to increase with the current, DOTS based programmatic response.

## 8.2 Limitations

Several limitations of this thesis should be noticed. Data quality is one of the greatest limitations in analysing TB epidemiology in Bangladesh. In **Chapter 3**, time series analysis was based on quarterly time series sequences. I used quarterly data in discussing cross correlations between times series sequences; however, measurements based on such long time intervals may be too coarse, and therefore the risk of bias cannot be precluded. Further, I could only adjust for a few important weather variables in the model. Many other important risk factors for TB were unavailable, including human activities and other environmental factors. Weather variables based on fixed monitoring sites do not completely gauge the true weather exposure of every individual. Therefore, more accurate data and additional TB risk factors could be included in the models to confirm their associations and mechanism of TB cases and continuing climate change. However, the assessment of weather-TB associations in the North-West region of Bangladesh provides new insight into the burden of the disease that can be attributed to varying weather conditions.

The two-strain SIR model presented in **Chapter 4** is not based on a data series and has not been validated against other models. It is therefore a theoretical model with the infectious agent unspecified, with the aim to simulate the prevalence of DS and DR disease strains and the emergence of drug resistance as a result of inadequate treatment. Future studies may compare models with real data to explore the dynamics of DS and DR strains due to the poor quality treatment to validate the model. Furthermore, studies may use the general findings of the model and specify the model to additional infectious diseases (viral or bacterial) in future.

In **Chapters 5, 6 and 7**, I used TB surveillance data, including prevalence, notification and incidence data, to estimate the model parameters. In Bangladesh, infectious disease surveillance is not fully recognized, lack of specificity of the TB symptoms, and limited access to health facilities, leads to under-reporting and misclassification of TB cases, and the risk of bias cannot be precluded. Therefore, more accurate data should be collected to address concerns related to TB. As our proposed intervention is data dependent, policy-makers need to adjust for data in adopting our proposed intervention. The seasonality component is not further incorporated into the mathematical models, in some cases, it may give a better fit to the data. Further, in **Chapters 5, 6 and 7**, I also considered the population is constant and mixes homogeneously. That means the only way a person can leave the susceptible compartment is to become infected and not all infected become infectious, some recover back to susceptible class and then the only way a person can leave the infectious compartment is to recover and die from TB once a person has recovered the person received immunity and death. Additionally, I also assumed that all populations were equally susceptible and the death rate was equal for each population compartment.

### **8.3 Significance and implications**

This project analyzed TB epidemiological surveillance data from the Bangladesh NTP and WHO, and investigated spatiotemporal trends in TB prevalence, notification, incidence and factors driving these trends. I modelled TB elimination strategies by the Bangladesh NTP and predicted their efficacy, and also determined the optimal combinations of interventions for particular scenarios. This work was done in close collaboration with the NTP and has the potential to directly inform the design of TB elimination strategies for Bangladesh. Furthermore, this work provides a better understanding of the changing epidemiology of DS-TB and emerging MDR-TB epidemics, and supports future policy and planning of TB control efforts in Bangladesh. Finally, the flexible modelling (both transmission and economic) framework developed here could be adaptable to other settings that experience high burdens of DS and MDR-TB.

### **8.4 Future directions**

More research is needed to explain the relationship between weather variables and the number of TB cases in Bangladesh. As mentioned earlier, only a few important weather variables were adjusted for in the time series analysis in the model. To capture the environmental changes in the coming years, other important variables, including human activity, population density and coverage of protective measures will need to be considered to improve the performance of predictive models. Linking more variables would be an important advance towards the development of an early warning system for NTP in Bangladesh.

In this thesis, I also developed a flexible mathematical model of TB transmission dynamics, including many of the important features of TB epidemiology: DS-TB and acquisition of MDR-TB, through the two possible mechanisms of amplification and primary transmission. The model incorporated important drivers for resistance, such as antibiotic pressure, poor use of antibiotics, weak health systems with poor follow-up, and increased risk of resistance developed following incomplete antibiotic courses. In the future, this model will be extended by incorporating two additional modules: one for pharmacokinetic pharmacodynamic (PKPD) information and another for information on strain diversity with respect to anti-mycobacterial resistance; the latter will be informed by publications based on drug resistance mutations and phenotype/genotype mutations.

Experimental PKPD models include *in vitro* and *in vivo* animal models. Measurement of the impact of a single or combinations of drugs on resistance emergence has accelerated recently with an *in vitro* model of drug delivery, the hollow glass fibre models (HFMs). The HFMs can predict the rate of

emergent resistant isolates with monotherapy or dual therapy under different population pharmacokinetic profiles. Inputs into the models are (i) the concentration of drug mimicking expected at the site of the TB infection under a range of different population pharmacokinetic profiles, and (ii) conditions at the site in terms of acidity and hypoxia mimicking abscess and different stages of TB infection. Outputs of the HFM are log kill time curves and rates of emergence of phenotypic DR-TB isolates. These allow careful titration to expose *Mtb* to the actual concentration that can be delivered in vitro to assess the probability of the development of resistance, including mono/multi/pan-resistance. Outputs from the PKPD model can be fed into the transmission dynamic model in terms of the likelihood of the emergence of a novel strain of *Mtb*. How this strain adapts in terms of fitness cost, sequential resistance and transmission can be further modelled by considering the multiple strain model.

The multiple strain model will include the diversity and evolution of TB and hence the subsequent disease dynamics that result through antibiotic selection pressure. This diversity will be parameterized through published data on frequency of resistance acquisition in clinical studies, fitness cost and compensatory mutations for each of the anti-mycobacterial agents being considered in the model. This novel model will make a tool with three interacting models. The TB triple tool is a creative approach to the global challenge of emerging drug resistance because it will combine three different scientific streams into one composite model to great effect. The result is an in 'silico' prediction of the efficacy and durability of combinations of antibiotics, specified to populations across the globe. The results will be generalizable to global TB epidemiology, and beyond that the methods used will have potential significance for other infectious agents and infection-antibiotic combinations.

## **8.5 Conclusion**

This thesis developed practical approaches to a better understanding of the changing epidemiology of TB dynamics in Bangladesh using geographic, demographic, and TB surveillance data. The presented framework is a marked development on earlier strategies for the modelling of TB transmission in Bangladesh. The framework highlights that estimation of the weather variables impacting TB transmission needs consideration of not only coarse aggregated weather patterns, including mean temperature, humidity, and rainfall, but also short and long scale variability in weather. In the mathematical modelling framework, this study carried out an analytical and numerical comparison of various TB model architectures to explore the impact of various assumptions on the transmission dynamics of DS and MDR-TB in Bangladesh. The study also assessed the consequences of different interventions and optimal elimination strategies and explored their interactions with spatial spread of DS and MDR-TB in Bangladesh. The results of this thesis will contribute to the evidence base available to the NTP in Bangladesh to plan for DS and MDR-TB elimination strategically and efficiently under the threat of drug resistance.

## References

1. Liu, M-Y., et al., *Spatial and temporal clustering analysis of tuberculosis in the mainland of China at the prefecture level, 2005–2015*. Infectious Diseases of Poverty, 2018. **7**(1): p. 106.
2. Xiao, Y., et al., *The influence of meteorological factors on tuberculosis incidence in Southwest China from 2006 to 2015*. Scientific Reports, 2018. **8**(1): p. 1-8.
3. Fernandes, F. M. D. C., et al., *Relationship between climatic factors and air quality with tuberculosis in the Federal District, Brazil, 2003-2012*. Brazilian Journal of Infectious Diseases, 2017. **21**(4): p. 369-375.
4. Trauer, J. M., Denholm, T. J., and McBryde, E. S., *Construction of a mathematical model for tuberculosis transmission in highly endemic regions of the Asia-Pacific*. Journal of Theoretical Biology, 2014. **358**: p. 74-84.
5. Gao, D-P., and Huang, N-J., *Optimal control analysis of a tuberculosis model*. Applied Mathematical Modelling, 2018. **58**: p. 47-64.
6. Kim, S., Aurelio, A., and Jung, E., *Mathematical model and intervention strategies for mitigating tuberculosis in the Philippines*. Journal of Theoretical Biology, 2018. **443**: p. 100-112.
7. Kim, S., et al., *What Does a Mathematical Model Tell About the Impact of Reinfection in Korean Tuberculosis Infection?* Osong Public Health and Research Perspectives, 2014. **5**(1): p. 40-45.
8. Okuonghae, D., and Ikhimwin, O. B., *Dynamics of a mathematical model for tuberculosis with variability in susceptibility and disease progressions due to difference in awareness level*. Frontiers in Microbiology, 2016. **6**: p. 1530.

\*\*\*\*\*